GEOLOGICAL SURVEY OF WESTERN AUSTRALIA

REPORT 37

PROFESSIONAL PAPERS

DEPARTMENT OF MINERALS AND ENERGY

GEOLOGICAL SURVEY OF WESTERN AUSTRALIA

REPORT 37

PROFESSIONAL PAPERS

Perth 1994

14732—1

MINISTER FOR MINES
The Hon. George Cash, J.P., M.L.C.

ACTING DIRECTOR GENERAL
L. C. Ranford

DIRECTOR, GEOLOGICAL SURVEY OF WESTERN AUSTRALIA
Pietro Guj

Copy editor: I. R. Nowak

National Library of Australia Card Number and ISBN 0 7309 4405 0

ISSN 0508–4741

ISSN 0812–8952

Copies available from:
Mining Information Centre
Department of Minerals and Energy
100 Plain Street
EAST PERTH Western Australia 6004
Telephone (09) 222 3459

Contents

Geology and hydrogeology of the Karridale Borehole Line, Perth Basin

by

L. J. Baddock

Abstract

The Karridale Line consists of sixteen bores drilled at seven sites across the southern Perth Basin, 250 km south of Perth. An aggregate depth of 9441 m was drilled during the program which investigated the geology and hydrogeology of the area. The deepest bore was 1682 m. Drilling intersected faulted, non-marine sediments of Permian to Early Cretaceous age after passing through the unconformably overlying, unfaulted Bunbury Basalt and Warnbro Group of Early Cretaceous age.

The southern Perth Basin consists of two structural units, the Bunbury Trough and the Vasse Shelf. The major aquifers in the Bunbury Trough are the Yarragadee Formation, Cockleshell Gully Formation and Lesueur Sandstone. The Yarragadee Formation, the most extensive aquifer and at least 1200 m thick in the eastern Bunbury Trough, contains fresh groundwater throughout the formation. The Cockleshell Gully Formation is over 800 m thick and contains up to 750 m of fresh groundwater. There is a regional groundwater flow system controlled by lithology and faulting.

On the Vasse Shelf the Lesueur Sandstone, which is up to 860 m thick, is the major aquifer. It contains two flow systems separated by a structural high in the Sue Coal Measures.

The Warnbro Group is a minor aquifer which forms local flow systems controlled by topography.

The salinity of the fresh groundwater in the major aquifers is generally less than 400 mg/L total dissolved solids, but there is a high iron content. The Sabina Sandstone and Sue Coal Measures usually contain brackish to saline groundwater.

KEYWORDS : Perth Basin, hydrogeology, geology, stratigraphy, groundwater

Introduction

The Karridale Line consists of sixteen exploratory water bores drilled to a maximum depth of 1682 m at seven sites on an east-trending line across the southern Perth Basin around latitude 34° 10' south. The line is located some 250 km south of Perth, and extends from 17 km north of Augusta to 23 km south of Nannup (Fig. 1).

Drilling on the Karridale Line was undertaken by the Geological Survey of Western Australia (GSWA) as part of the deep groundwater resources assessment of the Perth Basin. The Karridale Line is the most southern line in the assessment program, with the Cowaramup Line (Appleyard, 1989) located 33 km to the north. There is little information on groundwater in the area, and the only previous stratigraphic data came from four deep petroleum-exploration wells, and some shallow bores drilled for coal or mineral sands (Fig. 1).

Climate

The Augusta–Nannup area has a Mediterranean climate with warm, dry summers and cool, wet winters. The average annual rainfall ranges from 1000 mm to 1100 mm, and the average annual evaporation is about 1000 mm. Most rainfall occurs between the months of April and October.

The monthly average maximum and minimum daily temperatures at the closest climatological stations in the area range from 23.5°C in February to 11.0°C in July and August at Cape Leeuwin, and from 28.2°C in February to 8.0°C in August at Margaret River (Commonwealth Bureau of Meteorology).

Physiography and landuse

The Karridale Line is situated at the southern end of the Blackwood Plateau which is bounded by the Darling Plateau to the east, the Leeuwin–Naturaliste Ridge to the west, and the Scott Coastal Plain to the south. The Blackwood Plateau is gently undulating in this area, and ranges in elevation from about 120 m Australian Height Datum (AHD) in the east to about 20 m AHD in the west where it merges with the Scott Coastal Plain. The area is drained by the Blackwood River whose meandering course is incised into the plateau. Tributaries of the Blackwood

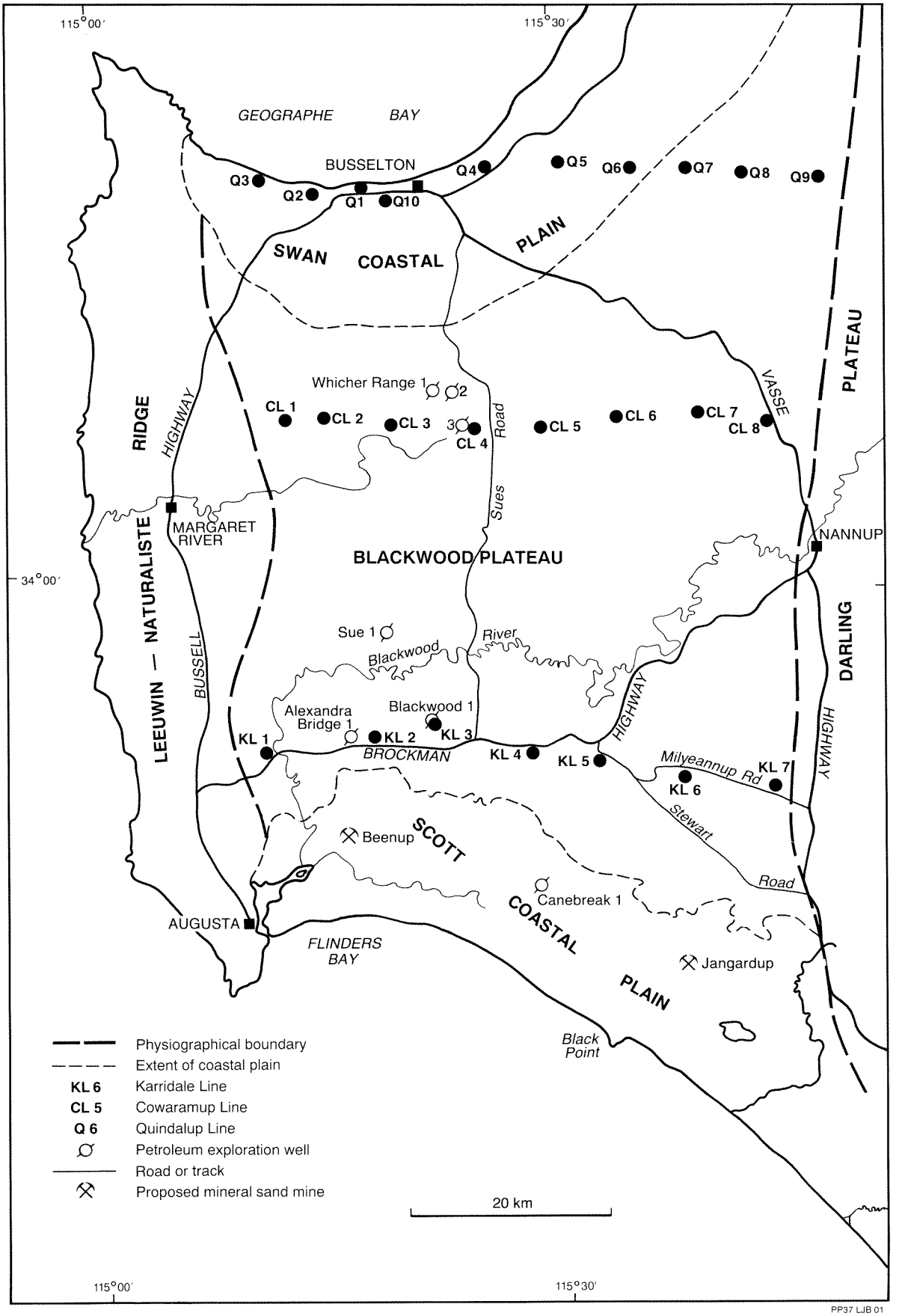

Figure 1. Location and physiography

River, and streams draining southwards to the Scott Coastal Plain, commonly contain swamps in areas of low gradient.

Most of the Blackwood Plateau lies within State Forest and is vegetated mainly by native jarrah–marri forest. The western part of the area has been cleared for agriculture and is used mainly as pasture for cattle raising.

Investigation program

The Karridale Line bores (prefix KL) were drilled between February 1989 and March 1990 by the Depart-ment of Mines Drilling Branch using a Midway–Skytop rig employing the mud-flush rotary drilling technique. At each site a deep exploratory bore (designated 'A') was drilled to between 655 and 1682 m depth. Shallow bores (designated 'B') were drilled at sites 2, 3, 4 and 7, and rig water-supply bores (designated 'W') were drilled at sites 1, 2, 5, 6 and 7. Bore depths range from 20 to 1682 m with an aggregate depth of 9441.6 m. A summary of drilling and bore information is given in Table 1.

Sludge samples were collected at 3 metre intervals from each of the deep exploratory bores for lithological logging, and are stored at the GSWA Core Library. Each deep hole was geophysically logged on completion of drilling, and sidewall cores taken from shale or siltstone beds for palynological analysis. All deep bores were cased and pressure cemented. Construction details of each bore are contained in the bore completion reports (Baddock, 1990).

Selected intervals in the deep exploratory bores were perforated with explosive charges over two or three 6-metre sections. With one interval perforated, the bores were developed by airlifting at the conclusion of which water samples were taken. The boreholes (except KL3) were then pumped to obtain an air-free water sample. After measuring the waterlevel, all remaining intervals were then perforated and developed. The initially perforated interval was then isolated, and in bores with three perforated intervals the middle interval was abandoned. The bottom and top intervals were then developed separately by airlifting and left for waterlevel monitoring.

The shallow bores (B) and water-supply bores (W) were completed with one observation interval, consisting of a 6-metre screen, and developed by airlifting.

Airlifted water samples collected from the deep and shallow bores were analysed by the Chemistry Centre. In a special sampling program, pumped air-free samples were obtained from both the deep bores and the water bores for carbon-14 dating and determination of dissolved iron and manganese.

Geology

Setting

The Karridale Line bores were drilled in the southern Perth Basin which, in this area, is a graben located between the Archaean Yilgarn Craton in the east and the Proterozoic Leeuwin Complex in the west. The southern Perth Basin is subdivided into two major structural units, the Bunbury Trough and the Vasse Shelf (Fig. 2). The Bunbury Trough is a deep graben which probably contains up to 10 000 metres of Phanerozoic sediments of Permian, Triassic, Jurassic, and Cretaceous age (Playford et al., 1976). The Vasse Shelf is an area of shallower basement which lies between the Bunbury Trough and the Leeuwin Complex and contains some 3000 metres of mostly Permian sedimentary rocks.

Rifting associated with the separation of south-western Australia from the rest of Gondwana during the Neocomian has resulted in an intensely block-faulted pre-Neocomian sequence. Basalt extrusion was associated with the breakup, and dolerite intrusions within the basin are considered to be comagmatic with the basalt (Playford et al., 1976). Above the Neocomian unconformity are comparatively undeformed Cretaceous sediments deposited during the tectonically quiet period following breakup. These sediments have been lateritized on the Blackwood Plateau, and are overlain by extensive thin Cainozoic deposits, especially on the coastal plains.

Stratigraphy

Formations intersected by the Karridale Line bores range in age from Early Permian to Quaternary. The stratigraphic succession is summarized in Table 2 and the formations are described below, in order, from oldest to youngest.

Sue Coal Measures

The Sue Coal Measures were intersected by KL1A and KL2A, and the formation has also been penetrated in this area by the petroleum-exploration wells Alexandra Bridge 1, Sue 1, Blackwood 1, and Canebreak 1. Extensive drilling of the Sue Coal Measures for coal has been conducted on the Vasse Shelf. The maximum thickness penetrated was 455 m in KL1A and the maximum known thickness of the Sue Coal Measures is 1838 m in Sue 1 (Williams and Nicholls, 1966).

The Sue Coal Measures unconformably overlie the Precambrian basement and are conformably overlain by the Sabina Sandstone. Over a limited area on the Vasse Shelf the Sue Coal Measures are unconformably overlain by the Warnbro Group (Ellis, 1985; Nolan, 1975), and occur close to the surface about 4 km southeast of KL1 (Utting, 1966).

The Sue Coal Measures consist of sequences of interbedded sandstone, siltstone, and coal. The sandstone constitutes 40–60% of the formation and normally comprises well-consolidated, fine- to medium-grained, poorly sorted to moderately well-sorted quartz. It is generally pale to dark grey-brown, or greenish (chloritic). Accessory minerals include feldspar, garnet, chlorite, pyrite and opaque heavy minerals, and the sandstone is occasionally calcareous. The siltstone is dark grey-brown to black, micaceous, carbonaceous and clayey, grading into

Table 1. Summary of bore completion data

Bore and interval	AMG Zone 50 East	AMG Zone 50 North	Construction Start	Construction Finish	Total depth (m bns)	Elevation NS (mAHD)	Elevation TOC (mAHD)	Perforated interval (m bns)	Formation	Potentiometric head (mAHD)	Salinity TDS (mg/L)	Airlift yield (m3/d)	Status
KL1A 1	332600	6217700	14.07.89	02.08.89	655.6	13.12	13.60	142 – 148	PTs	4.84	330	209	Obs
KL1A 2							13.80	216 – 222	Ps	5.67	2 060	61	Obs
KL1W			11.07.89	12.07.89	112	13.12	13.58	97.9 – 103.9	Tru	4.84	300	140	Obs
KL2A 1	341900	6219000	15.06.89	05.07.89	1 174.5	42.94	43.47	402 – 408	Tru	34.91	170	1 468	Obs
KL2A 2								600 – 606	Tru	34.60	190	979	Abd
KL2A 3							43.60	830 – 836	Tru	34.80	450	293	Obs
KL2B			06.07.89	06.07.89	20	42.94	43.61	17 – 20	Tru	36.78	120	14.4	Obs
KL2W			12.06.89	13.06.89	113.1	42.78	43.11	106 – 112	Tru	34.99	310	200	Obs
KL3A 1	348900	6219900	08.05.89	07.06.89	1 203	65.44	65.56	235 – 241	Juy	22.60	300	84	Obs
KL3A 2								760 – 766	Juy	19.69	380	5	Abd
KL3A 3							65.95	1 110 – 1 116	Juy	18.55	460	367	Obs
KL3B			08.06.89	08.06.89	37	65.33	66.27	31 – 37	Klw	44.97	720	20	Obs
KL4A 1	358100	6218700	30.08.89	25.09.89	1 207	84.64	85.14	279 – 285	Juy	27.88	390	839	Obs
KL4A 2								769 – 775	Juy	27.99	180	145	Abd
KL4A 3							85.50	1 160 – 1 166	Juy	21.24	500	380	Obs
KL4B			25.09.89	27.09.89	80.5	84.64	85.51	74 – 80	Klw	34.91	1 450	37	Obs
KL5A 1	364300	6218100	10.08.89	25.08.89	1 165.4	60.87	61.81	380 – 386	Juy	42.44	140	140	Obs
KL5A 2							61.53	622 – 628	Jlo	26.38	280	500	Obs
KL5W			20.02.89	21.02.89	33.8	60.65	61.20	27.8 – 33.8	Q	45.54	60	92	Obs
KL6A 1	373000	6216800	18.04.89	03.04.90	1 605	111.77	111.96	205 – 211	Juy	39.19	260	113	Obs
KL6A 2								685 – 691	Juy	39.33	220	259	Abd
KL6A 3							112.34	1 244 – 1 250	Jlo	27.91	260	35	Obs
KL6W			02.02.89	18.04.89	148.9	111.35	111.72	143 – 149	Juy	36.04	200	144	Obs
KL7A 1	382000	6216100	28.02.89	05.04.89	1 682	121.43	121.53	344 – 350	JKp	70.75	330	404	Obs
KL7A 2								994 – 1 000	Juy	37.98	180	457	Abd
KL7A 3							122.07	1 620 – 1 626	Juy	37.19	290	28	Obs
KL7B			29.03.89	30.03.89	35	121.37	122.01	28 – 34	Klw	107.70	240	26	Obs
KL7W			09.02.89	13.02.89	205.8	121.34	121.93	104 – 110	Klw	78.18	210	120	Obs

Notes: bns = below natural surface, AHD = Australian Height Datum, NS = natural surface, TOC = top of casing, Obs = monitored interval, Abd = abandoned interval, Q = Quaternary, Klw = Warnbro Group, JKp = Parmelia Formation, Juy = Yarragadee Formation, Jlo = Cockleshell Gully Formation, Tru = Lesueur Sandstone, PTs = Sabina Sandstone, Ps = Sue Coal Measures

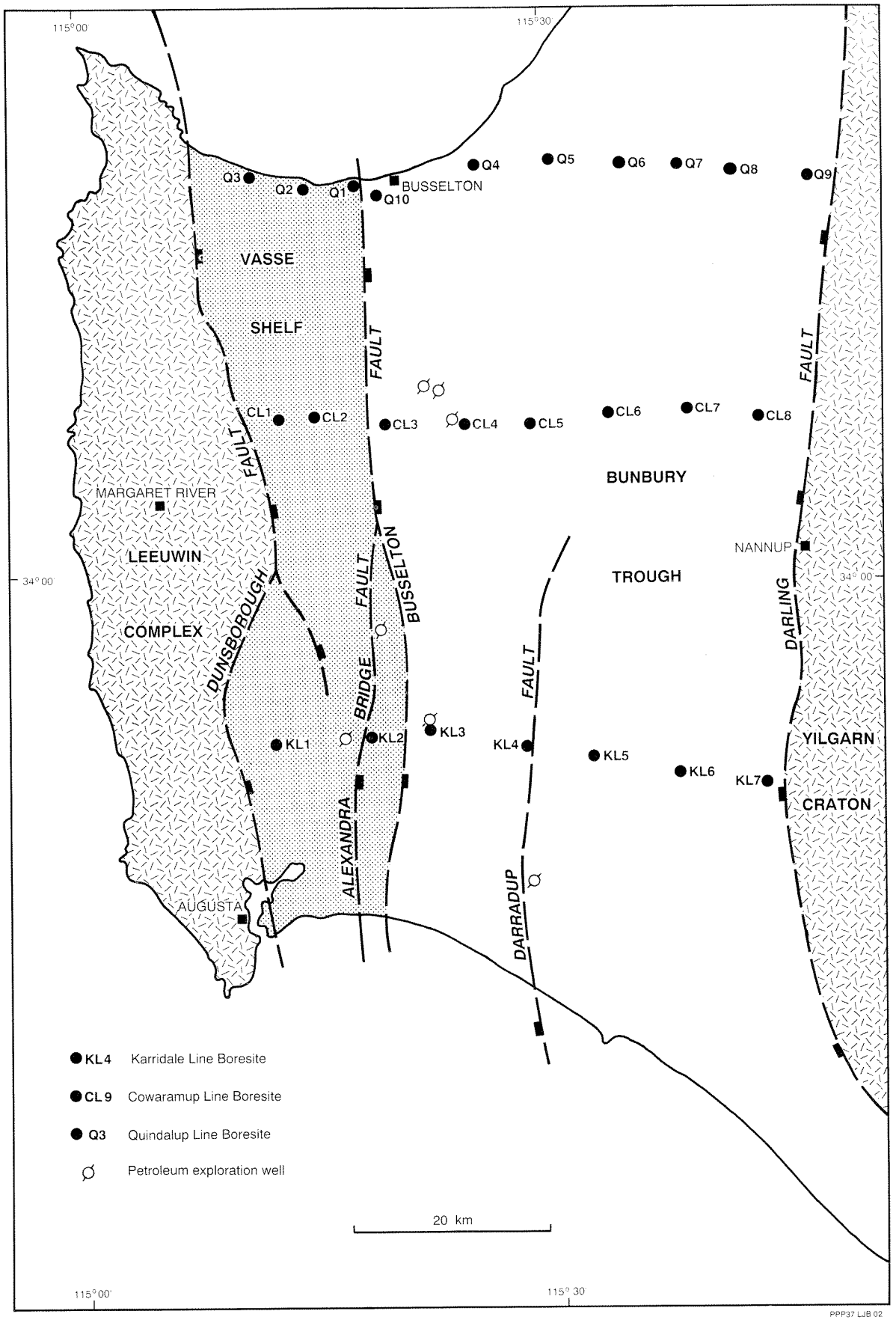

Figure 2. Structural units

Table 2. Stratigraphic table

Age		*Stratigraphic unit*	*Maximum thickness intersected (m)*	*Lithology*	*Aquifer potential*
QUATERNARY		Channel Sand	45	sand	minor aquifer
		UNCONFORMITY			
CRETACEOUS		Warnbro Group	235	shale, sand, coal silt	confining bed, minor aquifer
		DISCONFORMITY			
	Early	Bunbury Basalt	103	basalt	confining bed
		UNCONFORMITY			
JURASSIC		Parmelia Formation	217	sand, shale minor aquifer	confining bed,
	Late	Yarragadee Formation	1 202	sandstone, minor shale	major aquifer
	Early	Cockleshell Gully Formation	775	sandstone, siltstone, shale, claystone	major aquifer
TRIASSIC	Late	Lesueur Sandstone	860	sandstone	major aquifer
	Early	Sabina Sandstone	120	sandstone, claystone	minor aquifer
PERMIAN	Late	Sue Coal Measures	455	sandstone, coal	confining bed,
	Early			shale	minor aquifer

shale and low-grade coal. Seams of sub-bituminous coal occur through much of the formation.

Palynological assemblages from sidewall cores have been assigned to the *Dulhuntyispora parvithola* Assemblage and Upper Stage 5 Zone (Backhouse, 1989d, e) which are Late Permian in age. The formation was deposited in a continental environment, and rare acritarchs probably indicate brackish water conditions.

Sabina Sandstone

The Sabina Sandstone was intersected in KL1A and KL2A and has also been encountered in petroleum-exploration wells in the area. The type section is in Whicher Range 1 between 3666 and 3915 m. On the Karridale Line the maximum thickness encountered (in KL2A) was 120 m. The Sabina Sandstone is overlain, probably conformably, by the Lesueur Sandstone.

The Sabina Sandstone is a pale, grey-green to apple green, well-consolidated, commonly clayey, fine- to medium- and occasionally coarse-grained, moderately sorted quartz sand. Accessory minerals include feldspar, chlorite, pyrite, mica, garnet, and opaque heavy minerals. Minor interbedded grey shale and coal is present.

No palynomorphs were recovered from the formation, but the sandstone is believed to be predominantly a fluvial deposit of Late Permian to Early Triassic age (Playford et al., 1976).

Lesueur Sandstone

The Lesueur Sandstone was intersected in KL1A and KL2A. The maximum thickness intersected on the Karridale Line was 860 m in KL2A, and the maximum known thickness in the area is 1180 m intersected in Canebreak 1 (Lowry, 1982).

The Lesueur Sandstone is overlain conformably by the Cockleshell Gully Formation in the Bunbury Trough, and on the Vasse Shelf is unconformably overlain by the Warnbro Group.

The sandstone is characteristically weakly to well-consolidated, fine to very coarse-grained quartz sand with gravel, and is poorly to moderately sorted. The gravel and sand are pale brown and highly oxidized, commonly feldspathic and contain minor conglomerate and brown oxidized siltstone. Accessory carbonized wood, opaque heavy minerals, garnet, and mica are present.

Sidewall cores taken from the Lesueur Sandstone were barren of palynomorphs owing to both the scarcity of suitable lithology and its oxidized condition. The sandstone is believed to be a fluvial unit of Early Triassic age (Playford et al., 1976).

Cockleshell Gully Formation

The Cockleshell Gully Formation was intersected in KL5A and KL6A, with the thickest section of 775 m being encountered in KL5A. The formation may be as much as 1500 m thick in the Bunbury Trough, but the thickest known section is 1279 m intersected in Whicher Range 2 (Poynton and Hollams, 1980).

The Cockleshell Gully Formation is conformably overlain by the Yarragadee Formation, and unconformably overlain by the Bunbury Basalt in Canebreak 1 (Lowry, 1982). In some localities the formation may be unconformably overlain by the Warnbro Group.

The Cockleshell Gully Formation comprises two members; the Eneabba Member at the base, and the Cattamarra Member at the top. The Eneabba Member is a fine- to coarse-grained sandstone with characteristically multicoloured interbedded claystone and siltstone. In the Karridale Line bores, KL5A appears to have entered the Eneabba Member at about 950 m depth (-890 m AHD) and KL6A may have intersected the member from about 975 m depth (-864 m AHD). The sandstone is weakly to well consolidated, poorly sorted, pale grey-brown, occasionally kaolinitic and calcareous, and contains accessory feldspar, pyrite, garnet, and thin partings of coal. It contains brown, red, and green beds of siltstone and claystone. The member becomes more argillaceous eastwards from KL5A to KL6A.

The Cattamarra Member is a fine- to very coarse-grained sandstone with interbedded shale, siltstone, and narrow seams of sub-bituminous and shaly coal. In the Karridale Line bores the sandstone was generally well to poorly sorted, pale grey-brown, with interbedded dark grey, carbonaceous and micaceous shale, and siltstone. Accessory minerals include feldspar, kaolin clay, pyrite, garnet, chlorite, and opaque heavy minerals.

Palynological assemblages from sidewall-core samples include the *Corollina torosa, Callialasporites turbatus* and *Dictyotosporites complex* Miospore zones (Backhouse, 1989f, 1990a). These indicate an Early to Middle Jurassic age (Hettangian to Bathonian) for the formation, which is believed to be of fluvial origin. The lithological contact between the Cockleshell Gully Formation and the Yarragadee Formation is within the *D. complex* Miospore Zone, and the presence of reworked Permian miospores in KL5A (411 m) indicates erosion of Permian sediments during deposition of the formation.

Yarragadee Formation

The Yarragadee Formation was intersected in bores KL3A through to KL7A in the Bunbury Trough, but is absent on the Vasse Shelf. The maximum thickness intersected was 1202 m (base not reached) in KL7A.

The Yarragadee Formation is conformably overlain by the Parmelia Formation, or unconformably overlain by the Bunbury Basalt, Warnbro Group, or Quaternary deposits (KL5) to the south of the Karridale Line in the eastern part of the Scott Coastal Plain (Sharples, 1981).

The formation is an interbedded sequence of sandstone and siltstone with lesser amounts of shale, claystone, and conglomerate. Sandstone is the predominant lithology and makes up 70–90% of the formation, except in KL4A where the Yarragadee Formation is slightly more argillaceous in the middle section. The sandstone is weakly to moderately consolidated, grey, and pale brown. It is composed of poorly sorted, fine- to very coarse-grained quartz and is ferruginous in part, especially in the lower section. There are some seams of shaly coal, and accessory minerals include feldspar, kaolin, mica, pyrite, garnet, opaque heavy minerals, and chlorite. Argillaceous sediments are generally dark grey or grey-brown, micaceous and carbonaceous in the upper section, and in the lower part of the formation pale green and oxidized brown, yellow-brown, and red.

Sidewall core samples taken from the formation contained palynomorphs from the *Murospora florida, Contignisporites cooksoniae,* and *Dictyotosporites complex* assemblage zones, which are of Late Jurassic age. The formation is believed to be a continental fluvial deposit (Backhouse, 1989a,b,c,f, 1990a,b). Reworked very late Permian palynomorphs are present in KL4A (534.5 m), indicating that erosion of Permian sediments continued into the Late Jurassic (Backhouse, 1990a).

Parmelia Formation

The Parmelia Formation was intersected in KL4A and KL7A, with the thicker section of 217 m in KL7A. The Parmelia Formation was first encountered onshore in the southern Perth Basin in the Cowaramup Line (Appleyard, 1991), where the maximum thickness intersected was 70 m.

The formation is unconformably overlain by the Bunbury Basalt, or by the Warnbro Group. It consists of poorly consolidated clayey sandstone, siltstone, and shale. The siltstone and shale are carbonaceous, dark grey-brown to pale yellow-brown, and contain minor sub-bituminous coal. The sandstone is fine to coarse grained, and comprises moderately to poorly sorted quartz sand. Accessory minerals include feldspar, garnet, chlorite, and opaque heavy minerals.

Palynomorph assemblages from sidewall-core samples belong to the *Biretisporites eneabbaensis* Miospore Zone, which is Late Tithonian to Berriasian age (very Late Jurassic to very Early Cretaceous). The assemblages indicate a continental environment of deposition (Backhouse, 1989a, 1990a), compared with a non-marine

to shallow marine environment in the Cowaramup Line (Backhouse, 1988a,b).

Bunbury Basalt

The Bunbury Basalt was penetrated in KL6A where it is 103 m thick, and in KL7A where it is 28 m thick. The basalt is present discontinuously in the subsurface of the southern Perth Basin (Burgess, 1978), and outcrops at several localities between Bunbury and Black Point. The thickest section intersected in the subsurface is 106 m in Canebreak 1 (Lowry, 1982). The Bunbury Basalt is disconformably overlain by the Warnbro Group and locally is unconformably overlain by Quaternary sediments.

The basalt is an aphanitic to porphyritic tholeiite, is locally vesicular, and displays columnar jointing in outcrop (Trendall, 1963; Playford et al., 1976; Burgess, 1978). In the Karridale Line the basalt is predominantly fresh and lacks the weathered margins encountered elsewhere.

The basalt, which McDougall and Wellman (1976) found to be at least 90 million years old, is considered to be Neocomian in age (Playford et al., 1976), and a dolerite sill thought to be comagmatic with the Bunbury Basalt in Sue 1 gave a K–Ar age of 136 ± 3 Ma (Williams and Nicholls, 1966). The basalt probably represents one or more flows that, prior to deposition of the Warnbro Group, spread along valleys cut into the underlying rocks. Extrusion may have occurred along north-trending faults within the Perth Basin. The distribution of basalt is more extensive than indicated by aeromagnetic data.

Warnbro Group

The Warnbro Group was penetrated at all sites on the Karridale Line except KL2 and KL5. The unit becomes thicker towards the Darling Fault and the thickest section intersected was 235 m in KL7A. The group is widely distributed in the southern Perth Basin and is present over most of the Blackwood Plateau. The Warnbro Group reaches a maximum known thickness in the area of 250 m in Cowaramup Line 2A (Appleyard, 1991) but possibly exceeds 500 m in Quindalup Line 10A (Wharton, 1981). The Warnbro Group is lateritized on the Blackwood Plateau and is unconformably overlain by Quaternary and Tertiary deposits on the Scott Coastal Plain.

The unit consists of interbedded, poorly consolidated claystone, siltstone, sandstone, and coal. Argillaceous sediments dominate the upper section of the unit and are dark brown-grey, carbonaceous, and micaceous with associated thin coal seams. In the Karridale Line bores, sandstone is dominant in the lower section of the group, and consists of light-grey, fine- to very coarse-grained, poorly sorted quartz. Accessory minerals include feldspar, kaolin, mica, pyrite, chlorite, garnet, and opaque heavy minerals. In KL1 high concentrations of non-radioactive heavy minerals are present in the lower section of the unit, mainly between 48 and 87 m depth.

Palynological assemblages from sidewall cores taken from this unit belong to the *Balmeiopsis limbata* Miospore Zone, and range in age from Valanginian to Early Aptian within the Early Cretaceous (Backhouse, 1989a,e, 1990a). The environment of deposition is continental, but material from bores on the Scott Coastal Plain to the south show evidence of shallow-marine conditions (Backhouse, 1990c,d). Evidence for extensive reworking of Permian miospores was seen in core samples from 61 and 91 m in KL7A, indicating continuing erosion of Permian sediments during the Early Cretaceous.

Laterite and alluvium

Laterite is developed widely on the Blackwood Plateau, where it is dissected by stream and river channels. It consists of a pisolitic gravel, usually up to about 5 m thick, underlain by as much as 40 m of oxidized sand and mottled clay derived from the weathering in situ of Mesozoic and Palaeozoic sedimentary rocks. Laterite is present at the surface at each site on the Karridale Line. The laterite is considered to range from Tertiary to Quaternary age and may still be forming today (Lowry, 1965).

Alluvial sands of presumed Quaternary age were encountered at KL5. They are 45 m thick and have infilled a drainage channel cut into the Yarragadee Formation. The sand is pale brown, consists of fine to gravel-sized quartz sand with some feldspar, kaolin clay, and minor heavy minerals. The base of the channel is marked by basalt pebbles.

Structure

The inferred geological structure along the Karridale Line is shown in Figure 3. The section extends across the two major units in the Perth Basin: the Vasse Shelf bounded by the Busselton and Dunsborough Faults, and the Bunbury Trough bounded by the Busselton and Darling Faults.

On the Vasse Shelf the predominant unit preserved is the Permian Sue Coal Measures. The Lesueur and Sabina Sandstones are present on both sides of the shelf and are separated by a structural high in the Sue Coal Measures. On the western edge of the shelf a preserved section of Lesueur Sandstone dips towards the Dunsborough Fault where it abuts Proterozoic crystalline rocks. Seismic data in this area show complex faulting, including east-trending faults and step faulting.

Two faulted blocks are present on the eastern side of the Vasse Shelf. The block west of the Alexandra Bridge Fault has about 300 m of Lesueur Sandstone, while in the block west of the Busselton Fault 860 m of Lesueur Sandstone (KL2A) is preserved.

The Bunbury Trough is a deep graben between the Busselton Fault,with a displacement of about 1500 m, and the Darling Fault, which has a displacement of about 9000 m. Drilling encountered sediments of Triassic, Jurassic, and Cretaceous age which dip gently and thicken toward the east. The Jurassic formations are bounded by the Busselton Fault in the west, where they abut Permian and Triassic sediments on the Vasse Shelf. All formations

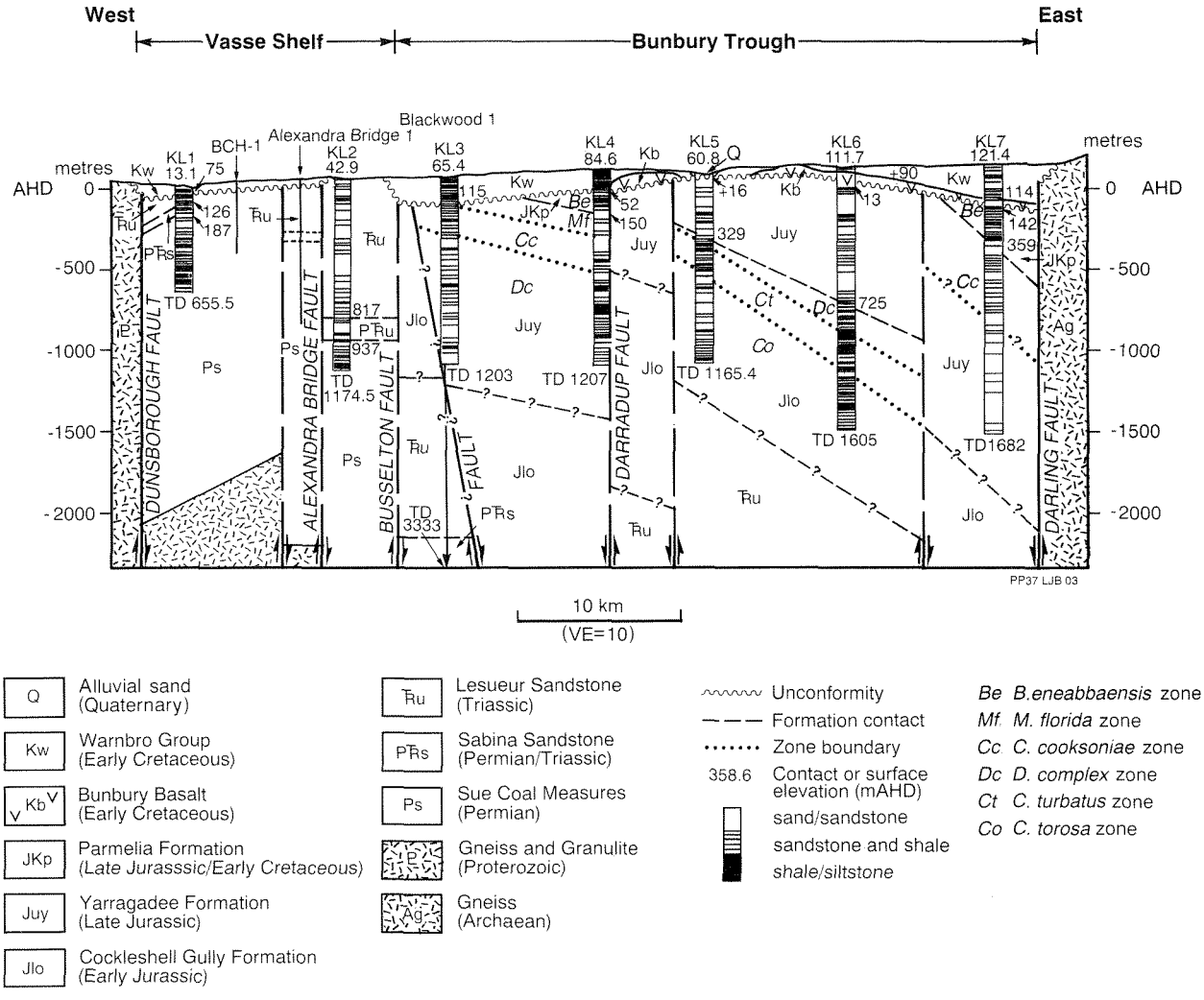

Figure 3. Geological section

abut the Archaean crystalline rocks of the Yilgarn Craton along the Darling Fault.

A number of north-trending faults cut the Bunbury Trough. Of these, the Darradup Fault, with a displacement of about 500 m, is the most significant on the Karridale Line. Some east-west faults are evident on seismic sections. In Blackwood 1, at the same site as KL3, the Cockleshell Gully Formation is absent and the Yarragadee Formation is apparently in faulted contact with the Lesueur Sandstone. The postulated fault, which would have a throw of about 1000 m, is not apparent on seismic data.

The Warnbro Group is draped over all the pre-Neocomian sediments and seems to be unfaulted, although it is absent at KL2 and KL5. Thickening of the Warnbro Group towards the Darling Fault in the eastern part of the basin is probably due to continuing subsidence or compaction of the underlying formations during deposition.

Hydrogeology

Aquifer systems

There are a number of structurally controlled regional meteoric flow systems in the pre-Neocomian sediments, and several local groundwater flow systems in the Warnbro Group on the Karridale Line (Fig. 4). Downward vertical head gradients occur along the entire Karridale Line, except locally at KL1 where the potentiometric head within the Sue Coal Measures is greater than in the overlying Lesueur Sandstone. Areas around KL2 and KL5, where the Warnbro Group is absent, appear to be groundwater recharge areas. There is also probably some downward leakage from the Warnbro Group into underlying aquifers. Upward heads and artesian flows have been encountered from the Lesueur Sandstone in the Blackwood River valley to the north of KL1 and Alexandra Bridge 1, and from the Yarragadee Formation

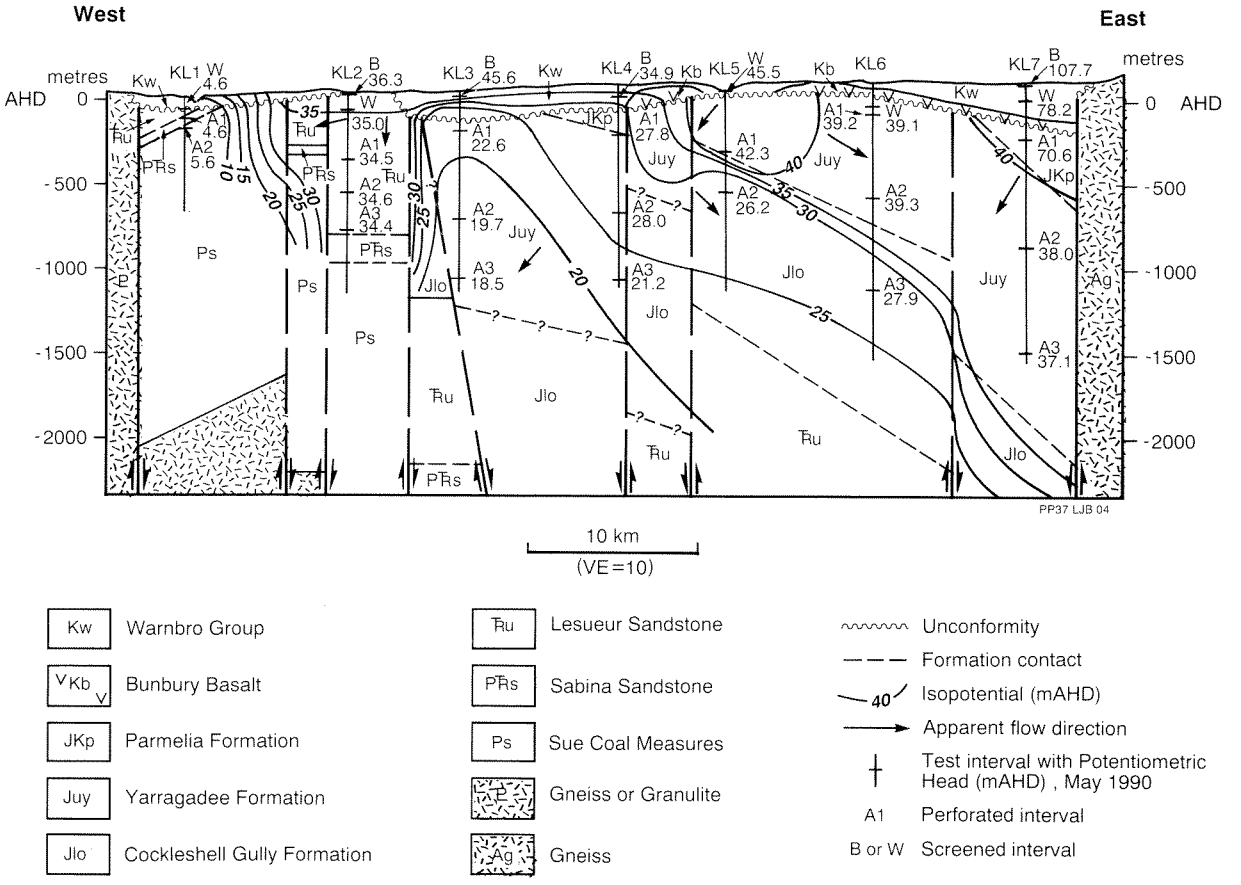

Figure 4. Isopotentials and apparent groundwater flow directions

and Lesueur Sandstone on the Scott Coastal Plain to the south (Fig. 5).

In the Bunbury Trough groundwater movement within the Jurassic formations forms a regional flow system, with an irregular base controlled by the presence of shales and faults which act as local barriers to groundwater movement. In the eastern part of the Bunbury Trough the groundwater flow system in the Yarragadee Formation reaches depths greater than 1600 m. However, to the west, thick argillaceous units within the Cockleshell Gully Formation limit the depth reached by the flow system. There appears to be hydraulic continuity of the fresh groundwater across faults, allowing groundwater movement between abutting formations, notably from the Yarragadee Formation into the Cockleshell Gully Formation east of the Darradup Fault. Thick argillaceous layers within the Cockleshell Gully formation would otherwise ensure than contained water is brackish to saline. The faults appear to become more effective barriers to groundwater movement with increasing depth.

On the Vasse Shelf, two flow systems separated by a structural high in the Sue Coal Measures occur in the Lesueur Sandstone. On the eastern part of the shelf there is a major groundwater flow system (eastern Lesueur Sandstone flow system) in which potentiometric heads are over 10 metres higher than in the Yarragadee flow system in the Yarragadee Formation to the east (Fig. 4). The Busselton Fault may be a partial hydraulic barrier between the two flow systems — a feature noted on the Cowaramup Borehole Line (Appleyard, 1991) — or a wedge of Cockleshell Gully Formation may separate the two flow systems. A smaller groundwater flow system within the Lesueur Sandstone on the western side of the Vasse Shelf (western Lesueur Sandstone flow system) has a potentiometric head about 30 metres lower than that in the eastern Lesueur Sandstone flow system (Fig. 4).

Aquifers

Warnbro Group

The Warnbro Group is a multilayered aquifer composed of shale and sandstone layers. Along the Karridale Line the upper part of the Warnbro Group is predominantly shale, whereas the lower part contains mainly sandstone.

Groundwater recharge is by direct rainfall infiltration through the overlying laterite. There is a seasonal potentiometric-head fluctuation of about 2 metres in shallow beds, and less in deeper beds. Groundwater is normally confined or semi-confined, and the watertable and shallow groundwater flow are often controlled by topography, forming local flow systems discharging to creeks and swamps (Appleyard, 1991). Groundwater leakage to underlying formations also occurs.

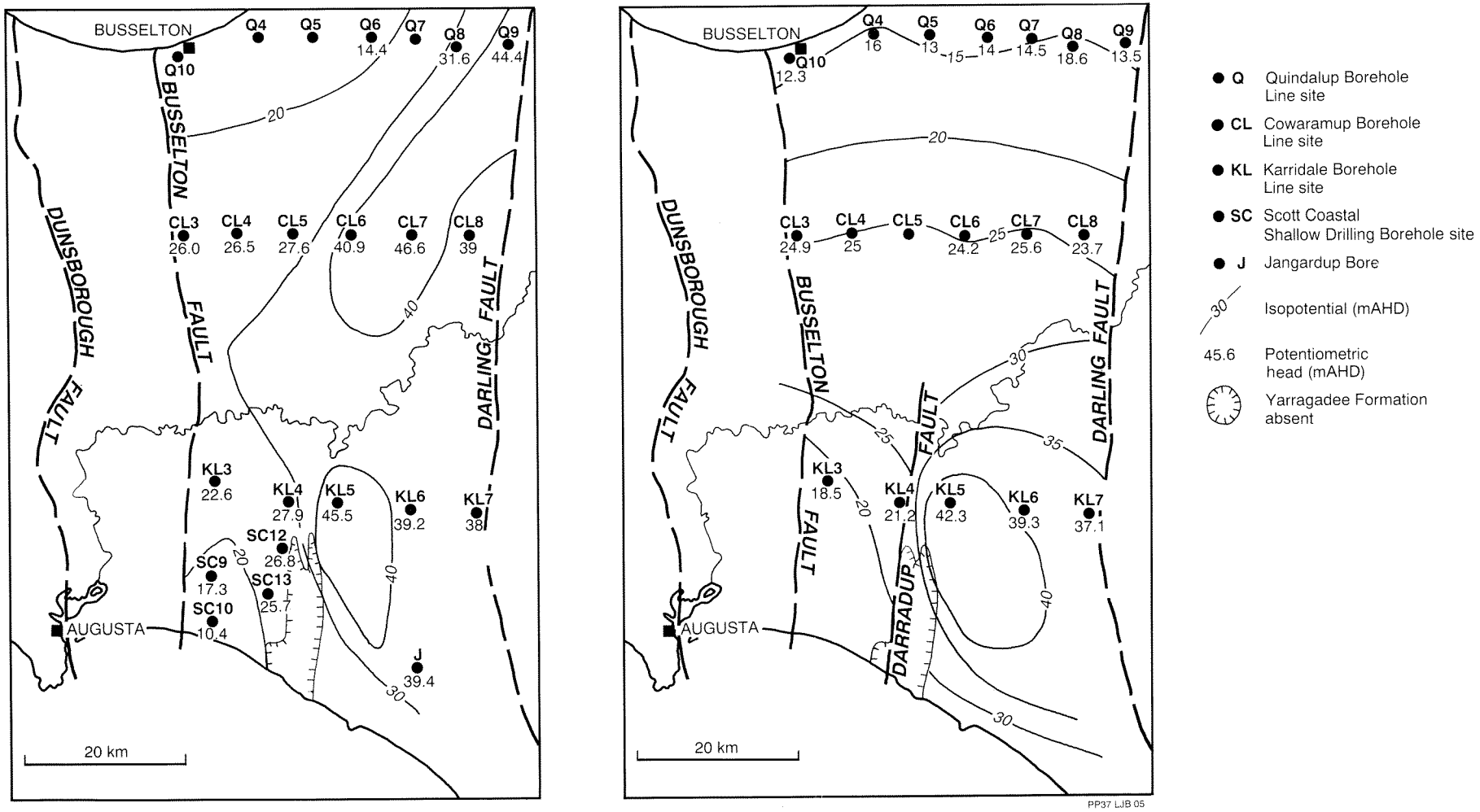

a) Top of Yarragadee Formation.

b) Bottom of Yarragadee Formation

Figure 5. Yarragadee Formation — regional isopotentials

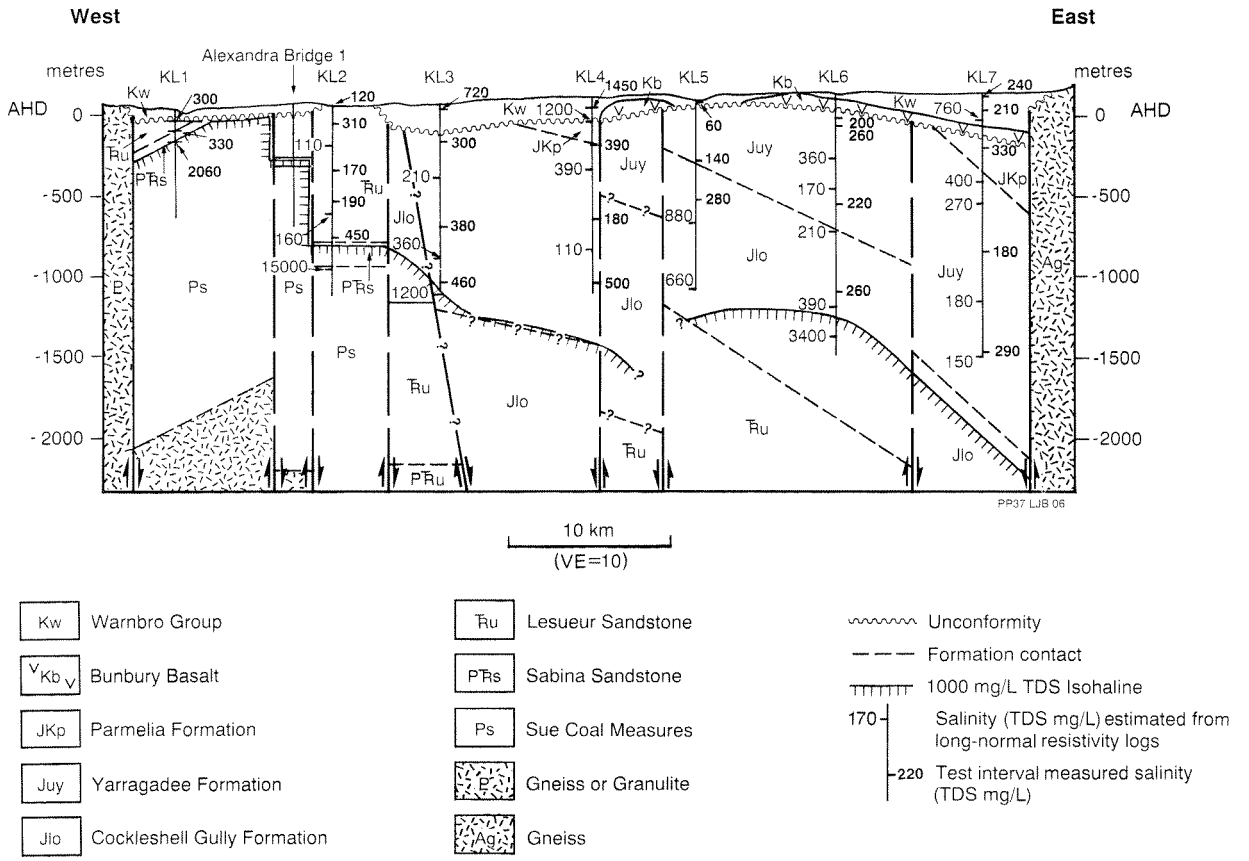

Figure 6. Groundwater salinity

The groundwater salinity in the Warnbro Group ranges from 210 mg/L total dissolved solids (TDS) to 1450 mg/L in the Karridale Line bores (Fig. 6). Groundwater from the Warnbro Group is typically high in iron and manganese, but only one sample from the formation was analysed for these (KL7W) and had values of 26 mg/L and 0.33 mg/L respectively. Boron and fluoride were 0.1 mg/L in all samples, except KL7B with 0.6 mg/L boron, and KL7W with 0.5 mg/L boron and 0.3 mg/L fluoride.

Groundwater pH was acidic in all samples, and one sample from KL4B was highly acidic with a pH of 2.9.

On the western side of the basin, groundwater from the Warnbro Group is used for watering stock. Small to moderate yields of groundwater, ranging to 20 to 120 m^3/day, were obtained from the Karridale Line bores by airlifting. The Warnbro Group is capable of further development for local domestic and stock water supplies.

Parmelia Formation

The Parmelia Formation consists of poorly con-solidated, interbedded siltstone, shale, and clayey sandstone.

Groundwater in the formation is confined and recharged by downward leakage from the Warnbro Group where the intervening Bunbury Basalt is absent. The vertical hydraulic conductivity of the Parmelia Formation is low as a result of its argillaceous nature, and it probably behaves as a semi-confining bed to the underlying Yarragadee Formation.

On the Karridale Line the only interval tested in the formation was KL7A1 in which groundwater had a salinity of 330 mg/L. The resistivity log of KL7A suggests that groundwater salinity is up to about 1000 mg/L in the Parmelia Formation.

Analysis of a groundwater sample from the Parmelia Formation yielded values for boron and fluoride of 0.6 mg/L and 0.2 mg/L respectively, and a pH of 8.1. The concentrations of iron and manganese, although not determined, are probably high.

Yarragadee Formation

The Yarragadee Formation is the largest and most extensive aquifer in the region. Sandstone generally constitutes 70–90% of the formation, which is at least 1200 m thick.

Along the Karridale Line, groundwater within the Yarragadee Formation is confined by the overlying Warnbro Group and Parmelia Formation, except around Karridale Line 5 where it is unconfined. The potentiometric-head distribution on the Karridale Line indicates recharge around KL5 (Fig. 3). Some recharge

to the formation also occurs by leakage from the overlying Warnbro Group and Parmelia Formation. A major source of groundwater recharge to the formation may be on the eastern Scott Coastal Plain inland from the coast.

Regional isopotentials for the top and base of the Yarragadee Formation are given in Figure 5. The isopotentials indicate that south of the Karridale Line groundwater probably discharges along the Scott Coastal Plain and offshore to the Southern Ocean. Between KL5 and KL7, east of the Darradup Fault, groundwater flow is apparently northwards.

The groundwater salinity in the Yarragadee Formation ranges between 180 mg/L and 500 mg/L. The entire formation in this area, which extends to a total depth of more than 1682 m in KL7A, appears to contain fresh groundwater.

All groundwater samples from the Yarragadee Formation have very high dissolved-iron concentrations, ranging from 14 mg/L to 33 mg/L, indicating high iron mobility. Manganese values are typically high, ranging from 0.11 mg/L to 0.84 mg/L. Boron is usually 0.1 mg/L or less, but values up to 0.4 mg/L were recorded, and two samples contained 0.7 mg/L (KL7A2 and 3). Fluoride is typically 0.1 mg/L, with some values up to 0.4 mg/L: one sample contained 1.0 mg/L (KL3A3).

Groundwater samples from the Yarragadee Formation east of the Darradup Fault (KL5, 6 and 7) were all acidic, with pH values from 5.3 to 6.5. However, west of the Darradup Fault (KL3 and 4) the groundwater was usually slightly alkaline, ranging from pH 7.6 to 8.8, with one acidic sample (6.3).

The Yarragadee Formation is the most extensive aquifer in the region and contains a large volume of fresh groundwater in storage. The only users of groundwater from the Yarragadee Formation in the southern end of the Perth Basin are a few farms on the Scott Coastal Plain and the Jangardup mineral-sand mine. The groundwater resources in the formation are capable of extensive development.

Cockleshell Gully Formation

The Cockleshell Gully Formation is composed of interbedded sandstone, siltstone, shale, and claystone. The sandstone is usually lithified and constitutes 40–65% of the formation. The formation is over 800 m thick on the Karridale Line.

Groundwater in the formation is recharged by downward leakage from the Yarragadee Formation, but most of the recharge may be across faulted contacts with the Yarragadee Formation. To the south of the Karridale Line, recharge to the formation may occur through overlying Warnbro Group or Quaternary sediments. Groundwater in the formation is confined, and downward head gradients are present throughout. There is probably some downward groundwater discharge to the underlying Lesueur Sandstone. The direction of groundwater movement is probably southward, in hydraulic connection with south-flowing groundwater in the Yarragadee Formation west of the Darradup Fault.

Groundwater salinity is generally less than 300 mg/L in the upper part of the Cockleshell Gully Formation east of the Darradup Fault, and two tested intervals recorded salinities of 280 mg/L (KL5A2) and 260 mg/L (KL6A3). Karridale Line 6A intersected brackish groundwater at a depth of 1420 m depth where salinity is estimated from the resistivity log to be 3400 mg/L. It is therefore likely that groundwater in the Cockleshell Gully Formation west of the Darradup Fault is saline (Fig. 6).

The two groundwater samples from the Cockleshell Gully Formation had boron concentrations of 0.2 mg/L and 0.3 mg/L, and fluoride concentrations of 0.3 mg/L and 0.4 mg/L. Bicarbonate was the dominant anion in both samples, with values of 144 mg/L (KL5A2) and 135 mg/L (KL6A3), and pH values were determined at 8.0 and 7.3. Iron and manganese were not determined.

The Cockleshell Gully Formation is a major aquifer which contains a large fresh-groundwater resource in the central section of the Bunbury Trough. Water from the aquifer is not utilized in this part of the basin.

Lesueur Sandstone

The Lesueur Sandstone is a major aquifer composed predominantly of sandstone, and containing minor siltstone and claystone.

On the Vasse Shelf, groundwater in the Lesueur Sandstone is recharged directly by rainfall or by downward infiltration through the overlying Warnbro Group. Groundwater flow is towards the south.

In much of the Bunbury Trough, groundwater in the Lesueur Sandstone probably has a high salinity due to its depth of burial and isolation from groundwater circulation. However, resistivity logging indicated low-salinity groundwater within the sandstone between 447 m and 1650 m in Canebreak 1, just east of the Darradup Fault (Lowry, 1982). It is estimated that whilst groundwater salinity is less than 500 mg/L in most of the aquifer, it may approach 1000 mg/L near the base. The formation is probably recharged by groundwater movement across faulted contacts with the Yarragadee Formation or Cockleshell Gully Formation. Groundwater in the sandstone probably discharges into the Southern Ocean.

On the Vasse Shelf, groundwater salinity in Karridale Line bores ranges from 120 mg/L (KL2B) to 450 mg/L (KL2A3). The base of the fresh groundwater generally coincides with the contact with Sabina Sandstone.

Groundwater samples from the Lesueur Sandstone contained dissolved iron ranging from 1.2 mg/L to 39 mg/L in Karridale Line bores, and manganese ranging from less than 0.02 mg/L to 0.37 mg/L. Boron values varied from less than 0.1 mg/L to 0.4 mg/L, and fluoride content was 0.1 mg/L or less, except for two samples (KL1W and KL2A3) which contained 0.7 mg/L. Bicarbonate was the dominant anion in one sample (KL1W), with a value of 150 mg/L, and another sample (KL2A3)

Table 3. Chemical analyses

Bore	*GSWA No.*	*pH*	*C (a)*	*TH (b)*	*TA (c)*	*TDS (d)*	*Ca*	*Mg*	*Na*	*K*	*HCO_3*	*CO_3*	*Cl*	*SO_4*	*SiO_2*	*B*	*F*	*Fe*	*Mn*
											(mg/L)								
KL1A1	103814	(e)7.8	57.1	21	101	330	5	2	109	7	123	<2	111	14	17	0.1	0.4	0.64	0.05
KL1A2	103815	8.6	36.7	199	85	2 060	55	15	675	16	94	5	1 000	229	16	0.6	0.3	-	-
KL1W	103811	(e)6.9	53.7	59	123	300	12	7	87	9	150	<2	88	14	12	0.2	0.7	1.8	0.06
KL2A1	103802	5.9	32.3	31	4	170	1	7	50	1	5	<2	83	15	12	0.3	0.1	-	-
KL2A2	103803	(e)5.8	40.4	34	7	190	2	7	54	2	8	<2	100	12	10	0.2	<0.1	39	0.37
KL2A3	103804	7.7	83.6	26	107	450	4	4	146	22	131	<2	173	24	15	0.4	0.7	-	-
KL2B	103812	6.1	20.6	20	8	120	3	3	28	3	10	<2	42	20	5	<0.1	<0.1	-	-
KL2W	103801	(e)4.4	61.5	51	3	310	4	10	95	<1	4	<2	172	16	7	0.1	<0.1	1.2	<0.02
KL3A1	103817	7.6	59	59	56	300	12	7	77	17	68	<2	129	16	4	0.1	0.3	-	-
KL3A2	103818	8.8	68.2	53	173	380	13	5	92	50	177	17	95	13	2	<0.1	<0.1	-	-
KL3A3	103819	8.6	83.3	40	140	460	6	6	144	22	156	7	159	20	19	0.4	1.0	-	-
KL3B	94159	5.9	140	96	11	720	4	21	231	6	14	<2	393	33	27	0.1	0.1	-	-
KL4A1	103823	7.8	73.8	121	110	390	27	13	75	32	134	<2	140	24	14	0.1	0.2	-	-
KL4A2	103824	(e)6.3	29.6	21	44	180	2	4	35	22	54	<2	47	20	18	<0.1	0.1	25	0.43
KL4A3	103825	7.8	91.3	87	130	500	10	15	123	41	158	<2	175	23	17	0.3	0.4	-	-
KL4B	103827	2.9	326	297	<2	1 450	30	54	403	14	<2	<2	871	41	32	0.1	0.1	-	-
KL5A1	103821	(e)5.3	25.4	21	19	140	2	4	37	3	23	<2	64	4	9	<0.1	<0.1	20	0.14
KL5A2	103820	8.0	48.8	31	118	280	4	5	76	24	144	<2	70	18	15	0.2	0.3	-	-
KL5W	103822	(e)4.2	10.8	8	11	60	<1	2	16	<1	13	<2	26	2	5	<0.1	<0.1	0.36	0.02
KL6A1	103839	5.8	48.7	36	7	260	3	7	72	10	8	<2	132	12	16	<0.1	0.1	-	-
KL6A2	103840	(e)5.7	39	26	28	220	2	5	60	9	34	<2	95	8	24	<0.1	0.1	14	0.11
KL6A3	103841	7.3	46.4	22	111	260	4	3	76	19	135	<2	68	12	11	0.3	0.4	-	-
KL6W	103846	6.4	36.8	24	7	200	3	4	54	8	8	<2	97	11	18	0.1	0.1	-	-
KL7A1	94155	8.1	57.5	139	156	330	36	12	61	9	190	<2	80	13	25	0.6	0.2	-	-
KL7A2	94153	6.1	34.3	30	12	180	2	6	42	11	15	<2	82	12	17	0.7	0.2	33	0.84
KL7A3	94156	6.5	57.9	68	15	290	6	13	59	30	18	<2	156	7	7	0.7	0.1	-	-
KL7B	94157	6.3	42.4	39	12	230	4	7	66	5	15	<2	108	16	18	0.6	0.1	-	-
KL7W	94150	(e)5.6	38.2	31	31	210	1	7	51	8	38	<2	83	13	28	0.5	0.3	26	0.33

Notes: (a) conductivity (mS/m at 25°C), (b) total hardness (as $CaCO_3$), (c) total alkalinity (as $CaCO_3$), (d) total dissolved solids (by calculation), (e) field pH measurement (otherwise laboratory)

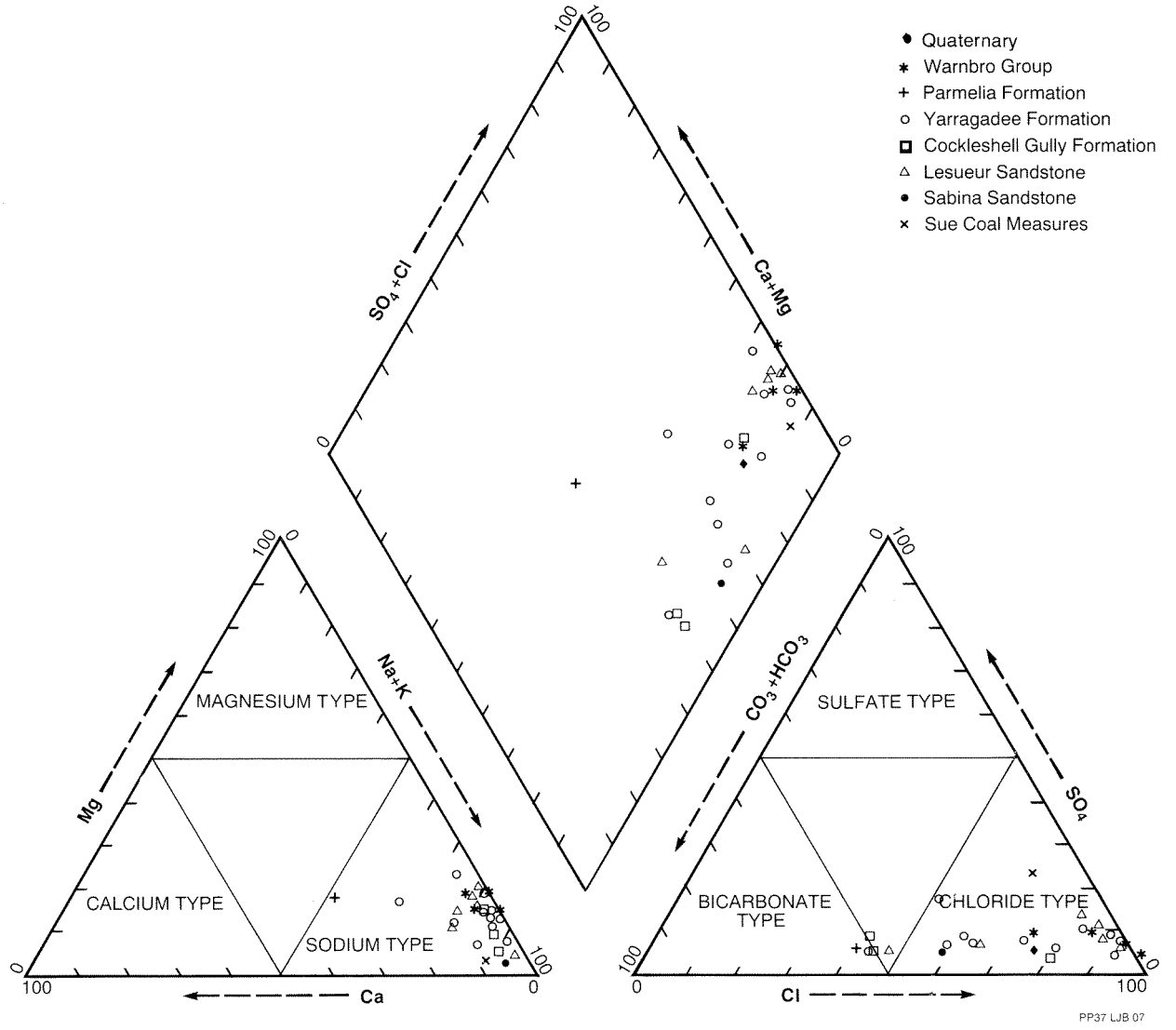

Figure 7. Piper trilinear diagram

contained 131 mg/L bicarbonate. Groundwater from the Lesueur Sandstone was acidic, with pH ranging from 4.4 to 6.9 in all samples except the deepest from KL2A3 (830–836 m), which was slightly alkaline (7.7).

Groundwater from the formation is used only for stock. However, at the proposed Beenup mineral-sand mine on the Scott Coastal Plain, it is intended that this groundwater be utilized for mining and plant operations. A bore in the Lesueur Sandstone was also drilled 6.5 km northeast of Augusta for a future town-water supply. The Lesueur Sandstone is a major aquifer on the eastern Vasse Shelf, containing very large fresh groundwater resources. On the western Vasse Shelf, the aquifer is less extensive but contains significant resources adjacent to the groundwater-deficient Leeuwin Complex.

Sue Coal Measures and Sabina Sandstone

The Sue Coal Measures are composed of sandstone, siltstone, shale, and coal, while the Sabina Sandstone is a clayey sandstone.

In the Karridale Line area there appears to be little recharge of groundwater to the Sabina Sandstone and Sue Coal Measures. Any groundwater recharge is by downward movement from overlying sediments or across fault zones, and direct recharge from rainfall where the units are present at the surface.

Groundwater salinity is high in both formations. Resistivity logs indicated brackish to saline groundwater in the two Karridale Line boreholes (KL1A and KL2A) that intersected part of the Sue Coal Measures. The only

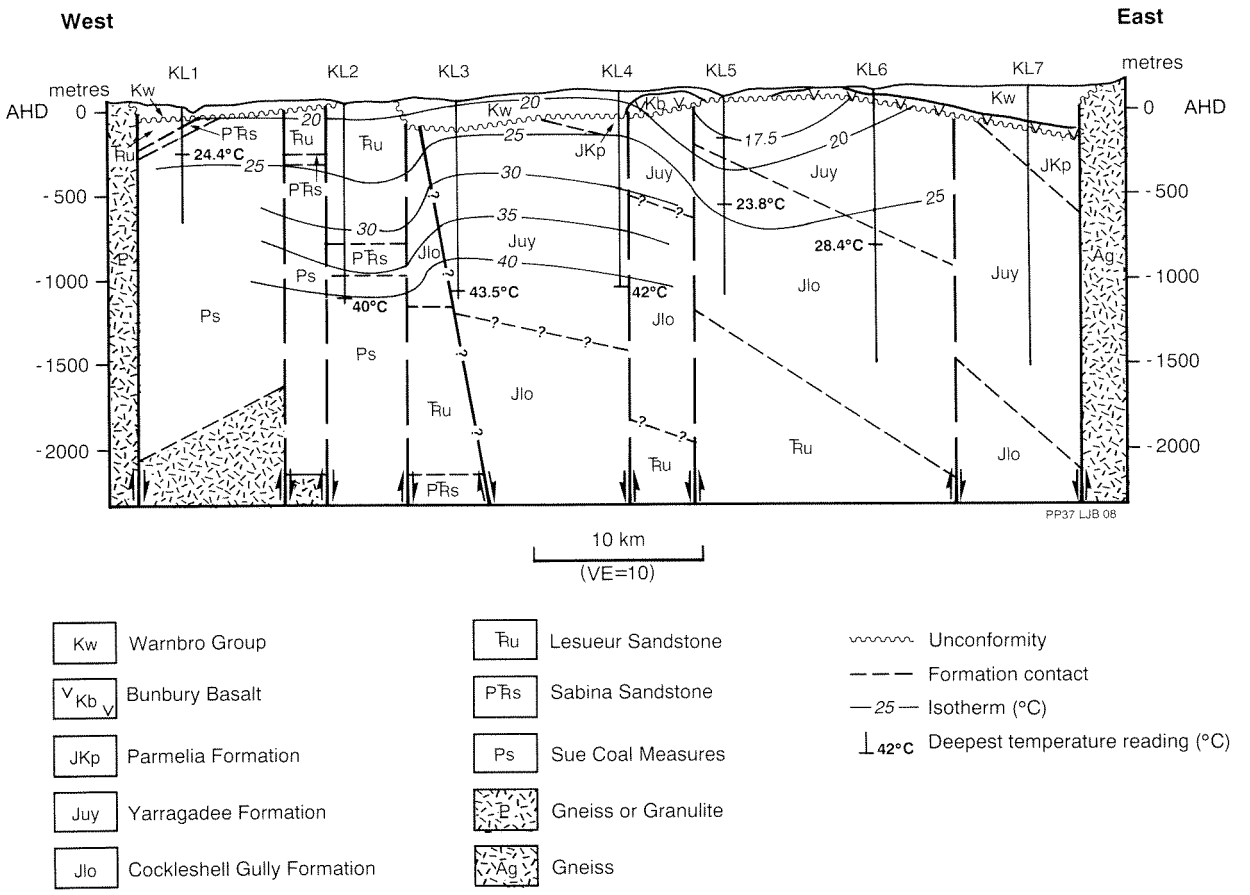

Figure 8. Isotherms

tested interval in the Sue Coal Measures (KL1A2) yielded water with a salinity of 2060 mg/L and contained 0.6 mg/L boron and 0.3 mg/L fluoride The sulfate value was high (229 mg/L), probably due to oxidation of sulfide-rich coal seams. Only the uppermost part of the Sabina Sandstone contains fresh water, where one interval (KL1A1) yielded water with a salinity of 330 mg/L. Composition of groundwater from the Sabina Sandstone was similar to groundwater from the overlying Lesueur Sandstone, from which it was probably derived. Groundwater from both formations is slightly alkaline, with a pH of 7.8 in the Sabina Sandstone and 8.6 in the Sue Coal Measures.

There are no known users of groundwater from the Sue Coal Measures or Sabina Sandstone near the Karridale Line, but the aquifer could be utilized for stock or industrial use, particularly where it outcrops or occurs below the Warnbro Group.

Hydrochemistry

Chemical analyses of water samples from the Karridale Line are presented in Table 3. The major ions are plotted as a percentage of their total milli-equivalent per litre concentrations on a trilinear diagram (Piper, 1944) in Figure 7.

In all water samples sodium is the principle cation and in most samples chloride is the dominant anion, although some samples are marginally dominant in bicarbonate.

The pH is generally between 4.2 and 8.8, with the acidic groundwater associated with the Warnbro Group, Yarragadee Formation, and Lesueur Sandstone. Slightly alkaline groundwater is typically associated with the Parmelia Formation, Cockleshell Gully Formation, Sabina Sandstone, and Sue Coal Measures. Groundwater from the Yarragadee Formation west of the Darradup Fault is usually slightly alkaline. Field-measured pH values are often substantially lower than those measured in the laboratory, suggesting that the carbon dioxide content of the groundwater is high.

Groundwater temperature

Groundwater temperatures measured by wire-line temperature logs are shown in Figure 8. Temperatures range from 16.9°C at the water table in KL5A, to 43.5°C at the bottom of KL3A. The geothermal gradient is higher over the Vasse Shelf than the Bunbury Trough, possibly reflecting the shallow basement on the Vasse Shelf. The geothermal gradient is high in the argillaceous formations: in the Sue Coal Measures, the geothermal gradient varies

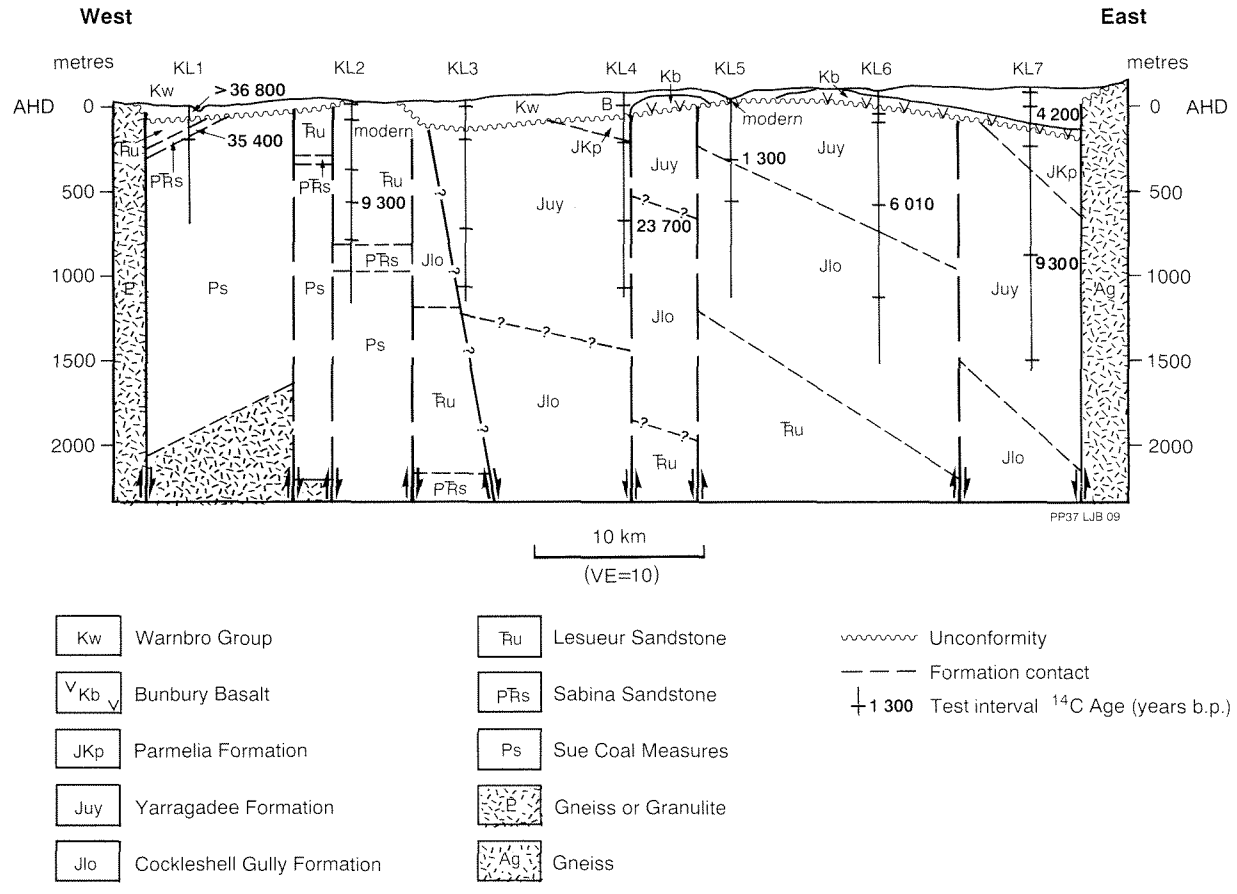

Figure 9. Groundwater age (carbon–14)

between 2.4 and 3.1°C/100 m; in the Sabina Sandstone it is about 2.6°C/100 m; about 3.2°C/100 m in the Parmelia Formation; in the Cockleshell Gully Formation the gradient lies between 2.0 and 2.2°C/100 m; and in the Warnbro Group there is a gradient of 1.4 to 2.3°C/100 m. The sandy formations have low geothermal gradients: 1.5°C/100 m in the Lesueur Sandstone, and 1.0 to 2.2°C/100 m for most of the Yarragadee Formation. A high rate of groundwater recharge in the area may account for the constant temperature of 16.9°C recorded in the Yarragadee Formation to a depth of 180 m at site KL5.

In the southern Perth Basin geothermal gradients tend to decrease toward the south. In the Yarragadee Formation geothermal gradients found in the deep-bore lines progressively change toward the south from 2.0 to 2.7°C/100 m in the Boyanup Line (Smith, 1984), 1.8 to 2.4°C/100 m in the Quindalup Line (Wharton, 1981), 1.8°C/100 m in the Cowaramup Line (Appleyard, 1991), to 1.0 to 2.2°C/100 m in the Karridale Line.

Carbon-14 dating

Groundwater was sampled from an interval in each deep bore (except KL3A), and some of the shallow bores, for carbon-14 dating: the results are depicted in Figure 9.

The carbon-14 ages (Thorpe, P. M., 1990, pers. comm.) correlate well with groundwater flow patterns determined from potentiometric heads. The dating indicates modern ages in recharge areas and relatively young groundwater in the Yarragadee Formation in the eastern Bunbury Trough. Young groundwater is also present in the Lesueur Sandstone on the eastern Vasse Shelf. However, groundwater in the Lesueur Sandstone aquifer on the western Vasse Shelf is much older and approaches the age limit for carbon-14 dating.

Conclusions

Drilling of the Karridale Line bores has extended knowledge of the geology and hydrogeology of the southern Perth Basin, and proved the existence of very thick sandstone formations containing low-salinity groundwater.

The drilling intersected the Sue Coal Measures, Sabina Sandstone and Lesueur Sandstone on the Vasse Shelf, and the Cockleshell Gully Formation, Yarragadee Formation, and Parmelia Formation in the Bunbury Trough. These formations are juxtaposed by faulting and overlain by the Warnbro Group, and in places by the Bunbury Basalt.

A number of groundwater flow systems complicated by the structural geology have been identified. The most important aquifer is the Yarragadee Formation in the Bunbury Trough which contains over 1200 m of sandstone with groundwater generally between 140 mg/L and 400 mg/L TDS. Over 500 m of aquifer containing fresh groundwater was discovered in the Cockleshell Gully Formation, and a further 1200 m in the Lesueur Sandstone south of the Karridale Line in the Bunbury Trough.

On the Vasse Shelf a previously unknown large resource of fresh groundwater was found in the Lesueur Sandstone to a maximum depth of 860 m. There are two groundwater flow systems within the Lesueur Sandstone on the Vasse Shelf, and these are separated by a structural high in the Sue Coal Measures.

Groundwater recharge to the Yarragadee Formation appears to be predominantly by rainfall with intake areas where the Warnbro Group is absent, while on the Vasse Shelf recharge to the Lesueur Sandstone is directly by rainfall or downward leakage from the Warnbro Group.

The Yarragadee Formation, Cockleshell Gully Formation, and Lesueur Sandstone contain a very large volume of fresh groundwater that is presently almost unutilized. These aquifers have the potential for substantial development as a source of high-quality water for the southwest of Western Australia.

References

APPLEYARD, S. J., 1991, The geology and hydrogeology of the Cowaramup borehole line, Perth Basin, Western Australia: Western Australia Geological Survey, Report 30, Professional Papers, p. 1–12.

BACKHOUSE, J., 1988a, Palynology of Cowaramup Line 6A: Western Australia Geological Survey, Palaeontology Report 1988/1 (unpublished).

BACKHOUSE, J., 1988b, Palynology of Cowaramup Line 7A: Western Australia Geological Survey, Palaeontology Report 1988/11 (unpublished).

BACKHOUSE, J., 1989a, Palynostratigraphy of Karridale Line 7A: Western Australia Geological Survey, Palaeontology Report 1989/10 (unpublished).

BACKHOUSE, J., 1989b, Palynology of two samples from Union Oil Blackwood 1: Western Australia Geological Survey, Palaeontology Report 1989/12 (unpublished).

BACKHOUSE, J., 1989c, Palynostratigraphy of Karridale Line 3A: Western Australia Geological Survey, Palaeontology Report 1989/18 (unpublished).

BACKHOUSE, J., 1989d, Palynostratigraphy of Karridale Line 2A: Western Australia Geological Survey, Palaeontology Report 1989/19 (unpublished).

BACKHOUSE, J., 1989e, Palynostratigraphy of Karridale Line 1A: Western Australia Geological Survey, Palaeontology Report 1989/20 (unpublished).

BACKHOUSE, J., 1989f, Palynostratigraphy of Karridale Line 5A: Western Australia Geological Survey, Palaeontology Report 1989/21 (unpublished).

BACKHOUSE, J., 1990a, Palynology of Karridale Line 4A: Western Australia Geological Survey, Palaeontology Report 1990/5 (unpublished).

BACKHOUSE, J., 1990b, Palynology of Karridale Line 6A: Western Australia Geological Survey, Palaeontology Report 1990/6 (unpublished).

BACKHOUSE, J., 1990c, Palynology of Karridale Line 10A: Western Australia Geological Survey, Palaeontology Report 1990/9 (unpublished).

BACKHOUSE, J., 1990d, Palynology of Scott Coastal 13A: Western Australia Geological Survey, Palaeontology Report 1990/20 (unpublished).

BADDOCK, L. J., 1990, Karridale Line bore completion reports: Western Australia Geological Survey, Hydrogeology Report 1990/63 (unpublished).

BURGESS, I. R., 1978, Geology and geochemistry of the Cretaceous Bunbury Tholeiite suite, Perth Basin, Western Australia: University of Western Australia, B.Sc. honours thesis (unpublished).

ELLIS, C. J., 1985, Final report on Blackwood Exploration Licence E 70/64 Augusta, Western Australia: CRA Exploration Pty Ltd (unpublished), Western Australia Geological Survey, S-series Open File, item 2798.

LOWRY, D. C., 1965, Geology of the southern Perth Basin: Western Australia Geological Survey, Record 1965/17 (unpublished).

LOWRY, D. C., 1982, Canebreak 1 well completion report: Weaver Oil and Gas Corporation, Australia (unpublished), Western Australia Geological Survey, S-series Open File, microfilm roll 628, item 2020.

McDOUGALL, I., and WELLMAN, P., 1976, Potassium–argon ages for some Australian Mesozoic igneous rocks: Geological Society of Australia, Journal, v. 23, p. 1–9.

NOLAN, R., 1975, Interim report coal exploration south Perth Basin, Western Australia: Broken Hill Proprietary Co. Ltd (unpublished).

PIPER, A. M., 1944, A graphic procedure for the geochemical interpretation of water-analysis: American Geophysical Union, Transactions of the 25th Annual Meeting, 1944, part 6, p. 914–923.

PLAYFORD, P. E., COCKBAIN, A. E., and LOW, G. H., 1976, Geology of the Perth Basin, Western Australia: Western Australia Geological Survey Bulletin 124.

POYNTON, D. J., and HOLLAMS, R. F. F., 1980, Whicher Range No. 2 well completion report: Mesa Australia Limited, Western Australia (unpublished), Western Australia Geological Survey, S-series Open File, microfilm rolls 629 and 630, item 1628.

SHARPLES, C. E., 1981, Report on coal exploration: temporary reserves 7669H, 7670H, 7425H, coal mining leases 70/4347-4448, 70/4661-4831, 70/4926-4960, and 70/8850-8851, south Perth Basin, Western Australia: BHP Report (unpublished).

SMITH, R. A., 1984, Geology and hydrogeology of the Boyanup bore line, Perth Basin: Western Australia Geological Survey, Report 12, Professional Papers for 1982, p. 72–81.

TRENDALL, A. F., 1963, Petrology of the Bunbury Basalt: Western Australia Geological Survey, Petrological Report 33 (unpublished).

UTTING, E. P., 1966, Exploration for coal, temporary reserve 3623H, Western Australia: Griffin Coal Mining Company (unpublished), Western Australia Geological Survey, S-series Open File, tem 273.

WHARTON, P. H., 1981, The geology and hydrogeology of the Quindalup Borehole Line: Western Australia Geological Survey, Annual Report 1980, p. 27–35.

WILLIAMS, C. T., and NICHOLLS, J., 1966, Sue No. 1 well completion report: Western Australian Petroleum Pty Ltd, Petroleum Search Subsidy Acts Report (unpublished), Western Australia Geological Survey, S-series Open File, microfilm roll 43, item 268.

The impact of stormwater infiltration basins on groundwater quality, Perth Metropolitan Region

by

S.J. Appleyard

Abstract

Twelve bores were sunk adjacent to three stormwater infiltration basins in the Perth suburbs of Myaree and Ardross to examine the impact of runoff on groundwater quality, and the hydrological response of the aquifer to runoff-recharge. The three basins were situated in a light-industrial area, a medium-density residential area, and a major arterial road. The bores were constructed at the watertable, at the base of the shallow aquifer, and at an intermediate depth. They were sampled in April 1990 and November 1990 to record groundwater quality before and after the winter rainfall period.

Automatic and manual waterlevel monitoring between April and November 1990 indicated that groundwater levels responded within minutes to recharge from the infiltration basins. Peak waterlevels of up to 2.5 m above rest levels occurred 6 to 24 hours after the commencement of ponding in the infiltration basins.

The main impact of runoff-recharge on groundwater quality was a marked reduction in salinity, and increase in dissolved-oxygen concentrations and bromide/chloride ratios in the upper part of the aquifer downgradient of the infiltration basins. Concentrations of toxic metals, nutrients, pesticides, and phenolic compounds in groundwater near the infiltration basins were low, and generally well within NHMRC guidelines. However, sediment in the base of an infiltration basin draining a major road contained in excess of 3500 ppm of lead. No faecal coliforms, streptococci or salmonella organisms were detected in groundwater near the infiltration basins.

Phthalates were detected in all but one bore near the infiltration basins. These compounds are US EPA priority pollutants and, while possibly derived from the PVC casing used to line boreholes, may be derived from the plastic litter which accumulates in the infiltration basins.

The concentration of iron in groundwater near the infiltration basins appears to be controlled by dissolved-oxygen concentrations, with high iron concentrations occurring where dissolved-oxygen concentrations are low. Pumping bores located near infiltration basins may suffer from iron-encrustation problems caused by the mixing of shallow, oxygenated groundwater with water containing higher concentrations of iron from deeper in the aquifer.

KEYWORDS : Groundwater quality, urban runoff, artificial groundwater recharge

Introduction

The city of Perth is the only capital in Australia that has developed over a large groundwater resource. Groundwater currently provides about 35% of the city's potable water supply, and about 70% of the city's water supply when abstraction by local government authorities, schools, and private householders is taken into account. Perth is one of the fastest growing capital cities in Australia, and the rapid increase in urban development could potentially have a deleterious impact on groundwater quality.

One possible source of groundwater contamination in the Perth metropolitan area is the large number of infiltration basins which are used to dispose of drainage water from roads and paved surfaces in the metropolitan area. There are over 900 such basins in the Perth area (Cargeeg et al., 1987), and these receive runoff from land developed for a variety of uses, ranging from low-density residential developments to heavy industry. Runoff from these areas could contain a wide range of contaminants, and these could be introduced into groundwater by recharge through the infiltration basins.

The purpose of this study was to examine the impact on groundwater quality of three infiltration basins in the Perth metropolitan area. The basins were selected to investigate the impact of runoff on groundwater quality from a light-industrial area, a medium-density residential area, and a major arterial road, as these were considered to be typical ways in which land is used in new urban areas.

Bores were drilled adjacent to each infiltration basin, and were sampled in April and November 1990 for a range of parameters including selected nutrients, bacteria, major ions, heavy metals, and a suite of organic compounds

including pesticides. Waterlevels were monitored continuously in bores at each site, and at two sites waterlevels were monitored in the infiltration basins to estimate the volume of water recharged through the basins.

The effect of urban runoff on groundwater quality

A considerable amount of work has been carried out to determine the impact of urban development on stormwater runoff, but relatively little work has been carried out examining the impact of recharging ground-water with urban stormwater.

In general, as a catchment is urbanized, the following changes take place:

(i) runoff is significantly increased because of an increase in the impervious area of the catchment,

(ii) runoff is discharged more quickly because of increased velocities in hydraulically more efficient drainage channels,

(iii) runoff may carry a significant load of contaminants resulting from the activities of man within the urbanized catchment (Table 1)

The impact on groundwater quality of recharging stormwater through drainage wells has been investigated by the US Geological Survey in a number of studies (Kimrey, 1978; Hull and Yurewicz, 1979; Schiner and German, 1983). Generally, these studies have been exploratory in nature and have neither attempted to quantify the amount of water recharged, nor provided comprehensive analyses of potential contaminants.

A more comprehensive study was carried out by Seaburn and Aronson (1974) who measured precipitation, stormwater inflow, seepage rates, groundwater responses, and also quantified groundwater recharge from three infiltration basins on Long Island, New York State. They also measured some water-quality parameters in storm-water inflow to the infiltration basins and in groundwater beneath the basins; pesticide analyses were included. They found that recharge from the infiltration basins had little impact on groundwater quality, and that pesticide concentrations in groundwater near the basins were negligible.

Another comprehensive study was carried out by German (1989), who studied the impact of stormwater recharge through two recharge wells in Florida, and included measurements of recharge volumes and analyses of a wide suite of chemical compounds. The study found that concentrations of iron, nitrogen and phosphorus, and bacterial counts, were generally higher in groundwater near the recharge wells than in samples taken from other bores in the area.

The effect of varying landuse on groundwater near stormwater infiltration basins in Sweden was investigated by Malmquist and Hård (1981), who investigated stormwater recharge in an industrial area, a residential area, and near a major highway. Several bores were sampled both upgradient and downgradient of each site to assess the impact of stormwater recharge. They found that stormwater recharge had a minimal impact on groundwater quality, despite the shallow watertables (1 to 2 m below ground). The major changes in chemical composition were reductions in the concentrations of nitrogen species downgradient of the infiltration basins, and increases in phosphorus concentrations. Increased levels of poly-aromatic hydrocarbons were detected in groundwater near the highway.

Table 1. Major sources of pollution of stormwater in urban catchments

1. Road pavement materials
2. Motor vehicles
   * Leakage of fuels
   * Lubricants
   * Hydraulic fluids
   * Coolants
   * Abraded material (from tyres, brake, and clutch linings etc.)
3. Atmospheric fallout
4. Litter
   * Packaging materials
   * Plant debris
   * Food discards
   * Animal and bird droppings
5. Spills
6. Unauthorized deliberate dumping

Source: Sartor and Boyd (1972)

Geological setting

The Perth metropolitan area is located in the Perth Basin, an elongate trough containing up to 15 000 m of sediments. The basin is bounded to the east by the northerly trending Darling Fault, which separates Phanerozoic sediments from Precambrian rocks of the Yilgarn Craton. The uppermost sediments in the Perth Basin range in age from Late Tertiary to Quaternary, and are collectively known as the superficial formations. These sediments consist predominantly of sand, clay, and limestone and range in thickness from 20 to 35 m in the study area.

The superficial formations form an extensive aquifer which underlies most of the metropolitan area, and contains two major groundwater flow systems: the Gnangara Mound to the north of Perth, and the Jandakot Mound to the south of Perth (Fig. 1). Groundwater flows radially from each of these groundwater mounds, and discharges into wetlands, rivers, the Swan estuary, and the ocean. The three infiltration-basin sites are located near the northern edge of the Jandakot mound in an area which is hydrogeologically similar to other parts of the Jandakot

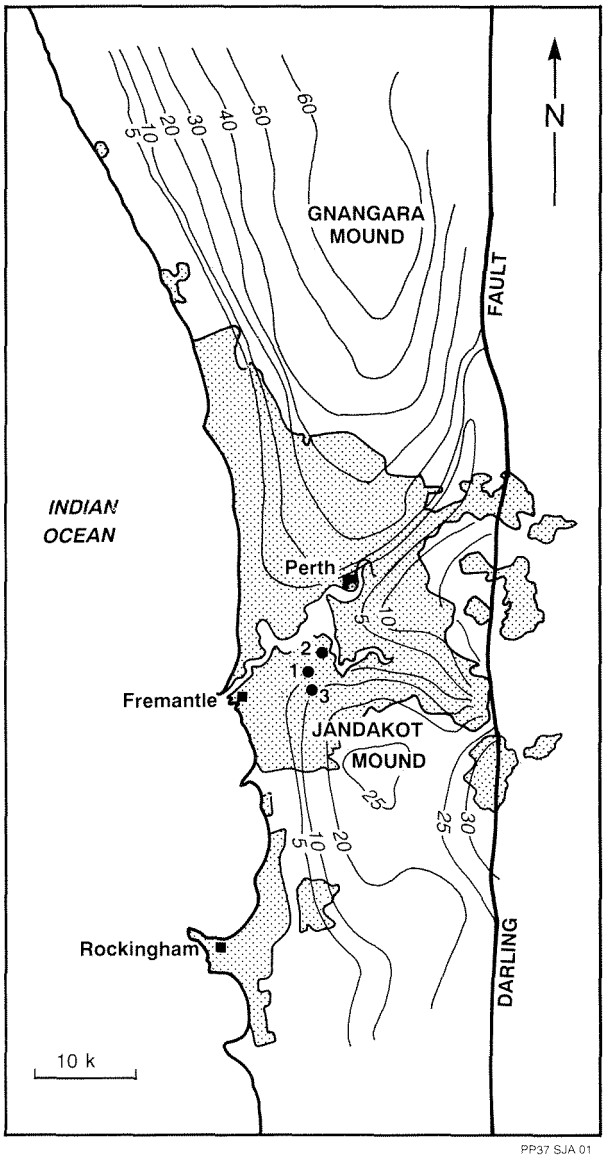

Figure 1. Location plan

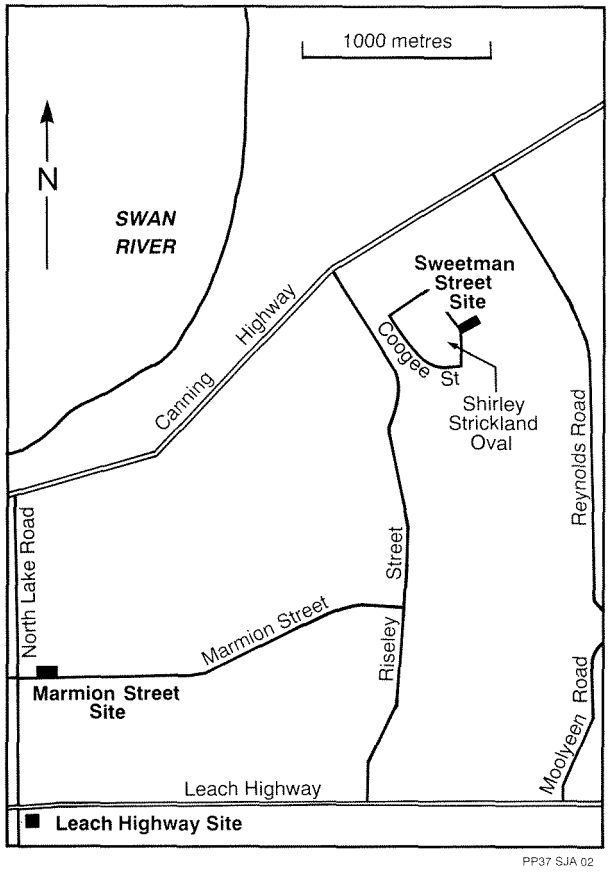

Figure 2. Location of the infiltration basins

mound where new urban developments have been proposed.

Description of the sites

Site 1: Marmion Street

Site 1 is located at the corner of Evershed and Marmion Streets in the suburb of Myaree (Fig. 2). The infiltration basin has a floor area of about 1200 m^2, and receives runoff from the Myaree light-industrial area and nearby residential areas. The exact size of the catchment is difficult to determine, because water is pumped to this basin from another infiltration basin in Myaree. However, the total impervious catchment area is at least 67 000 m^2.

Three bores were sunk adjacent to, and immediately upgradient of the Marmion Street infiltration basin (Fig. 3) during a drilling program in November 1989: a watertable bore (MIS1s); a bore slotted at the base of the superficial aquifer (MIS1d); and a bore sunk to an intermediate depth (MIS1i).

These bores were drilled immediately upgradient of the site, because of limited access on the downgradient side of the infiltration basin. However, the bores were considered to be sufficiently close to the basin to detect any chemical changes in groundwater caused by the infiltration basin. A fourth bore (MIS1wt) was drilled by hand in August 1990 to monitor the watertable immediately downgradient of the infiltration basin. Bore construction details for these and other bores drilled during this study are given in Table 2.

Site 2: Sweetman Street

Site 2 is located on Sweetman Street near the intersection with Klem Road in Applecross, and is adjacent to Shirley Strickland Oval (Fig. 2). The floor of the infiltration basin has a surface area of about 380 m^2, and receives runoff from a catchment with an area of about 74 000 m^2. The

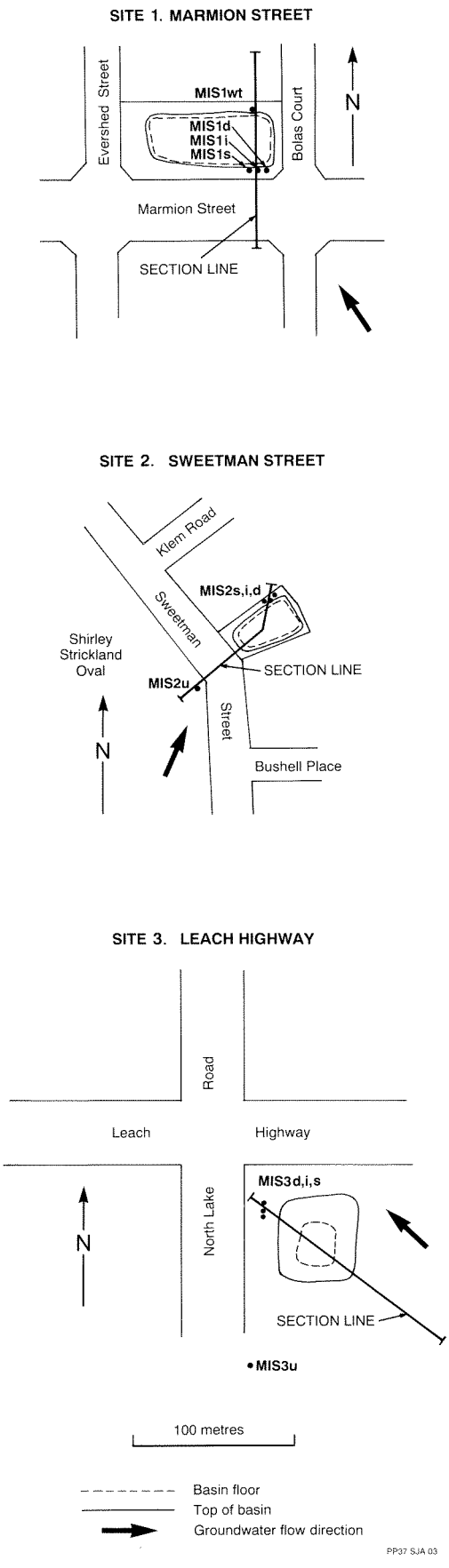

Figure 3. Bore locations at each site

catchment is covered with medium-density housing with an average block size of about 1000 m^2. An analysis carried out during the Perth Urban Water Balance Study (Cargeeg et al., 1987) indicated that 14% of this catchment was covered by impervious surfaces that generate surface runoff, giving an impervious catchment area of about 10 000 m^2.

The time taken for water to travel from the catchment boundaries to the infiltration basin (time of concentration) was estimated from the Bransby–Williams equation (Australian Institute of Engineers, 1987) to be 17 minutes (Appleyard, 1986). Continuous flow measurements in 1985 (Appleyard, 1986) indicated that discharge rates into the infiltration basin ranged between 0.01 and 0.4 m^3/second. The total volume of water discharged into the basin between May and October in 1985 was 4200 m^3, when 829 mm of rain was measured at this site during the same period.

Four bores were sunk near the Sweetman Street infiltration basin (Fig. 3; Table 2): three immediately downgradient of the basin (MIS2s, MIS2i, MIS2d), and one about 30 m upgradient of the basin (MIS2u) to measure background groundwater quality at the watertable.

Site 3: Leach Highway

Site 3 is located at the corner of Leach Highway and North Lake Road in Myaree (Fig. 2), and receives most runoff from Leach Highway, although some runoff is also received from a new residential development to the south of this arterial road. The infiltration basin has a floor area of about 600 m^2, and an impervious catchment area of about 58 000 m^2 (Evangelisti, M., 1990. pers. comm.).

Four bores were sunk adjacent to this infiltration basin (Fig. 3; Table 2): three downgradient of the basin (MIS3s, MIS3i, MIS3d) and one upgradient of the basin (MIS3u) in a way similar to that at Site 2.

Methods of investigation

Hydrological data collection

Groundwater levels at the watertable near each basin were measured continuously between April and October 1990 using WESDATA capacitive waterlevel probes and dataloggers recording at 15 minute intervals. Potentiometric levels at the base of the aquifer were also monitored at Site 3, and briefly at Site 2, to see if water recharging through the infiltration basins influenced potentiometric heads near the base of the aquifer. This was not carried out at Site 1 owing to a limited number of dataloggers.

The depth of water in the infiltration basins at Sites 2 and 3 were continuously monitored with dataloggers to measure the hydrological response of these basins to runoff. Waterlevels in the infiltration basins were related to volumes using the volume–height curves in Figure 4, and the total volume recharged to groundwater during each rainfall event was calculated.

Table 2. Bore completion details

Site	Bore	Date drilled	Total depth (m)	Elevation NS (mAHD)	Elevation TOC (mAHD)	Slotted interval (m)	Head (mAHD)	Salinity TDS (mg/L)	Airlift Rate (m^3/day)
1.	MIS1s	3 Nov 89	6	6.448	7.363	3–6	4.24	150	86
	MIS1i	3 Nov 89	15	6.568	7.408	12–15	4.25	240	56
	MISd	1 Nov 89	24	6.513	7.450	21–24	4.24	430	30
	MIS1wt	8 Aug 90	5.5	-	-	2.2–5.5	-	360	-
2.	MIS2s	7 Nov 89	10.5	9.496	10.464	7.5–10.5	2.96	90	19
	MIS2i	7 Nov 89	15	9.484	10.472	12–15	2.97	70	10
	MIS2d	6 Nov 89	28	9.512	-	25–28	-	450	26
	MIS2u	8 Nov 89	10.5	-	9.776	7.5–10.5	3.00	1 310	13
3.	MIS3s	10 Nov 89	10.5	13.202	14.202	7.5–10.5	5.33	80	56
	MIS3i	9 Nov 89	18	13.205	13.989	15–18	5.33	110	34
	MIS3d	8 Nov 89	30	13.227	14.000	27–30	5.33	-	-
	MIS3u	10 Nov 89	13	14.110	15.000	10–13	5.52	330	20

Notes: All bores except MIS1wt were constructed with 50 mm ID PVC casing. MIS1wt was constructed with 80 mm casing.

NS: natural surface; TOC: top of casing; TDS: total dissolved solids

All dataloggers were unloaded regularly (generally fortnightly), and manual waterlevels were taken to check the accuracy of the recorded data.

Daily rainfall information for the three sites was obtained from the Bureau of Meteorology weather station at Melville, which is located within 2.5 km of all infiltration-basin sites.

Groundwater sampling

Water samples were collected from all bores by pumping with 12 volt electric submersible pumps. The pumped water was passed through a perspex flow cell, where measurements of conductivity and dissolved oxygen were made with a Philips resistivity bridge, and a dissolved-oxygen meter. Each bore was pumped until at least three casing volumes of water had been displaced before samples were collected.

Two sampling rounds were carried out to test the effect of seasonal variations on groundwater quality: the first set of samples was collected in April 1990 before the onset of winter, and the second in October 1990 at the end of the winter rainfall season.

Separate samples were collected for the analysis of major ions, heavy metals, nutrients, pesticides and other trace organic compounds using sampling procedures and bottles recommended and supplied by the Chemistry Centre (W.A.). All samples collected were returned to the Chemistry Centre within 3 hours of collection to ensure that preservation and storage procedures were carried out correctly for subsequent chemical analysis.

During the April sampling round, samples were collected for microbiological analysis from bores MIS1s, MIS2s, MIS2u, MIS3s, and MIS3u to test whether groundwater downgradient of the infiltration basins had been contaminated with micro-organisms, and to test whether there were any microbiological differences between groundwater at the watertable downgradient and upgradient of the infiltration basins. An extra sample was collected from bore MIS3i to see whether the volume of water recharging through this basin had caused micro-biological contamination at depth in the aquifer.

Biological samples were collected in sterile glass bottles provided by the Health Department, cooled to 4°C, and taken to the Environmental Laboratory at the Queen Elizabeth II Medical Centre within 2 hours of sampling.

Hydrological response of groundwater to the infiltration basins

Measurements of waterlevels in infiltration basins and at the watertable at each site (Figs 5, 6, and 7) have indicated that the watertable responds rapidly to recharge from the basins. Watertable elevations at both the Sweetman Street and Leach Highway sites responded to a slug of runoff within minutes, and peak watertable elevations were recorded 6 to 24 hours after ponding occurred in the infiltration basins. The magnitude of the watertable response varied between 0.1 and 0.3 m at Sweetman Street, and 0.5 and 2.5 m at the Leach Highway site where the volume of runoff is larger. Datalogger measurements in deep bores indicated that a rapid but more subdued waterlevel response occurred near the base of the aquifer.

The impact of runoff recharge on groundwater levels can be most clearly seen where there is a single large rainfall event followed by a dry period. Such an event occurred on May 28, and the waterlevel responses to this event and interpreted groundwater isopotentials at the Leach Highway site are shown in Figures 8 and 9 respectively.

Four days before the rainfall event, manual waterlevel readings indicated that groundwater flowed laterally beneath the basin. Heavy rainfall on May 28 resulted in a 1.6 m depth of water in the infiltration basin, and a groundwater mound began to develop. Peak groundwater levels were recorded the following day, and the mound gradually collapsed as water disappeared from the basin. Groundwater levels returned to rest levels about three days after rainfall.

Rapid waterlevel rises at the watertable at the Sweetman Street site are superimposed on a trend of seasonal waterlevel variations: the mean watertable elevation rose from about 1.4 m AHD in April to a peak of about 1.9 m AHD in September (Fig. 6). A similar trend was observed at Marmion Street (Fig. 5) with peak waterlevels occurring in August. Short-term declines in groundwater levels at the watertable at Sweetman Street are probably caused by pumping from a nearby domestic bore.

Estimation of water volumes recharged to groundwater

The volume of water in infiltration basins available for groundwater recharge was estimated at the Sweetman Street and Leach Highway sites, where waterlevels were measured in the basins.

The volume of water discharged by drains into the infiltration basins was not measured at any of the sites, so it was not possible to directly measure the total volume of runoff discharged into the infiltration basins. However, the discharge volumes were estimated by converting infiltration basin waterlevels to water volumes, and incrementing positive volume changes for the period April 9 to November 16. Waterlevel records indicate that the seepage rate at Sweetman Street varied from 10 to 30 m^3/hour, and at the Leach Highway site from 25 to 40 m^3/hour. Seepage rates less than the maximum value at each site were assumed to be influenced by continuing discharge into the infiltration basins, and were included in the volume calculations.

The volume of runoff that was discharged to the infiltration basin at the Leach Highway site from individual rainfall events varied from about 200 to 900 m^3. The variations were probably caused by short-term fluctuations in rainfall intensity, rather than by daily rainfall totals. The total volume of water available for groundwater recharge during the period April 9 to November 16 is estimated to be at least 23 000 m^3, when the total rainfall recorded at Melville for this period was 588 mm.

Far less runoff was discharged to the infiltration basin at the Sweetman Street site than at Leach Highway, partly because of the smaller size of the Sweetman Street catchment, but also because a smaller percentage of that catchment is covered by impervious surfaces capable of producing runoff. Again, fewer runoff events were recorded at the Sweetman Street site, probably because a higher proportion were insufficiently large to cause ponding in the infiltration basin at this site. The volume

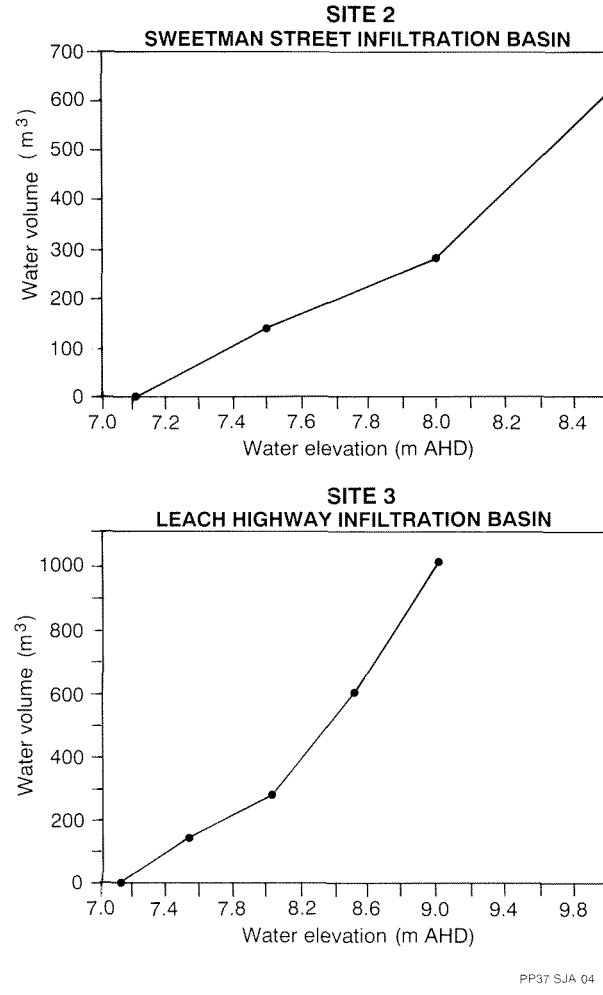

Figure 4. Volume/waterlevel curves for the Sweetman Street and Leach Highway sites

of runoff generated by individual rainfall events generally varied between 50 and 100 m^3 at the Sweetman Street site, although up to 200 m^3 flowed into this infiltration basin. The total volume of runoff discharged into the Sweetman Street infiltration basin between April 9 and November 16 was about 3000 m^3.

The volume of water which is potentially available for discharge into the infiltration basins can be estimated from the relationship:

Volume = A x R x P

where:

A = catchment area
R = rainfall
P = proportion of catchment with paved surfaces

For example, the total volume of runoff reaching the infiltration basin at Sweetman Street should be:

74 000 m^2 x 0.59 m x 0.14
~6000 m^3

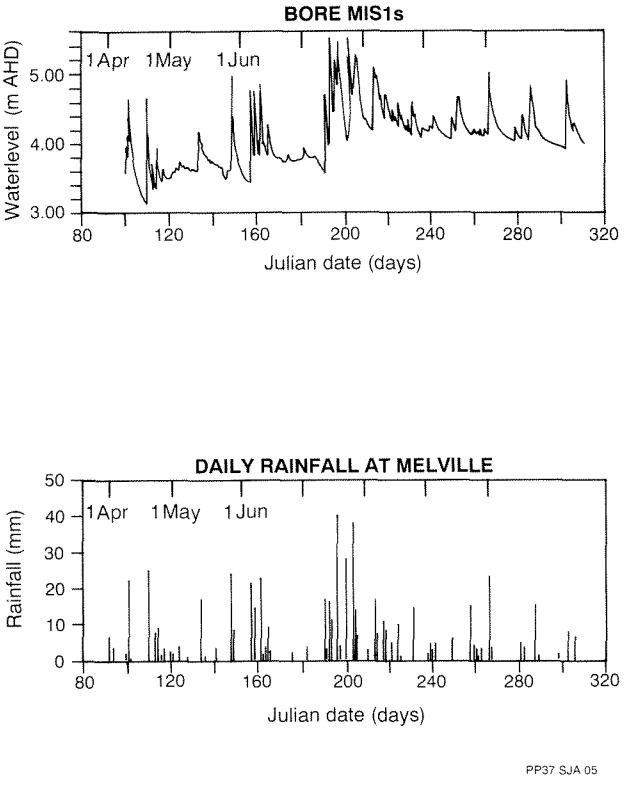

Figure 5. Variations in waterlevels at the Marmion Street site

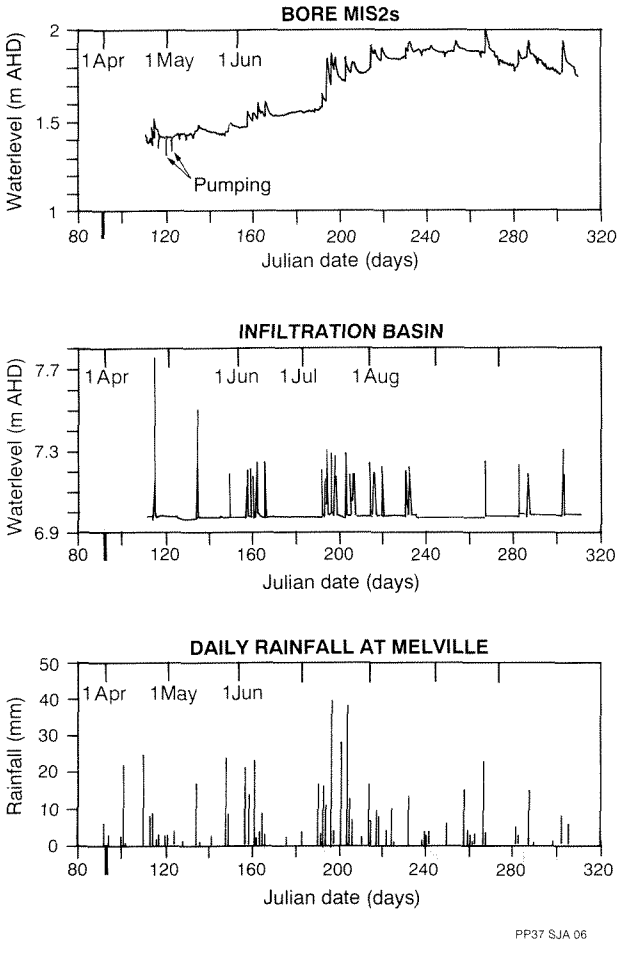

Figure 6. Variations in waterlevels at the Sweetman Street site

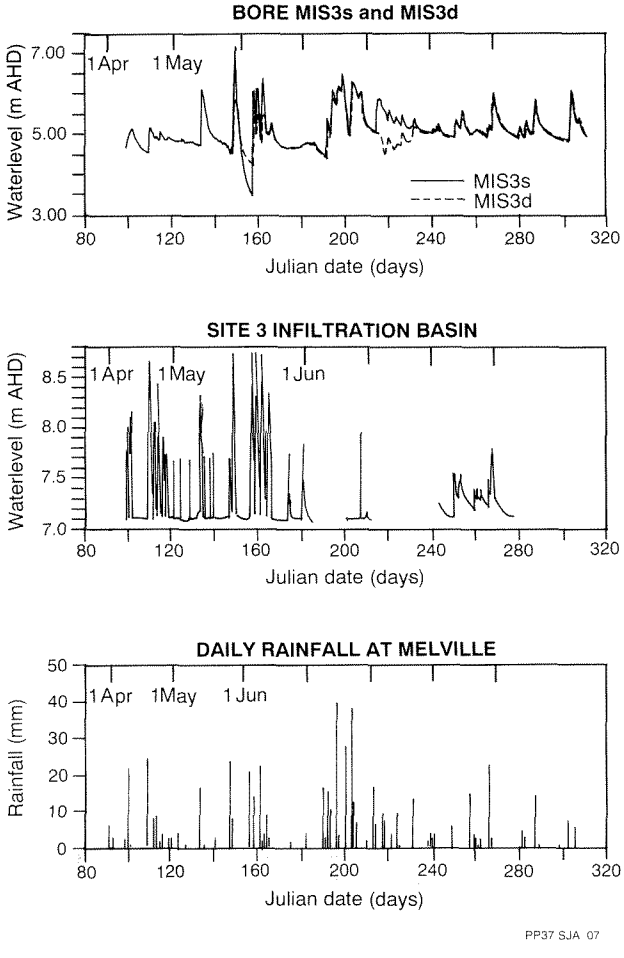

Figure 7. Variations in waterlevels at the Leach Highway site

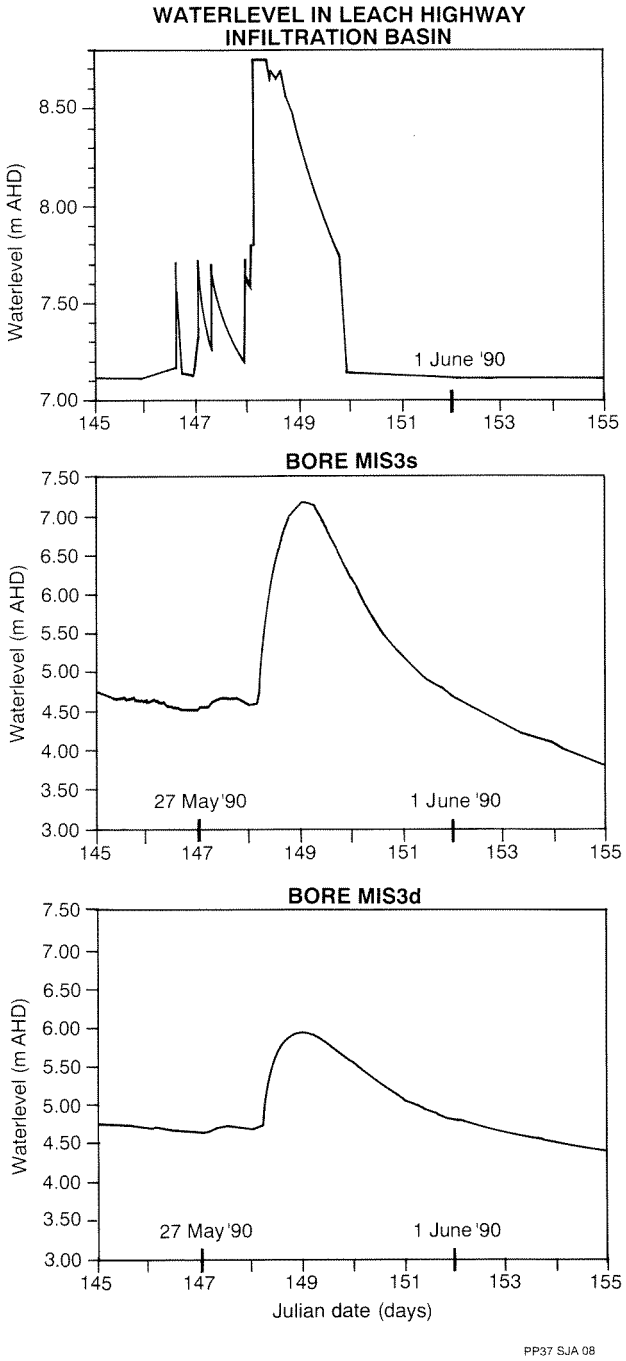

Figure 8. Variations in waterlevels at the Leach Highway site for the period May 25 to June 4, 1990

Similarly, the volume of water which was potentially available for discharge into the Leach Highway infiltration basin during the same period was 47 000 m^3.

The estimated volumes of runoff reaching the infiltration basins at the Sweetman Street and Leach Highway infiltration basins are about 50% of the potential discharge to these basins calculated from the catchment areas. There are several factors that could cause the differences between the two sets of figures, and these include:

(i) extensive leaks from stormwater drains,

(ii) periods of low discharge into the infiltration basins where ponding does not occur, and

(iii) evaporation from road surfaces in low-intensity rainfall events.

Effect of the infiltration basins on groundwater quality

Groundwater salinity

Major-ion analyses for samples collected from the infiltration basin bores in April and November 1990 are set out in Table 3. These data indicate that the major change in groundwater quality downgradient of the infiltration basins at each of the sites, is a marked reduction in total dissolved solids (Fig.10).

The natural groundwater salinity in the vicinity of the three sites lies in the range 250–500 mg/L total dissolved solids (TDS). However, salinities downgradient of the infiltration basins were lowered by runoff-recharge to 20–140 mg/L TDS to depths of more than 10 m below the watertable. The high groundwater salinity at the watertable upgradient of Site 2 is possibly due to heavy fertilizer use on Shirley Strickland oval, or the recycling of salts caused by irrigating the oval.

The low groundwater salinities near the infiltration basins are probably caused by the rapid nature of recharge from the basins. Fresh runoff flowing into these basins seeps rapidly to the watertable (very little is lost by evaporation) causing a plume of very fresh water to develop downgradient of the infiltration basins. The plume is less dense than the natural groundwater, and is confined to the upper part of the aquifer. The low-salinity plumes persist for long periods, and groundwater salinities did not change significantly between April and November 1990.

Ionic composition

Runoff-recharge has a negligible impact on the major-ion composition of groundwater near the infiltration basins. A Piper trilinear diagram (Fig.11) indicates that although there is a wide variation in the composition of groundwater at different depths in the superficial aquifer, there is no significant difference in composition between groundwater near the watertable affected by runoff-recharge, and groundwater near the base of the aquifer which is probably unaffected by runoff-recharge.

By contrast, the composition of halides in groundwater is affected by recharge through the infiltration basins. Although only limited data are available, the bromide/chloride weight ratio in groundwater near the watertable downgradient of the Sweetman Street and Leach Highway sites is as much as an order of magnitude greater than in groundwater near the base of the aquifer (Fig.12). This is due largely to the low concentration of chloride in groundwater affected by runoff-recharge.

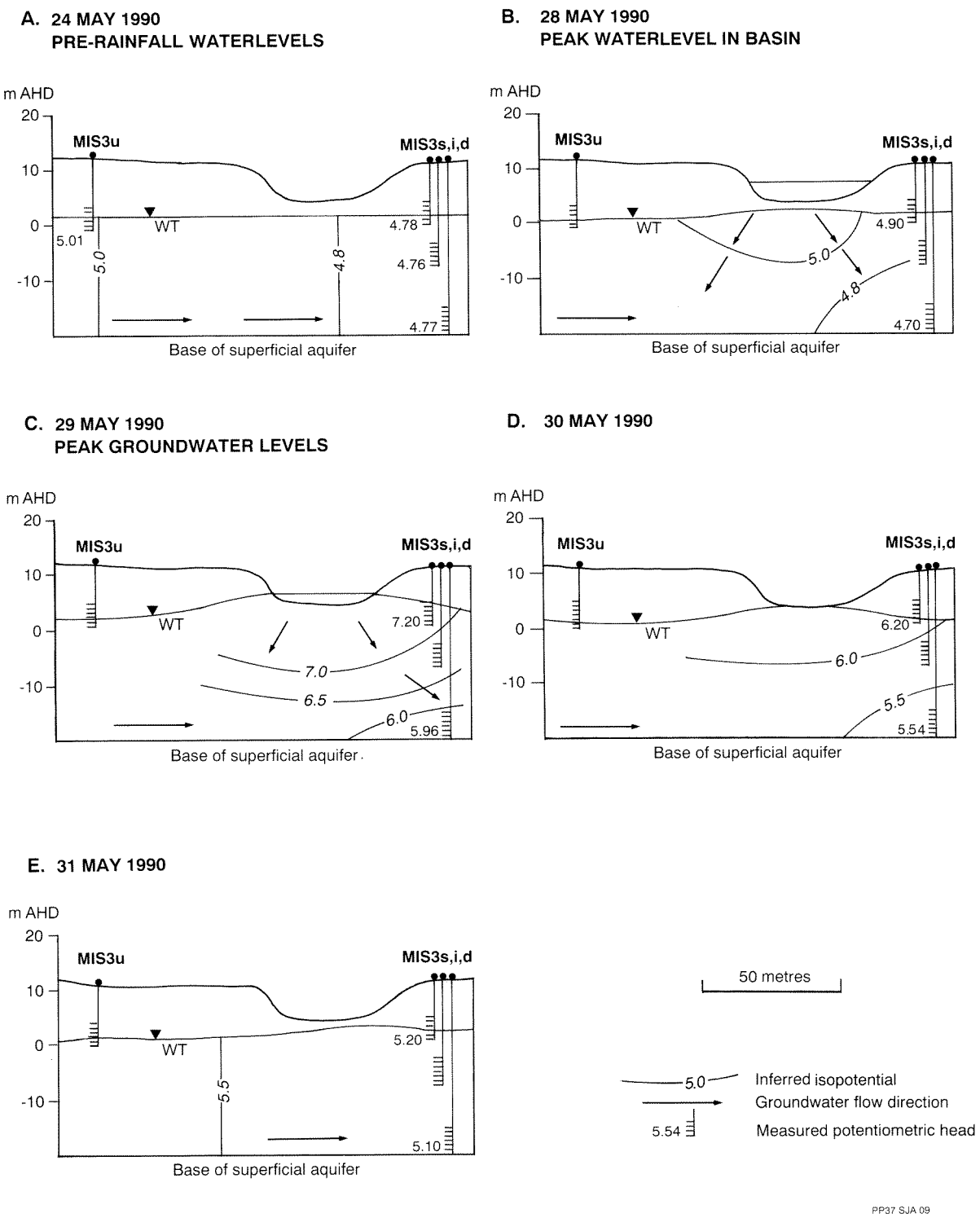

Figure 9. Interpreted isopotentials at the Leach Highway site for the period May 25 to June 4, 1990

Table 3. Major-ion chemical analyses

Bore	*Sample*	*pH*	*DO*	*TDS*	*Ca*	*Mg*	*Na*	*K*	*HCO_3*	*Cl*	*SO_4*	*SiO_2*	*B*	*Fe*	*Br*
										mg/L					
MIS1s1	5 Apr 90	6.9	NA	360	32	19	67	4	116	109	55	4	0.03	5.40	0.4
MIS1i	5 Apr 90	7.1	NA	270	23	14	40	3	83	51	48	19	<0.02	0.07	0.4
MIS1d	5 Apr 90	8.4	NA	360	68	7	51	4	211	85	19	14	<0.02	0.04	0.5
MIS2s	4 Apr 90	6.1	NA	20	1	2	2	<1	10	6	3	4	<0.02	0.09	0.1
MIS2i	4 Apr 90	6.3	NA	40	5	1	5	1	18	12	2	3	<0.02	0.16	0.1
MIS2d	4 Apr 90	8.5	NA	460	55	12	93	4	208	143	22	15	<0.02	1.50	0.5
MIS2u	4 Apr 90	5.1	NA	1 370	24	35	442	9	4	771	81	5	<0.02	0.17	0.8
MIS3s	3 Apr 90	6.9	NA	70	1	2	16	2	23	18	12	8	<0.02	0.48	0.5
MIS3i	3 Apr 90	7.4	NA	120	27	2	10	1	98	10	11	4	<0.02	0.09	0.7
MIS3d	3 Apr 90	8.6	NA	290	51	5	46	2	180	67	10	12	<0.02	1.40	0.6
MIS3u	3 Apr 90	7.8	NA	330	33	9	70	4	189	59	41	18	0.03	0.39	0.5
MIS1s	8 Nov 90	6.6	0.7	230	25	9	45	2	92	65	40	2	NA	3.40	NA
MIS1i	8 Nov 90	6.5	2.1	280	24	15	41	4	84	58	59	19	NA	0.05	NA
MIS1d	8 Nov 90	7.5	2.1	360	72	8	50	3	195	90	22	13	NA	0.26	NA
MIS1wt	8 Nov 90	7.4	1.4	40	4	1	7	1	28	6	5	2	NA	0.05	NA
MIS2s	9 Nov 90	5.9	8.3	30	1	3	4	1	10	12	2	3	NA	<0.05	NA
MIS2i	9 Nov 90	6.0	8.5	70	8	3	9	1	10	35	2	2	NA	<0.05	NA
MIS2d	9 Nov 90	7.4	1.5	460	54	11	100	4	225	140	20	15	NA	1.00	NA
MIS2u	9 Nov 90	5.9	3.6	1 210	21	31	397	9	13	652	82	5	NA	1.10	NA
MIS3s	8 Nov 90	6.5	4.8	80	5	2	15	2	45	10	13	6	NA	0.43	NA
MIS3i	8 Nov 90	7.1	8.0	140	26	2	26	1	104	18	10	2	NA	0.05	NA
MIS3d	8 Nov 90	7.4	2.1	320	58	6	54	2	201	78	10	11	NA	1.40	NA
MIS3u	8 Nov 90	7.0	7.8	340	39	13	63	4	214	60	36	13	NA	0.14	NA

Notes: DO: dissolved oxygen; TDS: total dissolved solids; NA: not analysed

Iron and dissolved oxygen

The solubility of iron in groundwater is controlled by a number of factors, including the redox potential of groundwater (largely controlled by the dissolved-oxygen concentration), pH, concentrations of carbonate and sulfur species, and the presence of organic compounds which can form soluble complexes with iron. Iron is most soluble under reducing conditions, where it exists in solution as free ferrous-ion or as soluble divalent iron complexes. In oxygenated groundwater iron concentrations are generally low, as ferrous-ion is oxidized to form ferric oxides and hydroxides which precipitate from solution.

Limited data from groundwater near the infiltration basins indicate that there is a weak relationship between iron and dissolved oxygen (Fig. 13; Table 3), with the highest iron concentrations occurring where dissolved-oxygen concentrations in groundwater are low. A similar relationship was noted by Martin (1980) in the Gwelup area to the north of Perth. Martin also detected dissolved oxygen in shallow groundwater in this area, whereas samples taken elsewhere contained no detectable dissolved oxygen. He attributed the presence of oxygen to increased drawdowns in iron-encrusted bores drawing in soil gas, but it is more likely that high dissolved-oxygen concentrations are associated with urban recharge.

The Sweetman Street infiltration basin appears to have a strong impact on the concentration of dissolved oxygen and iron in groundwater. Dissolved-oxygen concentrations at this site exceed 8 mg/L in the upper part of the aquifer (Fig. 14), which is probably near the saturation limit for this gas under the temperature and pressure conditions present in the aquifer (Matthess, 1982). Iron concentrations are correspondingly low in the upper part of the aquifer at this site, and increase with depth where oxygen concentrations are lower. A similar trend occurs at the Leach Highway site, although high dissolved-oxygen concentrations also occur at the watertable upgradient of this infiltration basin.

Low dissolved- oxygen concentrations at the watertable suggest that this infiltration basin is having little impact on oxygen levels in groundwater. Dissolved-oxygen concentrations near the base of the aquifer are higher at this site, possibly indicating that recharge upgradient of the site has oxygenated the entire aquifer thickness.

The impact of infiltration basins on oxygen and iron concentrations has implications for the management of bores located near these basins. Where, for instance, pumping from nearby bores induces mixing of water from different levels in the aquifer, bacterially catalysed precipitation of iron oxides could occur, creating encrustations on screens, which can substantially reduce bore yields. Encrustation problems have been noted in some Water Authority bores located near infiltration basins in the Gwelup borefield to the north of Perth (McLaughlan, 1991).

Toxic metals

High concentrations of metals such as copper, lead, zinc, and cadmium can be generated in surface runoff,

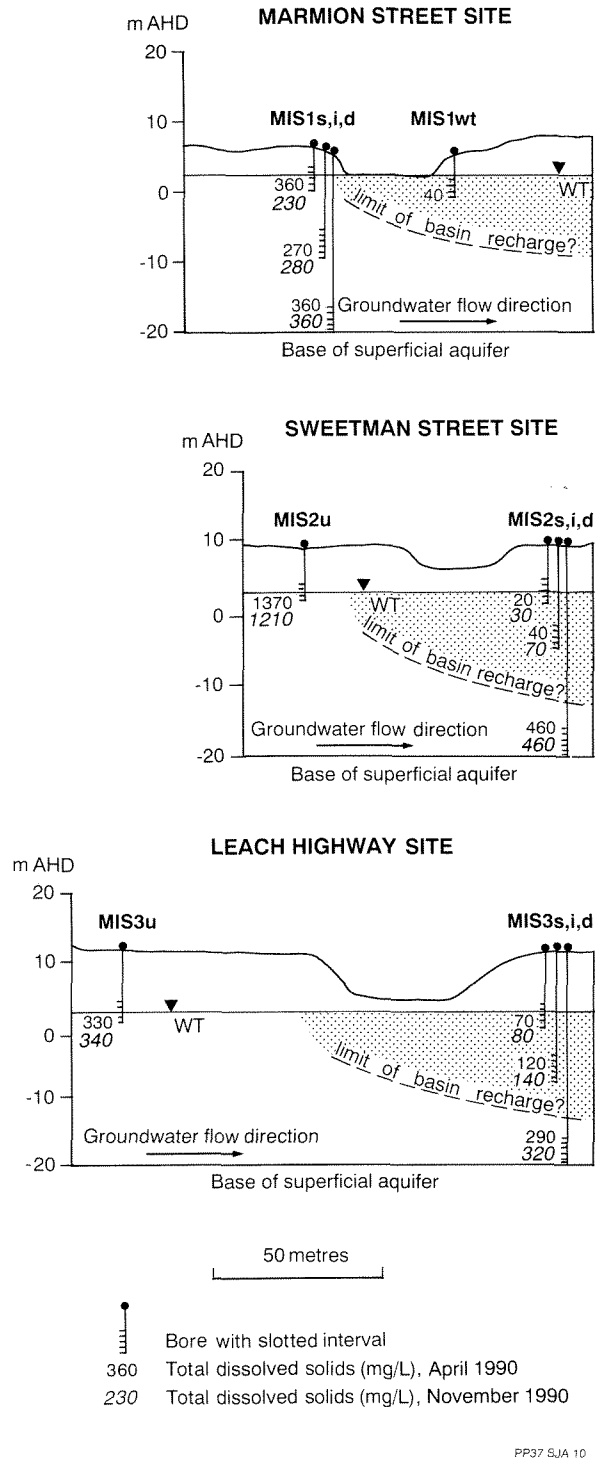

Figure 10. Vertical variations in total dissolved solids (mg/L) at each site

particularly in runoff after a long dry spell. The main sources of these metals are the combustion of fossil fuels, tyre wear, and metal particles abraded from vehicles, scheme water, and fertilisers. Gerritse et al. (1988) estimated that the annual input of the metals copper, lead, zinc, and cadmium to groundwater in the Perth metropolitan area is about 0.1, 0.6, 1, and 0.01 kg/ha respectively.

Trace-metal concentrations in samples collected from the infiltration basin bores in April and October 1990 are all low (Table 4), and were all below drinking-water criteria set by the National Health and Medical Research Council (NHMRC, 1987). The low groundwater concentrations of metals indicate that sediments within the infiltration basins are effective in adsorbing metals, despite the sandy nature of the sediment, and the rapid response of groundwater to recharge by runoff. Low concentrations of metals were also found in groundwater in the Perth metropolitan area in studies carried out by Cargeeg et al. (1987) and Gerritse et al. (1988).

A sample of sediment was collected from the top 2 cm of the base of the infiltration basin at the Leach Highway site, and analysed for cadmium, copper, lead, and zinc (Table 5). The sediment consisted of finely laminated silt to fine sand-sized quartz weakly cemented with clay minerals, iron oxides and a small amount of organic matter. The high concentration of lead in the sediment is probably caused by the strong adsorption of this element by iron oxides and clay minerals.

Lead concentrations are likely to be similar in sediments in other infiltration basins around the Perth metropolitan area. These basins are periodically scraped by local councils to remove fine sediment that reduces the water seepage rate. This material should be disposed of in a manner approved by the Health Department.

High concentrations of lead have also been observed by Nightingale (1975) in the top few centimetres of sediment in infiltration basins in California. Nightingale considered that lead concentrations in these sediments were sufficiently high to pose a health hazard where the infiltration basins were used for recreational purposes. Most infiltration basins in the Perth metropolitan area are fenced, and not used for public recreation.

Nitrogen and phosphorus

Concentrations of phosphorus and nitrogen species in groundwater near the infiltration basins were generally low (Table 6), and none of these parameters exceeded NHMRC drinking-water guidelines.

Concentrations of phosphorus were extremely low and generally did not exceed 0.01 mg/L phosphorus expressed as phosphate. The amount of phosphorus produced in residential areas in Perth has been estimated by Gerritse et al. (1988) to be between 40 and 80 kg/ha/year, a proportion of which probably ends up in urban runoff.

Most of the phosphorus is probably removed from runoff water by soil adsorption in the infiltration basins, although uptake by vegetation in these basins may also be an important sink for this element. Most of the nitrogen present in groundwater near the studied infiltration basins is in the form of nitrate, and concentrations of this ion generally did not exceed 1 mg/L NO_3-N. Relatively high nitrate concentrations upgradient of the Marmion Street infiltration basin may be due to a garden fertilizer or septic tank source, rather than from seepage from the infiltration basin.

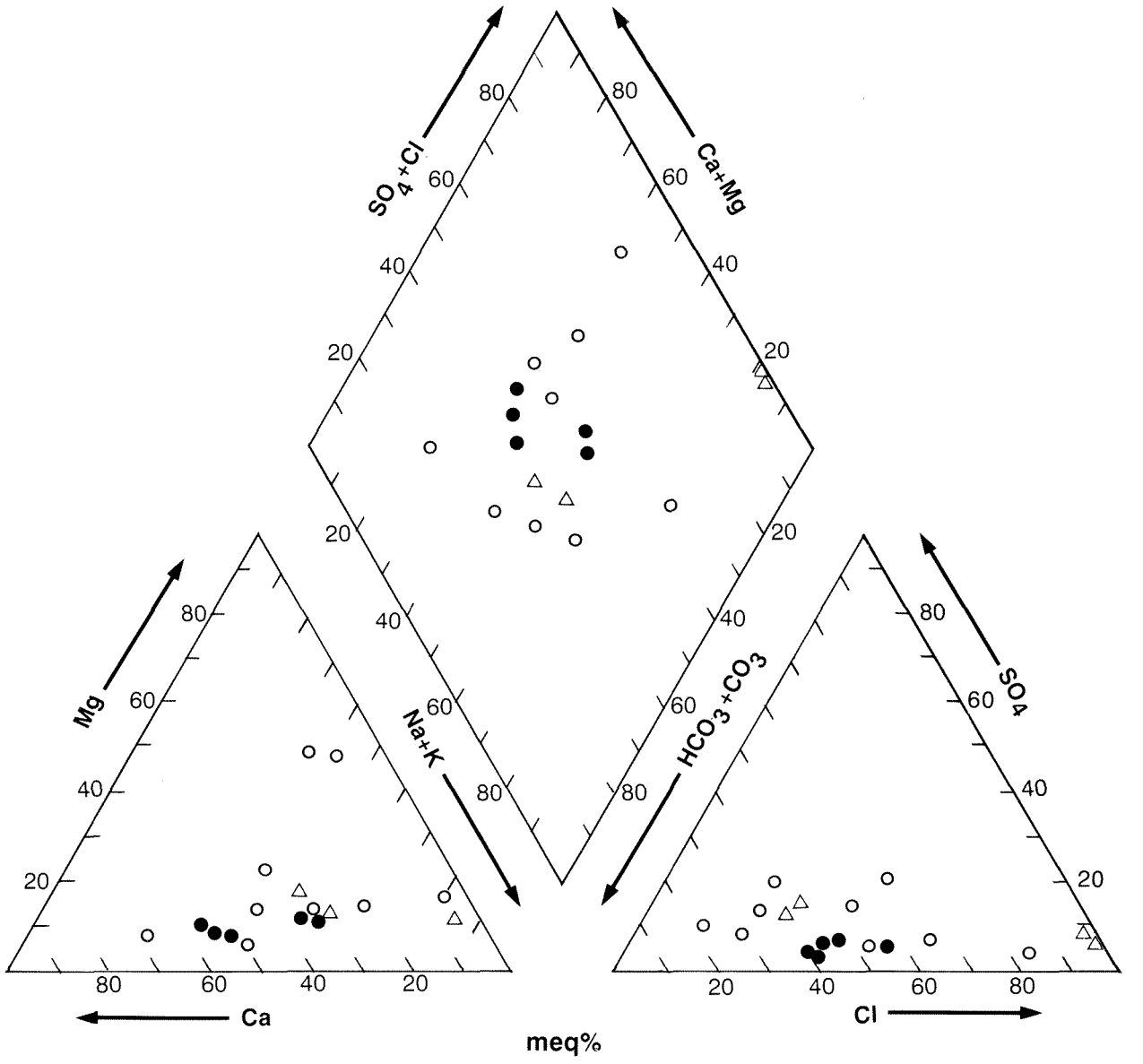

○ Shallow and intermediate bores affected by recharge from the infiltration basins

● Deep bores

△ Bores upgradient of the infiltration basins

PP37 SJA 11

Figure 11. Piper trilinear diagram showing variations in chemical composition at each site

Ammonia concentrations in groundwater were generally less than 0.02 mg/L NH_3-N, and did not show the consistent vertical changes in concentration that have been observed elsewhere in the metropolitan area (Cargeeg et al.,1987).

Gerritse et al. (1988) estimated that about 80 kg/ha/year of nitrogen is applied to gardens and parks in the Perth metropolitan area, and data given by Hart (1982) suggest that up to 10% of this nitrogen could be transported in urban runoff into stormwater infiltration basins. Nitrogen concentrations may be reduced in groundwater near these basins as a result of denitrification, and the direct uptake by vegetation in the infiltration basins.

Pesticides

Analyses of chlordane, DDT and their metabolites, and dieldrin (Table 7) indicate that concentrations of these pesticides generally approach their detection limit of

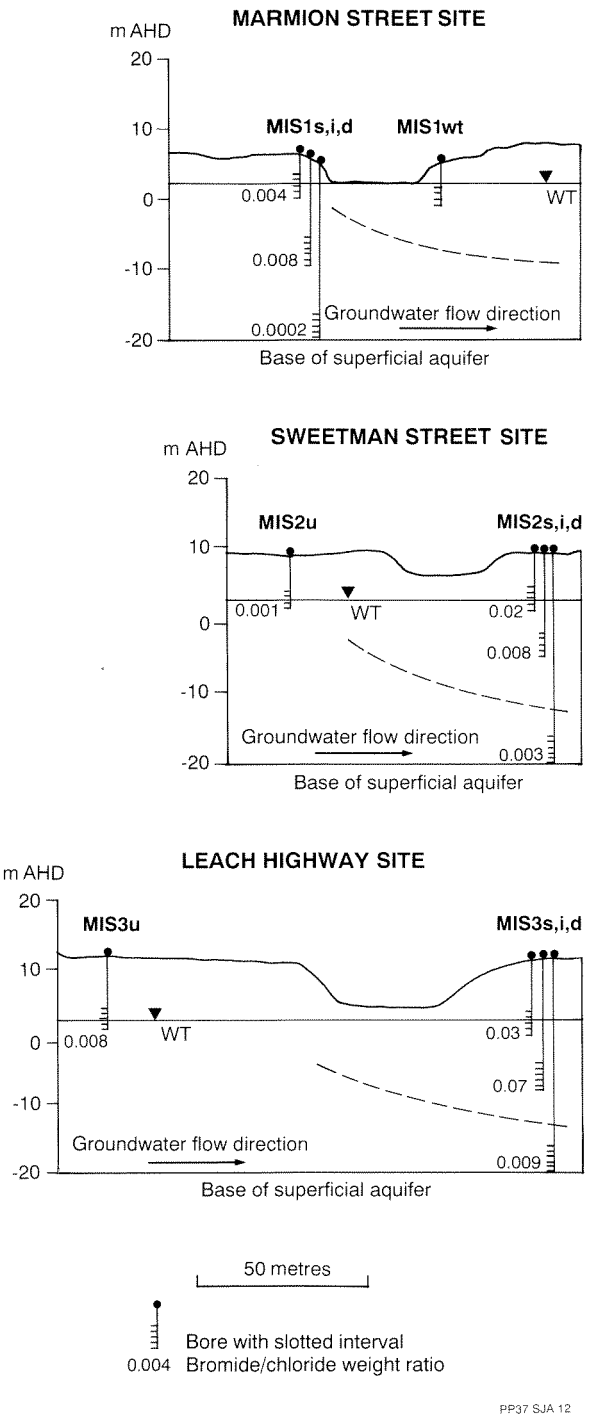

Figure 12. Variations in the bromide/chloride weight ratio in April 1990

0.002 µg/L. Dieldrin was the most commonly detected insecticide which had a peak concentration of 0.018 µg/L at Site 3. This is well below the NHMRC drinking-water guideline for this chemical of 1 µg/L.

No other common organochlorine or organophosphorus pesticides were detected in groundwater samples at levels greater than 0.002 µg/L.

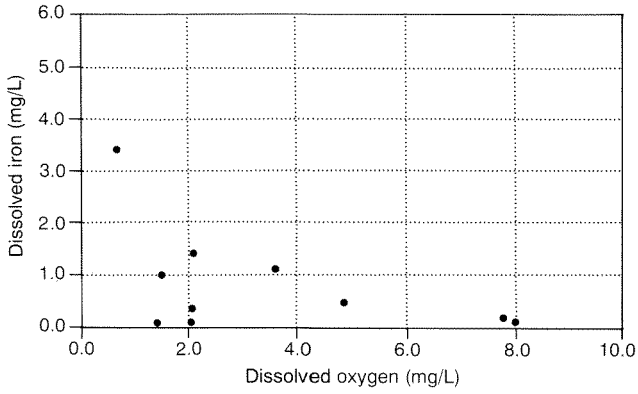

Figure 13. Relationship between dissolved oxygen and dissolved iron

Phenols

Phenols in urban runoff may be produced as a result of the weathering of road asphalt, fuel combustion, and from industrial effluent. Concentrations of phenolic compounds in groundwater samples (Table 7) generally exceeded the NHMRC desirable drinking-water level of 0.002 mg/L, but all concentrations were less than 0.01 mg/L, and are within the range of natural phenol levels detected in shallow bores used for garden reticulation in the Perth metropolitan area.

Other organic compounds

Solvent extracts of water samples were analysed for hydrocarbon (petrol, diesel, and other oil products) concentrations. Concentrations of these compounds were less than 10µg/L in all water samples. A broad scan of solvent extracts from water samples was carried out using gas chromatography–mass spectroscopy to indicate the presence of trace levels of other organic compounds (Table 8). A wide range of organic compounds was detected, some of which are likely to be of natural origin, and some of which are probably man-made.

Of the natural compounds, the most commonly detected were long-chain hydrocarbons which are probably derived from the decay of vegetation.

The most commonly detected compounds of probable man-made origin were phthalates. Phthalate esters (principally bis(2-ethylhexyl) phthalate) are widely used as plasticizers to produce a wide range of polymers with various properties. Phthalates are readily released on the breakdown of plastic materials, and could be released from the large amount of plastic litter washed into the infiltration basins. The compound bis(2-ethylhexyl) phthalate is a US EPA priority pollutant which has been identified in drinking-water supplies (US EPA, 1975) and in 98% of samples of groundwater from New York (Schroeder and Snavely, 1981).

It was not possible to determine phthalate concentrations in groundwater samples in this study because

Table 4. Trace-metal chemical analyses

Bore	*Sample date*	*Cd*	*Pb*	*Hg*	*Cu*	*Cr*	*Zn*
				mg/L			
MIS1s	5 Apr 90	<0.0005	<0.005	<0.0005	0.03	0.001	0.04
MIS1i	5 Apr 90	<0.0005	<0.005	NA	<0.01	<0.001	0.13
MIS1d	5 Apr 90	<0.0005	<0.005	NA	0.01	<0.001	0.02
MIS2s	4 Apr 90	<0.0005	<0.005	<0.0005	<0.01	0.002	0.04
MIS2i	4 Apr 90	<0.0005	<0.005	NA	0.01	0.002	0.09
MIS2d	4 Apr 90	<0.0005	<0.005	NA	<0.01	<0.001	0.03
MIS2u	4 Apr 90	<0.0005	<0.005	NA	0.01	0.005	0.03
MIS3s	3 Apr 90	<0.001	<0.005	<0.0005	<0.02	<0.005	0.05
MIS3i	3 Apr 90	<0.001	<0.005	<0.0005	<0.02	<0.005	0.03
MIS3d	3 Apr 90	<0.001	<0.005	NA	0.05	<0.005	0.02
MIS3u	3 Apr 90	<0.001	<0.005	NA	<0.02	<0.005	0.02
MIS1s	8 Nov 90	<0.001	<0.01	NA	<0.02	<0.02	0.05
MIS1i	8 Nov 90	<0.001	<0.01	NA	<0.02	<0.02	0.03
MIS1d	8 Nov 90	<0.001	<0.01	NA	<0.02	<0.02	0.02
MIS1wt	8 Nov 90	<0.001	<0.01	NA	<0.02	<0.02	0.05
MIS2s	9 Nov 90	<0.001	0.01	NA	<0.02	<0.02	0.07
MIS2i	9 Nov 90	<0.001	<0.01	NA	<0.02	<0.02	0.06
MIS2d	9 Nov 90	<0.001	<0.01	NA	<0.02	<0.02	0.03
MIS2u	9 Nov 90	0.03	0.04	NA	0.21	0.04	1.4
MIS3s	8 Nov 90	<0.001	<0.01	NA	<0.02	0.001	0.42
MIS3i	8 Nov 90	<0.001	<0.01	NA	<0.02	<0.001	0.02
MIS3d	8 Nov 90	<0.001	<0.01	NA	0.02	0.001	0.04
MIS3u	8 Nov 90	<0.001	<0.01	NA	<0.02	<0.001	0.06

Note: NA: not analysed

the PVC casing used to construct the bores was a possible source of contamination for these compounds. Future sampling would have to be carried out from metal-cased bores to verify the presence of phthalates in groundwater.

Micro-organisms

Faecal coliform, faecal streptococci, and salmonella counts were determined in water samples collected for micro-biological analysis. None of these micro-organisms was isolated in groundwater samples, indicating that sediments beneath the infiltration basins are efficiently filtering them out of infiltrating water.

Discussion

Water-quality sampling carried out during this study has indicated that infiltration basins have a negligible impact on groundwater quality, other than a marked reduction in salinity, and an increase in dissolved-oxygen concentrations in the top half of the superficial aquifer.

Substantial amounts of water are recharged to the aquifer from these basins, the volume depending on the catchment area and the percentage of the aquifer that is covered by impervious surfaces: the volume of water recharged annually at Site 2 is at least 3000 m^3, and at Site 3 is at least 23 000 m^3. There is, therefore, some scope for using urban runoff to augment groundwater supplies in those parts of the metropolitan area with limited throughflow and where urban runoff is discharged to the Swan estuary or the ocean. The possibility of using urban runoff to increase groundwater supplies in the Applecross area was examined by Cargeeg et al. (1987), who estimated that the vertical water flux into the superficial aquifer in this area was currently about 490 m^3/ha. They estimated that this could be increased to about 690 m^3/ha if four extra infiltration basins were constructed in areas where the depth to groundwater was greater than 5 m.

The benefits of using infiltration basins to increase recharge locally, however, may be partially offset by an increase in iron-encrustation problems in nearby pumping bores. The rapid recharge of water through the infiltration basins introduces a large amount of dissolved oxygen into the upper part of the aquifer at levels which may be close to saturation concentrations for this gas, and which may be out of equilibrium with iron concentrations in groundwater deeper in the aquifer.

Table 5. Metal concentrations in sediment from the filtration basin at Site 3

Metal	*Concentration (ppm)*
Cadmium	6
Chromium	55
Copper	122
Lead	3 570
Zinc	390

Note: Analysis of whole sediment digested in a mixture of hydrofluoric, nitric and perchloric acids

Table 6. Nutrient analyses

Bore	*Sample date*	*Nitrate*	*Ammonia*	*Total nitrogen*	*Total phosphorus*
MIS1s	5 Apr 90	2.6	<0.02	2.6	0.01
MIS1i	5 Apr 90	6.6	0.32	8.5	<0.01
MIS1d	5 Apr 90	1.1	0.02	1.2	<0.01
MIS2s	4 Apr 90	0.2	<0.02	0.42	<0.01
MIS2i	4 Apr 90	0.3	<0.02	0.3	<0.01
MIS2d	4 Apr 90	0.19	<0.02	0.45	<0.01
MIS2u	4 Apr 90	0.95	<0.02	1.1	<0.01
MIS3s	3 Apr 90	0.02	<0.02	0.14	<0.01
MIS3i	3 Apr 90	0.92	0.04	0.95	<0.01
MIS3d	3 Apr 90	0.19	<0.02	0.20	0.06
MIS3u	3 Apr 90	0.31	<0.02	0.42	<0.01
MIS1s	8 Nov 90	0.02	0.16	0.24	0.01
MIS1i	8 Nov 90	3.7	0.29	4.80	<0.01
MIS1d	8 Nov 90	1.7	0.12	2.20	0.01
MIS1wt	8 Nov 90	0.13	0.08	0.34	0.18
MIS2s	9 Nov 90	0.05	<0.02	0.07	0.01
MIS2i	9 Nov 90	0.03	<0.02	0.05	<0.01
MIS2d	9 Nov 90	0.07	<0.02	0.24	<0.01
MIS2u	9 Nov 90	2.0	<0.02	4.70	0.44
MIS3s	8 Nov 90	0.12	0.04	0.48	0.07
MIS3i	8 Nov 90	0.56	0.02	0.75	<0.01
MIS3d	8 Nov 90	0.03	0.05	0.08	0.01
MIS3u	8 Nov 90	0.45	0.02	0.61	<0.01

Notes: 1. All nitrogen species concentrations are expressed as mg/L of nitrogen
2. Total phosphorus concentrations are expressed as mg/L of phosphate

Table 7. Pesticide and phenol analyses

Bore	*Sample date*	*Phenols (mg/L)*	*Chlordane*	*DDT (µg/L)*	*Dieldrin*
MIS1s	5 Apr 90	<0.001	<0.002	<0.002	<0.002
MIS1i	5 Apr 90	0.002	0.004	<0.002	0.003
MIS1d	5 Apr 90	<0.002	0.002	<0.002	0.003
MIS2s	4 Apr 90	0.005	<0.002	<0.002	<0.002
MIS2i	4 Apr 90	0.004	<0.002	<0.002	0.003
MIS2d	4 Apr 90	0.006	<0.002	<0.002	<0.002
MIS2u	4 Apr 90	0.002	<0.002	<0.002	<0.002
MIS3s	3 Apr 90	0.005	<0.002	<0.002	0.003
MIS3i	3 Apr 90	0.003	0.004	0.002	0.018
MIS3d	3 Apr 90	<0.001	<0.002	<0.002	0.004
MIS3u	3 Apr 90	<0.001	<0.002	<0.002	<0.002
MIS1s	8 Nov 90	NA	NA	NA	0.004
MIS1i	8 Nov 90	NA	NA	NA	<0.002
MIS1d	8 Nov 90	NA	NA	NA	<0.002
MIS1wt	8 Nov 90	NA	NA	NA	0.011
MIS2s	9 Nov 90	NA	NA	NA	0.002
MIS2i	9 Nov 90	NA	NA	NA	0.002
MIS2d	9 Nov 90	NA	NA	NA	0.003
MIS2u	9 Nov 90	NA	NA	NA	0.010
MIS3s	8 Nov 90	NA	NA	NA	0.004
MIS3i	8 Nov 90	NA	NA	NA	0.025
MIS3d	8 Nov 90	NA	NA	NA	0.007
MIS3u	8 Nov 90	NA	NA	NA	0.004

Notes: NA: not analysed

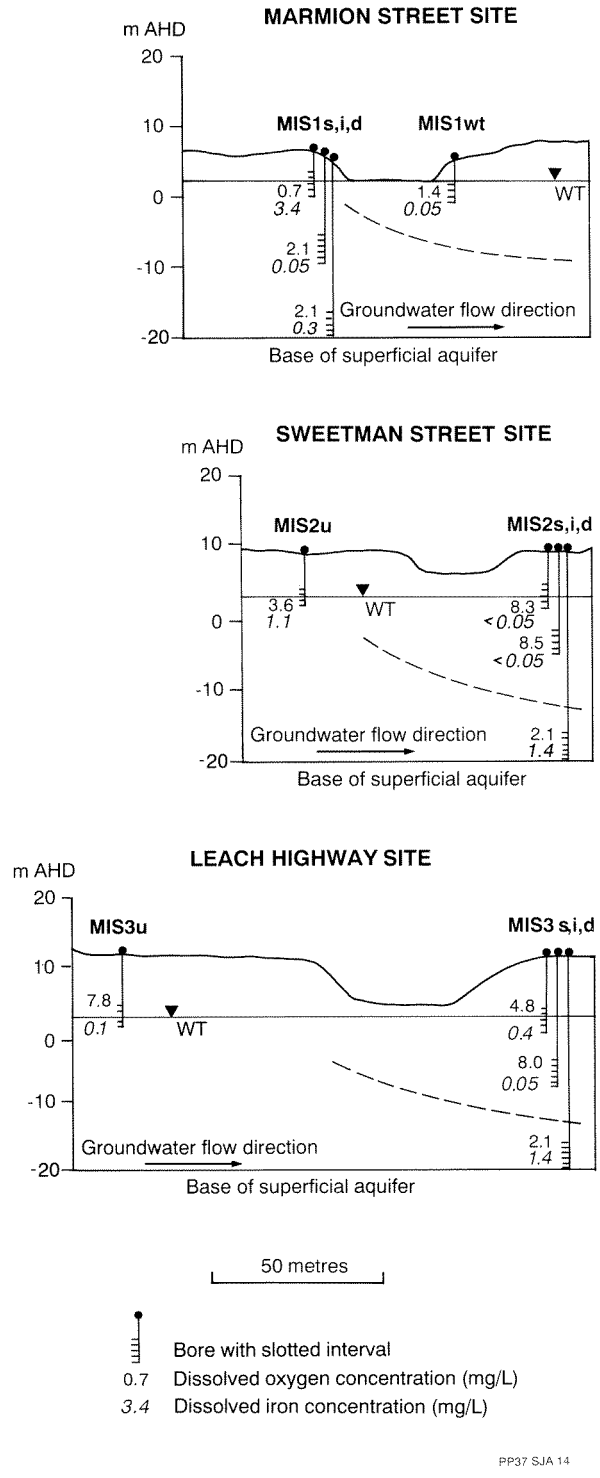

Figure 14. Variations in dissolved oxygen and dissolved iron (mg/L) in November 1990

Water from different levels in the aquifer mixes during pumping and may provide the correct conditions either for the direct precipitation, or the bacterially catalysed precipitation of iron oxides and hydroxides on bore screens. This may be a problem especially where water-supply production bores are located in urban areas, where lack of space limits the availability of sites to locate bores. Production bores in these areas are often located near infiltration basins, or are in parks near lakes which receive urban runoff.

Apart from the fact that production bores near infiltration basins could suffer from iron-encrustation problems, there could be other water-quality problems. Concentrations of phthalates could be unacceptably high in groundwater near these basins, and although concentrations of other organic compounds may not exceed drinking-water guidelines, they may be high enough to produce objectionable tastes or odours in groundwater. There is also the possibility that contaminants from accidental spills on road surfaces could be rapidly transported into groundwater, and produce contamination problems for bores located near infiltration basins. More information on the capacity of sediments beneath infiltration basins to attenuate contaminants is needed before the widespread use of such basins can be considered in Water Authority abstraction areas.

Conclusions

Continuous waterlevel measurements, made between April 9 and November 16 1990 in bores near three infiltration basins, have shown that groundwater levels respond rapidly to recharge from the infiltration basins. Potentiometric levels at the watertable responded within minutes to runoff infiltration, and peak waterlevels occurred within a few hours of the recharge event. Subdued increases in potentiometric levels were also recorded at the base of the superficial aquifer.

The main impact of runoff-recharge on groundwater quality is a marked reduction in salinity and an increase in dissolved-oxygen concentrations in the upper part of the superficial aquifer. The natural groundwater salinity in the study area is generally in the range of 250 to 500 mg/L total dissolved solids. The groundwater salinity in shallow and intermediate bores downgradient of infiltration basins varied between 20 and 140 mg/L, and the dissolved-oxygen concentrations varied between 1.4 and 8.5 mg/L.

The concentration of iron in groundwater near the infiltration basins appears to be controlled by dissolved-oxygen concentrations, with high iron concentrations occurring where dissolved-oxygen concentrations are low. Pumping bores located near infiltration basins may suffer from iron-encrustation problems caused by the mixing of shallow, oxygenated groundwater with water containing higher concentrations of iron.

Concentrations of toxic metals, nutrients, pesticides and phenolic compounds in groundwater near the infiltration basins were very low, and generally well within NHMRC drinking-water guidelines.

Sediment in the infiltration basin at Site 3 contains high concentrations of lead, and it is likely that other basins in the Perth area contain sediment with similar lead levels.

No faecal coliforms, streptococci or salmonella organisms were detected in groundwater near the infiltration basins.

Table 8. Other organic compounds present in water samples

Bore	*Compounds of probable natural origin*	*Compounds of probable man-made origin*
MIS1s	an aliphatic acid	phthalates
MIS1i	-	phthalates
MIS1d	an amide, aliphatic hydrocarbons	-
MIS2s	aliphatic hydrocarbons	phthalates
MIS2i	an aliphatic hydrocarbon	phthaltes
MIS2d	-	alicyclic hydrocarbons
MIS2u	an amide, aliphatic hydrocarbons	phthalates, a phosphate ester
MIS3s	aliphatic hydrocarbons, steroids, an amide	phthalates
MIS3i	steroids, an amide	phthalates
MIS3d	an amide, aliphatic hydrocarbons	phthalates
MIS3u	an amide, aliphatic hydrocarbons	phthalates

Notes: 1. Solvent extracts of samples were screened with GC/MS techniques — no attempt was made to estimate concentrations
2. Samples collected in April 1991

Phthalates were detected in all but one bore near the infiltration basins. These compounds are US EPA priority pollutants, and are possibly derived from the PVC casing used to line boreholes, but may also be derived from plastic litter which accumulates in the infiltration basins.

References

APPLEYARD, S. J., 1986, Rainfall and runoff in the Purdie Avenue catchment in Applecross: Western Australia Geological Survey, Hydrogeology Report 2710 (unpublished).

AUSTRALIAN INSTITUTE OF ENGINEERS, 1987, Australian Rainfall and Runoff: AIE Monograph, v.1 and 2.

CARGEEG, G. C., BOUGHTON, G. N., TOWNLEY, L. R., SMITH, G. R., APPLEYARD, S. J., and SMITH, R. A., 1987, The Perth Urban Water Balance study. Water Authority of Western Australia, 2 vols.

GERRITSE, R. G., BARBER, C., and ADENEY, J. A., 1988, The effect of urbanization on the quality of groundwater in Bassendean Sands: CSIRO Division of Water Resources, Water Resources Series no. 3, 27p.

GERMAN, E. R., 1989, Quantity and quality of stormwater runoff recharged to the Floridan aquifer system in the Orlando area, central Florida: U.S. Geological Survey, Water Supply Paper 2344, 23p.

HART, B. T., 1982, Water quality management: monitoring programs and diffuse runoff. Chisholm Institute of Technology, Water Studies Centre Monograph, p. 121–139.

HULL, R. W., and YUREWICZ, M. C., 1979, Quality of storm runoff to drainage wells in Live Oak, Florida: U.S. Geological Survey, Open File Report 79-1073, 40p.

KIMREY, J. O., 1978, Preliminary appraisal of the geohydrologic aspects of drainage wells, Orlando area, central Florida: U.S. Geological Survey, Water Resources Investigation 78–37, 24p.

McLAUGHLAN, R., 1991, Interim draft report on biofouling in wells and pumping equipment at the Mirrabooka and Gwelup wellfields, Perth, W.A.: University of New South Wales, Centre for Groundwater Management and Hydrogeology, Research Publication 6/91, 22p.

MALMQUIST, P. A., and HÅRD, S., 1981, Groundwater quality changes caused by stormwater infiltration, *in* Urban stormwater quality, management and planning *edited by* BEN CHIE YEN: Proceedings of the Second International Conference on Urban Storm Drainage, Illinois, USA, p. 89–97.

MARTIN, R., 1980, Hydrochemical study of an unconfined aquifer in the vicinity of Perth, Western Australia: University of Western Australia, Ph.D. thesis (unpublished).

MATTHESS, G., 1982, The properties of groundwater. John Wiley and Sons, 406p.

NATIONAL HEALTH AND MEDICAL RESEARCH COUNCIL, 1987, Guidelines for drinking water quality in Australia. NHMRC/AWRC Pamphlet, 33p.

NIGHTINGALE, H. I., 1975, Lead, zinc and copper in soils of urban storm runoff retention basins: Journal of the American Water Works Association, v. 67, p. 443–446.

SARTOR, J. D., and BOYD, G. B., 1972, Water pollution aspects of street surface contaminants: U.S. Environmental Protection Agency, Environment Technology Series Report EPA-R2-72-081.

SCHINER, G. R., and GERMAN, E. R., 1983, Effects of recharge wells on the quality of water in the Floridan aquifer in the Orlando area, central Florida: U.S. Geological Survey, Water-Resources Investigations 82-4094, 124p.

SCHROEDER, R. A., and SNAVELY, D. S., 1981, Survey of selected organic compounds in aquifers of New York state, excluding Long Island: U.S. Geological Survey, Water-Resources Investigations 81-47, 60p.

SEABURN, G. E., and ARONSON, D. A., 1974, Influence of recharge basins on the hydrology of Nassau and Suffolk Counties, Long Island, New York: U.S. Geological Survey, Water Supply Paper 2031, 65p.

U.S. ENVIRONMENTAL PROTECTION AGENCY, 1975, Identification of organic compounds in effluents from industrial sources: U.S. Environmental Protection Agency, Report EPA-560/3-75-002.

Mafic dykes in the Williams–Wandering area, Western Australia

by

J. D. Lewis

Abstract

A small area of the Late Proterozoic Boyagin dyke swarm, 150 km south-southeast of Perth, has been mapped in detail. The area also includes part of the 600 km-long Binneringie Dyke, and an associated hybridized dyke, both members of the early Proterozoic Widgiemooltha dyke swarm. The Boyagin swarm consists of dolerite dykes, generally between 10 m and 20 m thick, in two sets trending northwest and west-northwest, and a minor east-northeast set. In the vicinity of the Binneringie Dyke, the direction of the dyke swarm was deflected anti-clockwise about 20°. The pattern of the Boyagin dyke swarm is interpreted as reflecting intrusion along a conjugate set of Riedel shears associated with a sinistral wrench zone that was reactivated in the final phase of the Pinjarra Orogen. Major northwest-trending lineaments which terminate the Binneringie Dyke are interpreted as similar Riedel shears formed during an earlier ductile phase of orogenesis, at the time of the formation of the proto-Darling Fault.

Thirty chemical analyses are presented, to characterize the dyke swarms. The Binneringie Dyke is calc-alkaline basaltic andesite, and the Boyagin dyke swarm is quartz tholeiitic in composition.

KEYWORDS: Dyke swarms, chemical anayses, Pinjara Orogen, Western Australia

Introduction

A prominent feature of the western part of the Yilgarn Craton is the presence of a number of dense swarms of basaltic to gabbroic dykes of Late Proterozoic to Phanerozoic age (Fig. 1). The dykes occupy a zone about 200 km wide, bounded on the west by the trace of the Darling Fault and extending in a north–south direction for about 1000 km. The general trend of the dykes is northwest over most of the zone, and the swarm has been named the Boyagin dyke swarm by Myers (1990). In the northwest part of the Yilgarn Craton, the swarm is intersected by the Muggamurra dyke swarm, which trends northeast; in the south it is intersected by the Gnowangerup dyke swarm, which trends roughly east.

In addition to these dense swarms of narrow dykes, there is also a widespread, but less numerous, swarm of large east-northeasterly trending dykes which traverse the whole of the craton. These dykes, of Early Proterozoic age, form the Widgiemooltha dyke swarm, the 'Widgiemooltha Dyke Suite' of Sofoulis (1966).

Whereas the dykes of the western swarms can rarely be traced for more than a few kilometres, individual members of the Widgiemooltha dyke swarm can be followed, in outcrop or magnetically, for up to 600 km. Many basic dykes are noted on the 1:250 000-scale geological maps but, except for the large easterly trending dykes in the Eastern Goldfields (where they have been prospected for base metals and platinum) little notice has been taken of them. The principal causes of the neglect are the enormous extent of the dyke swarms, the poor exposure over most of the area, the uniformity of composition, and the presumed lack of economic mineral potential. This paper examines in some detail a relatively well-exposed part of the Boyagin dyke swarm about 150 km south-southeast of Perth, in the vicinity of Williams.

The Williams–Wandering area was chosen following an examination of the regional mapping on a scale of 1:250 000 (Wilde and Lowe, 1980; Wilde and Walker, 1982). In particular, the 1:100 000-scale maps, CROSSMAN and DARKAN, promised both numerous dykes and a variety of dyke directions. The area lies east of the Tertiary laterite sheet which blankets much of the Darling Range, and most of it has been cleared for agriculture, with the result that the trace of major dykes is not obscured by dense forest cover or scrub vegetation.

Previous investigations

Until recently, little work had been done on the basic dykes of the southwest of Western Australia. Prider (1945) summarized studies of a number of small areas along the Darling Scarp; and in later years, honours students of the University of Western Australia have mapped the scarp near Perth in great detail. To the east of Perth, in the vicinity of Meckering, Lewis (1970) described the

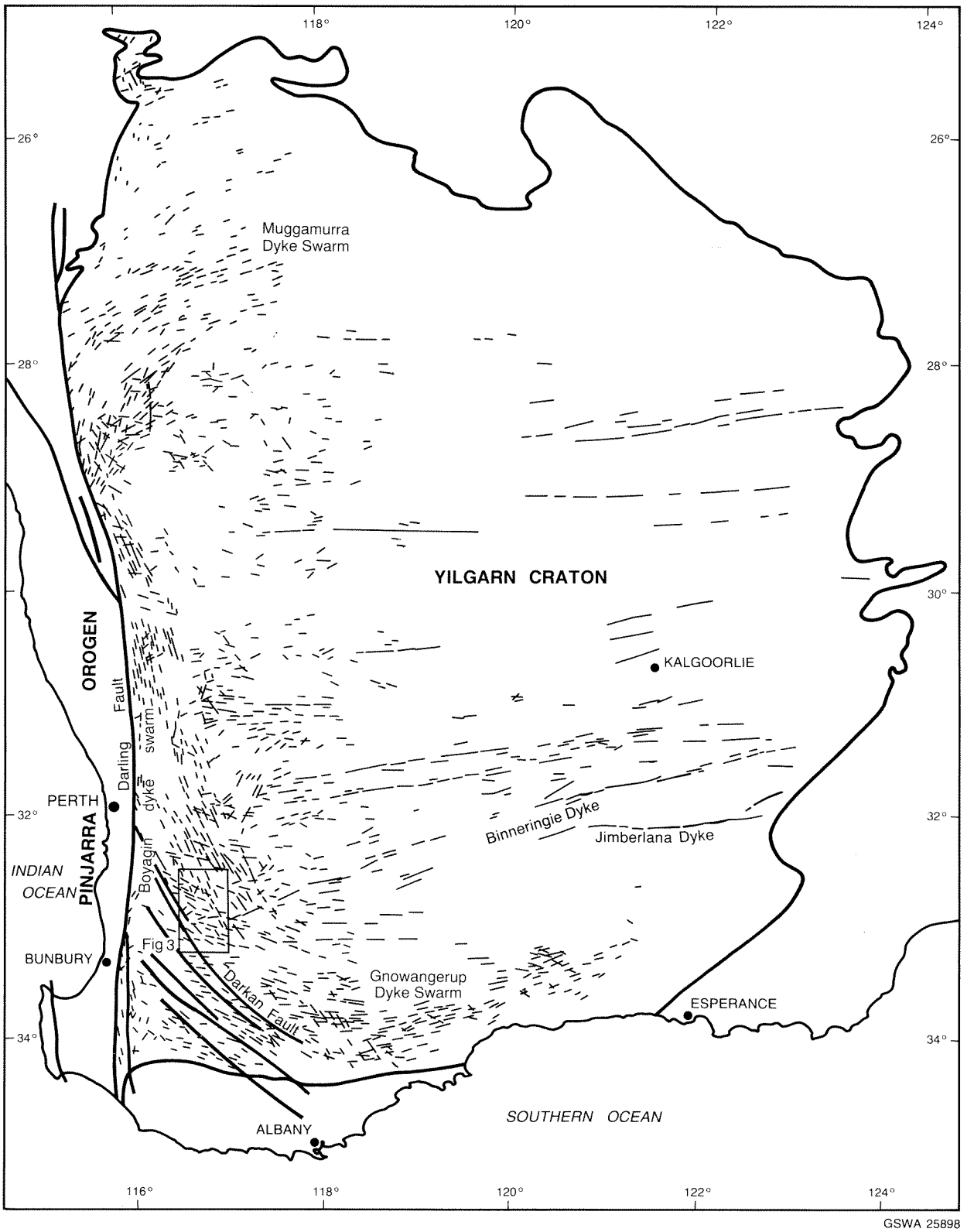

Figure 1. Mafic dyke swarms of the Yilgarn Craton (after Myers, 1990)

petrography and chemistry of a small number of basic dykes contaminated by numerous granitic xenoliths. The palaeomagnetism of basic dykes in the Perth region has been investigated by Giddings (1976), who concluded that five ages of dyke intrusion, ranging from 2500 Ma to 700 Ma, could be distinguished.

The availability of airborne magnetic surveys over the whole of the Yilgarn Craton in recent years has led to a renewed interest in the dyke swarms. Tucker and Boyd (1987) have shown that grey-scaled pixel maps produced from total magnetic intensity data can be used to detect the larger basic dykes in the southwest of Western Australia — particularly the large westerly trending dykes, which are shown to extend to the western margin of the craton. Individual dykes of the Widgiemooltha swarm — particularly the Jimberlana Dyke (Campbell, 1968, 1977; Campbell et al., 1970; Mazzuchelli and Robins, 1973; McClay and Campbell, 1976) and the Binneringie Dyke (McCall and Peers, 1971) — have received considerable attention; but there is no general account of the dyke swarm or of individual dykes outside the Eastern Goldfields Province of the Yilgarn Craton. Isles and Cooke (1990) distinguished six dyke suites in the Eastern Goldfields, and discussed their spatial relationship to pre-existing gold deposits. The only general accounts of all mafic dyke swarms of the Yilgarn are found in Parker et al. (1987), which provides only a short summary of each dyke swarm; and in Hallberg (1987), which reviews past work and provides some chemical data.

Regional geology

That part of the western margin of the Yilgarn Craton intruded by mafic dyke swarms is broadly coincident with the Western Gneiss Terrane of Gee et al. (1981). The terrane consists of repeatedly deformed and metamorphosed ortho- and paragneisses of a variety of ages, intruded by granites which have also been deformed. Enclosed greenstone belts are small and discontinuous, particularly when compared with their abundance in the remainder of the craton. The age of much of the gneiss is more than 3.0 Ga. Cores of detrital zircon from orthoquartzites have been dated at 3.34 Ga, and metamorphic overgrowths at 3.18 Ga (Nieuwland and Compston, 1981). Younger gneisses and deformed granites have Sm–Nd model ages between 3.11 and 2.74 Ga (Fletcher et al., 1983).

Undeformed granites, which intrude the gneiss, underlie large areas in the south of the Western Gneiss Terrane and have been dated by the Rb–Sr isochron method at 2.7–2.5 Ga (Libby and de Laeter, 1979), an age similar to the widespread granite intrusions throughout the remainder of the craton. Zircons from sediments and felsic volcanics of the Saddleback Greenstone Belt, a small greenstone belt enclosed by the granite, give a similar age of 2.65 Ga (Wilde and Pidgeon, 1986).

The Williams–Wandering area is underlain by a variety of granites which form part of the Darling Range Batholith (Wilde and Low, 1980); the largest (2.7–2.5 Ga) intruded the southern part of the Western Gneiss Terrane. The batholith is mostly undeformed, but encloses remnants of older migmatite and gneiss.

To the west, the Yilgarn Craton is terminated by the Darling Fault, a major normal fault that was active during Palaeozoic and Mesozoic times. During that time, up to 6 km of sedimentary rocks were deposited in the Perth Basin (Playford et al., 1976). Beneath the basin lies the largely unknown Pinjarra Orogen (Myers, 1990) of Proterozoic age. The intrusion of the basic dyke swarms in the neighbouring Archaean Yilgarn Craton is probably related to the final post-orogenic phase of development of the Pinjarra Orogen.

The basic dykes

Widgiemooltha dyke swarm

Two major parallel dykes of the Widgiemooltha dyke swarm are present in the Williams area. The Binneringie Dyke, which passes close to the town, extends a further 600 km eastwards to Norseman and beyond. A second dyke, parallel to the Binneringie Dyke and 6 km south of Williams, is confined to DARKAN (1:100 000) and is characterized by abundant granitic xenoliths. Both of the dykes are generally well exposed in the vicinity of Williams, although parts of the outcrop are capped by laterite.

Aeromagnetic data indicate that the Binneringie Dyke occupies a single, continuous fracture, and that it has a positive magnetic anomaly east of Narrogin and a negative anomaly to the west (Tucker and Boyd, 1987). In the field, however, the dyke is discontinuous in outcrop and occupies a series of parallel fractures over a total width of up to 3 km (Fig. 2). East of Wickepin, the dyke forms a positive physiographic feature, particularly in the Wedenin Hills northeast of Kulin where the dyke is at least 300 m wide and forms a ridge about 30 m high. At Walters Hill, 15 km east of Wickepin, the dyke occupies the summit ridge but is largely obscured by laterite. Elsewhere the Binneringie Dyke occurs as low ridges of boulders and small outcrops and is generally 150–200 m wide.

Between Wickepin and Narrogin, the dyke occupies at least four fractures, which step northward as the dyke continues to the west. Here the dyke commonly forms a distinct negative topographic feature, up to 300 m wide, mostly soil covered, but with a few small outcrops and scattered boulders. In the Williams area, and to its western termination south of Meridian Hill, the Binneringie Dyke again forms a strong positive feature. Individual segments of the dyke are up to 4 km long and 400 m wide, and are well exposed in narrow ridges up to 60 m high.

Throughout most of its length, the Binneringie Dyke occupies straight, parallel-sided, vertical fractures; but, in the Williams area and to the west, the dyke pinches, swells, and branches into short apophyses, and its trace is sinuous. In this section, the dyke appears to be a passive intrusion into the granite. For most of its length, the Binneringie

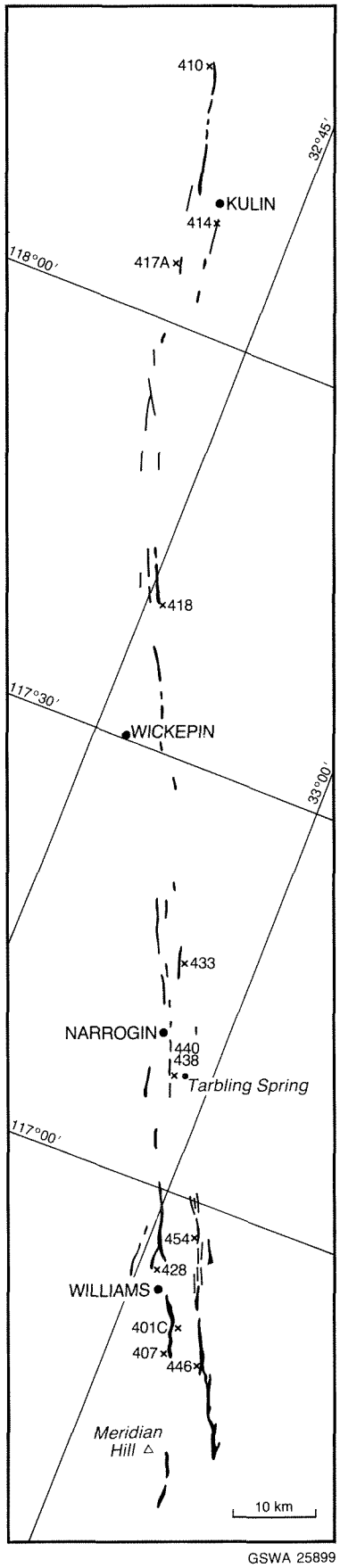

Figure 2. The Binneringie Dyke between Kulin and Williams, showing the location of analysed samples. See Table 1 for sample numbers

Dyke is a single intrusive phase of coarse-grained gabbro, similar in each of the separated outcrops. However, about 5 km north of Williams, a 75 m-wide dyke, similar in overall composition and parallel to the main dyke, dips 70°S and shows prominent banding on a 2–10 cm scale. Possible cross-bedding can be seen in parts. Similar features were described by McCall and Peers (1971) from the eastern end of the Binneringie Dyke, where the banding is believed to result from the combined effects of convection currents within the magma and progressive crystallization inwards from the dyke footwall.

Pods and veins, often several metres long and up to a metre across, of medium-grained, pink, aplitic rock are found throughout the length of the main dyke. There is no evidence of granitic xenoliths in the dyke: the pods are probably segregations of the final melt fraction.

At three locations in this area the Binneringie Dyke is a multiple dyke. At Tarbling Spring, southwest of Narrogin, a coarse dolerite dyke about 200 m wide forms a low ridge to the north of the main dyke and separated from it by a narrow screen of granite up to 50 m wide. A similar pattern is present 5 km southwest of Williams, where a gabbroic dyke, to the south of the main dyke, shows a well-developed chilled margin against an incomplete screen of granite pods each about 50 m long by 10 m wide. Farther southwest, near Meridian Hill, a doleritic phase is present on the northern side of the dyke; this may be a second intrusion or a wide, chilled margin of the main dyke.

South of Williams, a second member of the Widgiemooltha dyke swarm, here named the Binneringie Dyke South, is characterized by abundant granitic xenoliths. This dyke is complex, and occupies a narrow zone of fractures 30 km long, trending 070°, and parallel to the main Binneringie Dyke. Magnetic pixel maps of Tucker and Boyd (1987) show a faint negative anomaly continuing the same trend for a further 40 km west-southwest; but for much of this distance, the anomaly is coincident with a major water-supply pipeline. It is probable that the dyke terminates close to the westernmost outcrop; and almost certainly, neither the northern or southern Binneringie dykes extend west of the major northwesterly trending magnetic lineament of the Darkan Fault.

The Binneringie Dyke South is relatively rectilinear, and for most of its length, occupies a single fracture, or two fractures separated by a screen of granite several hundred metres wide. The dykes are generally 200–300 m wide; but where a single dyke is present, it may be up to 500 m wide. Where the dyke is crossed by the Albany Highway 6 km south of Williams, and continuing to its eastern termination, the Binneringie Dyke South is commonly made up of a number of parallel dykes, each about 30–50 m wide and together occupying a zone up to 1 km wide. Throughout its length, the dyke is notable for the presence of abundant xenocrysts of plagioclase and quartz, granitic xenoliths up to 10 cm across and, rarely, larger xenoliths up to 1 m across. It is probable that the dyke intrudes a contemporaneous fault zone.

Petrography

The Binneringie Dyke: Throughout its length, the Binneringie Dyke is fairly uniform, coarse-grained quartz gabbro, varying only in alteration products and the proportion of interstitial granophyric intergrowth. Essentially, the rock consists of prisms of anhedral to subhedral plagioclase 2–5 mm long — zoned from cores of labradorite (An_{66}) to narrow rims of oligoclase (An_{27}) — and abundant anhedral to subhedral augite aggregates 1–3 mm across. Ilmenite, and pseudomorphs after orthopyroxene, are common and rarely occurring grains of pigeonite are enclosed by augite. Late-stage crystallization has produced small amounts of olive-brown hornblende and biotite, and ubiquitous interstitial patches of granophyre and quartz. Accessory perthite, apatite, and a variety of secondary minerals, are also present, and baddelyite is a rare occurrence in some samples.

Most samples are partly altered: plagioclase is commonly saussuritized or sericitized, and augite may be schillerized and partly replaced by secondary amphiboles or chlorite. A few extensively epidotized specimens contain large interstitial masses of clinozoisite and prehnite.

The most prominent late-stage interstitial phase is a granophyre consisting of quartz and perthite or, less commonly, poorly twinned albite. Quartz and perthite may also form discrete, well-formed crystals. The proportion of granophyric material varies. West of Narrogin, the proportion is 5–10%, and the rock is a normal quartz gabbro; east of Narrogin, the proportion of granophyre increases to between 15 and 25% of the rock and forms an irregular granophyre network throughout the rock. The abundance of granophyre in some specimens produces the appearance of a hybrid rock with patches of gabbroic textured plagioclase, augite, and ilmenite in a 'sea' of granophyre, quartz, and perthite.

The granophyre has formed from the accumulation of a final 'granitic' residuum in the central and upper parts of the intrusion. Where this residuum completely separated from the crystallizing magma, it formed aplitic pods of perthite, oligoclase, quartz, and small amounts of hornblende. There are no partly resorbed xenocrysts of quartz or plagioclase to suggest an origin from assimilated granitic xenoliths. In the western part of the dyke, the residuum either did not separate or it migrated to a portion of the dyke now lost by erosion. It is possible that, in the western portion of the dyke, a deeper cross section has been exposed by uplift and erosion relative to the eastern section. The magnetic signature of the dyke also changes, from positive in the eastern section to negative in the western section.

The Binneringie Dyke South: The southern, xenolith-bearing member of the Widgiemooltha dyke swarm is a medium-grained hybrid rock containing, in varying proportions, xenocrysts of plagioclase and quartz and xenoliths of granite. The xenolithic material has been partly remelted, and its relationship to the surrounding granites cannot be determined; but no rock types other than granite have been found as xenoliths. Incorporation of the low-temperature-melt fraction from the xenoliths, and the complete assimilation of smaller fragments, has given rise to the hybrid nature of the bulk rock.

In thin section, the rock has a doleritic appearance. It contains abundant laths of altered plagioclase up to 1 mm long, anhedral grains of augite about 0.2 mm across, and acicular augite up to 2 mm long. Prismatic orthopyroxene up to 1 mm long is pseudomorphed by chlorite and actinolite, or serpentine. Also present are small patches of interstitial quartz, and abundant interstitial cloudy feldspathic material that constitutes up to 40% of the rock and proves to be extremely fine-grained intergrowths of quartz and feldspar.

Xenocrysts of plagioclase and quartz, up to 2 mm across, make up 10–15% of the rock. The plagioclase is rounded, strongly saussuritized, and contains abundant melt-channels along cleavages; the quartz is embayed and commonly fringed by small diopsidic augite crystals: both were derived from the disaggregation of granitic rocks. Granitic xenoliths within the magma show all stages of melting and disaggregation.

The Boyagin dyke swarm

The dykes of the Boyagin swarm were mapped by airphoto interpretation, and briefly checked in the field for accuracy and rock sampling. Only isolated and dissected remnants of laterite are present in the Williams–Wandering area. Outcrop is more commonly obscured by a thin residual sandy soil. Few dykes present a continuous outcrop through the Tertiary laterite or Quaternary soil. A number of easterly trending gabbroic dykes, particularly in the Williams area, are moderately well exposed for a kilometre or more; but most dolerite dykes are exposed for only a few metres, or are found only as cobbles and boulders in the soil. On airphotos, however, many dykes show up as dark lineaments in the soil, and can be easily plotted. A field check showed only rare examples of cultural features, e.g. fence lines, being mistaken for dykes. A number of dykes were present only as dark, lateritized ridges. The final dyke pattern, slightly simplified, is presented in Figure 3.

All dykes checked in the field were essentially vertical, and very rarely less than 10 m wide. However, in a number of areas, it was evident that many smaller dykes, which did not show up as photo-lineaments, were present; these ranged from less than 1 m, to as much as 10 or 15 m wide. With the exception of the Binneringie Dyke and its associates, the dykes plotted on Figure 3 range from about 10 to 50 m in width, but rare examples reach 100 metres. Figure 3 probably represents 80% of the dykes in this size range. Most omissions are closer to 10 m than 20 m wide, but it is difficult to estimate the proportion of the total dyke swarm omitted. For the dykes plotted on Figure 3, the average thickness is between 15 and 20 m. Dykes less than 10 m thick, and not plotted on Figure 3, probably represent at least an additional 40%, but many would be thin and impersistent.

As presented in Figure 3, the 2400 mafic dykes plotted in the Williams–Wandering area form a pattern only in limited areas where one dyke trend is predominant. When

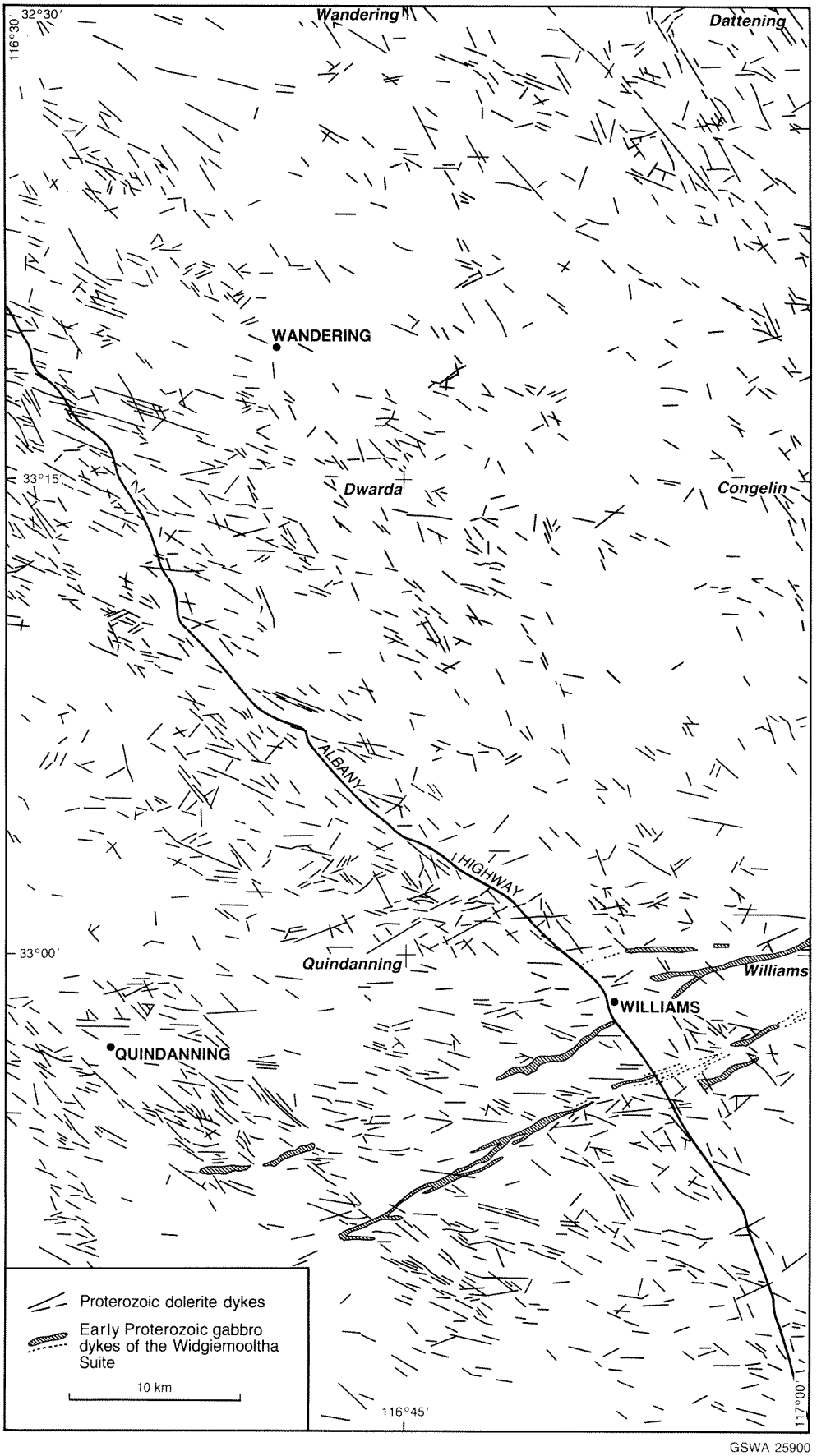

Figure 3. Mafic dykes in the Williams–Wandering area

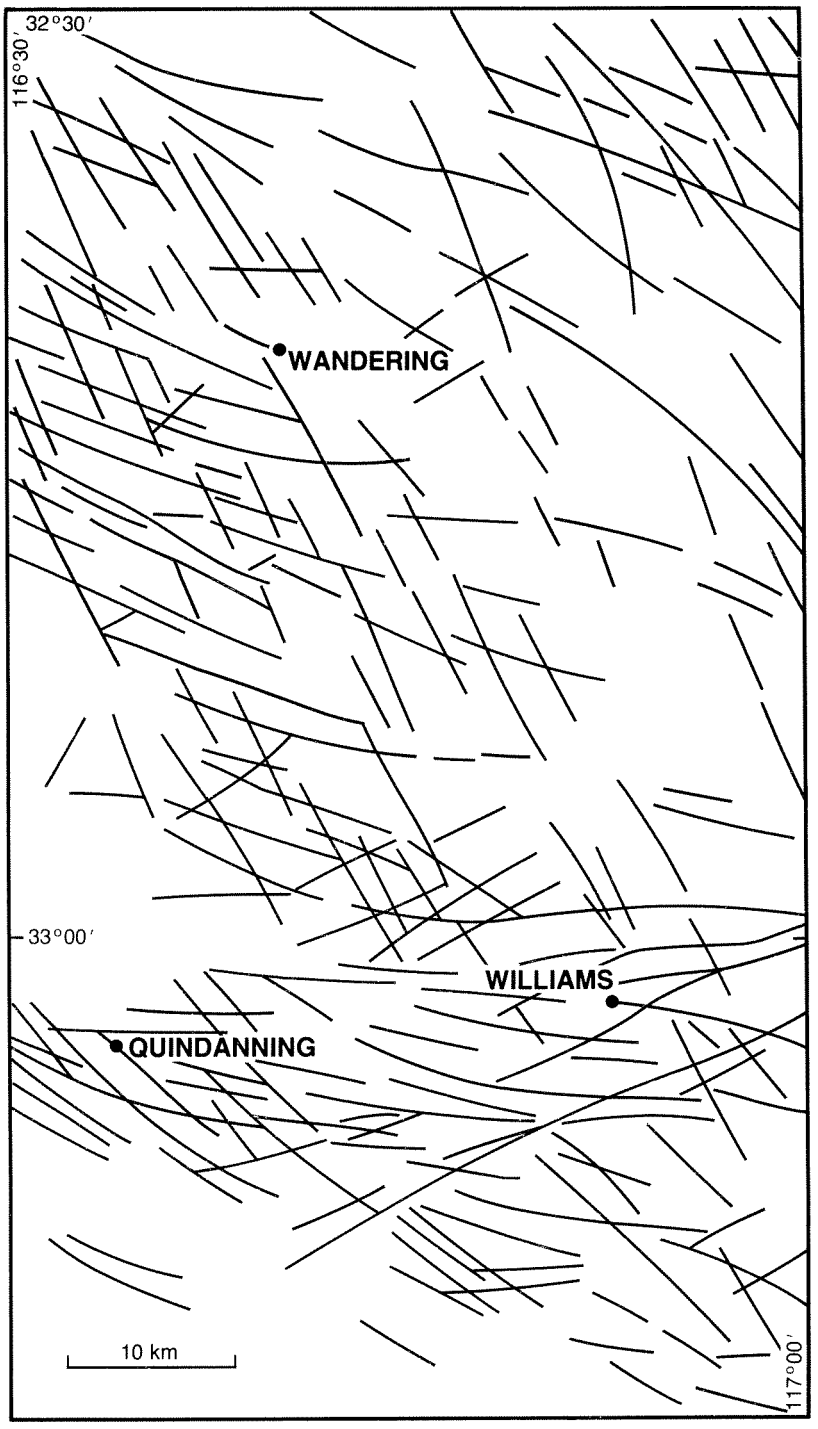

Figure 4. Generalized fracture pattern in the Williams–Wandering area

simplified as a generalized fracture pattern (Fig. 4), or plotted on a rose diagram (Fig. 5), it is evident that the dykes follow a limited number of trends and form distinct dyke sets which intersect each other. North of Williams two trends predominate: northwest (310–330°), and west-northwest (290°) dykes. A less prominent trend (070°) is also evident in some areas. In the Williams area, a number of large westerly (260–270°) trending dykes are present. The Binneringie Dyke, trending 070°, traverses the Williams area, but is not included in the rose diagrams of Figure 5.

Throughout the western and southern parts of the mapped area, dykes trending 270–290° form the most prominent swarm. Only in the Datenning and Congelin areas do dykes trending northwest outnumber those trending west-northwest (Fig. 3). In the Wandering and Dwarda areas the dykes most commonly trend between

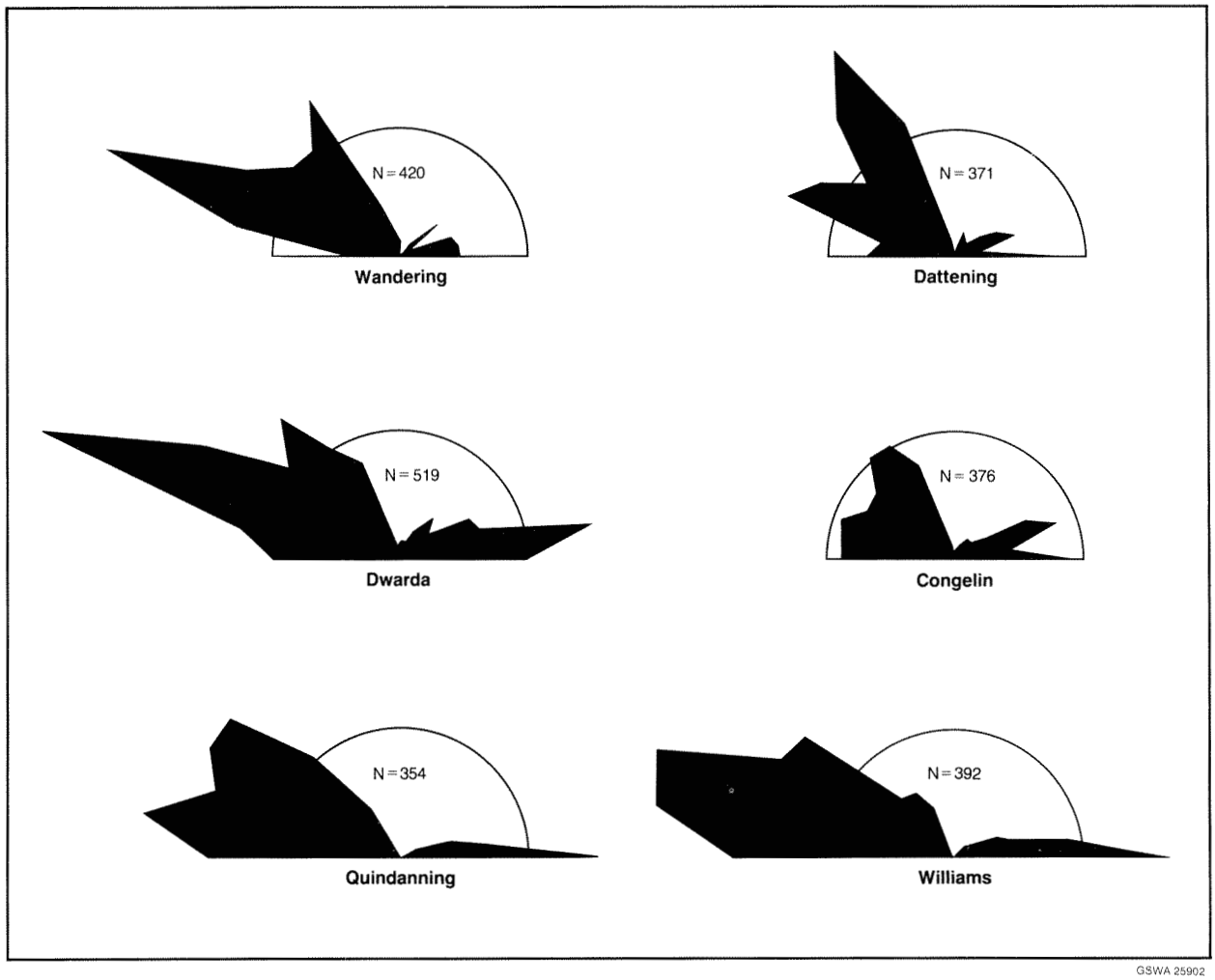

Figure 5. Rose diagrams of dyke direction and length for each 1:50 000 map sheet in the Williams–Wandering area (radius of circle = 20 km)

280 and 300°, but in the Quindanning and Williams areas there is also a strong 260–270° trend (Fig. 5). It appears that, in the southern parts of the region, the general trend of the dykes swings slightly from west-northwest to west; but from Figure 4 it is evident that they form a single dyke set.

The west-northwesterly trending dykes are of coarse-grained dolerite, and some show distinct chilled basaltic marginal zones. They range up to 100 m across, but are mostly about 30 m wide and occupy rectilinear or gently curving fractures. A number of dykes can be traced for up to 3 km, but exposures are generally poor. A common feature of the dykes is a prominent, raised, marginal zone of granite, generally a metre or so high and a few metres wide, with the dyke itself only poorly exposed. A few of the larger dykes in the Williams area occupy the crests of granite ridges that can be as much as 20 m high. In general, the presence of upstanding hornfelsed granitic margins appears to be a function of the width of the dyke, although not all large dykes have noticeable contact aureoles.

A second major dyke set, evident from Figures 4 and 5, trends approximately northwest. In the north of the mapped area, the most prominent dyke direction is 330°; but this progressively swings round to 310° in the Williams and Quindanning areas. The dykes are basaltic to doleritic in texture, between 10 and 20 m wide, and traceable on airphotos for less than 1 km. Groups of related dykes arranged en echelon may be traced for several kilometres, particularly in the Dattening area; many smaller dykes are not detectable on airphotos. Exposure of the dykes is poor: outcrops are rarely more than 100 m long and commonly consist only of scattered boulders. The few dykes which form strong positive features on the landscape are usually thoroughly lateritized.

A small number of dykes, particularly in the Congelin area, trend between 060 and 070°, and suggest a distinct

east-northeasterly trending set. These are narrow, doleritic dykes, petrographically distinct from the Binneringie Dyke, which has a similar trend; they probably occupy fractures conjugate to the west-northwesterly and northwesterly trending dykes.

The relative ages of the northwesterly and west-northwesterly trending dyke swarms is difficult to determine, as few examples of dykes intersecting each other were found in the field. From airphoto interpretation, and the few examples found in outcrop, the two dyke sets appear to be contemporaneous.

Petrography

The petrography of the Boyagin dyke swarm is fairly uniform: the dykes range from coarse-grained quartz dolerite to basalt. The principal minerals are plagioclase laths up to 3 mm long, prismatic to anhedral interstitial augite up to 2 mm across, small amounts of ilmenite, and varying proportions of interstitial quartz and granophyric intergrowth. In a few dykes, interstitial grains and cores of pigeonite are prominent. A small amount of late-stage olive-brown hornblende is commonly present, but biotite occurs rarely. Accessory apatite is common; zircon and baddelyite were rarely noted. A few dykes display ophitic or sub-ophitic texture, and the chilled basaltic marginal facies of many dykes carries abundant small augite phenocrysts.

Plagioclase is commonly zoned, ranging from cores of bytownite (An_{75}) to rims of andesine (An_{35}). Augite is mostly uniform in composition, but a few crystals show rhythmic zoning. Ilmenite varies from small anhedral grains about 0.2 mm across, to large skeletal crystals up to 2 mm across.

The most prominent variation is in the proportion of interstitial quartz and granophyric intergrowth. Most commonly, there is less than 5% of such intergrowth; however, the proportion may rise to about 15% — mostly quartz, but including patches of coarse granophyre. The granophyre is commonly confined to the coarse central part of the dyke; this suggests that it is the result of the late-stage accumulation of a 'granitic' residuum.

Most dykes are extensively altered, although the original textures are preserved. Plagioclase is saussuritized, and in some cases, partly replaced by prehnite. Ilmenite is leucoxenized, and augite has been replaced by actinolite and chlorite. Secondary epidote is common, and there are a few grains of secondary pyrite. A few dykes are completely fresh and preserve both original textures and mineralogy.

Chemistry

Thirty samples from the Binneringie Dyke and Boyagin dyke swarm were analysed for major and trace elements, and are reported in Tables 1–3. The locations of analysed specimens of the Binneringie Dyke are given on Figure 2. Variation diagrams (Fig. 6) show that, chemically, the Binneringie Dyke is easily distinguished from the Boyagin dyke swarm. In particular, the Binneringie Dyke is higher in SiO_2 and lower in MgO, TiO_2, and total FeO, than the later dyke swarm. The trends for (Na_2O + K_2O) versus CaO are similar, but the Binneringie Dyke is more alkalic and less calcic than the Boyagin dykes. Although the range of Mg/(Mg + Fe) ratio is similar for both groups of rocks, the MgO content (and hence FeO+Fe_2O_3) is consistently higher for the Boyagin dyke swarm. In general, the analyses show that the Binneringie Dyke is a calc-alkaline basaltic andesite, whereas the dykes of the Boyagin swarm are low-K tholeiites.

A plot of the analyses on a variety of triangular tectonomagmatic discrimination diagrams (Fig. 7) confirms the calc-alkaline nature of the Binneringie Dyke, and suggests that the Boyagin dyke swarm has a more primitive oceanic signature. Tectonic implications of these signatures (Pearce and Cann, 1973) suggest that the emplacement of the Binneringie Dyke, and hence the Widgiemooltha dyke swarm, was related to a converging plate margin, while the Boyagin swarm was related to a diverging plate margin. The Binneringie Dyke is reasonably related to the 'orogenic' field of Pearce et al. (1977), but the Boyagin dykes are scattered throughout the 'oceanic' and 'continental' fields (Fig. 7C). However, the discrimination is based on the composition and tectonic setting of young basalts and may not apply in detail to Proterozoic dykes.

The trace-element contents for the two groups of analyses are also significantly different. The Binneringie Dyke is comparatively enriched in Ba, LREE, Rb, Th, and Pb; but contains only half the amount of V and Cu; and has lower values for Cr, Sc, and Zn, than the Boyagin dykes.

Analyses of the Binneringie Dyke (Table 1) show a range of compositions, but no systematic variation along the length of the dyke. The variation probably reflects the proportion of interstitial granophyre present in each specimen. Consistent with the field and petrographic observations, the two samples from west of Williams (Table 1, 401C and 407) show least differentiation and are low in SiO_2 and alkalis, and high in Al_2O_3, MgO, and CaO, compared with the remainder of the samples. The two samples are almost identical in composition, but 401C is from a later dyke, chilled against the main dyke from which sample 407 was collected. Samples 440 and 414 are also relatively undifferentiated, and similar in composition to the Binneringie Dyke west of Williams; sample 440 is from a later dyke separated by a granite screen from the main dyke (sample 438), while sample 414 is from a narrow, doleritic portion of the main dyke, near Kulin.

The western portion of the Binneringie Dyke described here is similar in composition to the 'normal gabbro' described by McCall and Peers (1971) from the eastern end of the dyke, in the Eastern Goldfields. Although the dyke pinches and swells in the Williams area, it does not show the extreme variation in thickness or chemistry reported by McCall and Peers. Throughout the length of the main dyke, there is no evidence that the magma has been modified by high-level assimilation of xenoliths or of a low-melting fraction from the wall rocks. Any

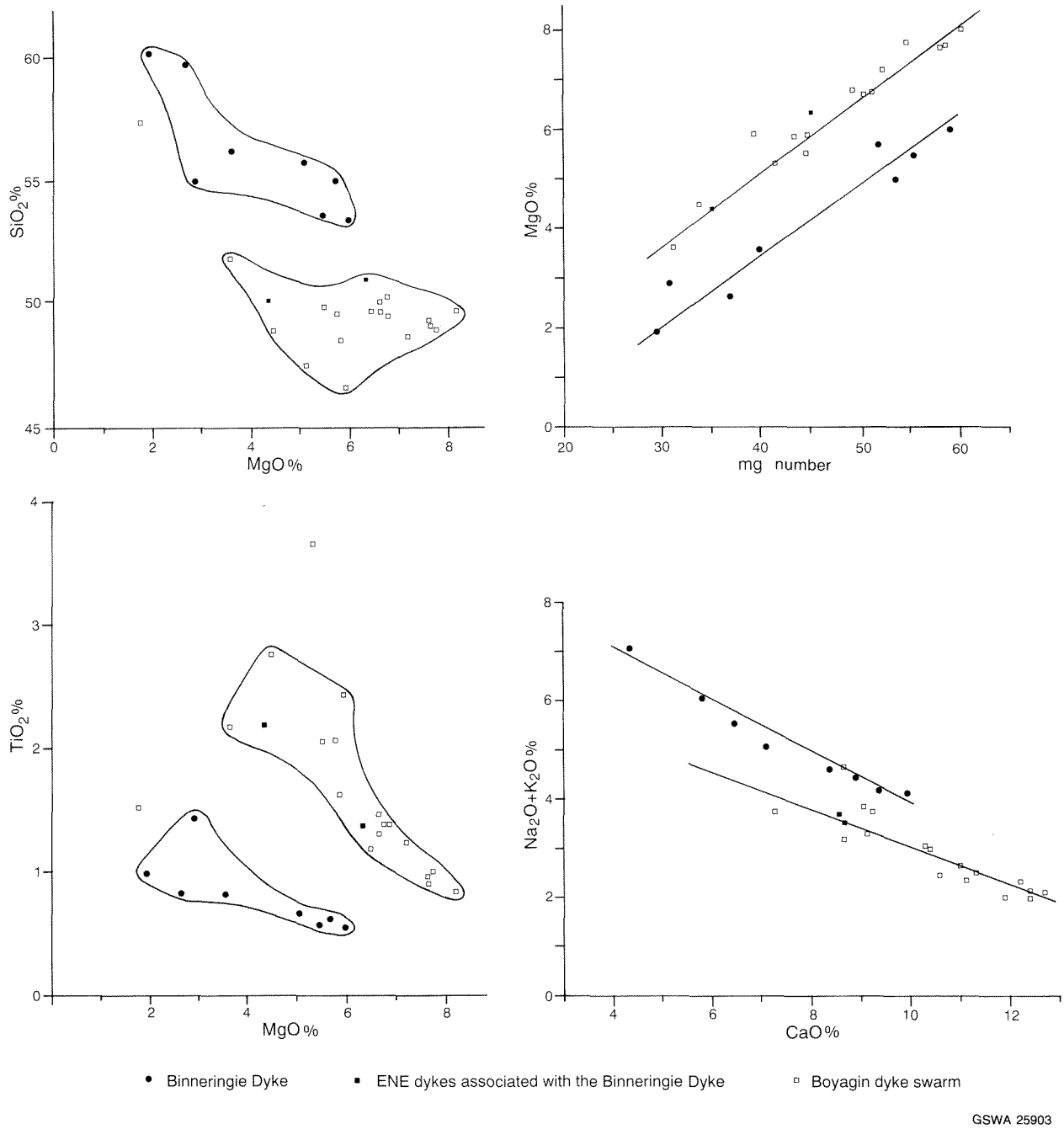

Figure 6. Major-element variation diagrams

modification of an original basltic magma to produce the present basaltic andesite, whether by fractionation or assimilation, must have occurred deep in the crust. However, the magma source, and the mechanism of intrusion for a dyke over 600 km long and of relatively uniform composition, remain problems.

The two analyses of the xenolith-rich Binneringie Dyke South (Table 1, samples 446 and 454) are difficult to interpret if the simple model of assimilation of granite, or a low melting point granitic fraction, by calc-alkaline magma is assumed. Silica and K_2O are suitably elevated, and CaO depressed, but Al_2O_3 is lower than both basalt and granite, and MgO remains high; among the trace elements, Cr at 300–400 ppm is exceptionally abundant. Although, on field and petrographic evidence, the dyke is probably related to the Binneringie Dyke, the nature of the original magma and its hybridization remains problematic.

Two specimens (Table 1, 428,433), collected as part of the Binneringie Dyke, are chemically dissimilar to the other analyses, and plot with the Boyagin dyke swarm in variation diagrams (Fig. 6). Both are coarse-grained gabbroic rocks which, apart from the paucity of interstitial granophyre, appear similar to the other Binneringie Dyke

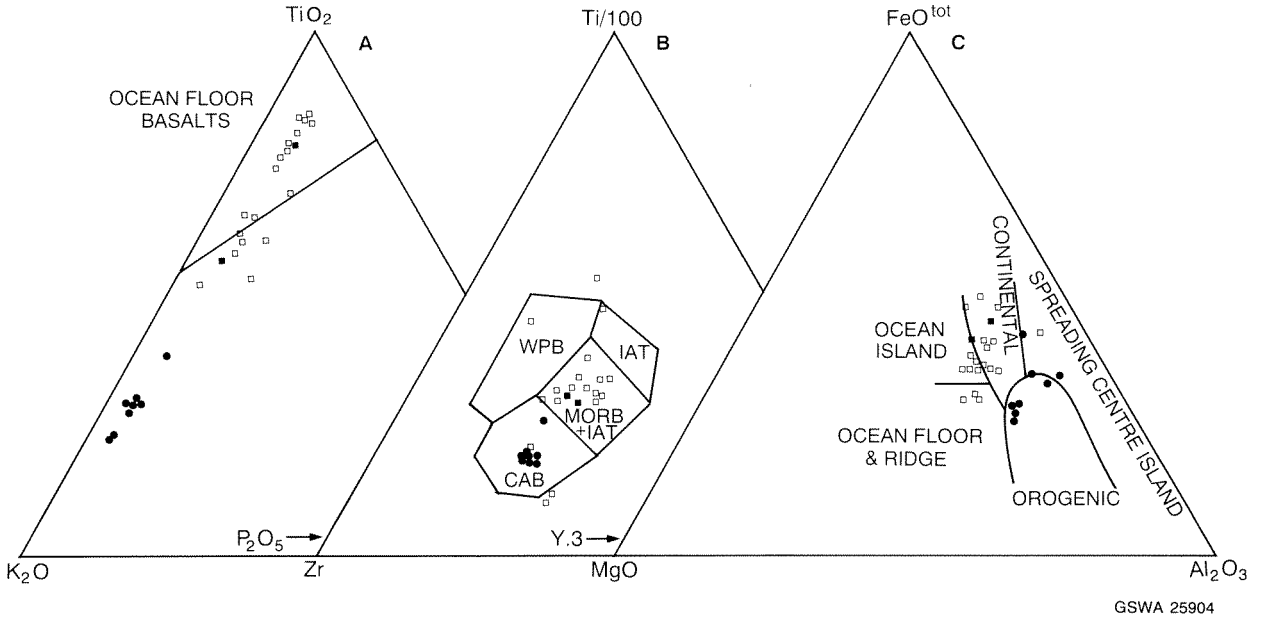

Figure 7. Triangular tectonomagmatic discrimination diagrams. Symbols as in Figure 6. A — after Pearce et al., 1975. B — after Pearce and Cann, 1973. C — after Pearce et al., 1977. (CAB, calc-alkaline basalt; MORB, mid ocean ridge basalt; IAT, island-arc tholeiite; WPB, within plate basalt)

samples. It is probable that the two dykes are east-northeasterly trending members of the Boyagin swarm, and occupy fractures conjugate to the principal west-northwesterly and northwesterly trending fractures. The intrusion of the dykes was possibly influenced by the pre-existing Binneringie Dyke, which follows the same east-northeasterly trend.

The mean compositions of the west-northwesterly and northwesterly trending dykes of the Boyagin dyke swarm are sufficiently similar to indicate that they are co-magmatic (Table 2, column B; Table 3, column C) and of quartz-tholeiite composition. In addition, the two east-northeasterly trending tholeiite dykes associated with the Binneringie Dyke (Table 1, samples 428 and 433) are of similar composition; this is consistent with their being part of the same dyke swarm. On variation diagrams (Figs 6, 7), all the dykes plot together, confirming that they are a single swarm.

Analyses of the northwesterly trending dykes (Table 3) cluster closely around the mean composition, while those of the west-northwesterly trending swarm are more variable in their major-element chemistry. This probably reflects the fact that the northwesterly trending dykes are commonly less than 20 m thick and were not subject to post-emplacement differentiation, whereas the west-northwesterly trending dykes are up to 100 m wide and often show the accumulation of a final granophyric phase in the central parts of the dyke. For example, specimen 476 (Table 2), from the central part of a large east-trending dyke, is high in SiO_2 and alkalis but low in CaO and MgO compared with the mean composition; the trace elements are enriched in LREE, Y, and Zr, and depleted in Cr, Ni, and V. In general, the trace-element contents of the two groups of dykes are comparable, and the only notable feature is a number of dykes with more than 200 ppm Cu.

All analyses except that for sample 552 (Table 3) are quartz normative, but this dyke is low in SiO_2 and CaO, has a high K_2O content and very high TiO_2, and is olivine normative. However, the trace elements Ba, LREE, Nb, and Sr are high, while Cr and Ni are low when compared with the quartz tholeiites. Petrographically the rock is similar to other members of the dyke swarm, but its chemistry is difficult to interpret.

Discussion

It is evident that members of two independent basic dyke swarms are present in the Williams area: the Binneringie Dyke, a member of the Widgiemooltha dyke swarm, centred on the eastern margin of the Yilgarn Craton; and the numerous basaltic and doleritic dykes of the Boyagin dyke swarm, which have been emplaced along the western margin of the craton. The dyke swarms differ in age, composition, and pattern of intrusion, although the presence of the large Binneringie Dyke appears to have locally influenced the trend of the later Boyagin swarm.

In the Kalgoorlie area, the Widgiemooltha dyke swarm is generally represented by a small number of very large dykes, often more than 200 km long, and up to a kilometre or more wide. The dykes are calc-alkaline, only lightly metamorphosed, and trend in two major directions, east-northeast and east. Aeromagnetic data used by Isles and Cooke (1990) suggest that many more dykes are concealed beneath Quaternary cover. Within this swarm, the

Table 1. Analyses of the Binneringie Dyke and associated dykes

	Binneringie Dyke									*Binneringie Dyke South*		*East-northeast-trending dolerite dykes*	
Sample number:	*104401C*	*104407*	*104410*	*104414*	*104417A*	*104418*	*104438*	*104440*	*A*	*104446*	*104454*	*104428*	*104433*
Map name:	*Darkan*	*Darkan*	*Kulin*	*Kulin*	*Kulin*	*Yealering*	*Narrogin*	*Narrogin*		*Darkan*	*Darkan*	*Darkan*	*Narrogin*
Grid reference:	*847424*	*823412*	*230910*	*060840*	*003865*	*626744*	*126532*	*126535*		*829378*	*962434*	*911470*	*248573*
							percent						
SiO_2	53.40	53.70	54.90	55.00	56.20	61.10	59.70	55.80	56.23	65.20	66.70	50.90	50.10
TiO_2	0.54	0.57	1.43	0.63	0.82	0.99	0.84	0.67	0.81	0.35	0.32	1.38	2.21
Al_2O_3	15.90	15.50	13.20	14.70	14.40	13.90	14.10	14.70	14.55	12.50	13.00	12.90	13.10
Fe_2O_3	1.54	1.76	3.99	1.43	2.65	3.17	1.92	1.62	2.26	1.26	1.14	3.48	4.00
FeO	5.96	6.22	8.18	6.37	7.19	5.40	6.27	6.33	6.49	2.88	2.61	10.10	10.50
MnO	0.15	0.15	0.19	0.15	0.18	0.15	0.14	0.15	0.16	0.08	0.07	0.25	0.24
MgO	5.98	5.47	2.92	5.72	3.58	1.94	2.65	5.08	4.17	4.24	3.48	6.33	4.36
CaO	9.90	9.36	6.45	8.87	7.10	4.33	5.72	8.34	7.51	3.96	3.40	8.63	8.57
Na_2O	2.95	2.90	3.46	3.02	3.22	3.83	3.49	2.95	3.23	3.08	3.49	2.61	3.28
K_2O	1.20	1.28	2.08	1.44	1.84	3.23	2.60	1.66	1.92	3.06	2.74	0.90	0.41
P_2O_5	0.08	0.08	0.22	0.08	0.15	0.17	0.13	0.10	0.13	0.05	0.06	0.13	0.21
CO_2	0.23	0.11	0.16	0.08	0.06	0.02	0.10	0.09	0.11	0.10	0.14	0.02	0.22
LOI	2.03	2.18	2.42	1.99	2.21	1.90	1.47	2.30	2.06	2.08	2.09	2.00	2.90
Rest	0.26	0.23	0.35	0.27	0.27	0.26	0.29	0.27	0.28	0.30	0.25	0.29	0.34
- O≡F,S	0.03	0.02	0.06	0.04	0.03	0.00	0.04	0.04	0.03	0.02	0.01	0.02	0.06
Total	**100.08**	**99.49**	**99.90**	**99.71**	**99.84**	**100.39**	**99.38**	**100.02**	**99.85**	**99.12**	**99.48**	**99.89**	**100.38**
							parts per million						
Ba	353	373	626	371	564	739	629	409	508	714	659	400	90
Ce	31	34	64	41	59	80	66	47	53	50	54	33	24
Cr	114	59	4	163	8	5	7	125	61	406	296	106	31
Cu	92	107	89	86	93	50	57	81	82	36	31	203	125
F	220	172	480	260	410	475	385	270	334	247	229	260	290
Ga	16	16	18	17	18	17	18	16	17	14	15	19	22
La	17	22	28	21	30	40	30	23	26	30	27	17	10
Li	13	10	19	12	11	7	13	15	12	21	15	12	12
Nb	<7	< 7	9	< 7	< 7	8	7	< 7	< 7	< 7	< 7	9	12
Ni	123	105	35	121	50	30	41	96	75	132	95	103	40
Pb	8	12	16	13	17	23	22	15	16	36	22	8	< 4
Rb	47	41	74	51	59	111	89	61	67	116	84	37	13
S	500	300	700	500	300	< 100	500	500	419	200	100	200	1 000
Sc	28	27	29	26	26	18	21	24	25	11	10	34	37
Sn	< 4	< 4	< 4	< 4	< 4	<4	4	< 4	< 4	< 4	< 4	< 4	< 4
Sr	244	247	202	191	222	150	183	182	203	176	185	205	381
Th	6	7	12	10	10	16	15	9	11	16	17	4	< 2
U	<2	< 2	2	2	< 2	3	4	< 2	2	4	3	2	< 2
V	166	166	269	168	138	155	152	168	173	74	65	323	381
Y	16	15	29	17	26	28	24	19	22	13	13	29	40
Zn	66	72	123	70	97	85	81	75	84	51	43	127	135
Zr	93	101	164	112	153	182	156	119	135	132	137	122	186

Note: A = average for Binneringie Dyke

Table 2. Analyses of the Boyagin dyke swarm (west-northwesterly trending dykes)

Sample number :	*104461A*	*104463B*	*104476*	*104477*	*104479A*	*104482*	*104486*	*104489*	*104490D*	
Map name :	*Darkan*	*Darkan*	*Crossman*	*Crossman*	*Crossman*	*Crossman*	*Crossman*	*Crossman*	*Crossman*	*B*
Grid reference :	*832298*	*905418*	*978845*	*793945*	*678817*	*637655*	*977848*	*550838*	*571806*	
					percent					
SiO_2	46.60	49.70	57.40	49.30	48.90	49.00	51.90	49.10	48.70	50.07
TiO_2	2.45	1.31	1.51	0.91	2.77	1.00	2.18	0.96	1.24	1.59
Al_2O_3	12.10	13.40	12.80	14.20	11.70	13.20	12.30	14.70	13.70	13.12
Fe_2O_3	5.45	3.21	3.15	2.84	3.93	2.87	4.46	2.88	2.96	3.53
FeO	11.30	8.70	8.02	7.01	12.10	8.81	10.20	6.92	9.02	9.12
MnO	0.31	0.22	0.21	0.20	0.29	0.23	0.24	0.18	0.22	0.23
MgO	5.94	6.66	1.78	7.62	4.49	7.74	3.57	7.65	7.20	5.85
CaO	9.09	11.10	5.88	12.40	8.65	12.40	7.26	12.70	11.90	10.15
Na_2O	2.91	2.10	3.60	1.73	2.88	1.88	3.15	1.86	1.89	2.44
K_2O	0.37	0.27	0.97	0.40	0.29	0.11	0.60	0.25	0.12	0.38
P_2O_5	0.19	0.11	0.36	0.08	0.27	0.08	0.35	0.08	0.10	0.18
CO_2	0.15	0.17	0.17	0.10	0.29	0.16	0.12	0.13	0.15	0.16
LOI	3.01	2.08	2.55	2.14	2.78	1.73	3.07	2.52	1.96	2.43
Rest	0.31	0.27	0.44	0.23	0.41	0.23	0.31	0.24	0.26	0.30
-O≡F,S	0.05	0.04	0.09	0.02	0.09	0.03	0.05	0.03	0.04	0.05
Total	**100.14**	**99.26**	**98.74**	**99.14**	**99.65**	**99.41**	**99.66**	**100.13**	**99.37**	**99.50**
					parts per million					
Ba	95	77	238	217	107	59	138	77	36	116
Ce	20	12	106	12	36	10	50	13	6	29
Cr	32	143	7	196	58	111	28	175	127	97
Cu	216	209	177	134	135	165	116	138	162	161
F	260	203	970	135	475	160	500	170	188	340
Ga	23	17	27	14	22	17	24	14	15	19
La	6	5	40	6	14	< 5	17	< 5	< 5	11
Li	14	11	12	20	13	< 6	16	9	19	13
Nb	7	< 7	22	< 7	14	< 7	13	< 7	< 7	8
Ni	58	92	14	121	44	105	34	130	102	78
Pb	< 4	< 4	< 4	4	< 4	< 4	5	<4	< 4	< 4
Rb	22	13	27	22	8	3	23	14	6	15
S	700	700	1 000	200	1 500	500	500	500	700	700
Sc	42	41	22	38	37	43	30	36	40	37
Sn	4	< 4	5	< 4	< 4	< 4	6	< 4	< 4	< 4
Sr	166	156	197	147	180	132	160	154	134	158
Th	< 2	< 2	5	< 2	< 2	< 2	2	< 2	< 2	< 2
U	< 2	< 2	< 2	< 2	< 2	< 2	< 2	< 2	< 2	< 2
V	475	319	165	283	418	324	328	280	325	324
Y	35	21	100	17	47	19	58	17	21	37
Zn	149	97	151	90	138	90	190	71	92	119
Zr	138	90	509	68	217	61	285	65	76	168

Note: B = average for WNW dykes

Binneringie Dyke, which extends across most of the width of the craton, is the longest. Two members of the swarm have been dated at about 2.4 Ga (Turek, 1966; Fletcher et al., 1987), and intrusion followed a widespread period of tectonism and granite intrusion at about 2.6 Ga.

The western termination of the Binneringie Dyke, and that of the associated xenolith-rich Binneringie Dyke South, appear to be at, or close to, the Darkan Fault, one of a number of prominent northwest-trending magnetically defined lineaments cutting the southwest corner of the Yilgarn Craton (Tucker and D'Addario, 1986). These faults or fracture zones are associated with the Pinjarra Orogen, which is believed to have been initiated between 2.0 and 1.1 Ga (Myers, 1990), and are known to displace parts of the Albany–Fraser Orogen, which is dated between 1.8 and 1.0 Ga. However, the Darkan Fault is also associated with the Saddleback greenstone belt, dated at 2.65 Ga (Wilde and Pidgeon, 1986), and pegmatite intruding a similar shear zone in the Greenbushes area is dated at 2.53 Ga (Partington et al., 1986). It is possible that the earliest movement on the Darkan Fault and other shear zones in the southwest is related to the 2.65 Ga proto-Darling Fault (Blight et al., 1981), and that further displacement occurred intermittently over an extended period. If this is so, the Darkan Fault would have existed before 2.4 Ga, and could have formed a terminating cross-fracture when the Binneringie Dyke was intruded.

Intrusion of the Boyagin dyke swarm followed the formation of the Pinjarra Orogen, a narrow belt of granites and gneisses west of the Darling Fault that is mostly buried

Table 3. Analyses of the Boyagin dyke swarm (northwesterly trending dykes)

Sample Number :	*104508*	*104512*	*104520*	*104527*	*104536*	*104540*	*104548*	*104551*		*104552*
Map Name :	*Darkan*	*Darkan*	*Darkan*	*Crossman*	*Crossman*	*Crossman*	*Crossman*	*Crossman*	*C*	*Crossman*
Grid reference :	*961371*	*987287*	*678379*	*868493*	*671720*	*982847*	*907966*	*790943*		*672807*
					percent					
SiO_2	49.90	49.80	48.50	49.60	49.50	50.30	49.70	50.10	49.67	47.50
TiO_2	2.06	1.19	1.63	2.08	1.39	1.39	0.84	1.47	1.51	3.67
Al_2O_3	14.20	14.90	13.90	13.80	13.40	13.80	14.10	13.90	14.00	14.00
Fe_2O_3	2.57	3.12	3.89	2.56	2.79	2.38	3.26	2.14	2.84	3.54
FeO	9.81	8.39	10.00	10.30	9.90	9.18	6.49	9.62	9.21	10.00
MnO	0.22	0.22	0.24	0.24	0.24	0.22	0.19	0.23	0.22	0.25
MgO	5.51	6.49	5.84	5.77	6.80	6.76	8.02	6.63	6.48	5.31
CaO	9.21	11.30	10.50	9.03	11.00	10.30	12.20	10.40	10.49	8.58
Na_2O	2.66	2.28	2.27	2.60	2.36	2.34	1.64	2.36	2.31	2.95
K_2O	1.09	0.22	0.20	1.25	0.32	0.71	0.70	0.63	0.64	1.70
P_2O_5	0.25	0.09	0.11	0.26	0.11	0.15	0.07	0.15	0.15	0.71
CO_2	0.09	0.10	0.19	0.14	0.19	0.14	0.12	0.14	0.14	0.15
LOI	1.56	1.84	2.22	2.23	2.23	1.82	2.36	1.69	1.99	1.72
Rest	0.34	0.23	0.30	0.35	0.29	0.28	0.25	0.30	0.30	0.50
-O≡F,S	0.05	0.03	0.06	0.05	0.06	0.04	0.04	0.05	0.05	0.07
Total	**99.43**	**100.14**	**99.74**	**100.16**	**100.47**	**99.73**	**99.91**	**99.71**	**99.91**	**100.51**
					parts per million					
Ba	446	60	60	445	53	196	125	231	202	1 176
Ce	62	10	13	64	16	34	11	30	30	85
Cr	94	86	33	77	69	156	203	150	108	49
Cu	58	202	237	72	197	97	125	105	137	40
F	510	154	183	510	187	315	255	320	304	800
Ga	20	17	18	18	17	17	13	17	17	19
La	30	< 5	5	30	<5	16	7	17	14	43
Li	< 6	< 6	< 6	13	10	10	23	8	9	8
Nb	16	< 7	< 7	17	< 7	8	< 7	8	8	18
Ni	51	83	64	58	76	77	115	71	74	42
Pb	7	< 4	< 4	6	< 4	5	5	< 4	4	5
Rb	33	8	8	45	16	27	52	24	27	30
S	500	500	1 000	500	1 000	500	500	700	650	700
Sc	32	39	37	33	39	37	37	26	35	25
Sn	< 4	< 4	< 4	< 4	4	< 4	<4	< 4	< 4	< 4
Sr	283	146	146	261	127	212	141	231	193	598
Th	5	< 2	2	4	< 2	2	< 2	2	2	4
U	2	< 2	< 2	< 2	< 2	< 2	< 2	< 2	< 2	<2
V	347	327	439	350	368	304	265	307	338	344
Y	31	21	24	32	25	24	18	23	25	22
Zn	113	103	118	137	113	96	79	99	107	91
Zr	194	74	88	200	88	126	62	123	119	204

Note: C = average for NW dykes

beneath a thick cover of Phanerozoic sediments forming the Perth Basin. Basement rocks of the orogen have Sm–Nd model ages between 2.1 and 1.1 Ga (Fletcher et al., 1985); but, between 1.1 and 0.7 Ga, there was a final phase of tectonic and metamorphic activity dominated by sinistral transcurrent faulting (Harris, 1987). Normal faulting continued on the Darling Fault into Palaeozoic and Mesozoic times. Dykes are not known to intrude the Leeuwin Complex, the only exposed portion of the southern part of the Pinjarra Orogen, but are found cutting the Moora and Cardup Group sedimentary rocks along the Darling Fault. The age of the Cardup Group is thought to be between 750 and 600 Ma (Compston and Pidgeon, 1962; Playford et al., 1976). Northeasterly trending dykes of the Muggamurra dyke swarm, which is broadly similar in age to the Boyagin swarm, intrude the Northampton Complex and have been dated at 750 and 550 Ma (Embleton and Schmidt, 1985). The only age determination on a dyke of the Boyagin swarm is from a sheared and metasomatized dyke margin; it gave an age of 560–590 Ma (Compston and Arriens, 1968). However, this dyke is from an elongated zone east of the Darling Fault, where biotite Rb–Sr ages have been extensively reset to 450–500 Ma (Libby and de Laeter, 1979), and the dating of the dyke may reflect this event. Thus, the age of the Boyagin dyke swarm is between 750 and 500 Ma, most probably around 650 Ma.

In the area studied, and for much of the area of the swarm, the structural pattern of the Boyagin dyke swarm is defined by two sets of dykes trending northwest and west-northwest, with a minor set trending east-northeast.

The northwesterly trending dykes follow the general geological grain of the region, particularly the major fracture zones of the Darkan Fault and its associates, the Saddleback greenstone belt, and the zone of ancient gneisses east of Perth. The west-northwesterly trending swarm of dykes truncates these structures at an angle of about 40°. The resulting dyke pattern is that of a conjugate set of Riedel shears produced within a broad wrench zone with sinistral principal displacement. As noted earlier, the final tectonic phase of the Pinjarra Orogen was dominated by sinistral transcurrent faulting concentrated in the proto-Darling Fault. Thus, the Boyagin dyke swarm may be seen as the final, post-orogenic phase of the Pinjarra Orogen. In addition, the major lineaments of the Darkan Fault, and the other shear zones which transect the southwest of the Yilgarn Craton, can also be interpreted as Riedel shears formed in the earliest, ductile phases of pre-orogenic sinistral movement along the proto-Darling Fault.

Between the time of formation of the Darkan Fault and its associated lineaments, and the emplacement of the Boyagin dyke swarm, the Binneringie Dyke was intruded. The emplacement of the dyke was the result of tectonic events in the eastern parts of the craton; but at its western end, its course may have been influenced by residual stresses associated with the proto-Darling Fault. As a result, the presence of the Binneringie Dyke influenced the emplacement of the Boyagin dyke swarm when sinistral stress was renewed in late Proterozoic times, causing the dyke trends to be deflected anticlockwise through about 20°.

Conclusions

The results of this study can be briefly summarized as follows:

1. In the Williams area there are two independent mafic dyke swarms:

   (a) the Widgiemooltha dyke swarm of calc-alkaline composition and Early Proterozoic age — represented by the large, gabbroic Binneringie Dyke, and the smaller, xenolith-rich Binneringie Dyke South; and

   (b) the Boyagin dyke swarm of quartz-tholeiite composition and Late Proterozoic (or early Palaeozoic) age — represented by many thin and impersistent dolerite dykes.

2. The Binneringie Dyke extends more than 600 km in a west-southwest direction across the width of the Yilgarn Craton and includes a parallel xenolith-rich dyke in the Williams area. Both dykes terminate at, or close to, the prominent magnetic lineament of the Darkan Fault.

3. The Boyagin dyke swarm comprises two intersecting sets of dykes, one trending northwesterly and the other trending west-northwesterly, and a minor set that trends east-northeasterly. The three sets of dykes are contemporaneous. The dyke pattern is best explained as intrusion along a conjugate set of Riedel shears formed in a broad sinistral wrench zone along the western margin of the Yilgarn Craton. The wrench zone is associated with the Pinjarra Orogen and its principal displacement was localized along the proto-Darling Fault.

4. The implications for the structural development of the southwest of Western Australia are that the prominent magnetic lineaments of the area are Riedel shears, which formed during the earliest and most ductile phase of deformation in a wrench zone that preceded the development of the Pinjarra Orogen and the emplacement of the Binneringie Dyke. The wrench zone (and associated shear zones), with its principal displacement localized along the proto-Darling Fault, continued to develop throughout the Pinjarra Orogeny.

The Boyagin dyke swarm intrudes Riedel shears of a reactivated wrench zone that represents the final phase of brittle deformation of the Pinjarra Orogen.

References

BLIGHT, D. F., COMPSTON, W., and WILDE, S. A., 1981, The Logue Brook Granite — Age and significance of deformation zones along the Darling Scarp: Western Australia Geological Survey, Annual Report 1980, p. 72–80.

CAMPBELL, I. H., 1968, The origin of heteradcumulate and adcumulate textures in the Jimberlana Norite: Geological Magazine, v. 105, p. 378–383.

CAMPBELL, I. H., 1977, A study of the macrorhythmic layering and cumulate processes in the Jimberlana intrusion, Western Australia, Part 1 — The upper layered series: Journal of Petrology, v. 18, p. 183–215.

CAMPBELL, I. H., McCALL, G. J. H., and TYRWHITT, D. S., 1970, The Jimberlana Norite, Western Australia — A smaller analogue of the Great Dyke of Rhodesia: Geological Magazine, v. 107, p. 1–12.

COMPSTON, W., and ARRIENS, P. A., 1968, The Precambrian geochronology of Australia: Canadian Journal of Earth Sciences, v. 5, p. 561–583.

COMPSTON, W., and PIGEON, R. T., 1962, Rubidium–strontium dating of shales by the total-rock method: Journal of Geophysical Research, v. 67, p. 3493–3502.

EMBLETON, B. J. J., and SCHMIDT, P. W., 1985, Age and significance of magnetization in dolerite dykes from the Northampton Block, Western Australia: Australian Journal of Earth Sciences, v. 32, p. 279–286.

FLETCHER, I. R., LIBBY, W. G., and ROSMAN, K. J. R., 1987, Sm–Nd dating of the 2411 Ma Jimberlana Dyke, Yilgarn Block, Western Australia: Australian Journal of Earth Sciences, v. 34, p. 523–525.

FLETCHER, I. R., WILDE, S. A., LIBBY, W. G., and ROSMAN, K. J. R., 1983, Sm–Nd model ages across the margins of the Archaean Yilgarn Block, Western Australia, II — The southwest transect into the Proterozoic Albany–Fraser Province: Journal of Geological Society of Australia, v. 30, p. 333–340.

FLETCHER, I. R., WILDE, S. A., and ROSMAN, K. J. R., 1985, Sm–Nd model ages across the margins of the Archaean Yilgarn Block, Western Australia, III — The western margin: Australian Journal of Earth Sciences, v. 32, p. 73–82.

GEE, R. D., BAXTER, J. L., WILDE, S. A., and WILLIAMS, I. R., 1981, Crustal development in the Archaean Yilgarn Block, Western Australia, *in* Archaean Geology *edited by* J. E. GLOVER and D. I. GROVES: International Archaean Symposium, 2nd, Perth, Western Australia, 1980, Geological Society of Australia, Special Publication 7, p. 43–56.

GIDDINGS, J. W., 1976, Precambrian palaeomagnetism in Australia, I — Basic dykes and volcanics from the Yilgarn Block: Tectonophysics, v. 30, p. 91–108.

HALLBERG, J. A., 1987, Postcratonization mafic and ultramafic dykes of the Yilgarn Block: Australian Journal of Earth Sciences, v. 34, p. 135–149.

HARRIS, L. B., 1987, A tectonic framework for the Western Australian Shield and its significance to gold mineralization – A personal view, *in* Recent advances in understanding Precambrian gold deposits *edited by* S. E. HO and D. I. GROVES: University of Western Australia, Geology Department and University Extension, Publication 11, p. 1–128.

ISLES, D. J., and COOKE, A. C., 1990, Spatial associations between post-cratonization dykes and gold deposits in the Yilgarn Block, Western Australia, *in*, Mafic dykes and emplacement mechanisms *edited* by A. J. PARKER, P. C. RICKWOOD, and D. H. TUCKER: Rotterdam, Balkema, p. 157–162.

LEWIS, J. D., 1970, Petrography and significance of some xenolith-bearing dykes of the Meckering district, Western Australia: Western Australia Geological Survey, Annual Report 1969, p. 46–54.

LIBBY, W. G., and de LAETER, J. R., 1979, Biotite dates and cooling history of the western margin of the Yilgarn Block: Western Australia Geological Survey, Annual Report 1978, p. 79–87.

MAZZUCCHELLI, R. H., and ROBBINS, T. W., 1973, Geochemical exploration for base and precious metal sulphides associated with the Jimberlana Dyke, Western Australia: Journal of Geochemical Exploration, v. 2, p. 383–392.

McCALL, G. J. H., and PEERS, R., 1971, Geology of the Binneringie Dyke, Western Australia: Geologische Rundschau, v. 60, p. 1174–1263.

McCLAY, K. R., and CAMPBELL, I. H., 1976, The structure and shape of the Jimberlana Intrusion, Western Australia, as indicated by an investigation of the bronzite complex: Geological Magazine, v. 113, p. 129–139.

MYERS, J. S., 1990, Pinjarra Orogen, *in* Geology and mineral resources of Western Australia: Western Australia Geological Survey, Memoir 3, p. 265–274.

NIEUWLAND, D. A., and COMPSTON, W., 1981, Crustal evolution of the Yilgarn Block near Perth, Western Australia, *in* Archaean geology *edited by* J. E. GLOVER and D. I. GROVES: International Archaean Symposium, Second, Perth, Western Australia, 1980, Geological Society of Australia, Special Publication 7, p. 159–72.

PARKER, A. J., RICKWOOD, P. C., BAILLIE, P. W., McCLENAGHAN, M. P., BOYD, D. M., FREEMAN, M. J., PIETSCH, B. A., MURRAY, C. G., and MYERS, J. S., 1987, Mafic dyke swarms of Australia, *in* Mafic dyke swarms *edited by* H. C. HALLS and W. F. FAHRIG: Geological Association of Canada, Special Paper 34, p. 401–417.

PARTINGTON, G. A., McNAUGHTON, N. J., KEPERT, D. A., COMPSTON, W., and WILLIAMS, I. S., 1986, Geochronology of the Balingup metamorphic belt — Constraints on the temporal evolution of the Greenbushes pegmatite district, *in* Genesis of *tin–tungsten deposits and associated granitoids* (IGCP Project 220): Australia Bureau of Mineral Resources, Record 1986/10, p. 55–56 (unpublished).

PEARCE, J. A., and CANN, J. R., 1973, Tectonic setting of basic volcanic rocks determined using trace element analysis: Earth and Planetary Science Letters, v. 19, p. 290–300.

PEARCE, T. H., GORMAN, B. E., and BIRKETT, T. C., 1975, The TiO_2–K_2O–P_2O_5 diagram — A method of discriminating between oceanic and non-oceanic basalts: Earth and Planetary Science Letters, v. 24, p. 419–426.

PEARCE, T. H., GORMAN, B. E., and BIRKETT, T. C., 1977, The relationship between major element chemistry and tectonic environment of basic and intermediate volcanic rocks: Earth and Planetary Science Letters, v. 36, p. 121–132.

PLAYFORD, P. E., COCKBAIN, A. E., and LOW, G. H., 1976, Geology of the Perth Basin, Western Australia: Western Australia Geological Survey, Bulletin 124.

PRIDER, R. T., 1945, Igneous activity, metamorphism and ore-formation in Western Australia: Royal Society of Western Australia, Journal, v. 31, p. 43–84.

SOFOULIS, J., 1966, Widgiemooltha, Western Australia: Western Australia Geological Survey, 1:250 000 Geological Series Explanatory Notes, 25p.

TUCKER, D. H., and BOYD, D. M., 1987, Dykes of Australia detected by airborne magnetic surveys, *in* Mafic dyke swarms *edited by* H. C. HALLS and W. F. FAHRIG: Geological Association of Canada, Special Paper 34, p. 163–172.

TUCKER, D. H., and D'ADDARIO, G. W., 1986, Albany — Magnetic domains (1:1 000 000 map): Australia Bureau of Mineral Resources.

TUREK, A., 1966, Geochronology of the Kalgoorlie area: Canberra, Australian National University, Ph.D thesis (unpublished).

WILDE, S. A., and LOW, G. H., 1980, Pinjarra, Western Australia: Western Australia Geological Survey, 1:250 000 Geological Series Explanatory Notes, 31p.

WILDE, S. A., and PIDGEON, R. T., 1986, Geology and geochronology of the Saddleback Greenstone Belt in the Archaean Yilgarn Block, southwestern Australia: Australian Journal of Earth Sciences, v. 33, p. 491–501.

WILDE, S. A., and WALKER, I. W., 1982, Collie, Western Australia: Western Australia Geological Survey, 1:250 000 Geological Series Explanatory Notes, 39p.

Chlorine-36 and carbon-14 measurements on hypersaline groundwater in Tertiary palaeochannels near Kalgoorlie, Western Australia

by

D.P. Commander, L.K. Fifield[1], P.M. Thorpe, R.F. Davie[1], J.R. Bird[2], and J.V. Turner[3]

Abstract

Chlorine-36 and carbon-14 isotopic determinations were applied to understanding the recharge regime of saline and hypersaline groundwater in the Eastern Goldfields of Western Australia. Groundwater samples were taken from palaeochannels in the Kalgoorlie area and a site near Lake Ballard. The groundwater chlorine-36/chlorine-35 ratios fall within a relatively narrow range (39–68 x 10^{-15}), between the values measured in local salt lakes and the calculated rainfall value. A high ratio in the lower salinity groundwater reflects the rainfall source, whereas low values in groundwater, similar to the levels in the salt lakes, indicate chloride residence times of the order of hundreds of thousands of years.

The groundwater carbon-14 dates, which range from 3600 to 16 600 years, also demonstrate that recharge is occurring under the present rainfall regime, and confirm that a substantial component of salts remobilized from salt lakes contributes to the groundwater salinity.

KEYWORDS : Groundwater, hypersalinity, isotopes, chlorine-36, carbon-14, palaeochannels, Kalgoorlie

Introduction

Hypersaline groundwater is used extensively in the Eastern Goldfields of Western Australia for the treatment of gold ore. The major groundwater resources are in the Early Tertiary Wollubar Sandstone, a fluviatile deposit which occurs in former courses of palaeorivers known locally as palaeochannels (Smyth and Button, 1989; Kern and Commander, 1993). Because of the importance of this groundwater in a region generally without major water resources, the Geological Survey of Western Australia (GSWA) commenced in 1987 a study of the hydrogeology of a palaeochannel near Menzies, between Lake Ballard and Lake Marmion in the Rebecca Palaeodrainage (Fig.1). This investigation was followed in 1988 by a regional investigation of groundwater resources in the Kalgoorlie area, involving the drilling of bores along twenty-three section lines across palaeochannels in the Roe Palaeodrainage (Commander et al. 1992).

Commander et al. (1992) suggested that a period of the order of 70 000 years was necessary to accumulate the salts stored in groundwater in the Roe Palaeodrainage, assuming that atmospheric precipitation was the source of the salts. McArthur et al. (1989) had previously suggested that the salts are derived from marine aerosols (rather than rock weathering), however the time scale of accumulation was uncertain. This was based on a study of sulfur and strontium isotopes in shallow groundwater from beneath salt lakes in the Cowan Palaeodrainage to the south. McArthur et al. (1989) further suggested the possibility of remnants existing of sequestered seawater from a Middle Miocene marine transgression, which implied a maximum groundwater age of about 10 Ma. Recently, the chlorine-36 (^{36}Cl) isotope has been used to date groundwater as old as 1.5 Ma (Calf et al., 1988; Davie et al., 1989). Thus it appeared that this isotope may have the potential to define the order of magnitude of the time needed to accumulate chloride in the groundwater. Combined with carbon-14 (^{14}C) age determinations of the carbon in groundwater, new information on the recharge to the palaeochannels would result.

Groundwater from selected bores was therefore sampled for ^{14}C age determination. At the same time, the GSWA collaborated with the Australian National University (ANU) and the Australian Nuclear Science and Technology Organisation in investigating the potential use of the ^{36}Cl isotope. Chlorine-36 had not previously been used in the study of hypersaline groundwaters.

[1] Australian National University, Canberra, ACT
[2] Australian Nuclear Science and Technology Organisation, Lucas Heights Research Laboratory, Menai, NSW
[3] CSIRO Division of Water Resources, Perth, WA

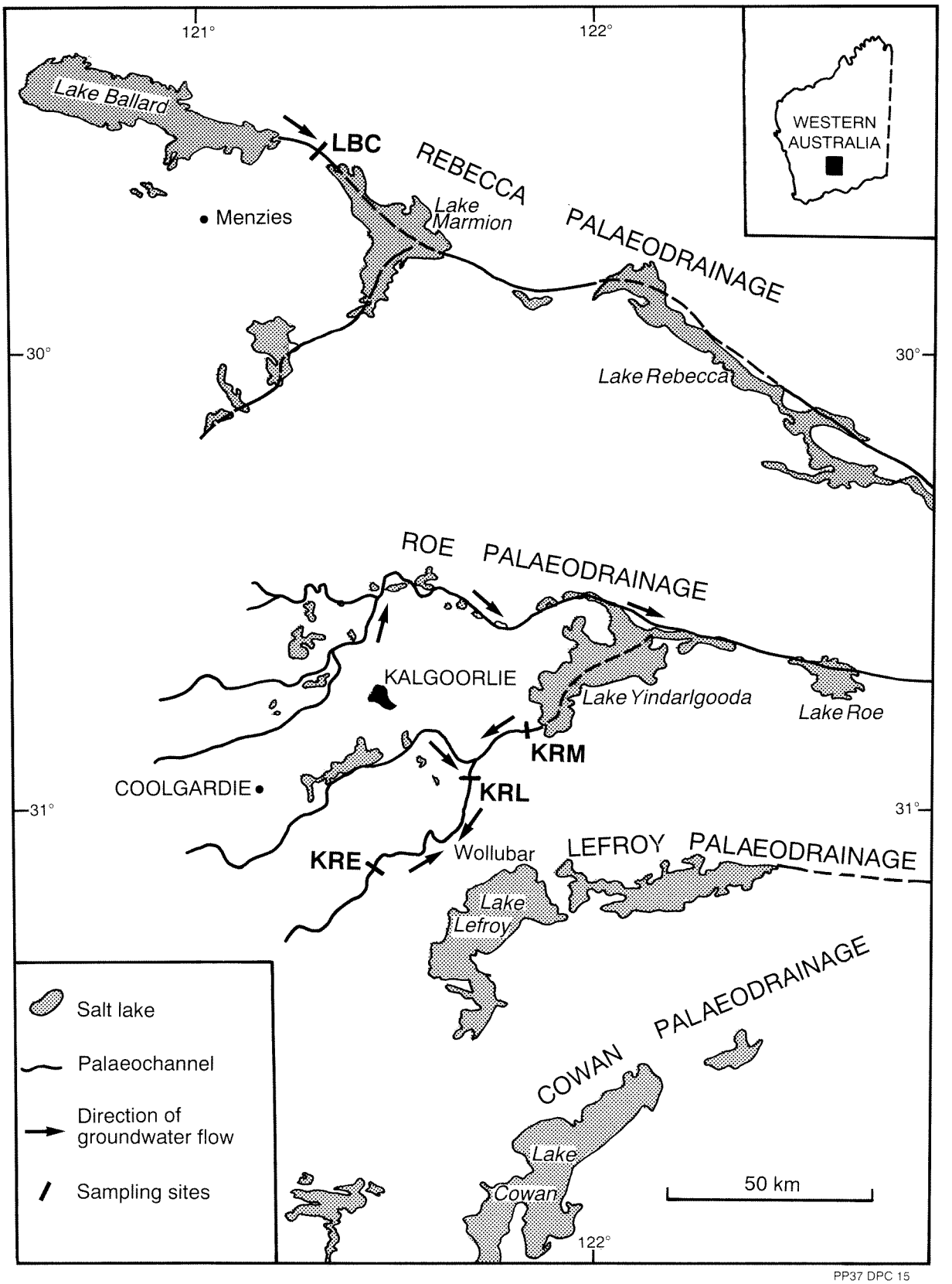

Figure 1. Location map

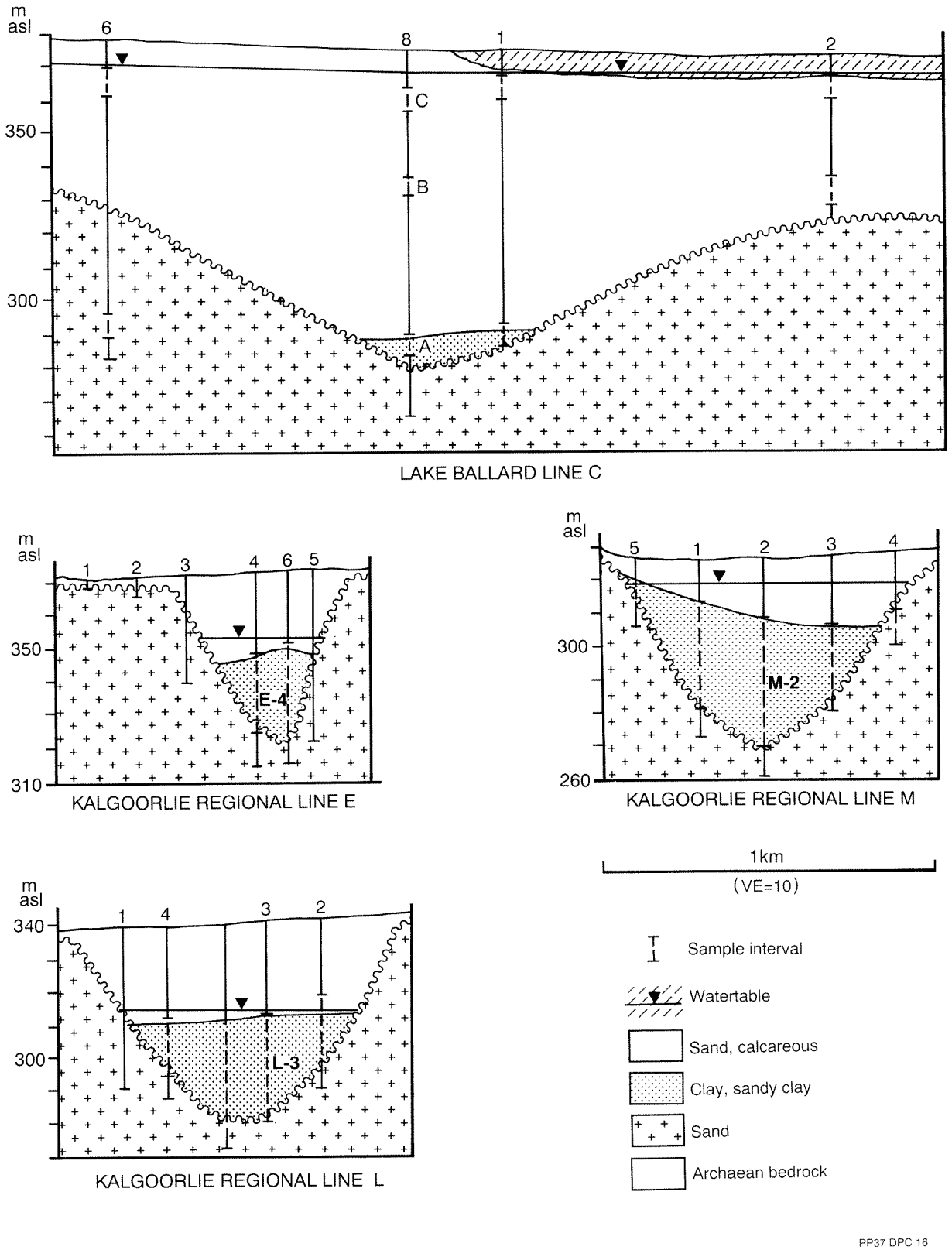

Figure 2. Geological cross sections

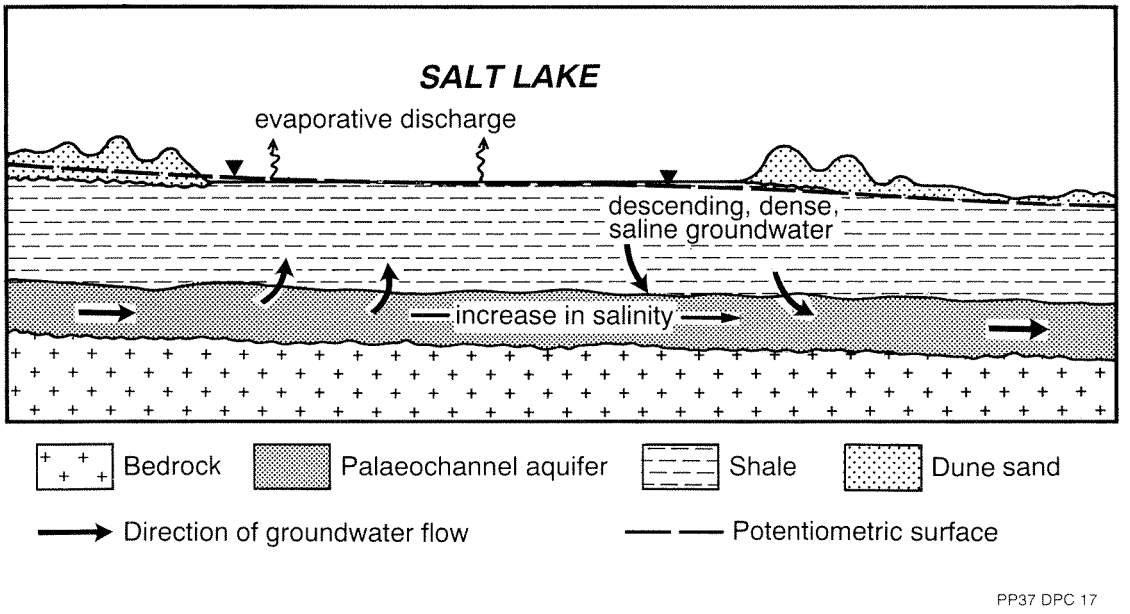

Figure 3. Diagrammatic section showing hydraulic relationship between palaeochannel and salt lake

Hydrogeological setting

The Kalgoorlie area lies within the Eastern Goldfields province of the Yilgarn Craton. The Yilgarn Craton, a granite–greenstone terrane of Archaean age with linear northerly trending belts of supracrustal rocks, consists essentially of metasedimentary and volcanic material, intruded by granite. The present topography comprises a dissected peneplain on the Archaean rocks, incised by a Cretaceous or early Tertiary palaeodrainage system which drained eastwards into the Eucla Basin.

The two study areas fall within the Rebecca and Roe Palaeodrainages (Fig. 1), which are infilled with sediments of Eocene age (Smyth and Button, 1989; Kern and Commander, 1993). The basal Wollubar Sandstone (Middle to Late Eocene) is the main aquifer in the Roe Palaeodrainage (Commander et al., 1992), and there is a similar sandstone in the Rebecca Palaeodrainage (Fig. 2). The basal sandstone is overlain and hydraulically confined by the Perkolilli Shale in the Roe Palaeodrainage, and by a similar sequence in the Rebecca Palaeodrainage. These Tertiary formations are concealed by a variety of Quaternary sediments and by discontinuous belts of terminal playas (salt lakes) occupying the present-day broad valleys.

The groundwater in the palaeochannels is saline or hypersaline, ranging from 30 g/L total dissolved solids (TDS) in the upper parts of the Roe Palaeodrainage system up to 200 g/L TDS near Lake Yindarlgooda, and 250 g/L TDS at Lake Ballard. The groundwater is predominantly sodium chloride type, but saturation is reached only locally and seasonally at the surface of the salt lakes. A marked increase in the groundwater salinity of the palaeochannels, which takes place beneath the salt lakes, indicates that the salt lakes concentrate the salts in the groundwater through evaporation. Hydraulic connection between the salt lakes and the palaeochannels is therefore inferred to exist (Fig. 3), similar to salt lakes elsewhere (Bowler, 1986; Torgerson et al., 1986). There is a slow groundwater outflow through the palaeochannels which, in the Roe Palaeodrainage, represents around 0.003% of the rainfall on the catchment area (Commander et al., 1992).

Origin of chlorine-36 and carbon-14 in groundwater

Chlorine-36 originates mainly from the spallation of argon by cosmic rays in the upper atmosphere. The rate of cosmogenic fallout of the isotope, which is dependent on geomagnetic latitude, is estimated from the work of Lal and Peters (1962, 1967) and Bentley et al. (1986) to be 20 atoms m^{-2} sec^{-1}, as there have been no direct measurements made of ^{36}Cl in atmospheric precipitation in the region. This ^{36}Cl is carried to the ground in precipitation together with other chloride in the atmosphere, which is derived predominantly from marine sources and contains negligible quantities of ^{36}Cl. The ratio of ^{36}Cl to stable chloride in rainfall can then be calculated from the estimated fallout of cosmogenically produced ^{36}Cl, and the measured chloride level in rainfall. This calculated ratio is approximately 35×10^{-15} in the study area.

Considering the Kalgoorlie region is some 350 km from the ocean, atmospheric saltfall is relatively high. The elevated levels are thought to result mainly from the uptake of salts from salt lakes in the vicinity (Hingston and Gailitis, 1976). These have a significant ^{36}Cl content, the $^{36}Cl/Cl$ ratios of near-surface halite in Lakes Lefroy and Ballard having been measured at $30 \pm 5 \times 10^{-15}$ and $41 \pm 7 \times 10^{-15}$ respectively (Chivas et al., 1987, 1988). The ratios in salt lake halite may reflect local production of

Table 1. Isotopic results for groundwaters from palaeochannels

Bore	$^{36}Cl/Cl$ ($x10^{-15}$)	Cl (g/L)	^{36}Cl (10^9 atoms/L)	GSWA no.	pH	CO_2 (mg/L)	HCO_3 (mg/L)	^{14}C (pmC)	$\delta^{13}C$ (‰PDB)	^{14}C age (years)	$\delta^{18}O$ (‰SMOW)	$\delta^{2}H$ (‰SMOW)
KRE-4	68 ± 6	19.6	22 ± 2	247	4.0	400	<2	34.8 ± 3.1	-15.1	8 700 ± 700	-3.3	-28.6
KRL-3	51 ± 5	53.3	65 ± 5	-	-	-	-	-	-	-	-	-
KRM-2	45 ± 6	106	79 ± 10	248	6.2	410	400	64.4 ± 3.2	-16.4	3 600 ± 400	+1.6	-8.0
LBC-8A	39 ± 3	136	88 ± 7	249	5.5	240	45	13.5 ± 2.0	-10.9	(a)16 600 ± 1 100	+2.8	-2.8
LBC-8B	47 ± 3	84.7	66 ± 5	250	5.8	160	120	(b)	-9.6	-	+1.1	-21.1
LBC-8C	47 ± 3	6.99	5.5 ± 3	175	7.1	50	410	59.5 ± 2.0	-10.3	4 300 ± 300	-4.8	-37.2

Notes: pmC = percent modern carbon; PDB = Pee Dee Belemnite, marine carbonate standard; SMOW = standard mean ocean water
(a) average of two independent (and concordant) measurements; (b) insufficient recovery of carbon to process

^{36}Cl due to radioactivity from uranium and thorium in the granitic bedrock. Granite commonly has a $^{36}Cl/Cl$ secular equilibrium ratio of 30–40 x 10^{-15} (Chivas et al., 1988; Bentley et al., 1986).

If halite from local salt lakes provides the dominant contribution to atmospheric saltfall the assumed ratio of $^{36}Cl/Cl$ in atmospheric precipitation in the area becomes about 70 x 10^{-15} (the sum of the calculated ratio in precipitation and the average measured ratio of halite in the two salt lakes). In the groundwater system, ^{36}Cl decays with a half life of 301 000 years, and the changing $^{36}Cl/Cl$ ratio may therefore be used as a measure of chloride residence time.

Carbon-14 is also produced in the upper atmosphere, by the action of cosmic rays on nitrogen atoms. The ^{14}C is quickly oxidized to CO_2 which enters groundwater in the unsaturated zone as dissolved CO_2, and as carbonate and bicarbonate ions. The radioactive decay of ^{14}C (half-life of 5730 years) can be used as a measure of the carbon residence time after the ^{14}C has moved below the watertable.

Sampling and analysis

Three sample points in the Kalgoorlie area were selected along a palaeochannel to investigate isotopic changes along a flow line (Fig. 1). It was originally assumed that groundwater flow was eastwards from Line E through Line L to Line M. However, subsequent levelling showed that the direction of flow in the eastern part of the palaeochannel was reversed, and that groundwater flowed westwards from Line M through Line L to discharge in the Wollubar area. In order to investigate vertical changes in isotopic composition in the vicinity of a palaeochannel, a site was also sampled at Lake Ballard where three bores had been drilled to various depths, with the deepest penetrating the sand at the base of the palaeochannel (Fig. 2).

Samples of airfree groundwater were obtained with a submersible pump from exploratory bores cased with 40 mm diameter slotted PVC pipe. The samples represent mixtures as the slotted lengths ranged from 6–38 m.

The samples analysed for ^{36}Cl were collected originally for analysis of heavy metals (Commander et al., 1992), and were initially filtered and acidified with high-purity nitric acid. Further chemical purification was then undertaken at the Chemistry Centre (W.A.) where the chloride was extracted from the water sample in the form of silver chloride precipitate. The silver chloride sample material was then used for Accelerator Mass Spectrometry (AMS) analysis on the 14 MV tandem accelerator at the Department of Nuclear Physics, ANU (Fifield et al., 1987). As a check on possible contamination, a blank of Weeks Island Halite was prepared at the same time, and its $^{36}Cl/Cl$ ratio determined in the same batch as the groundwater samples. The ratio for the blank of 0.3 ± 2.0 x 10^{-15} indicated that no ^{36}Cl contamination was introduced at either the processing or analysis stages.

The groundwater carbonate used for ^{14}C and ^{13}C analysis was extracted from large-volume samples (100 to 400 L) by field precipitation of the total dissolved carbonates. The method involved the addition of carbonate-free sodium hydroxide and barium chloride. Precautions were taken to trap all dissolved carbon dioxide (CO_2) gas in the groundwater and prevent contamination with atmospheric CO_2. Measurements of pH, alkalinity and water temperature were made on site at the time of sampling. The field precipitation of carbonates was attended by problems due to the low bicarbonate and high sulfate composition of the groundwater. Two of the samples collected, from LBC-8A and LBC-8B, could not be processed for liquid-scintillation counting owing to high sulfate levels which caused scavenging of the precipitation chemicals. Additional small-volume (1L) samples were then collected from LBC-8A and processed for measurement by AMS. The liquid-scintillation ^{14}C measurements were carried out in the GSWA Isotope Hydrogeology Laboratory, and the AMS measurements were performed at the Department of Nuclear Physics, ANU.

Groundwater carbon-13, deuterium and oxygen-18 analyses were carried out at the CSIRO Division of Water Resources in Perth.

Results

The $^{36}Cl/Cl$ ratios in groundwater (Table 1) all lie within a relatively narrow range (39–68 x 10^{-15}), falling between the values determined for the salt lake halite and

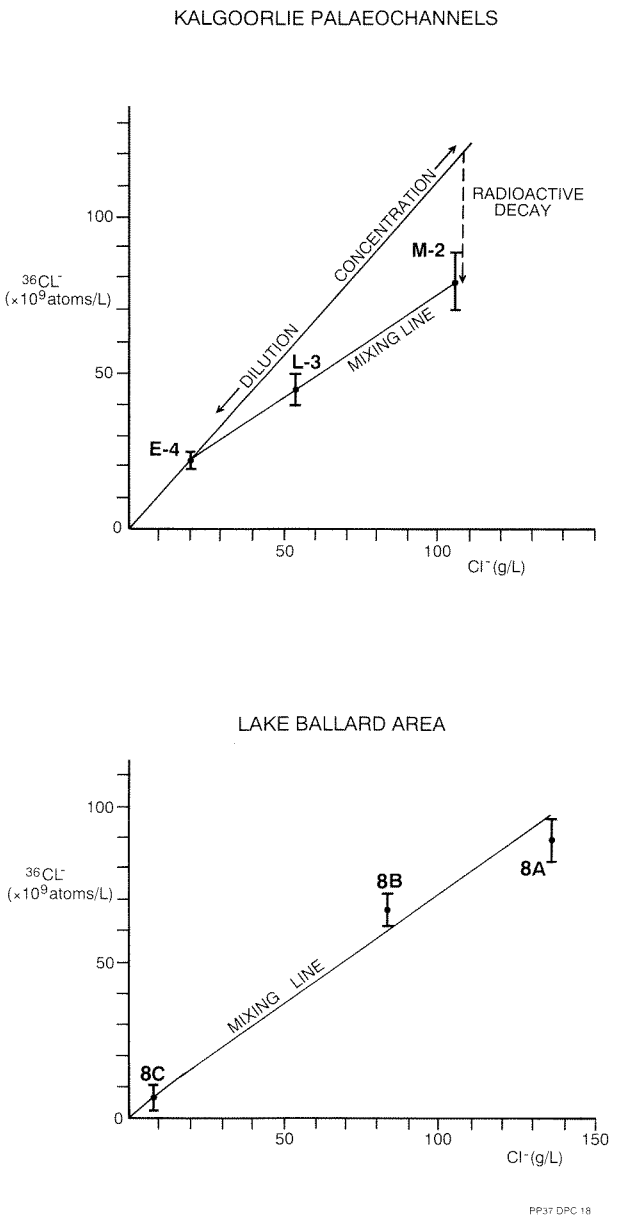

Figure 4. Chloride-36 compared with total chloride concentration

the calculated value for atmospheric precipitation. The ^{36}Cl concentration increases with increasing chloride concentration in all samples (Fig. 4).

The groundwater ^{14}C dates range from 3600 to 16 600 years. These dates were not corrected for dissolution of mineral carbonate, as there is uncertainty regarding the ^{13}C and ^{14}C composition of solid carbonate minerals in the area, and doubt as to whether possible dissolution took place under open or closed system conditions with respect to soil-zone carbon dioxide. Groundwater ^{13}C values (Table 1) were higher in samples from near Lake Ballard, where calcrete occurs in the subsurface, than in the samples from the Kalgoorlie area.

The groundwater oxygen-18 and deuterium results plot close to a straight line of lower gradient than the local meteoric water line (Fig. 5). This indicates that evaporation has led to progressive enrichment of stable isotopes with increasing salinity.

Discussion

If the value of the $^{36}Cl/Cl$ ratio in KRE-4 (68×10^{-15}) is taken to be close to the value in atmospheric precipi-tation, a period of approximately one half-life (301 000 years) is required for radioactive decay to the value in the salt lake halite. This suggests that the salts could have been in the landscape or groundwater system for at least several hundred thousand years. A similar minimum residence time for the chloride in the Kalgoorlie region was estimated from a catchment salt balance (Commander et al., 1992).

The distribution of points on plots of ^{36}Cl against Cl (Fig. 4) for the groundwaters could be interpreted as a result either of concentration and radioactive decay, or of mixing between a dilute and a concentrated end member. However, the ^{14}C results indicate that the water in both systems has been in contact with the atmosphere for a time which is short compared with the ^{36}Cl half-life. Hence the observed variations in ^{36}Cl in the groundwater are more likely to be due to mixing than radioactive decay.

Since the two study areas were sampled in different ways it is convenient to discuss the two systems separately.

Kalgoorlie palaeochannels

It can be inferred from the hydrogeology of the area that the salt and water in the palaeochannel at KRE-4 are derived wholly from precipitation, groundwater recharge and subsequent groundwater flow within the catchment area. The $^{36}Cl/Cl$ ratio is close to the value expected in rainfall and the ^{14}C age of 8700 years reflects the mean time taken for groundwater to reach KRE-4. The salinity is typical of groundwater from both palaeochannels and bedrock in the area.

In the palaeochannel at KRM-2, the measured $^{36}Cl/Cl$ ratio and ^{14}C is consistent with both the water and salt having their origin in Lake Yindarlgooda. The comparatively young ^{14}C age of 3600 years simply reflects proximity to the western edge of the lake and implies a groundwater flow rate of about 1 m/year, although there may also be local recharge to the palaeochannel.

The groundwater in KRL-3 is likely to be a mixture of water derived from Lake Yindarlgooda, and from the Hannan Palaeochannel in which the salinity is lower (about 100 g/L) and where the $^{36}Cl/Cl$ ratio could be expected to be higher. The measured $^{36}Cl/Cl$ ratio is consistent with this expectation.

All the Kalgoorlie groundwaters show enrichment of the heavier isotopes ^{18}O and ^{2}H (Fig. 5 and Table 1) consistent with evaporation.

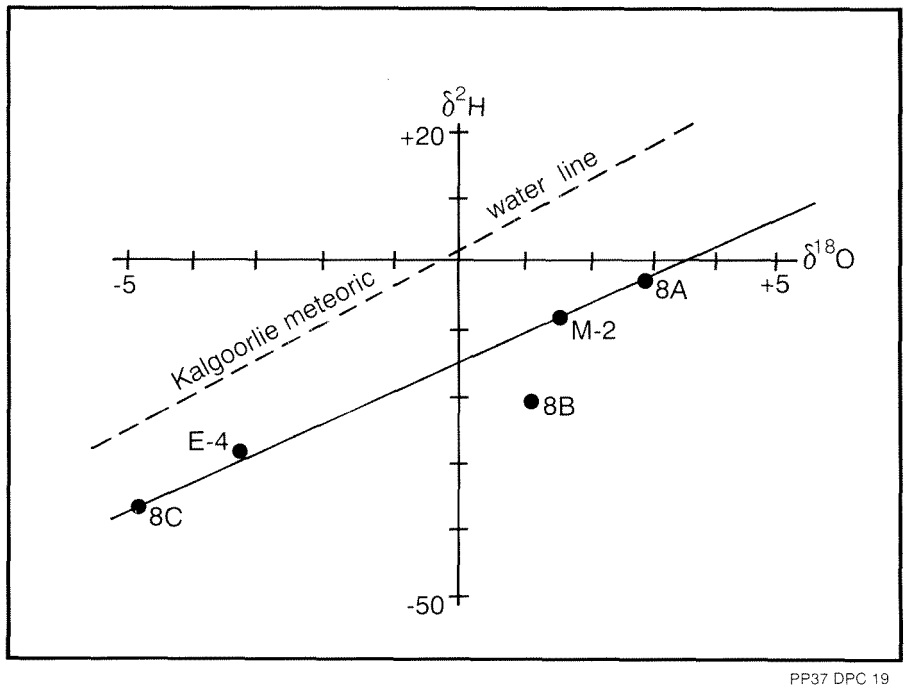

Figure 5. Plot of $\delta^{18}O$ against $\delta^{2}H$

Lake Ballard area

The $^{36}Cl/Cl$ ratio (39×10^{-15}) of groundwater in the palaeochannel at LBC-8A is consistent with a source of chloride from Lake Ballard halite ($^{36}Cl/Cl$ ratio of 41×10^{-15}). The ^{14}C age of 16 600 years suggests a minimum flow rate of the order of 1 m/a from the eastern tip of the lake to LBC-8A (10 km away).

The shallow groundwater in LBC-8C has a relatively young ^{14}C age and the deuterium/oxygen-18 ratio shows little effect of evaporation. However, the $^{36}Cl/Cl$ ratio is well below the expected rainfall value. This can be explained by the mixing of low-salinity modern recharge with saline groundwater either from lateral groundwater flow between Lakes Ballard and Marmion, or from vertical diffusion from the sands in the palaeochannel. The groundwater in LBC-8B is intermediate in salinity and $^{36}Cl/Cl$ ratio (taking into account the uncertainty), as would be expected from mixing between the deep and shallow groundwater.

The $d^{13}C$ values are all significantly lower than those determined in samples from the Kalgoorlie palaeochannels. This is probably due to solution of calcrete, which occurs near Lake Ballard but which is absent in the Kalgoorlie region.

Conclusions

Analysis of the ^{36}Cl and ^{14}C isotopes in hypersaline groundwater has facilitated the differentiation of sources of salt in groundwater.

The $^{36}Cl/Cl$ ratios in groundwater were found to lie between the calculated value in atmospheric precipitation and the measured values in salt lakes. Radioactive decay over hundreds of thousands of years is required to achieve the observed ratios in salt lake halite from a rainfall source. However a better estimate of the $^{36}Cl/Cl$ ratio in atmospheric precipitation or in low salinity groundwater is required.

The presence of groundwater containing appreciable ^{14}C but with low $^{36}Cl/Cl$ ratios is consistent with a hydraulic regime of low recharge, continual concentration of salts by evaporation from salt lakes, mixing of groundwaters of differing salinities, and circulation between the salt lakes and underlying palaeochannel sands.

Carbon-14 can be used to determine groundwater flow rates in the palaeochannel aquifers. Chlorine-36 is useful for determining the origin of chloride in groundwater, but has potential for dating groundwater only where there is no remobilization of chloride from salt lake halite.

References

BENTLEY, H. W., PHILLIPS, F. M., and DAVIS, S. N., 1986, Chlorine-36 in the terrestrial environment, *in* Handbook of Environmental Isotope Geochemistry, vol. 2. The Terrestrial Environment, B *edited by* P. FRITZ and J. Ch. FONTES: Amsterdam, Elsevier, p. 427–480.

BOWLER, J. M., 1986, Spatial variability and hydrologic evolution of Australian lake basins, analogue for Pleistocene hydrologic change and evaporite formation: Palaeogeography, Palaeoclimatology, Palaeoecology, v. 54, p. 21–41.

CALF, G. E., BIRD, J. R., DAVIE, R. F., FIFIELD, L. K., OPHEL, T. R., EVANS, W. R., KELLETT, J. R., and HABERMEHL, M. A., 1988, The

role of ^{36}Cl and ^{14}C measurements in Australian groundwater studies: 13th International Radiocarbon Conference, Dubrovnik, June 1986.

CHIVAS, A. R., FIFIELD, L. K., DAVIE, R. F., BIRD, J. R., OPHEL, T. R., and KISS, E., 1987, Chlorine-36 investigations of Australian salt lakes: Australian National University SLEADS Workshop, 1987, p. 23.

CHIVAS, A. R., FIFIELD, L. K., DAVIE, R. F., BIRD, J. R., OPHEL, T. R., and KISS, E., 1988, Chlorine-36 investigations of Australian salt lakes: Australian National University SLEADS Conference, 1988, p. 13.

COMMANDER, D. P., KERN, A. M., and SMITH, R. A., 1992, Hydrogeology of the Tertiary palaeochannels in the Kalgoorlie Region (Roe Palaeodrainage): Western Australia Geological Survey, Record 1991/10.

DAVIE, R. F., KELLETT, J. R., FIFIELD, L. K., EVANS, W. R., CALF, G. E., BIRD, J. R., TOPHAM, S., and OPHEL, T. R., 1989, ^{36}Cl measurements in the Murray Basin: preliminary results from the Victorian and South Australian Mallee Region: Australia BMR, Journal of Australian Geology and Geophysics, v. 11, p. 261–272.

FIFIELD, L. K., OPHEL, T. R., BIRD, J. R., CALF, G. E., ALLISON, G. B., and CHIVAS, A. R., 1987, The ^{36}Cl measurement program at the Australian National University: Nuclear Instruments and Methods in Physics Research, No. B29, p. 114–119.

HINGSTON, F. J., and GAILITIS, V., 1976, The geographic variation of salt precipitation over Western Australia: Australian Journal of Soil Research, v. 14, p. 319–335.

KERN, A. M., and COMMANDER, D. P., 1993, Cainozoic stratigraphy in the Roe Palaeodrainage of the Kalgoorlie Region: Western Australia Geological Survey, Report 34, Professional Papers, p. 1–11.

LAL, D., and PETERS, B., 1962, Cosmic ray produced isotopes and their application to problems in geophysics: Progress in Elementary Particle and Cosmic Ray Physics, v. 6, p. 3–74.

LAL, D., and PETERS, B., 1967, Cosmic ray produced radioactivity on the Earth, *in* Handbuch der Physik XLVI, part 2 *edited by* S. FLUGGE: Berlin, Springer-Verlag, p. 551–612.

McARTHUR, J. M., TURNER, J. V., LYONS, W. B., and THIRWALL, M. F., 1989, Salt sources and water rock interaction on the Yilgarn Block, Australia; isotopic and major element tracers: Applied Geochemistry, v. 4, p. 79–92.

SMYTH, E. L., and BUTTON, A., 1989, Gold exploration in the Tertiary palaeodrainage systems of Western Australia, *in* Gold Forum on Technology and practices — World Gold '89, Chapter 2, p. 13–22, Reno, Nevada, Nov. 1989 *edited by* R. S. BHAPPU and R. J. HARDEN: Society for Mining, Metallurgy, and Exploration Inc., Littleton, Colorado.

TORGERSEN, T., DE DECKKER, P., CHIVAS, A. R., and BOWLER, J. M., 1986, Salt lakes: a discussion of processes influencing palaeoenvironmental interpretation and recommendations for future study: Palaeogeography, Palaeoclimatology, Palaeoecology, v. 54, p. 7–19.

Sm–Nd model ages of granitoid rocks in the Yilgarn Craton

by

I. R. Fletcher [1], W. G. Libby and K. J. R. Rosman [1]

Abstract

Sm–Nd data are presented for 44 granitoid rocks from across the Yilgarn Craton. With more than 100 analyses now available, model age (T_{CR}) distributions show strong differences between the structural subdivisions of the craton. These differences are generally in keeping with recognized regional age differences but the distributions seen in the Murchison Province and Southern Cross Province apparently extend to include all areas of the Western Gneiss Terrane except the recognized ancient gneiss complexes. There are apparent T_{CR} peaks at 3.7 Ga, 3.3 Ga, 3.0 Ga and 2.7 Ga. The full range of T_{CR} is represented amongst granitic rocks with emplacement ages about 2.7 Ga. In contrast, the few available data pairs for (possible basement) gneisses show a rough correlation between T_{CR} and protolith crystallization age.

KEYWORDS: crustal evolution, Sm–Nd, Yilgarn Craton

Introduction

In the decade since Sm–Nd analyses were first carried out on Western Australian rocks (McCulloch and Wasserburg, 1978) they have been applied to a wide variety of geological problems in different areas. Amongst the data now available are more than one hundred analyses of granitoid rocks of the Yilgarn Craton, sufficient to attempt a broad-scale synthesis for this major Archaean crustal unit.

Sm–Nd model ages are commonly used as indicators of the time of extraction of crustal material from the mantle, though they are not as accurate as analytical precisions suggest and there is considerable uncertainty surrounding the process of extraction, the time span between possible stages of evolution, and the effects of crustal mixing (e.g. Harley, 1987; Arndt and Goldstein, 1987). It may be more appropriate to regard model ages as indicators of the time of derivation of felsic material from basaltic crust, whose prior age cannot be assessed. Whichever view is taken, they can be used to elucidate various aspects of Precambrian crustal evolution, particularly when used in conjunction with methods which more directly date pluton emplacement (e.g. Nelson and de Paolo, 1985). On the scale of continental or cratonic blocks, model ages alone can identify major lateral growth trends or distinguish terranes of different ages, provided the time differences involved are sufficiently large (>100 m.y.). Major changes corresponding to the recognized margins of the Yilgarn Craton have previously been demonstrated (Fletcher et al., 1983a,b, 1985; McCulloch, 1987).

In this paper we present new Sm–Nd analyses, drawn from a variety of mapping and other projects, for a variety of granitic rocks and gneisses from across the Yilgarn Craton. To these we have added all comparable published data (to 1988) in an attempt to characterize major trends across the block. Some subsets of the data are discussed in detail, relative to complementary isotope geochronological data which are available.

Samples

Locality names and brief descriptions of all samples analysed are given in Table 1; more details on most samples can be obtained from the references listed there. Sample locations are shown in Figure 1, as are sample localities for all other data quoted in later discussion or used in plots. All samples have been classified for later discussion as gneiss ('N' in Table 1) or syn- or post-tectonic granitic rock ('G', hereafter referred to as 'granite'), though the distinction is sometimes unclear. Paragneiss from unequivocal metasedimentary sequences (e.g. Mount Narryer metasedimentary rocks) has been omitted, as have greenstone belt volcanic rocks.

[1] Department of Applied Physics, Curtin University of Technology, GPO Box U1987, Perth 6001, Australia

Table 1. Locations and descriptions of samples for which new Sm–Nd data are reported

	Location (a)	*Latitude and longitude (b)*	*Sample number (c)*	*Description (d)*	*Ref. (e)*
Western Gneiss Terrane					
NARRYER GNEISS COMPLEX					
(a)	Meegea Hill	26°04'50"S 116°24'00"E	80316 80322	(N) Leucocratic granite gneiss (?Dugel Gneiss)	
		26°04'40"S 116°25'05"E	80316 80322	(N) as above	
(b)	West of Mount Dugel	26°20'04"S 116°21'10"E		(G) Deformed porphyritic monzogranite	
		26°19'20"S 116°22'50"E	80313	(G) as above	
(c)	New Forest	27°24'55"S 115°41'30"E	77270	(G) Deformed porphyritic monzogranite	
		27°24'55"S 115°41'30"E	77272	(G) Deformed leucocratic monzogranite	
OTHER					
(d)	Weiragoo Range	26°24'50"S 116°47'05"E	77391	(G) Recrystallized seriate biotite monzogranite	
			77392	(G) Fine-grained phase of the above	
(e)	Tching Range	26°31'33"S 116°52'50"E	77334	(G) Recrystallized fine-grained tonalite	
			77337A	(G) Recrystallized fine-grained monzogranite	
(f)	Mount Nicolay	27°07'25"S 116°23'35"E	77346	(G) Recrystallized fine-grained monzogranite cutting 77350 (Murgoo Gneiss)	
			77350	(N) Recrystallized fine-grained porphyritic monzogranite (Murgoo Gneiss)	
		27°09'20"S 116°23'25"E	77353	(N) Recrystallized porphyritic monzogranite (Murgoo Gneiss)	
(g)	Greenough River crossing	28°10'35"S 115°40'20"S	77362	(N) Recrystallized leucocratic granodiorite (Murgoo Gneiss)	
			77366	(G) Recrystallized monzogranite sheet cutting 77362	
(h)	Wongan Hills		WH-5	(G) Fine-grained, grey, hypidio- to allotriomorphic granular monzogranite	1
(i)	North of Narrogin	32°40'45"S 117°14'50"E	59925	(G) Even-grained monzogranite	
(j)	Wickepin	32°44'25"S 117°35'30"E	59926	(G) Seriate to porphyritic monzogranite	
(k)	Joyces Prospect		W-15	(N) Fine-grained leucocratic quartz–feldspar–biotite (granulite) gneiss	2
Saddleback Greenstone Belt					
(1)	6km northwest of Mount Saddleback		W-13	(G) Weakly foliated fine- to medium-grained mesocratic monzogranite	3
Murchison Province					
(m)	Northwest of Tragedy Bore	27°24'S 117°19'E	17808	(G) Porphyritic granite	4
(n)	South of Mardah Well	27°59'S 117°01'E	17810	(G) Foliated granodiorite	4
Southern Cross Province					
NOONDIE BATHOLITH					
(p)	New Well	28°33'00"S 119°05'00"E	71125	(G) Fine-grained hornblende–biotite monzogranite	

Table 1. (*continued*)

	Location (a)	*Latitude and longitude (b)*	*Sample number (c)*	*Description (d)*	*Ref. (e)*
(q)	Little Noondie Hill	28°42'00"S 119°08'10"E	71124	(G) Allotriomorphic granular biotite monzogranite	
(r)	Bulga Downs	28°31'10"S 119°44'15"E	71122	(G) Weakly seriate hypidiomorphic granular leucocratic biotite monzogranite	
(s)	White Cloud	28°39'15"S 119°52'35"E	71123	(N) Deformed hornblende–biotite granodiorite	
DIEMALS AREA					
(t)	Rainy Rocks		UWA87975	(G) Intensely lineated recrystallized granodiorite–monzogranite	5,6
(u)	Milky Soak		UWA87955	(G) Weakly foliated porphyritic granodiorite–monzogranite	
(v)	E. Koolyanobbing		UWA81884	(N) Banded gneiss	5,6
(w)	Merredin quarry	31°27'00"S 118°17'40"E	59956A	(G) Seriate to porphyritic monzogranite	
BOORABBIN					
(x)	Boorabbin Rock	31°12'30"S 120°17'20"E	56477	(G) Biotite monzogranite	
(y)	5km north of Diamond Rock	31°32'30"S 120°32'40"E	56478	(G) Biotite monzogranite	
Eastern Goldfields Province					
(z)	Perseverence		74/120 to 74/124	(N) Silicic gneiss with a folded foliated (Perseverence Gneiss)	7
1)	Woorana Well	27°28'15"S 121°12'40"E	59046 A	(G) Seriate clinopyroxene–albite–microcline quartz syenite	8
			59046 C	(G) Crystalloblastic albite– clinopyroxene–microcline, quartz-bearing syenite	
			59047	(G) Seriate clinopyroxene–amphibole–albite–microcline alkali granite	
(2)	Mount Boreas	27°50'55"S 121°53'10"E	40591A	(G) Coarse-grained hypidiomorphic granular monzogranite	
		27°51'55"S 121°53'10"E	40592A	(G) Medium-grained biotite monzogranite	9, 10
(3)	Isolated Hill	28°44'55"S 123°46'05"S	40597A	(G) Partially recrystallized porphyritic hornblende–biotite monzogranite	11
			40597F	(G) Porphyritic leucocratic monzogranite, intruding 40597A	

(a) Letters in parentheses correspond to sites shown on Figure 1
(b) For GSWA samples only; reported to the nearest 5"
(c) Five-digit sample numbers are GSWA numbers; others are as used in references
(d) (G) = granite; (N) = gneiss
(e) References for additional field and petrographic information and/or complementary isotopic age data:

1 = Pidgeon et al. (1990); 2 = Wilde and Pidgeon (1987); 3 = Wilde and Pidgeon (1986); 4 = Muhling and de Laeter (1971); 5 = Chapman et al. (1981); 6 = Bickle et al. (1983); 7 = Cooper et al. (1978); 8 = Libby and de Laeter (1981); 9 = Bunting and Williams (1979); 10 = Stuckless et al. (1981); 11 = Bunting et al. (1976)

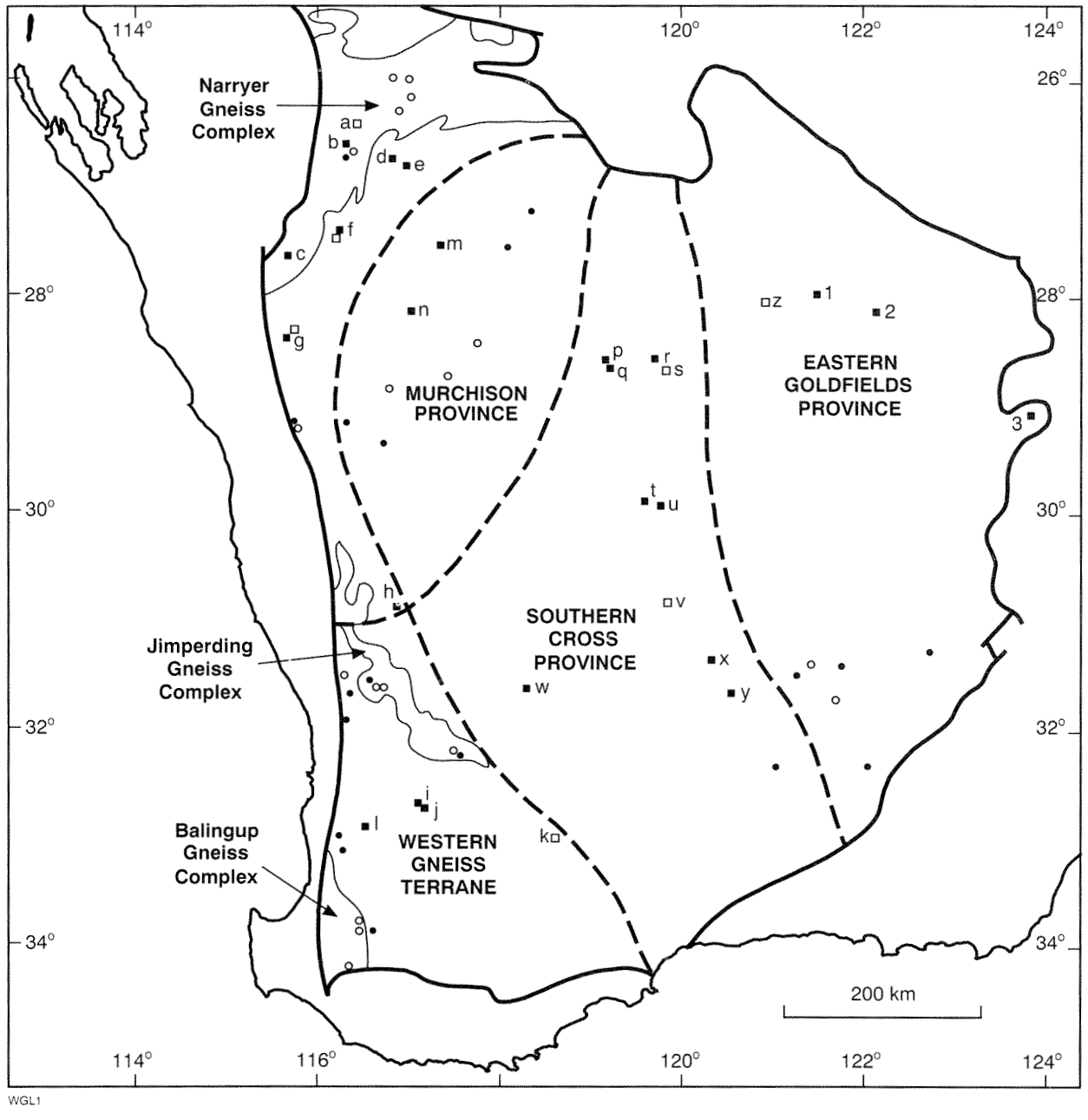

Figure 1. **Major structural subdivisions of the Yilgarn Craton (after Gee et al., 1981; Myers, 1990). The dashed line is the possible extension of the Murchison–Southern Cross province boundary discussed in text. Sample localities shown by solid symbols are classified as 'granite', open symbols are 'gneiss' (see text). Lettered squares are localities given in Table 1 and the references listed there. Circles show additional sites for which published data are plotted in later figures**

Analytical procedures

Data were obtained over several years, using the procedures described by Fletcher et al. (1984) and Fletcher et al. (1991). The older data are normalized to $^{146}Nd/^{142}Nd = 0.632265$ while more recent analyses use $^{146}Nd/^{144}Nd = 0.7219$. The two normalizations are essentially equivalent, the measured $^{143}Nd/^{144}Nd$ values for BCR-1 being 0.512630 ± 12 and 0.512622 ± 6 (95% C.L.), respectively.

Model ages

Model ages are computed parameters which have the dimensions of time. Unfortunately, the term implies a strictly chronological significance which is not justified, and considerable caution is required in using model ages as indicators of the ages of rocks or 'events' (see Arndt and Goldstein, 1987, for a review of the limitations inherent in the case of Sm–Nd). In general, compari-

sons between the model ages of samples — provided the same model is used and it is equally applicable to all samples — are of greater significance than the numerical values of individual model ages.

A variety of definitions has been used for Sm–Nd model ages, the differences reflecting different assumptions about the composition and evolution of the mantle from which continental crust is derived. There is no established convention for referring to different models, and care is required when comparing model ages from different laboratories.

Earlier publications, including some from this laboratory, use

$$T_{CHUR} = \lambda^{-1}\ln\left\{1+\frac{[^{143}Nd/^{144}Nd]_{Sample}-[^{143}Nd/^{144}Nd]_{CHUR}}{[^{147}Nd/^{144}Nd]_{Sample}-[^{147}Nd/^{144}Nd]_{CHUR}}\right\}$$

where λ is the decay constant of ^{147}Sm (= 6.54 x 10^{-12} a^{-1}), CHUR refers to unfractionated mantle of chondritic Sm–Nd composition, and the CHUR parameters are present-day values; the values used in this study are $[^{143}Nd/^{144}Nd]_{CHUR}$ = 0.51262, and $[^{147}Sm/^{144}Nd]_{CHUR}$ = 0.1967.

This model is an extreme case, ignoring the fact that the Sm–Nd system of the mantle has been fractionated, predominantly by the extraction of crustal material.

A second model which is now fairly widely used is

$$T_{MORB} = \lambda^{-1}\ln\left\{1+\frac{[^{143}Nd/^{144}Nd]_{Sample}-[^{143}Nd/^{144}Nd]_{MORB}}{[^{147}Nd/^{144}Nd]_{Sample}-[^{147}Nd/^{144}Nd]_{MORB}}\right\}$$

where MORB refers to a mantle which had chondritic $^{143}Nd/^{144}Nd$ at T ~ 4500 Ma but a $^{147}Sm/^{144}Nd$ composition that leads to a present-day mantle $^{143}Nd/^{144}Nd$ corresponding to the average composition recorded in mid-ocean ridge basalts. This is also an extreme model, since (assuming a chondritic primordial earth) it implies that the dominant REE fractionation in the mantle occurred 'instantaneously' following formation of the earth. The model parameters used here are $[^{143}Nd/^{144}Nd]_{MORB}$ = 0.513151, and $[^{147}Sm/^{144}Nd]_{MORB}$ = 0.2136.

In the data tables below, both T_{CHUR} and T_{MORB} are listed: T_{CHUR} allows direct comparison with most previously published Yilgarn Craton data; T_{MORB} and T_{CHUR} together give the range of 'reasonable' possible model ages.

There are several more-subtle models, notably the T_{DM} of de Paolo (1981), which attempt to allow for progressive changes in mantle composition throughout the history of the earth. As yet, the dynamics of mantle evolution are not sufficiently well characterized to allow the adoption of a universally applicable model.

Another expression commonly used is T_{CR} — 'crustal residence' age. This is variously defined by different authors, sometimes as T_{MORB} or T_{DM}, sometimes by other more specific models (e.g. McCulloch, 1987). For the plots presented below we use $T_{CR} = (T_{MORB} + T_{CHUR})/2$ which is computationally convenient, avoids the extreme assumptions of T_{MORB} and T_{CHUR}, and satisfies the condition that T_{CR} equals or exceeds the emplacement age in all cases where this is known for the samples considered. For Archaean samples, T_{CR} values are numerically close to T_{DM}.

Data and discussion

Sm–Nd data are given in Table 2 for the samples listed in Table 1. Data have also been drawn from published sources for some parts of the following discussion and are plotted in compilation figures. The relevant sample locations are shown in Figure 1; the sources are:

Fletcher et al. (1983a,b, 1985); de Laeter et al. (1981, 1985); Kinny (1986); Nieuwland and Compston (1981); McCulloch et al. (1983a,b); Dobos et al. (1986); Compston and Arriens (1968); Compston et al. (1986); McCulloch and Compston (1981); Claoué-Long et al. (1986b); Bunting et al. (1976), Oversby (1975); McCulloch (1987); Campbell and Hill (1988); Hill et al. (1989); Watkins et al. (1991) and J. S. Myers (1987, pers. comm.).

1. Isochron plots

In several instances, samples were chosen from sample suites which had previously been used for Rb–Sr isochron studies. In each case the Sm–Nd data disperse appreciably on isochron plots, but in no case is a simple isochron age determination possible.

Data for the Perseverence Gneiss (site z) scatter around a best-fit line (Fig. 2a) and disperse so widely that the protolith was almost certainly of mixed parentage. This supports the contention of some workers in this region (Cooper, J., 1981, pers. comm.) that it was sedimentary. Given this, the well-fitted (MSWD = 2.86) 2625 ± 34 Ma Rb–Sr isochron of Cooper et al. (1978) must date metamorphism.

The analysed samples from the Woorana Well alkaline granite (site 1) probably are cogenetic but the data spread (Fig. 2b) is not sufficient to define a precise isochron age. The best-fit line shown in Figure 2b suggests a 'typical Yilgarn' age of ~2700 Ma with initial ε_{Nd}~3.0. Rb–Sr data for seven samples from the Woorana Well locality (Libby and de Laeter, 1981) give a date, interpreted by them as an emplacement age, of 2520 ± 113 Ma. Stuckless et al. (1981) propose a Pb/Pb age, based on a regional sampling of syenites including Woorana Well, of 2760 ± 210 Ma. The Sm–Nd data are compatible with either of these dates; they would easily allow an age of 2760 Ma (with initial ε_{Nd} ~4), and possibly as low as 2520 Ma (initial ε_{Nd} ~0).

A strikingly different case is seen in the data for Isolated Hill (site 3). The two samples were chosen as typical, albeit quite distinguishable, granites from the area. They are from a suite analysed by Bunting et al. (1976) who interpreted the resulting Rb–Sr date of 2537 ± 25 Ma as a metamorphic age. The two Sm–Nd data points separate widely (Fig. 2c) with the $^{147}Sm/^{144}Nd$ of sample 40597F being extremely high for a granite, particularly for

Table 2. Sm–Nd analytical data and model ages

Location (a)	Sample Number	Sm (b) (ppm)	Nd (b) (ppm)	$^{147}Sm/^{144}Nd$ (d)	$^{143}Nd/^{144}Nd$ (d)	T_{CHUR} (e) (Ma)	T_{MORB} (e) (Ma)
Western Gneiss Terrane							
NARRYER GNEISS COMPLEX							
(a) Meegea Hill							
	80316	1.0	6.0	0.10210	0.510795 ± 10	2 922	3 197
	80322	1.4	6.9	0.12764	0.511107 ± 10	3 314	3 695
(b) West of Mount Dugel							
	80309	4.7	34	0.08323	0.510298 ± 10	3 097	3 310
	80313	9.0	62	0.08815	0.510444 ± 10	3 034	3 264
(c) New Forest							
	77270	1.7	9.8	0.10213	0.510792 ± 10	2 927	3 202
	77272	2.6	12.9	0.12131	0.511116 ± 10	3 020	3 335
OTHER							
(d) Weiragoo Range							
	77391	7.1	42	0.10303	0.510856 ± 10	2 853	3 141
	77392	7.4	36	0.12248	0.511052 ± 10	3 197	3 482
(e) Tching Range							
	77334	3.2	22.5	0.08710	0.510533 ± 10	2 884	3 132
	77337A	10.7	72	0.08979	0.510630 ± 10	2 820	3 082
(f) Mount Nicolay							
	77346	4.3	35	0.14834	0.511379 ± 10	-	-
	77350	14.3	116	0.07438	0.510079 ± 10	3 144	3 337
	77353	4.9	16.9	0.08764	0.510451 ± 10	3 011	3 243
(g) Greenough River crossing							
	77362	1.5	12.8	0.07298	0.510238 ± 10	2 916	3 135
	77366	3.0	22.6	0.07912	0.510362 ± 10	2 909	3 139
(h) Wongan Hills							
	WH-5	7.3	47	0.0956	0.510701 ± 22	2 875	3 142
(i) North of Narrogin							
	59925	5.9	34	0.1058	0.510936 ± 20	2 805	3 109
(j) Wickepin							
	59926	8.1	58	0.0846	0.510530 ± 21	2 825	3 076
(k) Joyces Prospect							
	W-15	1.3	8.0	0.0955	0.510772 ± 23	2 768	3 051
(l) Northwest of Mount Saddleback							
	W-13	3.5	18.1	0.1173	0.511239 ± 22	2 637	3 006
Murchison Province							
(m) Northwest of Tragedy Bore							
	17808	4.1	27.6	0.091*	0.510651 ± 25		
		4.7	31.3	0.0910	0.510657 ± 21	2 813	3 079
(n) South of Mardah Well							
	17810	1.9	11.8	0.098*	0.510849 ± 25		
		2.2	13.7	0.09703	0.510877 ± 11	2 650	2 954
Southern Cross Province							
(p) New Well							
	71125	3.1	21.9	0.0867	0.510583 ± 25	2 804	3 062
(q) Little Noondie Hill							
	71124	3.6	23.3	0.0926	0.510678 ± 25	2 826	3 093
(r) Bulga Downs							
	71122	3.0	22.1	0.0824	0.510369 ± 25		
		2.9	21.3	0.0821	0.510369 ± 20	2 974	3 201
(s) White Cloud							
	71123	3.3	24.0	0.0827	0.510380 ± 25	2 974	3 202

Table 2. (*continued*)

Location (a)	Sample Number	Sm (b) (ppm)	Nd (b) (ppm)	$^{147}Sm/^{144}Nd$ (d)	$^{143}Nd/^{144}Nd$ (d)	T_{CHUR} (e) (Ma)	T_{MORB} (e) (Ma)
(t) Rainy Rocks							
	UWA87975	8.6	67	0.0779	0.510474 ± 20	2 737	2 986
(u) Milky Soak							
	UWA87955	6.1	37	0.0995	0.510680 ± 20	3021	3 276
(v) East Koolyanobbing							
	UWA81884	2.8	20.6	0.0815	0.510484 ± 22	2 809	3 056
(w) Merredin quarry							
	59956A	5.3	39	0.0833	0.510520 ± 24	2 806	3 057
(x) Boorabbin Rock							
	56477	4.6	29.3	0.0949	0.510714 ± 32	2 837	3 108
(y) North of Diamond Rock							
	56478	4.6	31.8	0.0866	0.510593 ± 21	2 789	3 049
Eastern Goldfields Province							
(z) Perseverence Gneiss							
	74/120	3.1	10.6	0.176*	0.512210 ± 25	-	-
		3.1	10.6	0.1757	0.512224 ± 32	-	-
	74/121	2.3	13.1	0.1075	0.511042 ± 25	2 681	3 009
	74/122	3.1	12.2	0.154*	0.511943 ± 29	-	-
		3.0	11.8	0.1527	0.511953 ± 21	-	-
	74/123	2.5	11.1	0.1362	0.511548 ± 27	2 686	3 134
	74/124	3.6	12.1	0.181*	0.512340 ± 25	-	-
(1) Woorana Well	59046A	3.8	27.0	0.0858	0.510792 ± 25	2 500	2 796
	59046C	12.6	95	0.0807	0.510672 ± 25	2 547	2 826
	59047	13.4	82	0.0992	0.511006 ± 32	2 509	2 839
(2) Mount Boreas	40591A	12.8	109	0.0708	0.510463 ± 20	2 597	2 851
	40592A	14.1	117	0.0727	0.510467 ± 20	2 632	2 885
(3) Isolated Hill	40597A	5.5	40	0.0829	0.510655 ± 27	2 618	2 893
	40597F	1.8	5.5	0.2009	0.512788 ± 26	-	-

(a) Lettered as in Table 1 and Figure 1. Unnumbered data are complete re-analyses
(b) Reproducibility for small powdered samples is ~3%
(c) Data quoted to four figures have 95% C.L., including calibration and internal precision, of ±0.2%. A few cases (marked *) are known to have small additional uncertainties due to incomplete sample digestion. Data quoted to five figures are ±0.1%
(d) Normalized to $^{146}Nd/^{142}Nd = 0.632265$ or $^{146}Nd/^{144}Nd = 0.7219$ (see text). Uncertainties listed are 95% C.L. in the last figures quoted and include reproducibility and precision
(e) Defined in text; not calculated in cases with $^{147}Sm/^{144}Nd > 0.14$. Analytical uncertainties are ±20–40 m.y.

a highly fractionated one (as indicated by its high Rb/Sr). The two-point line does not define an age because the two samples are almost certainly not cogenetic. The unusual Sm–Nd character of sample 40597F is similar to that of some mixed gneiss/amphibolite rocks in the ductile deformation zone at the western edge of the ~1300 Ma Fraser Complex, about 500 km south of Isolated Hill. In that case, the samples have low Rb contents (<1 ppm) and low Rb/Sr, and the isotopic features have been interpreted as the imprint of purging of the zone by mantle-derived fluids at ~1300 Ma (Fletcher et al., 1991). There is no evidence for similar activity at Isolated Hill.

The other cases which give differing data for samples from restricted areas cannot be interpreted by isochron techniques. For Mount Nicolay, the only possible interpretation is that the components of the gneiss have not evolved as closed systems since its formation and/or that they were never fully equilibrated. Similarly, the two samples from Meegea Hill (site a) and the two from Weiragoo Range (site d) have analytically well-defined separations, but the directions of separation have no time significance in either case.

2. Comparisons between model ages and emplacement ages

A comparison between T_{CR} and the crystallization ages of granites or the protoliths of gneisses is given in Figure 3. Only U–Pb zircon data and several examples of Pb/Pb whole rock isochron data have been accepted as giving accurate crystallization ages. The Rb–Sr system is well known to be subject to post-emplacement resetting (e.g. Bickle et al., 1983) and in some cases published Pb/Pb isochrons are not well defined or are of uncertain significance. Data have been plotted only for cases where T_{CR} and emplacement age were measured on the same samples, or where there is a well-defined correlation

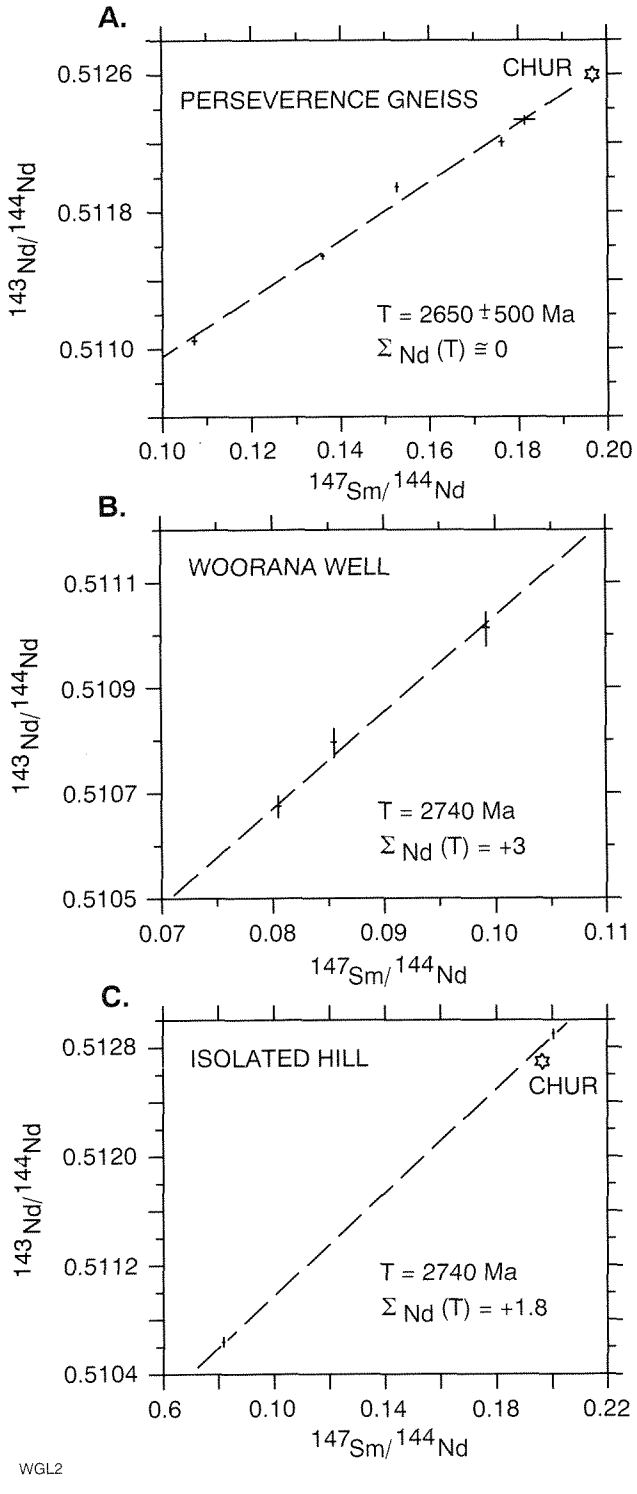

Figure 2. Sm–Nd isochron plots

(a) Perseverence Gneiss. The alignment is probably not a valid isochron
(b) Alkaline granitoids near Woorana Well. The isochron has large uncertainties
(c) Granites at Isolated Hill. Despite their general similarities the two samples have very different $^{147}Sm/^{144}Nd$ and they are unlikely to be cogenetic, i.e. the 2-point line is unlikely to be a valid isochron

between the rocks analysed. Where appropriate Sm–Nd data have been averaged and the plotting symbol spans the data; for single analyses analytical uncertainties (±30 m.y.) are used. For plotting purposes, a *minimum* uncertainty of ±10 m.y. is applied to the emplacement ages.

The most striking feature of Figure 3 is the clustering of data for the syn- and post-tectonic granites. All the emplacement ages fall in the range 2600–2700 Ma, while the corresponding T_{CR} values span the range 2680–3310 Ma. If T_{CR} (as defined above) is a valid estimator of crustal residence age then the pre-emplacement ages of material in the granites ranges from zero to ~700 Ma. This group of samples has representatives in all major regional divisions of the craton.

In contrast to the granites, data for the gneisses cover a wide range of both T_{CR} and crystallization age. The data are few, but they appear to define a diffuse elongate field parallel to the diagonal limiting line in Figure 3, with a mean pre-crystallization age of ~200 Ma.

3. Narryer Gneiss Complex

The granite samples from west of Mount Dugel (site b) have been shown by zircon U–Pb analysis to be similar in crystallization age (~2.63 Ga) to post-tectonic granites close to Mount Narryer (Myers, J. S., 1987, pers. comm.), though the granites at the two localities are chemically distinct. The bulk compositions of the Mount Dugel granites and the two granitic samples from New Forest (site c) show some similarity to components of the old gneisses at Mount Narryer. However, their model ages clearly show them to be unrelated. Their T_{CHUR} dates range from 2927 Ma to 3097 Ma (Table 2) and are quite distinct from the 3620 Ma to 3710 Ma values recorded for Meeberrie Gneiss, and 3510 Ma to 3540 Ma for Dugel Gneiss, in the type area near Mount Narryer (de Laeter et al., 1985). Even the T_{MORB} values are less than the crystallization age of Dugel Gneiss protoliths in the type area (3381 ± 22 Ma; Kinny et al., 1988). The granites from both of the new localities appear to correlate with late Archaean granites in the Mount Narryer area, two of which have given T_{CHUR} values of 3070 Ma and 3120 Ma (de Laeter et al., 1985).

The two samples of gneiss from Meegea Hill (site a), which were tentatively correlated in the field with Dugel Gneiss, give quite different model ages (T_{CHUR} = 2922 Ma and 3314 Ma, Table 2). These dates are distinctly less than the 3510 Ma to 3540 Ma values recorded for Dugel Gneiss in the type area near Mount Narryer (de Laeter et al., 1985) and at Errabiddy (Fletcher et al., 1983b).

4. Model age compilations

Compilations of all available Sm–Nd model age data (to 1988) are shown in Figure 4, for several different regional groupings. Data from published sources have been classified using the same granite/gneiss distinction applied to samples in Table 1. Data for the Jimperding and Balingup Gneiss Complexes have been grouped together

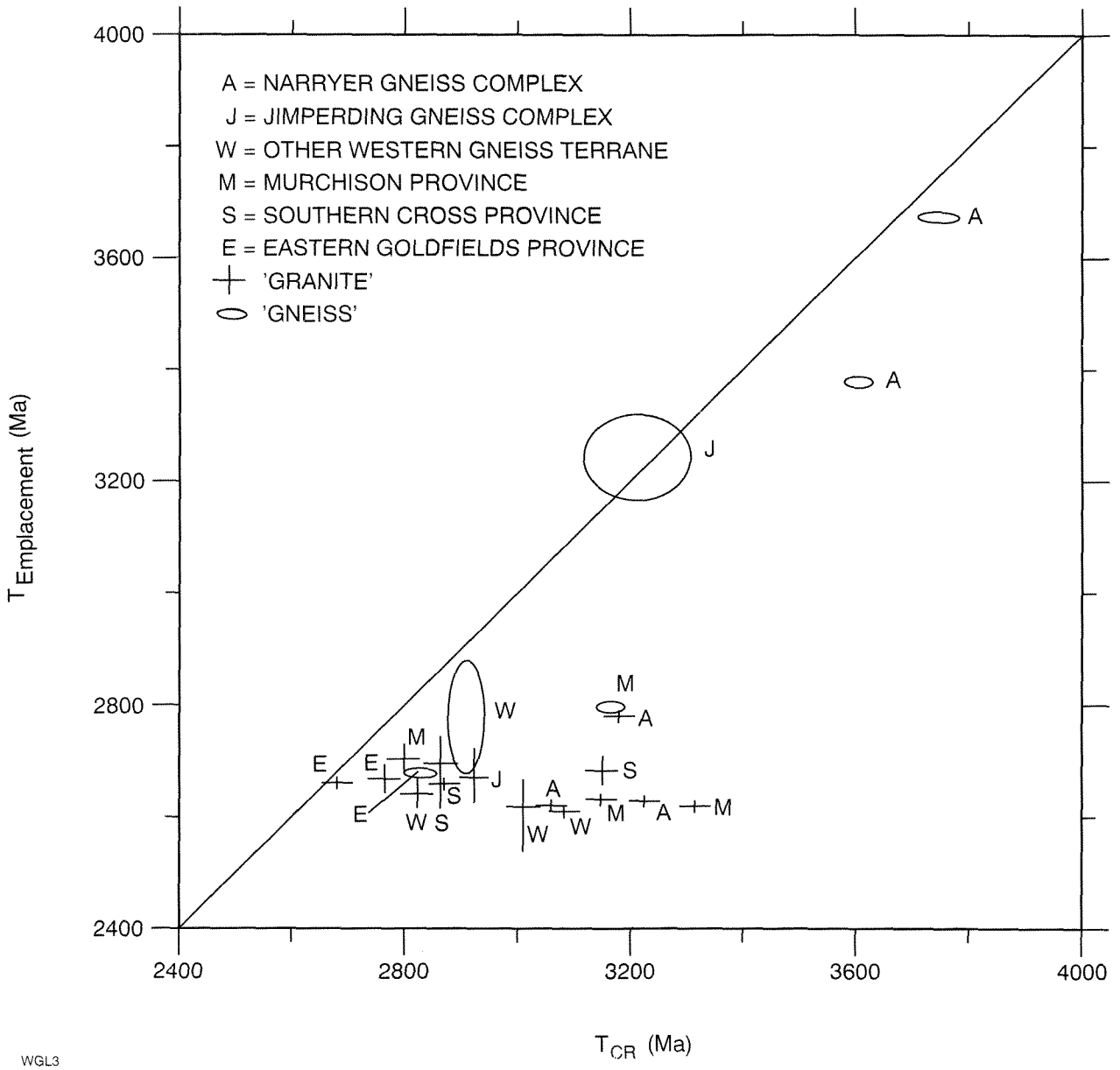

Figure 3. Comparison between Sm–Nd model ages (T_{CR}) and emplacement (or crystallization) ages of Yilgarn 'granites' and 'gneisses'. The diagonal line represents T_{CR} = emplacement age; any data falling to the left of the line would invalidate the model adopted for T_{CR}

because there are only limited data for each area and the two data sets almost completely overlap.

The top row of Figure 4 (a–d) shows data for the commonly used regional subdivisions reproduced in Figure 1. The second row (e–g, d) is a variant on this, in which the Western Gneiss Terrane is, in effect, reduced to include only the three recognized 'older' gneiss complexes, the remainder of the area of the Western Gneiss Terrane being apportioned between the Murchison and Southern Cross Provinces (following the dotted line in Fig. 1). These extensions do not change the character of the profiles for either of the provinces. That of the Southern Cross Province is still particularly narrow, even though the augmented province includes almost half of the area of the Yilgarn Craton.

Interpretations of Figure 4 are limited by the possibly unrepresentative nature of sampling, by the constraints inherent in model ages, and by ambiguities in some of the granite/gneiss classifications. Nonetheless, some broad-scale features stand out. One is the strong decrease in recorded model ages from the extreme northwest of the craton (the Narryer Gneiss Complex, Fig. 4h) to the Eastern Goldfields Province (Fig. 4d). The existence of abundant ~3350 Ma and rare ~3650 Ma zircons in the Maynard Hills quartzite, which lies just east of sites (r) and (s) in the Southern Cross Province (Froude et al., 1983)

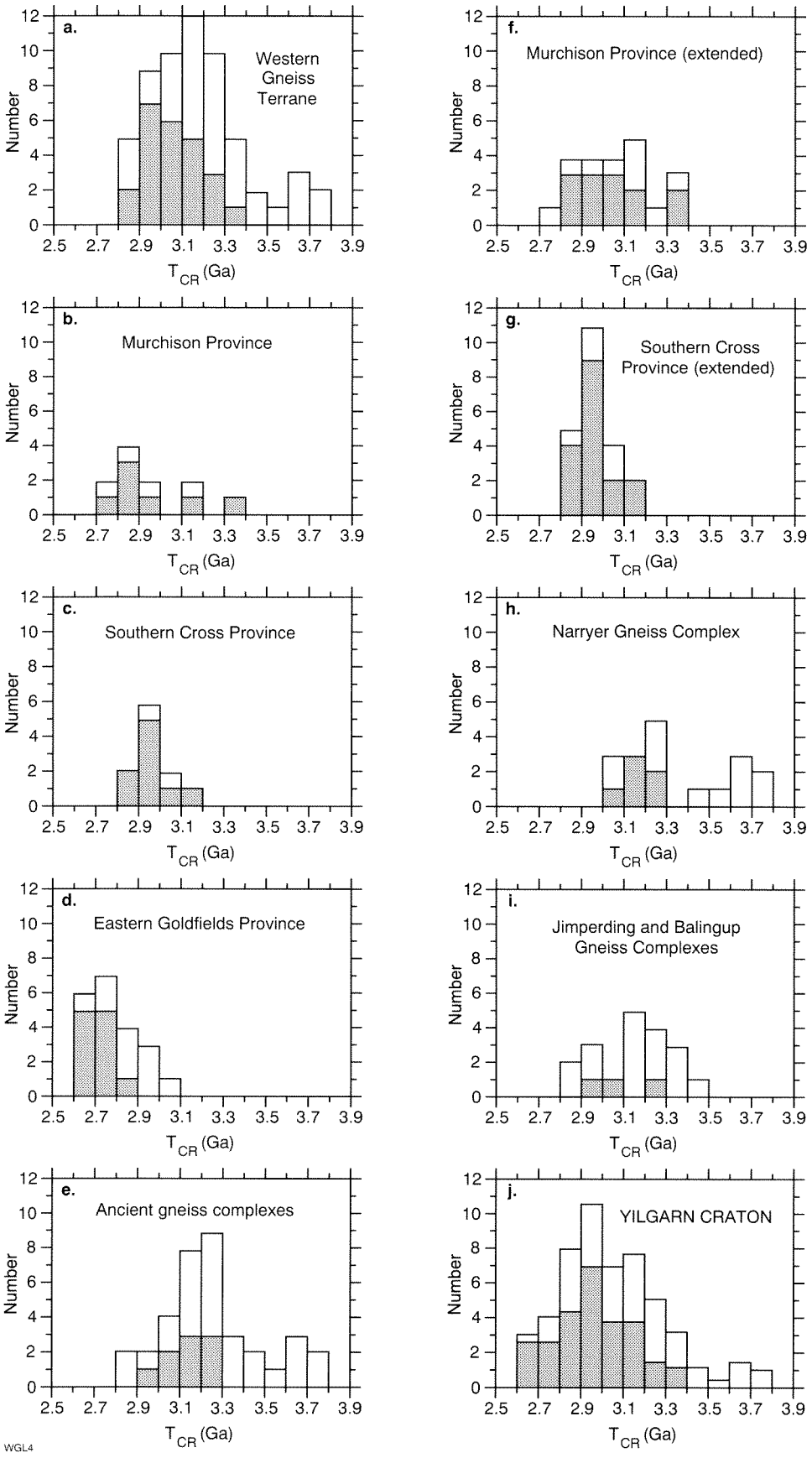

Figure 4. Compiled crustal residence ages (T_{CR}) for the Yilgarn Craton and the subdivisions outlined in Figure 1. Shaded blocks = 'granites', open blocks = 'gneisses'. Data from Table 2

and ~3400 Ma zircons at Kambalda in the Eastern Goldfields Province (e.g. Claoué-Long et al., 1986a) demonstrates that remnants of crust of at least these ages have been incorporated into the rocks now exposed in these provinces. Figure 4a shows, however, that these remnants can only be a minor component of the rock units analysed. It might be argued (e.g. Gee, 1979) that Proterozoic tilting of the Yilgarn Block has exposed older deep crustal rocks in western areas and that similar old crust may underlie the eastern provinces. This may be true, but it cannot explain the extent of the differences seen unless Archaean crust is stratified to an extent not generally recognized. As noted above, extending the central provinces to the west, to include some 'younger' high-grade areas such as the Murgoo Gneiss Complex and the Chittering Metamorphic Belt (as well as granite-dominated areas), does not change the character of their model age profiles.

Another feature in the data for the Narryer Gneiss Complex (Fig. 4h) is the bimodal distribution. This could be an artifact of sampling, since some of the gneiss samples were collected as representing possible 'oldest basement'. However, given that some of these samples fall in the younger model age group, it seems unlikely that further sampling would obliterate the bimodality.

The Southern Cross Province distribution (Fig. 4c or 4g) is remarkably narrow, considering the extent of the province (Fig. 1). This, together with the bimodal nature of the Narryer Gneiss Complex plot and the fairly narrow Eastern Goldfields profile, suggests an episodic sequence of additions of material to the craton, though it gives no clues as to how or when the provinces may have accreted into a single craton. The apparent growth pulses are at ~3700 Ma, ~3300 Ma, ~3000 Ma and ~2700 Ma. These dates are strongly model dependent, but they might be valid ages given that they correspond well with emplacement ages (established by ziron U–Pb data) for various rock types in the corresponding areas. The peaks of crustal growth are strongly associated with particular provinces and they have significant width (in time), so that in a compilation for the whole Yilgarn Craton (Fig. 4j) much of the detail is averaged out. Only the 3600–3700 Ma and 2900–3000 Ma peaks are still apparent in the total profile; the 2900–3000 Ma peak also shows up in the granites.

The Murchison Province profile (Fig. 4b or 4f) has a strong overlap with that of the Southern Cross Province (Fig. 4c or 4g), but it is somewhat broader and considerably less peaked than either the Southern Cross or Eastern Goldfields Province profiles, suggesting that material of more diverse ages is included here than is the case for the eastern granite–greenstone provinces.

The Jimperding and Balingup Complexes have a (combined) profile (Fig. 4i) quite different from that of the Narryer Complex (Fig. 4h), though the younger peak in the Narryer Complex profile falls near the centre of the Jimperding–Balingup data spread. More data would be needed from the Jimperding and Balingup complexes to make more detailed comparisons.

Conclusions

Each of the provinces of the Yilgarn Craton has a distinctive T_{CR} distribution, which probably reflects a distinct early history. Recorded values of T_{CR} range from a distinct grouping of gneisses with T_{CR} ~3.7 Ga in the Narryer Gneiss Complex to the T_{CR} ~2.7 Ga which dominate in the Eastern Goldfields Province. The regional character of the T_{CR} distributions lies predominantly in the older dates within each distribution. The rocks which these older dates represent are, however, only a minor (though very important) component of each region. For example, rocks with T_{CR} >3.4 Ga have been found only locally within the Narryer Gneiss Complex. Similarly, in the Eastern Goldfields Province, the remnants of felsic crustal material older than 3.0 Ga, whose existence is indicated by preservation of zircons of that age (but not yet by Sm–Nd model ages), constituted only a minor component of that province when the craton stabilized at about 2.6 Ga.

The Murchison Province appears to be a more mixed crustal segment than either of the other granite–greenstone provinces, and it may be transitional between the Narryer Gneiss Complex and the rest of the craton. Its T_{CR} dates span the ~3.3 Ga and ~3.0 Ga maxima seen elsewhere. It is notable that this is the only granite–greenstone province in which supracrustal sequences of two distinct ages are known to occur (Watkins and Hickman, 1990), the Luke Creek Group being ~3.0 Ga (Pidgeon and Wilde, 1990) and the Mount Farmer Group being younger, possibly ~2.8 Ga. It is not possible to rationally redefine the boundaries of the Murchison Province in a way which separates ~3.0 Ga and ~3.3 Ga model age areas, and this model age pattern apparently extends west as far as the Darling Fault and the contacts of the Narryer and Jimperding Gneiss Complexes.

The distinctive T_{CR} signature of granitoid rocks in the Southern Cross Province contrasts with the picture given by dates of major eruptive events in greenstone belts, which are similar (at ~2.7 Ga) in the Eastern Goldfields and Southern Cross Provinces (Pidgeon and Wilde, 1990). This emphasises the point that the provinces might be most readily distinguished on the basis of their early histories. In this context, the data suggest that the Southern Cross Province could be redefined to include the southern half of the Western Gneiss Terrane, except for the recognized ancient gneiss complexes within the latter.

Syn- and post-tectonic graintoid rocks have T_{CR} varying up to ~3.3 Ga, but throughout the craton they have emplacement ages of 2.6–2.7 Ga. Relatively few of the gneisses have well-determined protolith crystallization ages. These few show a crude correlation between T_{CR} and crystallization age, the majority of cases indicating crystallization from crustal material which was, at the time, no older than 300 million years.

The model ages suggest a periodicity when they are considered by structural province. There are frequency peaks at ~3.7 Ga and ~3.3 Ga in the Narryer Complex, ~3.0 Ga in the Southern Cross Province and ~2.7 Ga in

the Eastern Goldfields Province. No T_{CR} values less than ~2.6 Ga have been reported for granitoid rocks in the Yilgarn Craton, although there was widespread intrusion of mafic dykes in the early Proterozoic, and there was an apparent surge in crust formation marginal to the craton at ~2.2 Ga when development of the surrounding orogens began.

Given sufficient breadth of sampling, regional mapping of T_{CR} can provide a first-order view of the sequence of development of various crustal segments. At this level of approximation, the Narryer Gneiss Complex is the oldest crustal segment in the Yilgarn Craton and the Eastern Goldfields Province is the youngest. The remaining areas of the Western Gneiss Terrane, the Murchison Province and the Southern Cross Province are of intermediate crustal age, progressively younger from west to east. The indication of steps, or periodicity, in this progression is taken to reflect successive stages of crustal development rather than a progressive admixture of young crust with old. It is not clear whether the progression represents growth around a continental nucleus centred in the Mount Narryer area, repeated rifting of an ancient continent, or later juxtaposition of crustal plates which developed separately.

Acknowledgements

We are indebted to S. A. Wilde and R. T. Pidgeon (Curtin University of Technology), M. J. Bickle (then at University of Western Australia), J. A. Cooper (University of Adelaide) and numerous present and past GSWA staff who collected or provided samples analysed in this study. R. D. Gee and A. F. Trendall contributed to many discussions related to this study; S. A. Wilde, J. S. Myers and D. R. Nelson provided comments on earlier drafts of this paper. This work was supported by the Australian Research Council.

References

ARNDT, N. T., and GOLDSTEIN, S. L., 1987, Use and abuse of crust-formation ages: Geology, v. 15, p. 893—895.

BICKLE, M. J., CHAPMAN, H. J., BETTENAY, L. F., and GROVES, D. I., 1983, Lead ages, reset rubidium–strontium ages and implications for the Archaean crustal evaluation of the Diemals area, Central Yilgarn Block, Western Australia: Geochimica et Cosmochimica Acta, v. 47, p. 907–914.

BUNTING, J. A., de LAETER, J. R., and LIBBY, W. G., 1976, Tectonic subdivisions and geochronology of the northeastern part of the Albany–Fraser Province, Western Australia: Western Australia Geological Survey, Annual. Report 1975, p. 117–126.

BUNTING, J. A., and WILLIAMS, S. J., 1979, Sir Samuel, W.A.: Western Australia Geological Survey, 1:250 000 Geology Series Explanatory Notes.

CAMPBELL, I. H., and HILL, R. I., 1988, A two-stage model for the formation of the granite–greenstone terrains of the Kalgoorlie–Norseman area, Western Australia: Earth and Planetary Science Letters, v. 90, p. 11–25.

CHAPMAN, H. J., BICKLE, M. J., de LAETER, J. R., BETTENAY, L. F., GROVES, D. I., ANDERSEN, L. S., BINNS, R. A., and GORTON, M., 1981, Rb–Sr geochronology of granitic rocks from the Diemals area, central Yilgarn Block, Western Australia, *in* Archaean Geology: Geological Society of Australia, Special Publication 7, p. 173–186.

CLAOUÉ-LONG, J. C., COMPSTON, W., and WILLIAMS, I. S., 1986a, The elusive basement to the Kambalda–Kalgoorlie mineral belt: Australian National University, Research School of Earth Sciences, Annual Report 1986, p. 69.

CLAOUÉ-LONG, J. C., COMPSTON, W., WILLIAMS, I. S., and FOSTER, J. J., 1986b, Crustal history of the Kambalda greenstones: Australian National University Research School of Earth Sciences, Annual Report. 1986, p. 69–70.

COMPSTON, W., and ARRIENS, P. A., 1968, The Precambrian geochronology of Australia: Canadian Journal of Earth Sciences, v. 5, p. 561–583.

COMPSTON, W., WILLIAMS, I. S., and McCULLOCH, M. T., 1986, Contrasting zircon U–Pb and model Sm–Nd ages for the Archaean Logue Brook Granite: Australian Journal of Earth Sciences, v. 33, p. 193–200.

COOPER, J. A., NESBITT, R. W., PLATT, J. P., and MORTIMER, G. E., 1978, Crustal development in the Agnew region, Western Australia, as shown by Rb–Sr isotopic and geochemical studies: Precambrian Research, v. 7, p. 31–59.

de LAETER, J. R., FLETCHER, I. R., BICKLE, M. J., MYERS, J. S., LIBBY, W. G., and WILLIAMS, I. R., 1985, Rb–Sr, Sm–Nd and Pb–Pb geochronology of ancient gneisses from Mt Narryer, Western Australia: Australian Journal of Earth Sciences, v. 32, p. 349–358.

de LAETER, J. R., FLETCHER, I. R., ROSMAN, K. J. R., WILLIAMS, I. R., GEE, R. D., and LIBBY, W. G., 1981, Early Archaean gneisses from the Yilgarn Block, Western Australia: Nature, v. 292, p. 322–324.

de PAOLO, D. J., 1981, Neodymium isotopes in the Colorado Front Range and crust–mantle evolution in the Proterozic: Nature, v. 291, p. 193–196.

DOBOS, S. K., JACOBSEN, S. B., DERRY, L. A., and GOLDSTEIN, S. J., 1986, A Nd and Sr isotopic study of metasediments from the Western Gneiss Belt (WGB) of Western Australia (abs.): Eos, v. 67, p. 1265.

FLETCHER, I. R., MYERS, J. S., and AHMAT, A. L., 1991, Isotopic evidence on the age and origin of the Fraser Complex, Western Australia; a sample of mid-Proterozoic lower crust. Chemical Geology, v. 87, p. 197–216.

FLETCHER, I. R., ROSMAN, K. J. R., WILLIAMS, I. R., HICKMAN, A. H., and BAXTER, J. L., 1984, Sm–Nd geochronology of greenstone belts in the Yilgarn Block, Western Australia: Precambrian Research, v. 26, p. 333–361.

FLETCHER, I. R., WILDE, S. A., LIBBY, W. G., and ROSMAN, K. J. R., 1983a, Sm–Nd model ages across the margins of the Archaean Yilgarn Block, Western Australia — II; southwest transect into the Proterozoic Albany–Fraser Province: Journal of the Geological Society of Australia, v. 30, p. 333–340.

FLETCHER, I. R., WILDE, S. A., and ROSMAN, K. J. R., 1985, Sm–Nd model ages across the margins of the Archaean Yilgarn Block, Western Australia — III. The western margin: Australian Journal of Earth Sciences, v. 32, p. 73–82.

FLETCHER, I. R., WILLIAMS, S. J., GEE, R. D., and ROSMAN, K. J. R., 1983b, Sm–Nd model ages across the margins of the Archaean Yilgarn Block, Western Australia; northwest transect into the Proterozoic Gascoyne Province: Journal of the Geological Society of Australia, v. 30, p. 167–174.

FROUDE, D. O., COMPSTON, W., and WILLIAMS, I. S., 1983, Early Archaean zircon analyses from the central Yilgarn Block: Australian National University, Research School of Earth Sciences, Annual Report 1983, p. 124–126.

GEE, R. D., 1979, Structure and tectonic style of the Western Australian shield: Tectonophys, v. 58, p. 327–369.

GEE, R. D., BAXTER, J. L., WILDE, S. A., and WILLIAMS, I. R., 1981, Crustal development in the Archaean Yilgarn Block, Western Australia, *in* Archaean Geology: Geological Society of Australia, Special Publication 7, p. 43–56.

HARLEY, S. L., 1987, Origin and growth of continents : Nature, v. 329, p. 108–109.

HILL, R. I., CAMPBELL, I. H., and COMPSTON, W., 1989, Age and origin of granitic rocks in the Kalgoorlie–Norseman region of Western Australia: Implications for the origin of Archaean Crust: Geochimica et Cosmochimica Acta, v. 53, p. 1259–1275.

KINNY, P.D., 1986, Zircon ages from the Narryer Metamorphic Belt: Geological Society of Australia, Abstracts, v. 15, p. 107–108.

KINNY, P. D., WILLIAMS, I. S., FROUDE, D. O., IRELAND, T. R., and COMPSTON, W., 1988, Early Archaean zircon ages from orthogneisses and anorthosites at Mount Narryer, Western Australia: Precambrian Research, v. 38, p. 325–341.

LIBBY, W. G., and de LAETER, J. R., 1981, Rb–Sr geochronology of alkaline granitic rocks in the Eastern Goldfields Province : Western Australia Geological Survey, Annual Report 1980, p. 98–103.

McCULLOCH, M. T., 1987, Sm–Nd isotopic constraints on the evolution of Precambrian crust in the Australian continent, *in* Proterozoic Lithospheric Evolution, Geodynamics Series, v. 17, International Lithosphere Program Publication no. 0130, p. 115–130.

McCULLOCH, M. T., COLLERSON, K. D., and COMPSTON, W., 1983a, Growth of Archaean crust within the Western Gneiss Terrain, Yilgarn Block, Western Australia: Journal of the Geological Society of Australia, v. 30, p. 155–160.

McCULLOCH, M. T., and COMPSTON, W., 1981, Sm–Nd age of Kambalda and Kanowna greenstones and heterogeneity in the Archaean mantle: Nature, v. 294, p. 322–327.

McCULLOCH, M. T., COMPSTON, W., and FROUDE, D., 1983b, Sm–Nd and Rb–Sr dating of Archaean gneisses, eastern Yilgarn Block, Western Australia: Journal Geological Society Australia, v. 30, p. 149–153.

McCULLOCH, M. T., and WASSERBURG, G. J., 1978, Sm–Nd and Rb–Sr chronology of continental crust formation: Science, v. 200, p. 1003–1011.

MUHLING, P. C., and de LAETER, J. R., 1971, Ages of granitic rocks in the Poona–Dalgaranga area of the Yilgarn Block, Western Australia: Geological Society of Australia, Special Publication 3, p. 25–31.

MYERS, J. S., 1990, Western Gneiss Terrane, *in* Geology and Mineral Deposits of Western Australia: Western Australia Geological Survey, Memoir 3, p. 13–32.

NELSON, B. K., and de PAOLO, D. J., 1985, Rapid production of continental crust 1.7–1.9 G.y. ago: Nd and Sr isotopic evidence from the basement of the North American mid continent: Geological Society of America, Bulletin 96, p. 746–754.

NIEUWLAND, D. A., and COMPSTON, W., 1981, Crustal evolution in the Yilgarn Block near Perth, Western Australia, *in* Archaean Geology: Geological Society of Australia, Special Publication 7, p. 159–171.

OVERSBY, V. M., 1975, Lead isotope systematics and ages of Archaean acid intrusives in the Kalgoorlie–Norseman area, Western Australia: Geochimica et Cosmochimica Acta, v. 39, p. 1107–1125.

PIDGEON, R. T., and WILDE, S. A., 1990, The distribution of 3.0 and 2.7 Ga volcanic episodes in the Yilgarn Craton of Western Australia: Precambrian Research, v. 48, p. 309–325.

PIDGEON, R. T., WILDE, S. A., COMPSTON, W., and SHIELD, M. W., 1990, Archaean evolution of the Wongan Hills Greenstone Belt, Yilgarn Craton, Western Australia: Australian Journal of Earth Sciences, v. 37, p. 279–292.

STUCKLESS, J. S., BUNTING, J. A., and NKOMO, I. T., 1981, U–Th–Pb systematics of some granitoids from the northeastern Yilgarn Block, Western Australia and implications for uranium source rock potential: Journal of the Geological Society of Australia, v. 28, p. 365–375.

WATKINS, K. P., FLETCHER, I. R., and de LAETER, J. R., 1991, Crustal Evolution of Archaean Granitoids in the Murchison Province, Western Australia: Precambrian Research, v. 50, p. 311–336.

WATKINS, K. P., and HICKMAN, A. H., 1990, Geological Evolution and mineralization of the Murchison Province, Western Australia: Western Australia Geological Survey, Bulletin 137, p. 267.

WILDE, S. A., and PIDGEON, R. T., 1986, Geology and geochronology of the Saddleback Greenstone Belt in the Archaean Yilgarn Block, southwestern Australia: Australian Journal of Earth Sciences, v. 33, p. 491–501.

WILDE, S. A., and PIDGEON, R. T., 1987, U–Pb geochronology, geothermometry and petrology of the main areas of gold mineralization in the 'Wheat Belt' region of Western Australia: WAMPRI Project 30, Final Report.

Hydrogeology of the Robe River alluvium, Ashburton Plain, Carnarvon Basin

by

D. P. Commander

Abstract

Twenty-two exploratory bores were drilled into a Quaternary alluvial aquifer along the Robe River. This aquifer extends 15 km along the river, where it crosses the coastal plain 80 km east of Onslow. It is 3 to 6 km wide, and has a saturated thickness of as much as 13 m. The gravelly portion contains pebbles up to 100 mm diameter, but the gravel passes laterally into less-permeable clay and silt. The unit rests unconformably on Proterozoic schist, Cretaceous conglomerate and siltstone, and Tertiary pisolite and limestone. The aquifer is recharged directly through the river bed by periodic streamflow, and the groundwater salinity ranges from about 450 mg/L (similar to the flow-weighted average river salinity of 398 mg/L) up to 1200 mg/L. Test-pumping at four sites yielded from 980 to 1340 m^3/day, and indicated a hydraulic conductivity of about 250 m/day, a figure that is supported by modelling. Estimates based on the observed fluctuations of the watertable, suggest that average recharge to the aquifer is about 12 x 10^6 m^3 per year.

KEYWORDS: Carnarvon Basin, Robe River, Yarraloola, hydrogeology, ground water, unconfined aquifer

Introduction

Location

The Robe River, in the Pilbara region of Western Australia, crosses the Ashburton Plain near Yarraloola Homestead (Fig. 1). The nearest towns are Pannawonnica, 50 km to the east; Onslow, 80 km to the west; and Karratha, 150 km to the northeast. The North West Coastal Highway crosses the Robe River 6 km upstream of the homestead, and access to the area is provided by station tracks (Fig. 2).

Purpose and scope

The Geological Survey of Western Australia has carried out a number of exploratory drilling projects to locate groundwater supplies for towns along the Pilbara coast. Alluvium along the Robe River was recognized as having potential for large supplies of potable groundwater. This report describes the results of the exploratory drilling and test pumping of the alluvium carried out between 1983 and 1985. The investigation was jointly funded by the State and Commonwealth governments under the 'National Water Resources Assessment Program'.

Previous investigations

In 1965, following the discovery of large deposits of pisolitic iron ore in the Robe River valley, the Broken Hill Proprietary Company (BHP) drilled nineteen exploratory water bores. These bores were drilled between 5 km and 10 km upstream from the present investigation area (Fig. 1) and intersected a maximum thickness of 18 m of saturated alluvium. Bore yields ranged up to 1000 m^3/day, and the groundwater salinity was between 900 mg/L and 1400 mg/L TDS (milligrams per litre total dissolved solids).

The occurrence of low-salinity groundwater in alluvium along the Robe River downstream from Yarraloola Homestead was subsequently recognized in a survey of pastoral bores and wells by Davidson (1975). Following his recommendations, a seismic survey (Fig. 2) was carried out to assess the thickness of alluvium; but the seismic refraction method could not distinguish the alluvium from underlying sediments, and seismic velocities were too high to indicate water-bearing material (Nowak, 1979).

In 1982, two bores were drilled for the State Energy Commission (SEC) near Yarraloola Homestead to provide water for hydrostatic testing of the Dampier–Perth natural gas pipeline (Rockwater, 1982). The bores yielded 1000 m^3/day of water with a salinity of about 500 mg/L from the alluvium.

During a seismic survey for oil in 1966–67, artesian groundwater was encountered when a deep shot hole — at 77 m — blew out with an oil-cut flow from the basal Cretaceous aquifer (Thomas, 1978). Subsequent exploratory drilling for oil and uranium has provided additional information on the Cretaceous aquifer (Muggeridge, 1978; Tyrwhitt and Sargeant, 1978). Allen

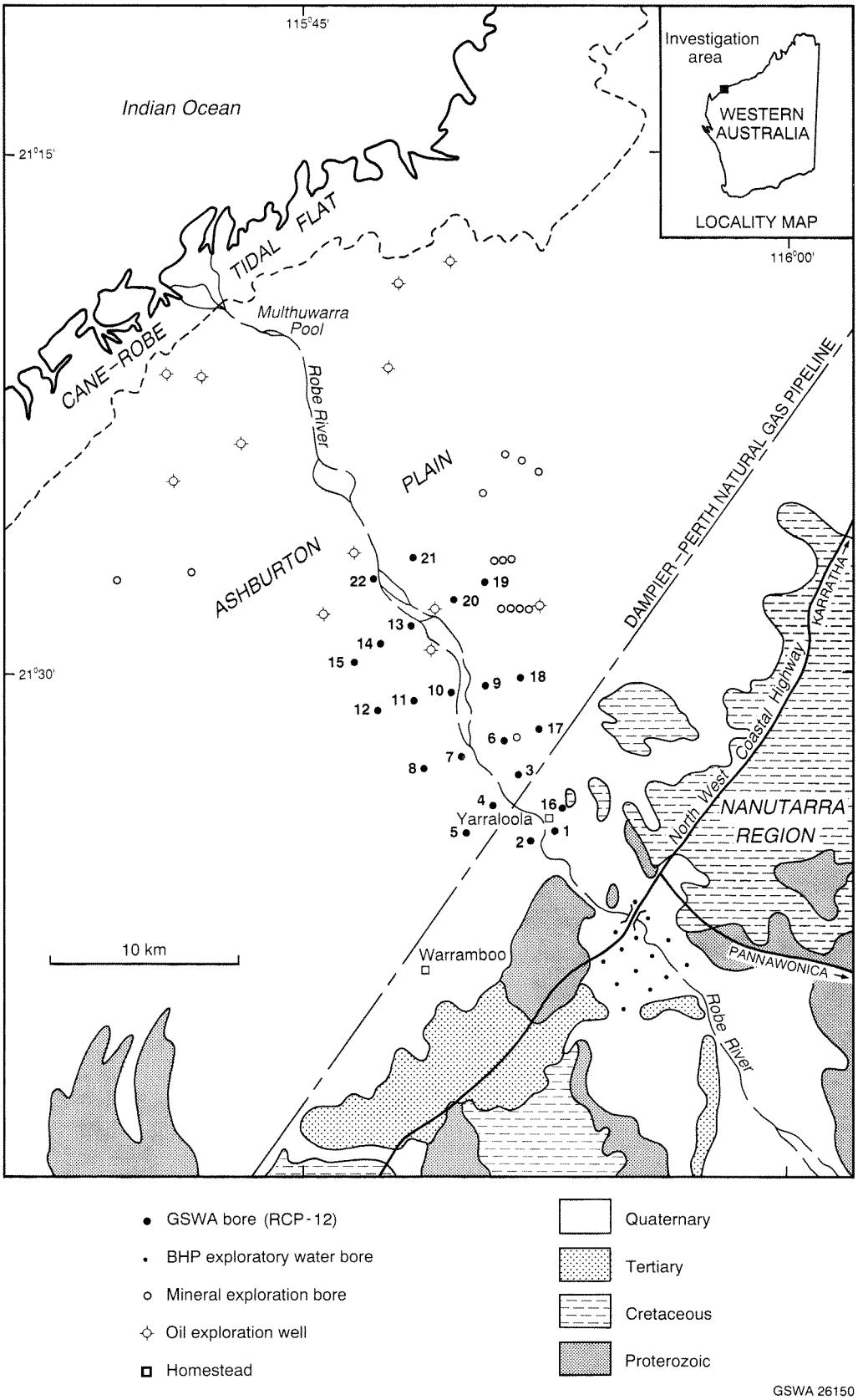

Figure 1. Location and geology

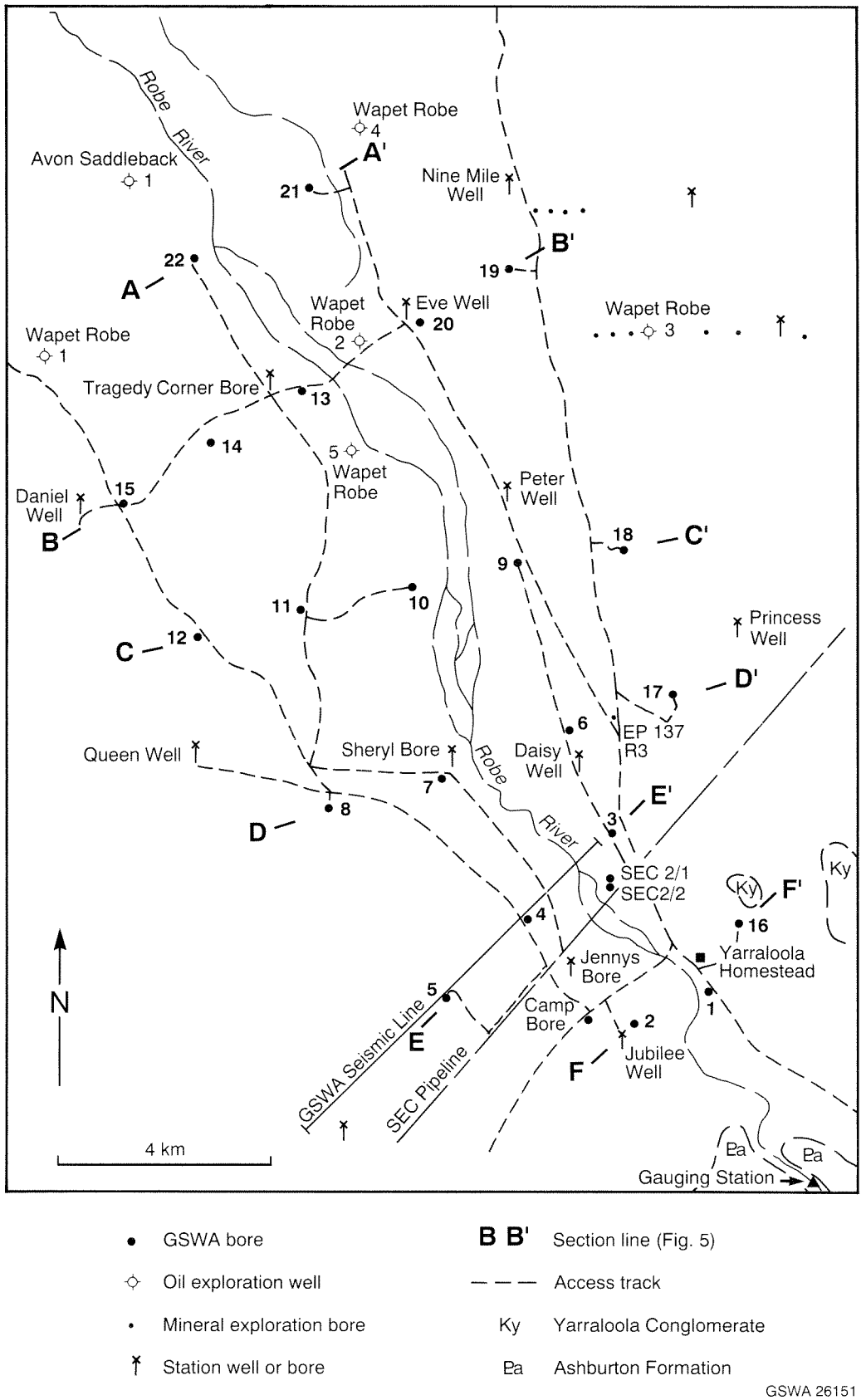

- GSWA bore
- Oil exploration well
- Mineral exploration bore
- Station well or bore

B B' Section line (Fig. 5)

— — — Access track

Ky Yarraloola Conglomerate

Pa Ashburton Formation

GSWA 26151

Figure 2. Bore locations

Table 1. Exploratory-bore data

Bore	*Date drilled*	*Elevation of casing top (a) (m)*	*Total depth (m)*	*Slotted interval level (b) (m)*	*Static water (m)*	*Salinity(c) (mg/L)*	*Airlift yield (m^3/d)*
1	01.10.83	50.89	30	2–18	8.17	992	84
2	10–11.10.83	50.37	30	0–18	7.94	601	12
3	05.10.83	45.07	30	5.5–21.5	7.00	1 011	27
4	11.10.83	49.09	36	5–35	8.47	902	144
5A	21–26.09.83	46.94	66	30–42	8.33	2 086	6
5B	29.09.83	46.85	18.5	5–18	8.14	2 259	8
6	06.10.83	41.71	23.5	5–23	7.15	1 030	36
7	12–14.10.83	40.66	30	2–21	6.70	454	–
8	14.10.83	38.52	33	5–11	6.52	940	7
9	07.10.83	37.91	29	10–24	6.21	1 086	62
10	21–22.10.83	36.50	30	5–10 14–23	7.13	716	–
11	20.10.83	34.34	24	5–16	6.61	755	–
12	15.10.83	32.10	30	5–11	6.57	723	14
13	19.10.83	29.20	27	5–14 18–22	5.52	704	86
14	18.10.83	29.25	29	5–13	6.34	672	48
15	17.10.83	27.94	35	5–14	6.51	684	86
16	29.08.84	49.30	28	13–23	6.57	800	247
17	22.08.84	43.89	29.5	5–29	8.77	1 126	69
18	20.08.84	38.19	29.5	5–26	7.34	1 286	69
19	17.08.84	29.49	32.5	20–30	6.37	3 027	60
20	23.08.84	29.74	32.5	5–15	6.55	729	101
21	24.08.84	25.31	35.5	5–28	6.83	524	172
22	12.06.84	25.33	32.5	4–25	7.00	844	216
Camp Bore	01–19.09.83	48.69	30	26–30	7.50	640	63

Note: (a) relative to Australian Height Datum (AHD)
(b) at 12 November 1985
(c) total dissolved solids (TDS) from conductivity (mS/m at 25°C) x 6.4

(1987), in a review of the groundwater in the Carnarvon Basin, has briefly described the groundwater resouces in the area.

Investigation program

Exploratory bores were drilled at twenty-two sites to delineate the extent of the aquifer (Fig. 2). Fifteen sites were drilled in 1983, and a further seven were drilled in 1984. Test-pumping bores and additional observation bores were drilled and tested in 1985.

The drilling was carried out by the Mines Department Drilling Branch using the mud-rotary drilling method. This method was found satisfactory; however, there was some loss of circulation where gravel was encountered.

These exploratory bores, known as the 'Robe Coastal Plain Bores', (prefix RCP) ranged from 18.5 to 66 m deep but were generally about 30 m deep (Table 1). The aggregate depth drilled was 751 m. The shallow exploratory bores were 130 mm diameter, and were cased with 80 mm PVC casing slotted over the water-bearing interval. The deepest exploratory bore (RCP 5A), and the test-pumping bores RCP 4P and RCP 10P, were 200 mm diameter, cased with 155 mm diameter steel casing, and equipped with in-line stainless steel screens. At the four test-pumping sites (Table 2), which included two bores previously drilled for the SEC, an additional observation bore was drilled 20 m away from each pumping bore and constructed with 80 mm PVC casing slotted at the same depth as the screens in the pumping bore.

The strata were lithologically logged during drilling to permit differentiation between thin gravel and clay beds; however, samples were only retained at 3 metre intervals. Gamma-ray logs were run in the cased bores after the completion of drilling in August 1984. Details of bore construction, strata, and geophysical logs are in the bore-completion reports (Commander, 1988).

On completion, the bores were developed by airlifting to obtain a clear water sample for chemical analysis by the Chemistry Centre (W.A.).

Pumping tests, including a six-stage step-drawdown test followed by an eight-hour constant-rate test at rates of 980 to 1340 m^3/day, were carried out in RCP 4P, RCP 10P, SEC2-1, and SEC2-2, during October and November 1985.

During the investigation period, waterlevels in the bores were monitored at intervals of between 2 weeks and 3 months, depending on the flow stage of the river and

Table 2. Monthly rainfall in millimetres 1983–86

	Jan	*Feb*	*Mar*	*Apr*	*May*	*Jun*	*Jul*	*Aug*	*Sep*	*Oct*	*Nov*	*Dec*	***Total***
Yarraloola homestead (a)													
1983	13	3	86	14	0	19	7	1	6	0	0	7	**156**
1984	31	73	79	23	223	0	36	4	10	0	0	12	**491**
1985	26	104	20	31	-	-	-	0	0	0	0	0	(c) **181**
1986	61	97	27	0	2	99	3	0	6	0	0	-	(c) **295**
Pannawonica (b)													
1983	14	9	137	20	0	16	24	1	7	0	50	37	**315**
1984	35	50	170	3	179	0	46	8	4	0	16	22	**533**
1985	28	31	25	51	3	6	34	0	0	3	0	0	**181**
1986	143	82	46	0	0	65	4	0	3	0	0	0	**343**

Note: (a) station 5032 — annual average 293 mm
(b) station 5069 — annual average 371 mm
(c) incomplete record

Source: Commonwealth Bureau of Meteorology

access. The more closely spaced measurements were made immediately following river flow. The Water Authority of Western Australia (WAWA) has undertaken the task of monitoring in November each year from 1986 to the present. The bores have been levelled to Australian Height Datum (AHD).

Environment

Physiography and vegetation

The investigation area lies on the Ashburton Plain (Hocking et al., 1987), which rises gently from the Cane–Robe Tidal Flats at the coast to about 50 m above sea level at the foot of an escarpment bordering the Nanutarra Region. The Robe River passes through a gap in the scarp, and crosses the coastal plain in a narrow channel (or anastomosing channels) that is incised as much as 5 m below the general level of the plain. Several small, shallow, distributary channels run from above the river banks in a northwesterly direction, but these carry water only at flood peaks.

The coastal plain is a flat mosaic of stony plains and intervening areas of cracking clay soils (gilgai). The stony plains are a shrub steppe dominated by snakewood (*Acacia xiphophylla*), whereas the gilgai supports mixed grasses (Beard, 1975). The river is flanked by a tree or shrub savannah of mixed grasses and scattered eucalypts, and the banks are lined with river gums. The vegetation along the river banks becomes progressively thicker downstream from the investigation area, but it terminates at a salt seep in Multhuwarra Pool (Fig. 1). Over the last hundred years, much of the floodplain has been denuded of native vegetation by grazing sheep.

Climate

The region is arid; summers are hot and winters warm. Infrequent, but intense, rainfall usually results from tropical cyclones and thunderstorms between December and March, and from cold fronts between May and July. Very little rainfall is recorded in August, September or October. The average annual rainfall is 290 mm, but the range is from zero to several times the average. Potential annual evaporation is 2500 mm. Monthly rainfalls for the investigation period from Yarraloola Homestead and Pannawonica are shown in Table 2.

Streamflow

Streamflow in the Robe River has been measured at the Yarraloola gauging station since January 1972. The station is 4 km upstream from the investigation area (Fig. 2) and measures runoff from a catchment of 7250 km^2.

Run-off occurs only after heavy rain — usually following cyclonic storms — on the catchment, and flows generally persist for about a month. Gauging records show an average of one flow per year but, during the fifteen-year period of records, there were three years when the river flowed more than once, and three years when it did not flow (Fig. 3) (Public Works Department, 1984; WAWA, unpublished data).

From 1972 to 1986 inclusive, the mean annual flow was 51 x 10^6 m^3, and the range from 8 x 10^6 m^3 to 160 x 10^6 m^3. The median of the fourteen flows is 38 x 10^6 m^3. Only large flows reach the sea, and none of the flows between 1976 and 1982 did so (Patterson, M., 1985, pers. comm.).

The salinity of the river water has been measured intermittently since 1976 (WAWA, unpublished data). While individual measurements ranged from 107–1154 mg/L, flow-weighted average annual salinities ranged from 161–486 mg/L, and the overall flow-weighted average salinity for the period was 398 mg/L. The salinity measurements taken during the flow following tropical cyclone Chloë in March 1984 are the most complete; they show that the salinity was about 120 mg/L at the flood peak, and thereafter increased steadily to about 550 mg/L (Fig. 4).

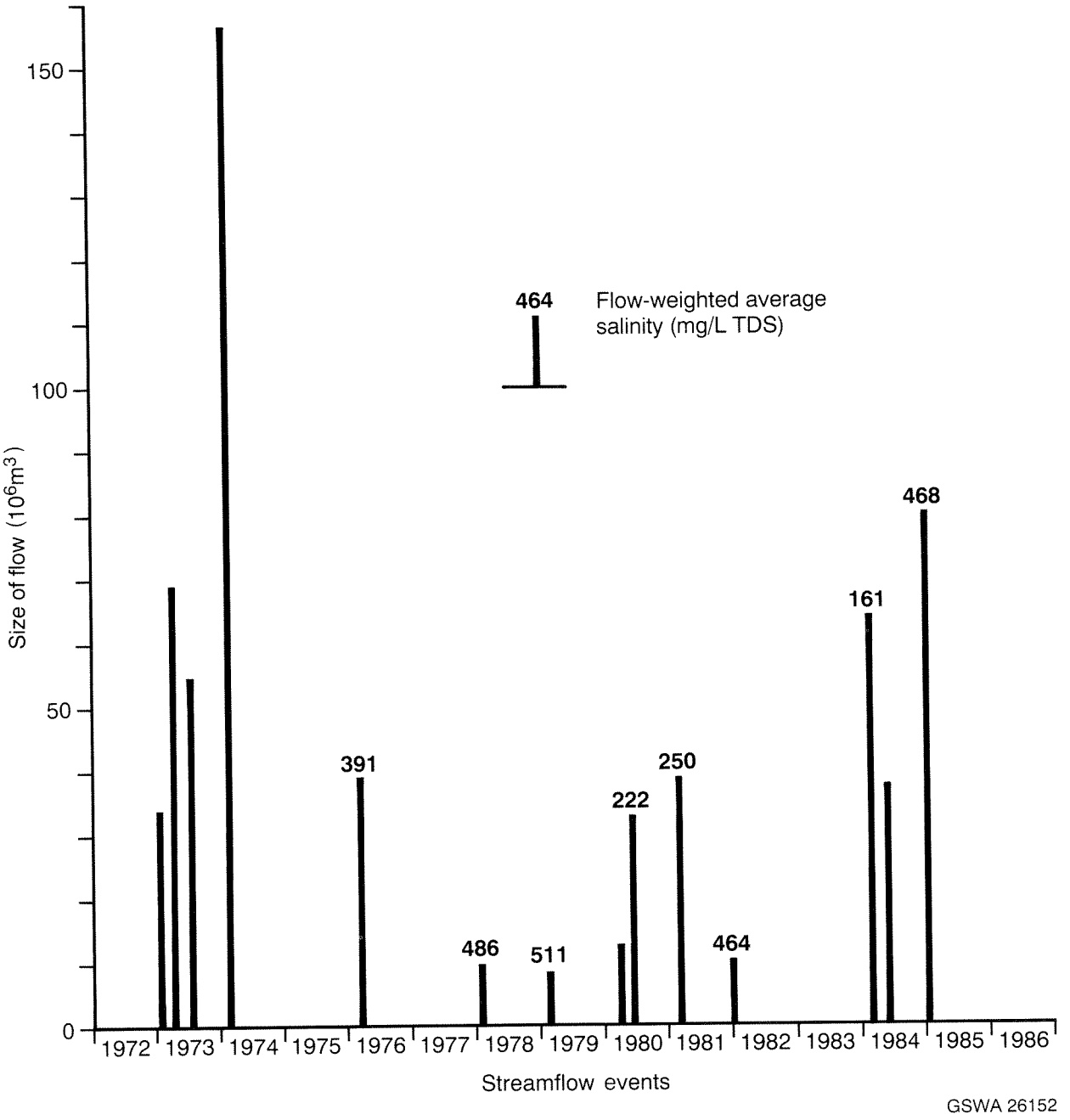

Figure 3. **Robe River — Streamflows (1972–86) and weighted average salinity (1976–85). Water Authority of Western Australia, station number 707002**

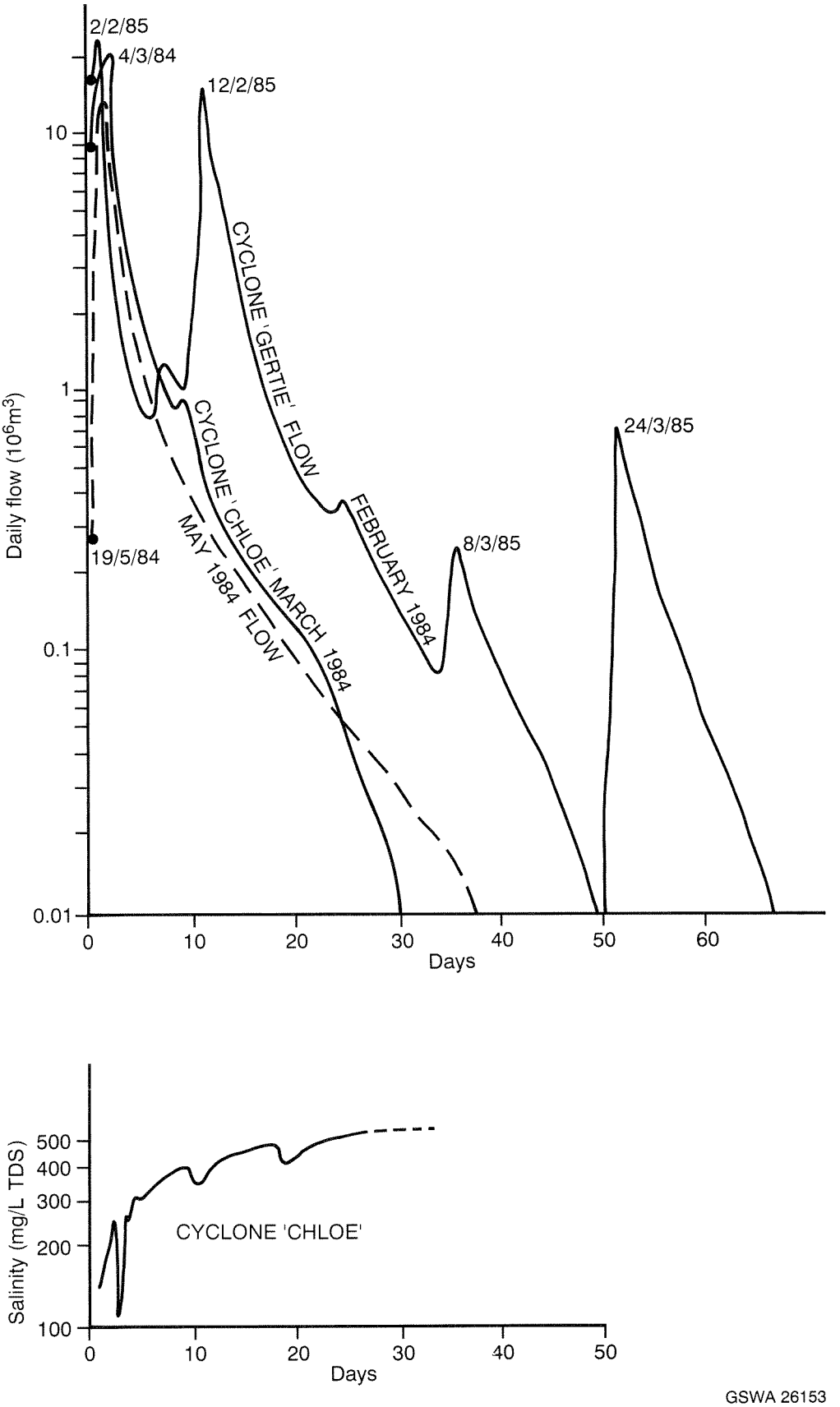

Figure 4. Robe River — Daily flow rate (1984–85) and salinity (1984). Water Authority of Western Australia, station number 707002

During the investigation period, there were three periods of streamflow: that following tropical cyclone Chloë in March 1984; that following heavy rain May 1984; and that following tropical cyclone Gertie in February 1985 (Fig. 4). The shapes of the flood hydrographs are similar, but subsidiary flows were superimposed on the flood following Gertie

Geology

Setting

The investigation area lies mainly within the Phaner-ozoic Carnarvon Basin, but also extends into the Precambrian Ashburton Basin. The coastal portion of the Peedamullah Shelf, a subdivision of the Carnarvon Basin (Hocking et al., 1987), contains Devonian–Carboniferous sedimentary rocks. These rocks, which were not intersected in the drilling program, are unconformably overlain by as much as 200 m of gently northwesterly dipping Cretaceous sediments. Although the Cretaceous sequence thins landwards, it extends onto the Proterozoic rocks of the Ashburton Basin that mark the inland margin of the Ashburton Plain, and occurs as a discontinuous capping in the Nanutarra Region (Fig. 1).

Overlying the Cretaceous and Proterozoic rocks of the coastal plain are Tertiary and Quaternary sediments, which reach a maximum thickness of 30 m.

The stratigraphic succession of formations intersected by drilling is shown in Table 3.

Stratigraphy

Ashburton Formation

The Ashburton Formation (Williams, 1968) outcrops in the hills on either side of the Robe River (Fig. 1) and was encountered in bores in the southeast of the investigation area (Figs 5, 6).

The formation is a quartz–mica schist, indurated in outcrop, but weathered in the subsurface to a white to grey clay that contains sericitic feldspar and minor amounts of quartz.

The Ashburton Formation is Proterozoic (Williams, 1968), and is unconformably overlain by Palaeozoic, Cretaceous, Tertiary, and Quaternary sedimentary rocks.

Yarraloola Conglomerate

The Yarraloola Conglomerate (Williams, 1968) outcrops on the tops of low hills near Yarraloola Homestead (Fig. 1) and was encountered in bores RCP 4, RCP 5A and RCP 17 (Figs 5, 6).

The formation includes pebble conglomerate with white to yellow clay matrix, subordinate shale, and thin layers of pale-grey sand. The pebbles, which range up to 100 mm diameter, are rounded white quartz, basalt, and tabular, banded jaspilite; the sand is medium- to coarse-grained, subangular, clear and white quartz. The formation ranges from about 3 m thick in RCP 17, to 22 m in RCP 5A.

The Yarraloola Conglomerate rests unconformably on the irregular upper surface of the Ashburton Formation. The conglomerate, which was deposited in a fluvial environment, is Early Cretaceous. It grades laterally into Nanutarra Formation and Birdrong Sandstone (Hocking and van de Graaff, 1978).

Muderong Shale and Windalia Radiolarite

Dark-green and dark-blue to brown and black clay and siltstone, which may belong to either the Muderong Shale or the Windalia Radiolarite (Condon, 1954), were encountered below the Cainozoic sequence in the central and eastern part of the area (Figs 5, 6). A maximum thickness of 8 m was penetrated in RCP 11.

The samples contained no palynomorphs, and the sediments are correlated with the Early Cretaceous Muderong Shale or the Windalia Radiolarite on the basis of their lithology and stratigraphic position. Both formations are shallow-marine deposits that conformably overlie the Nanutarra Formation.

Toolonga Calcilutite

In the north and west of the area, yellow and light-green to white clay with thin bands of claystone or marly limestone was encountered at the base of the Cainozoic sequence (Figs 5, 6). This is correlated with the Late Cretaceous Toolonga Calcilutite (Johnston et al., 1958), and a maximum thickness of 6 m was penetrated in RCP 12. A bluish-green colouration at the top of the sequence is thought to be due to weathering. The Toolonga Calcilutite disconformably overlies the Windalia Radiolarite.

Robe Pisolite

The Robe Pisolite (de la Hunty, 1965) outcrops in the Robe River valley (Fig. 1) and is present beneath the coastal plain near Warramboo to the southwest (Williams, 1968). In the investigation area, the formation is preserved in the subsurface on either side of the present course of the river (Fig. 6).

In outcrop the formation consists of pisolitic and massive iron oxides, detrital material, fossil wood, and seams of clay. In the Robe River Coastal Plain Bores, the formation includes red-brown and black pisolitic ironstone, yellow clay, and mottled red and yellow vitreous silcrete. The formation is 7 m thick at RCP 18 and RCP 19, where it directly overlies Cretaceous rocks. The Robe Pisolite is a fluvial deposit, probably of Late Eocene age, and may have been subjected to lateritization and silicification in the Oligocene (Hocking et al., 1987).

Trealla Limestone

Limestone and clay in the centre of the investigation area are assigned to the Trealla Limestone, which extends over

Table 3. Stratigraphic sequence

Age		*Formation*	*Thickness (a) (m)*	*Lithology*
QUATERNARY		Alluvium	30	Clay, gravel (calcrete close to watertable)
		~~ *unconformity* ~~~~~~~~~		
TERTIARY	Miocene	Trealla Limestone	17	Limestone, clay, marl
		~~ *unconformity* ~~~~~~~~~		
	Eocene	Robe Pisolite	6	Pisolitic ironstone, silcrete, clay
		~~ *unconformity* ~~~~~~~~~		
CRETACEOUS		Toolonga Calcilutite	6	Clay, claystone
		~~ *disconformity* ~~~~~~~~		
		Windalia Radiolarite	8	Siltstone
		Muderong Shale	8	Shale
		Yarraloola Conglomerate	23	Conglomerate, sand, clay
		~~ *unconformity* ~~~~~~~~~		
PROTEROZOIC		Ashburton Formation	22	Schist

Note: (a) maximum thickness intersected during drilling

much of the coastal plain (Hocking et al., 1987). The formation ranges from a finely crystalline limestone to a pale, cream and yellow clay, often with a greenish tinge. Dendritic manganese is common on broken surfaces of the limestone. The maximum thickness encountered was 17 m in RCP 4, where the limestone is indurated; elsewhere in the area, the formation appears to have been eroded and is less than 10 m thick. It unconformably overlies Cretaceous and older Tertiary sediments, and is unconformably overlain by Quaternary alluvium.

The Trealla Limestone is a marine or lagoonal deposit of Middle Miocene age (Hocking et al., 1987). The limestone is similar in lithology to the Millstream Dolomite (Barnett and Commander, 1986), which bears the same stratigraphic relationship to the Robe Pisolite in the headwaters of the Robe River 90 km to the east.

Alluvium

Flood deposits of the Robe River as much as 30 m thick cover the coastal plain and form a delta at the mouth of the river. On the coastal plain, the sediments are mainly overbank deposits of clay and silt. Gravel bed-load deposits outcrop in the river bed, and occur in the subsurface within 3 km of the river where they are concealed by the overbank deposits.

The gravel in the river bed consists of rounded, tabular pebbles of banded chert and jaspilite up to 100 mm diameter and 50 mm thick, together with rounded pebbles of basalt and quartz. The chert, jaspilite, and basalt were derived from Archaean or Lower Proterozoic rocks of the Hamersley Basin, which outcrop in the upper reaches of the catchment 40 km upstream. Some have also been reworked from the Yarraloola Conglomerate. The gravel is generally loose, but some surface cementation can be seen near semi-permanent river pools.

At RCP 10, the gravel between 10 m and 23 m is conspicuously different from the overlying material in that the pebbles have weathered and coated surfaces. This suggests they are from a considerably older deposit.

The gravel is thickest (15 m) close to the present river course at Yarraloola Homestead. It thins laterally away from the river, and also progressively downstream where it is interbedded with clay. At RCP 21 and 22, at the northern end of the area, individual gravel beds are less than 3.5 m thick.

The clay and silt are generally reddish brown, indurated, and contain local thin layers of fine pebbles and grains of jaspilite and basalt.

Pisolitic ironstone, probably derived from the Robe Pisolite, is present at the base of the gravel sequence in RCP 17 and 18, and also within the clay in RCP 12. Bright-blue clay at the base of the gravel in RCP 9 (overlying Trealla Limestone) appears to have been derived from the erosion of Cretaceous sediments.

Hydrochemical action has produced widespread calcrete within the alluvium. The calcrete is commonly developed close to, and to a depth of 5 m below, the watertable. A complete sequence from slightly calcareous clay, through white to pink clay with calcite veining, to

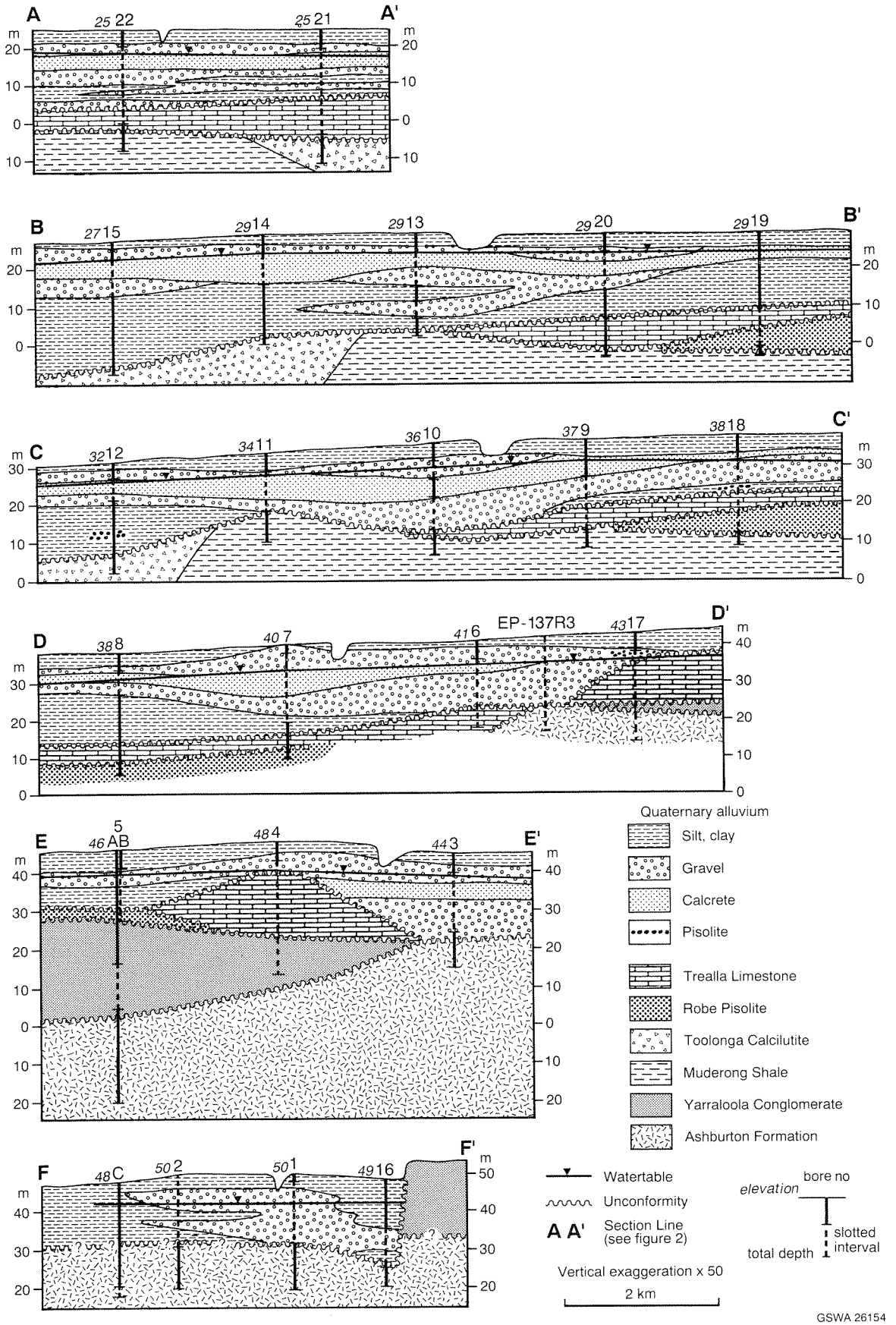

Figure 5. Geological sections

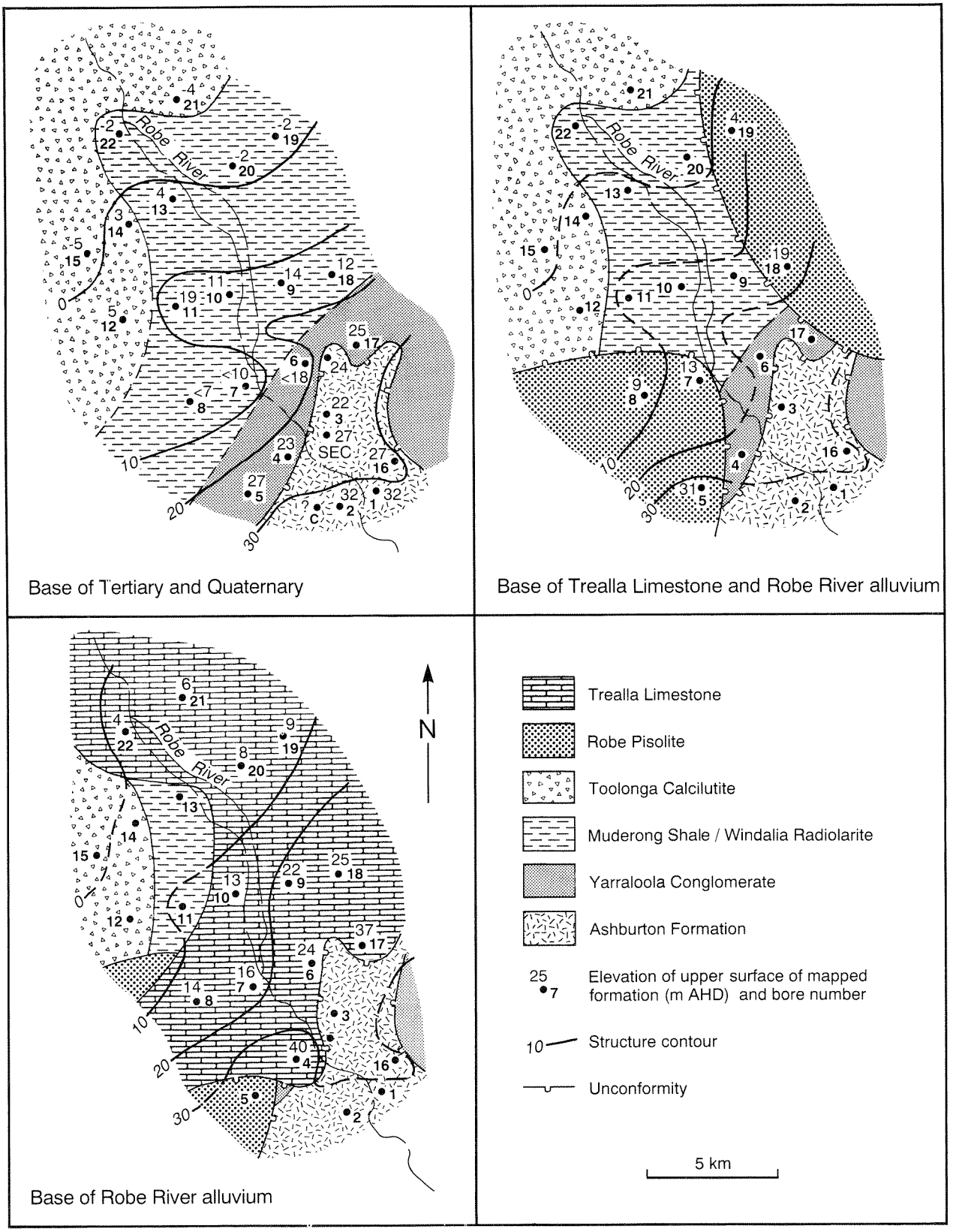

Figure 6. Subcrop and structure-contour maps. A — Base of Tertiary and Quaternary. B — Base of Trealla Limestone and Robe River alluvium. C — Base of Robe River alluvium

finely crystalline calcrete can be seen in the borehole samples. The gravel is generally unaffected; but at RCP 10, deposits of crystalline calcite in concentric rings, up to an aggregate thickness of 2 mm, were observed on pebbles between depths of 13 and 14 m. The finely crystalline calcrete resembles the limestone in RCP 4, which, on the basis of its thickness and uniform lithology, was correlated with the Tertiary Trealla Limestone.

The alluvium, which coalesces with more clayey deposits of adjacent small drainage lines, is part of an alluvial fan deposited by the Robe River where it discharges onto the Ashburton Plain. It unconformably overlies Proterozoic, Cretaceous, and Quaternary rocks, from which it is separated by an irregular erosion surface. The alluvium is periodically reworked by river floods.

Hydrogeology

Alluvium

The gravel (former bed-load component) of the Robe River alluvium is a major aquifer. The aquifer grades laterally into floodplain silts and clays, which have a very much lower transmissivity.

The gravel is thickest and deepest adjacent to the Robe River (Fig. 7). The thickest saturated section of gravel penetrated by the drilling aggregates 13 m at RCP 10. The aquifer thins away from the river and towards the downstream end of the investigation area, where individual gravel beds are only a few metres thick and become progressively intercalated with clay (Fig. 5, section A–A_1). The gravel is exposed only in the river bed: elsewhere it is covered by between 2 m and 5 m of overbank silt.

The alluvial gravels overlie relatively impermeable Tertiary, Cretaceous and Proterozoic rocks. The Trealla Limestone is mostly clayey and impermeable, but fissured limestone was found in one bore. The permeability of the Robe Pisolite is low in this area, but elsewhere it is a highly transmissive aquifer (Barnett and Commander, 1986). The Toolonga Calcilutite, Windalia Radiolarite, Muderong Shale, and Ashburton Formation, also form an impermeable base to the alluvial aquifer. Some downward leakage into the Yarraloola Conglomerate may take place, but it is considered to be small.

Watertable configuration

The watertable is generally between 5 m and 9 m below ground level (Fig. 8) but, in bores close to the river, it is subject to seasonal and annual fluctuations of as much as 4.5 m (Fig. 9).

The watertable slopes northwestwards from about 43 m where the Robe River enters the coastal plain to 18 m AHD in the northwest of the area (Fig. 8). The watertable also slopes away from the river, depending on the time elapsed since it last flowed.

The gravel is only partially saturated and, throughout the area (especially to the west of the river), several metres of unsaturated gravel occur above the highest observed watertable level (Fig. 5).

Recharge

Recharge to the alluvial gravel takes place by direct infiltration through the river bed during periods of flow. The amount of recharge is controlled by the frequency, size, and duration of flows.

The response of the watertable to recharge from river flows during the period 1983–86 is shown on Figures 9, 10A, and 10B. Close to the river, the watertable rises rapidly during a flow; farther from the river, the response is delayed and reduced. Waterlevels in RCP 5 and RCP 19, which are beyond the boundary of the gravel in alluvial silt and clay, showed little or no response to the river flow in the period 1983–86. The area of riverine recharge is, therefore, limited to the area of alluvial gravel; and the floodplain silts are probably recharged mainly by local rainfall and runoff.

During the investigation period the river flowed on three occasions (Figs 3, 4); twice in 1984, and once in 1985. The recharge to the aquifer that resulted from these flows can be estimated from the volumetric change between the watertable level before and after flow (Figs 10A, B), using an assumed specific yield of 0.1. The waterlevels used were measured values in the bores, except for the pre-flow levels in January 1984 which were extrapolated from measurements made the previous year. The differences in watertable levels were contoured and the volumes calculated from areal measurement.

The calculated recharge (Table 4) does not account for the groundwater outflow during the period, and is therefore an underestimate.

Watertable levels in bores close to the river reached a slightly higher elevation (Fig. 9) following the 1985 flow, owing to the higher pre-flow watertable level, and to the longer duration of flow.

Storage

The total groundwater storage in the alluvial gravel can be calculated from the volume of saturated aquifer multiplied by the specific yield. The volume of saturated gravel on 12 November 1985 — within the boundaries shown on Figure 7 — was estimated by measuring the area within each isopach of aggregate thickness, and multiplying by the average thickness. The volumes of groundwater in storage have been estimated by using an assumed specific yield of 0.1, and are given in Table 5.

Table 4. Calculated recharge in 1984 and 1985

Year	*Period of rising watertable*	*Recharge ($10^6 m^3$)*
1984	24 Feb–24 Jul	24
1985	30 Jan–03 Apr	10

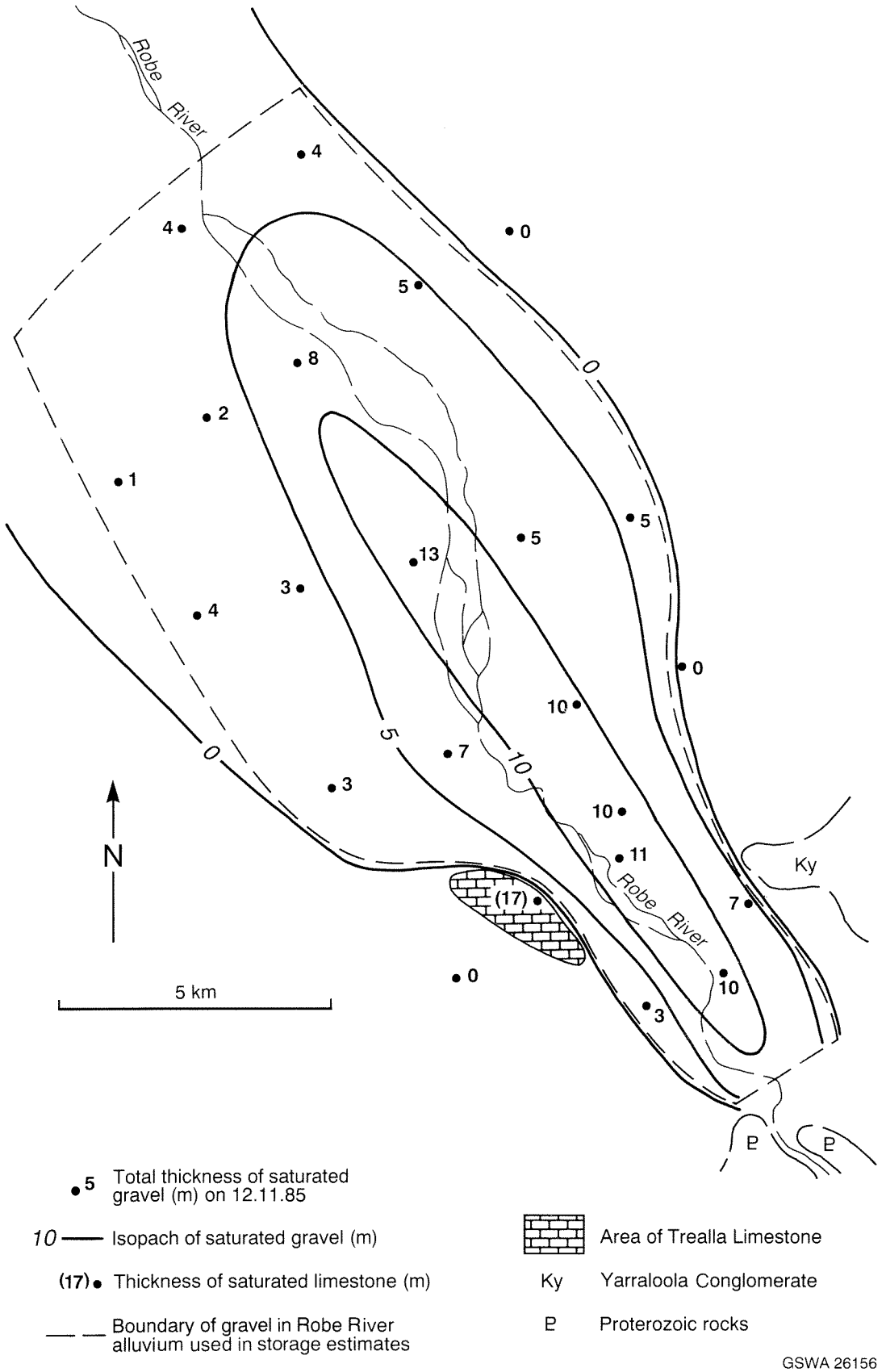

Figure 7. Extent and estimated aggregate thickness of alluvium

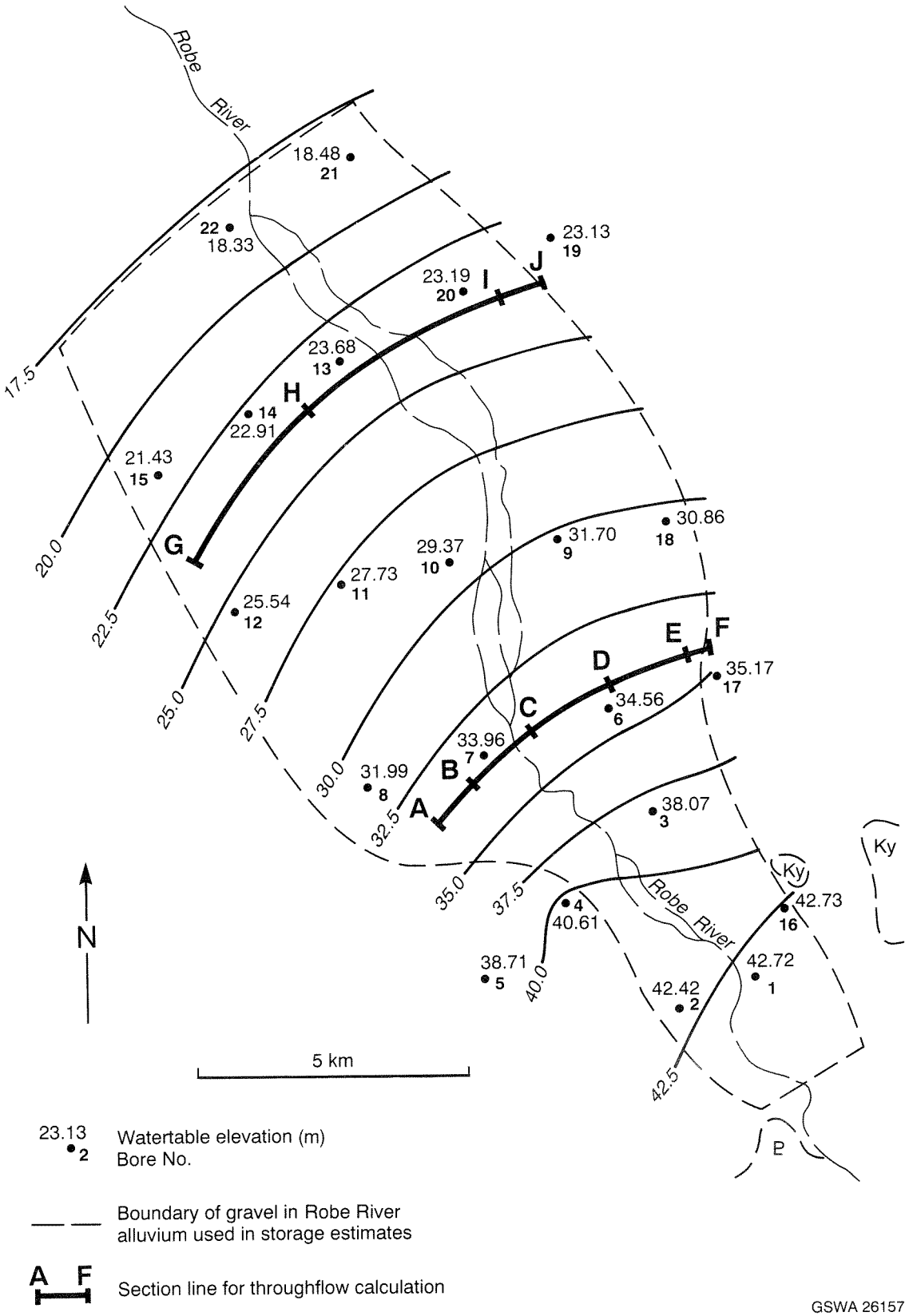

Figure 8. Elevation of watertable (12 November 1985)

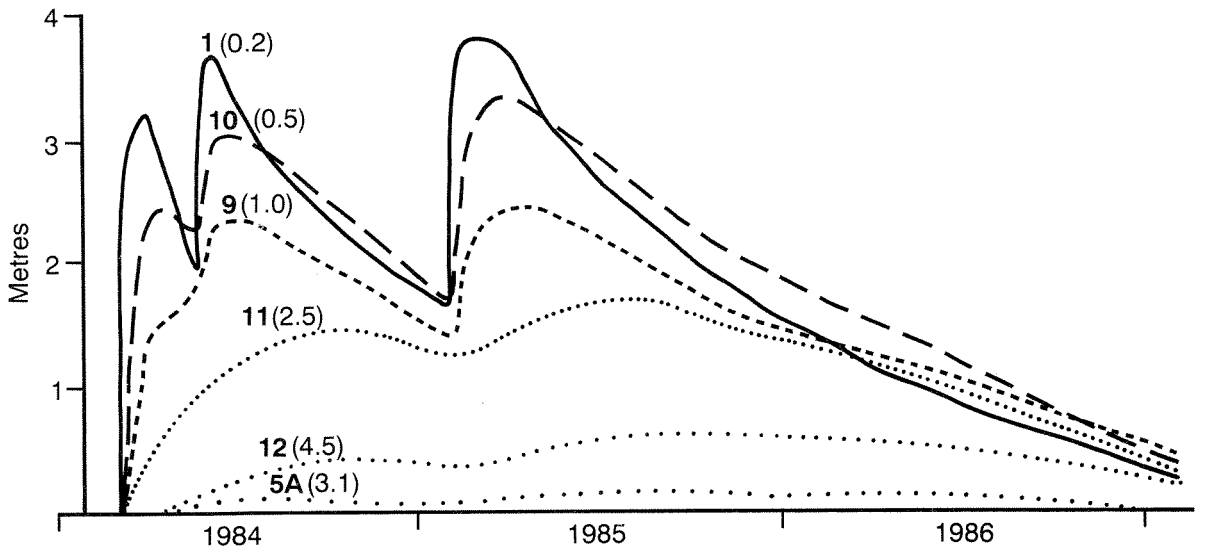

5A (3.1) Bore number (distance from river bank in kilometres)

GSWA 26158

Figure 9. Selected hydrographs showing watertable change from level immediately preceding cyclone 'Chloë'

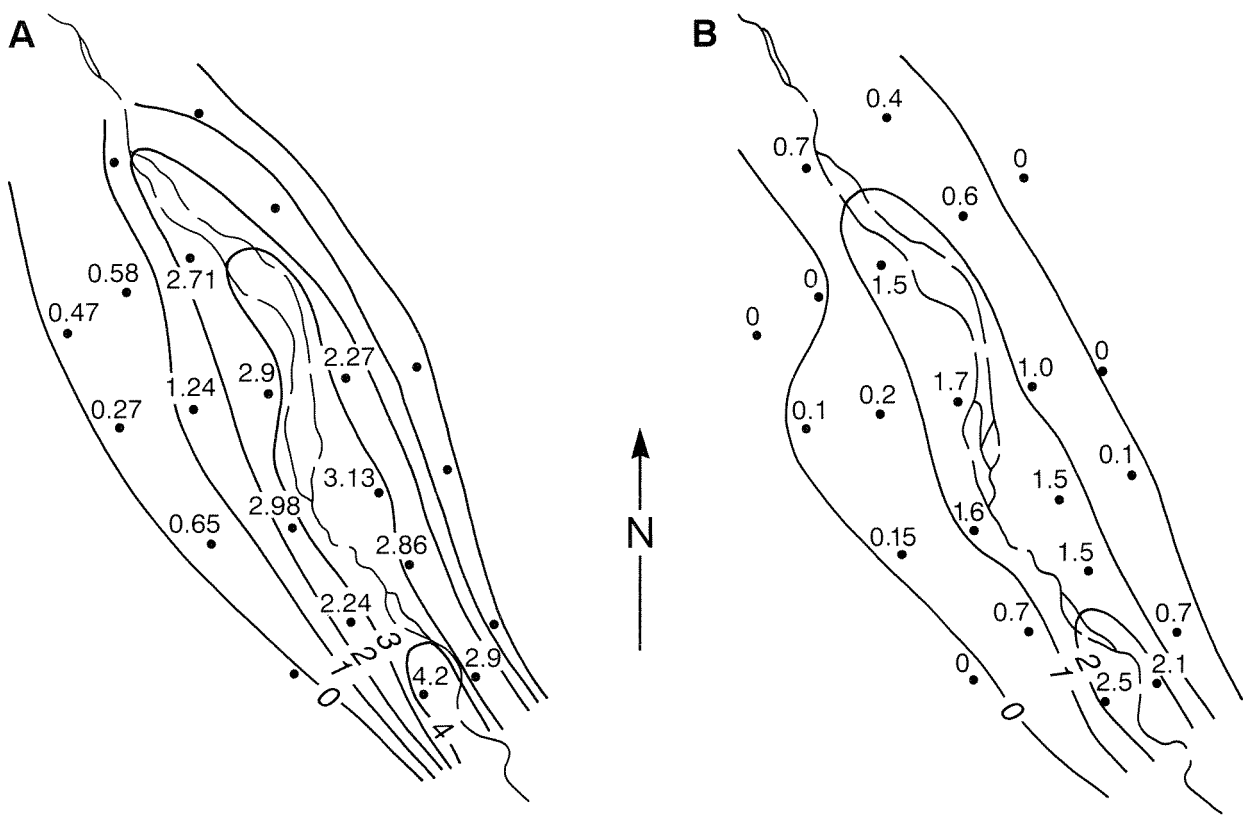

3.13 m rise in watertable between 24 Feb. and 24 July 1984

1.7 m rise in watertable between 30 Jan. and 3 April 1985

GSWA 26159

Figure 10. Rise in watertable. A — Following cyclone 'Chloë'. B — Following cyclone 'Gertie'

Table 5. Groundwater storage

Isopach interval (m)	*Average thickness (m)*	*Area (km^2)*	*Volume (a) ($10^6 m^3$)*
0–5	2.5	56	14
5–10	7.5	48	36
>10	10	20	20
		Total	**70**

Notes: (a) specific yield of 0.1

The annual change in storage during the investigation period can be calculated in the same way as above; from the change in level of the watertable (taken for convenience) from November to October of the subsequent year (Table 6).

Historical waterlevel changes

Watertable levels have been measured in station wells (Fig. 2) at intervals since 1964, and data from selected wells are given in Table 7. They show an approximate correlation with periods of river flow (Fig. 3), being relatively high following the large flow of 1974, and low in 1979 and 1983. The lowest levels were measured at the end of 1983 following the longest period without flow since 1972.

Table 6. Annual change in storage

Period	*Change in storage (a) ($10^6 m^3$)*
Nov 1983—Oct 1984	+16
Nov 1984—Oct 1985	-2
Nov 1985—Oct 1986	-12

Note: (a) specific yield of 0.1

Table 7. Historical waterlevels in station wells (metres below surface reference point)

Well	*1964 10 Oct*	*1974 22 Jun*	*1979 9 Nov*	*1983 5 Oct*	*1984 29 Aug*
Eve Well	5.5	4.40	6.80	8.18	6.85
Daisy Well	4.9	4.80	7.30	8.12	5.80
Princess Well	8.2	7.30	9.75	-	8.50
Queen Well	7.3	5.15	7.05	7.30	-

Source: GSWA records

Hydraulic conductivity

RCP 10P and the two SEC pumping bores in the gravel aquifer were pumped at rates of 980 to 1340 m^3/day with 1.1 to 4.4 m of drawdown (Table 8). Drawdowns in the observation bores, located 20 m from the pumping bores, ranged from 0.25 m to 0.29 m and gave transmissivities (derived from matching time–drawdown data to non-equilibrium type curves) of 1300 to 4900 m^2/day.

Estimates of hydraulic conductivity in the Robe River alluvium, derived from the pumping tests (Table 8), ranged from 150 m/day in partly cemented gravel at RCP 10 to 260 and 400 m/day in clean gravel at SEC2-1 and SEC2-2 respectively.

The hydraulic conductivity can also be estimated by modelling the response of the watertable to river flow, assuming the aquifer is of constant thickness. Observed waterlevel rises thirty days after the first river flow in March 1984 were plotted against distance from the river (Fig. 11). The best-fit curve to these data points was obtained from the equation given by Gill (1985):

$$s/s_o = 4\pi^{-1} \sum_{n=1,3,5,\ldots}^{\infty} n^{-1} \exp\left[-kn^2\pi^2 t\,(H_o - S_o)/4NL^2\right] \sin(n\pi x/2L)$$

where:

- s_o = rise in watertable at the river (3.75 m);
- $s_o - s$ = rise (m) in the watertable at a distance x metres from the river;
- H_o = final saturated thickness of the aquifer at the river (12 m);
- L = width of the aquifer (2000 m);
- t = time elapsed since river flow commenced (30 days);
- k = hydraulic conductivity (m/day); and
- N = specific yield (assumed to be 0.1).

The derived hydraulic conductivity of 250 m/day from the best-fit curve to data from seven bores up to 1.6 km from the river is in broad agreement with the values derived from pumping tests, even though the pumping tests apply to a small part of the aquifer close to the pumped bore.

Groundwater flow

Groundwater in the alluvial gravels flows in a general northwesterly direction, approximately parallel to the river (Fig. 8). When the river flows, a groundwater mound builds up beneath the river bed as recharge occurs to the shallow gravels flanking the river (Fig. 12A); the mound subsides when the river ceases to flow (Fig. 12B).

The volume of groundwater flow, Q, can be estimated from the Darcy equation:

$$Q = kbil$$

where:

- k = hydraulic conductivity (m/day);
- b = aquifer thickness (m);
- i = hydraulic gradient (dimensionless); and
- l = cross-sectional width (m)

Table 8. Test-pumping data

Bore	Pump bore				Observation bore (a)			
	Pumping rate	*Drawdown at 8 hrs*	*Specific capacity at 8 hrs*	*Specific (b) capacity at 30 min*	*Drawdown at 8 hrs*	*T*	*b*	*k*
	(m^3/d)	*(m)*	*(m^2/d)*	*(m^2/d)*	*(m)*	*(m^2/d)*	*(m)*	*(m/day)*
RCP4P	980	4.4	220	2 000	0.29	3 500	16	220
RCP10P	1 320	3.3	400	1 250	0.29	1 300	9	150
SEC2-1	1 170	2.8	420	1 250	0.25	3 100	12	260
SEC2-2	1 340	1.1	1 200	2 500	0.26	4 900	12	400

Notes: T = transmissivity; b = aquifer thickness; k = hydraulic conductivity
(a) situated 20 m from pumping bore; (b) calculated according to the method of Sheahan (1971)

Based on the watertable configuration in November 1985, the average annual groundwater throughflow across sections A–F and G–J in the alluvial gravel are about the same. Depending on the value of hydraulic conductivity (k), the throughflow ranges from 2.9 x 10^6 m^3 to 7.6 x 10^6 m^3 (Table 9).

Discharge

The average annual discharge from the aquifer can be equated to the decline in storage in a year with no recharge. Between November 1985 and October 1986 there was no river flow and the annual storage depletion (Table 6) was estimated to be 12 x 10^6 m^3 (using a specific yield of 0.1). This decline in storage is accounted for by groundwater flow out of the area and by evapotranspiration within the area.

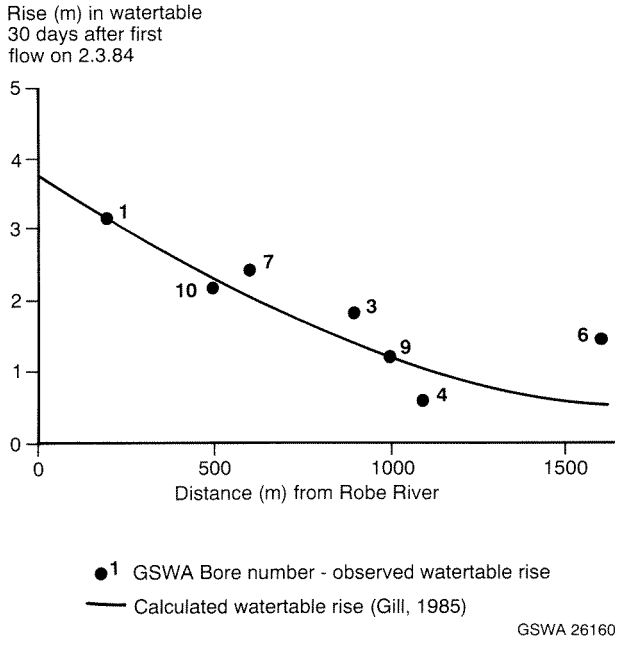

Figure 11. Relationship between rise of watertable 30 days after flow and distance from Robe River

The groundwater which flows downstream from the investigation area discharges by transpiration from thick vegetation which occupies the river bed for 10 km upstream from the saline seep at Multhuwarra Pool.

Water loss from this vegetation can be estimated by assuming that annual transpiration is 80% of the pan evaporation — approximately 2 m. The total annual water loss from an area 10 km long and 200 m wide is therefore about 4 x 10^6 m^3.

Discharge to the northwest of the investigation area is indicated by the presence (there) of low-salinity groundwater (Fig. 13). However, vegetation in this area is sparse, and it is likely that discharge occurs from the watertable by evaporation through the unsaturated zone at a relatively low rate over a large area.

Groundwater model

A groundwater-flow model of the alluvial gravels was constructed to assist in the determination of hydraulic conductivity, specific yield, and recharge. The modelling was carried out by S. J. Appleyard using the United States Geological Survey MODFLOW finite-difference groundwater flow model (McDonald and Harbaugh, 1984). A one-layer model consisting of 228 x 1 km^2 cells was used. The model dimensions were based on the extent and saturated thickness of the aquifer given in Figure 7. A constant-flux boundary at the input end, and a constant-head boundary at the output end were used to simulate groundwater inflow and outflow; and no-flow boundary conditions were used to simulate the outer limits of the aquifer. River flow was simulated with the river-leakage package of the model.

Calibration of the model was carried out using 1985 waterlevel and streamflow data, when a large flow was followed by a long period of falling waterlevel. A good fit between simulated and actual waterlevels was obtained using a hydraulic conductivity of 200 m/day and a specific yield of 0.15 for the aquifer (Figs 14, 15). The simulation indicated that recharge to the aquifer in 1985 was about 8 x 10^6 m^3; this agrees well with the value of 10 x 10^6 m^3 previously estimated by the analysis of hydrographs (although in the latter a specific yield of 0.1 was used).

Table 9. Throughflow calculations

Section	*Aquifer thickness (m)*	*Hydraulic gradient (10^{-3})*	*Length (m)*	*Annual throughflow ($10^6 m^3$)*	
				k = 150 m/d	*k = 400 m/d*
A–B	3	1.4	1 000	0.23	0.6
B–C	7.5	1.2	1 500	0.74	2.0
C–D	11	1.1	1 700	1.1	3.0
D–F	7.5	1.2	1 500	0.74	2.0
E–F	2.5	1.6	500	0.1	0.3
Total A–F				**2.9**	**7.9**
G–H	2.5	1.4	3 500	0.67	1.8
H–I	7	1.2	4 300	2.0	5.3
I–J	2.5	0.8	800	0.1	0.2
Total G–J				**2.8**	**7.3**

The simulation also gave a groundwater throughflow of about 5 x 10^6 m^3, within the range indicated in Table 9.

Salinity

The regional pattern of groundwater salinity in the alluvial deposits of the coastal plain shows a lobe of low-salinity groundwater around the Robe River (Fig. 13). The salinities of groundwater samples collected from bores in this lobe ranged from 454 mg/L to 3027 mg/L (Fig. 16).

In the alluvial gravels, the groundwater salinity ranges from 454 mg/L near the river to 1280 mg/L at the margin. The groundwater salinity is directly related to the salinity of the recharge water from the river, but it increases at the edge of the aquifer because of mixing with higher salinity water from the floodplain deposits.

The lobe of low-salinity groundwater extends northwestwards from the river in the direction of groundwater flow (Fig. 13). The lowest salinity groundwater occurs at RCP 7, where it is almost the same as the weighted average salinity (398 mg/L) of the river flows (Public Works Department, 1984). On the eastern side of the river, where the groundwater salinity is generally higher than on the western side, it ranges up to nearly 1300 mg/L (RCP18).

The groundwater salinity in the Robe River alluvium generally decreases with depth below the watertable. This is believed to be associated with evapotranspiration and can be shown by comparing the groundwater salinity in shallow station wells and bores with that in the deeper exploratory bores (Fig. 16).

Periodic sampling of the station wells in the area revealed little variation in salinity during the investigation period, except in Tragedy Corner Bore (Table 10). This bore is unusual both for its high salinity compared with nearby exploratory bores RCP 13, 14 and 22, and for its salinity variation from 1400 to 4500 mg/L. The more saline readings were obtained following river flows when waterlevels were high, and the salinity decreased thereafter as waterlevels declined.

Hydrochemistry

With increasing total salinity, the groundwater in the Robe Coastal Plain Bores shows a progressive enrichment of sodium chloride at the expense of calcium and bicarbonate (Fig. 17). Evidence of calcrete formation close to the watertable suggests that calcium bicarbonate is precipitated. In addition, there is a slight decrease in the proportion of magnesium and an increase in the proportion of sulfate with increasing salinity.

The groundwater is hard to very hard and ranges from 250 to 470 mg/L total hardness (Table 11). Nitrate is present at concentrations ranging up to 12 mg/L, and fluoride ranges from 0.3 to 1.6 mg/L. In potable groundwater (with a salinity of less than 1000 mg/L), there is a maximum nitrate content of 6 mg/L and a maximum fluoride content of 1.1 mg/L. Boron ranges from 0.2 to 0.7 mg/L, and silica concentrations are generally in the range 45 to 65 mg/L. Only non-aerated samples from pumped bores were analysed for iron, which was found to be present in concentrations of less than 0.13 mg/L (Table 11).

Temperature

The temperature of groundwater measured during pumping tests was 31.5°C.

Trealla Limestone

The Trealla Limestone, which is mostly clay, generally forms an impermeable base to the Robe River alluvium. However, at RCP 4 it is composed of fissured limestone which is in hydraulic continuity with the alluvial gravel (Fig. 5, section E–E_1).

An 8-hour pumping test carried out at RCP 4 at a rate of 980 m^3/day indicated a hydraulic conductivity of 220 m/day, similar to the gravel of the Robe River alluvium.

In spite of the marked difference in lithology, the salinity and chemical composition of the groundwater at

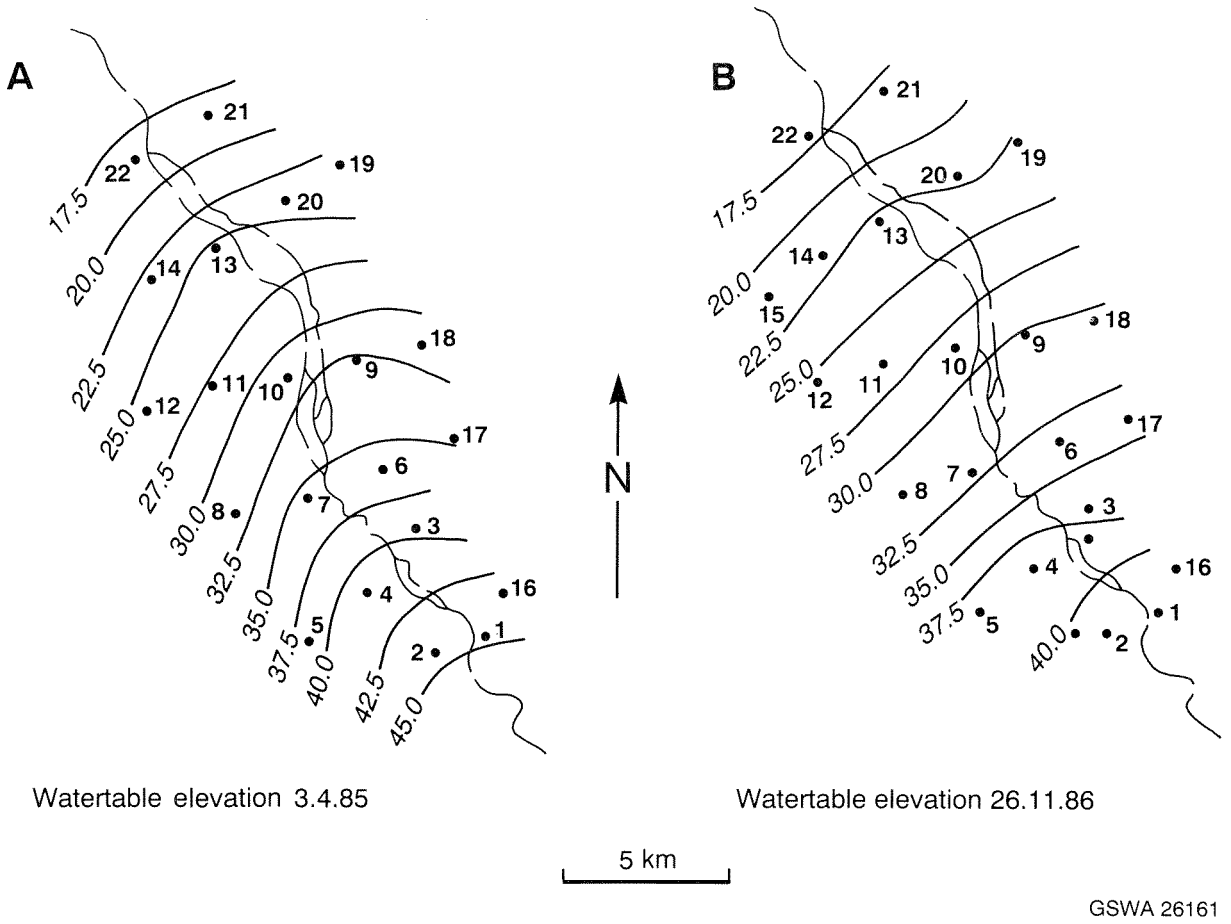

Figure 12. Elevation of watertable. A — maximum. B — minimum

RCP 4 is similar to that in the Robe River alluvium (Fig. 15).

Yarraloola Conglomerate

The Yarraloola Conglomerate was encountered at RCP 4 and RCP 5A, where it underlies Trealla Limestone and alluvium respectively. To the northwest it underlies impermeable Cretaceous and Tertiary sediments, and grades laterally into the Birdrong Sandstone, which is an aquifer throughout the Carnarvon Basin (Allen, 1987). The base of the formation is exposed in outcrops south and east of the investigation area, and these isolated outcrops are, therefore, unsaturated.

Table 10. Salinity variation in Tragedy Corner Bore 1983–85

Year	*Date*	*Salinity (mg/L)*
1983	5 Oct	1 400
1984	29 Aug	3 700
	8 Dec	2 300
1985	22 Feb	1 700
	3 Apr	4 500
	7 May	4 200
	12 Nov	2 100

Note: TDS by conductivity

The Yarraloola Conglomerate has a low permeability where intersected below the Robe alluvial aquifer. For example, RCP 5A was drilled in a zone of low seismic velocity (Nowak, 1979), usually indicative of relatively high porosity, but the bore yield was very low.

The Birdrong Sandstone aquifer beneath the coastal plain is presumably recharged through the Robe River alluvium where the Robe River enters the coastal plain. Pressure data from oil wells in the formation indicate a potentiometric head of about 40 m above sea level throughout the area (Thomas, 1978). This is consistent with a very low rate of recharge originating in the subcrop beneath the Robe River alluvium where the watertable is 40–43 m above sea level. Artesian flows from the formation have been encountered in the northern part of the investigation area and along the coast (Thomas, 1978).

The groundwater salinity in the Yarraloola Conglomerate rises from 2000 mg/L at RCP 5A, to about

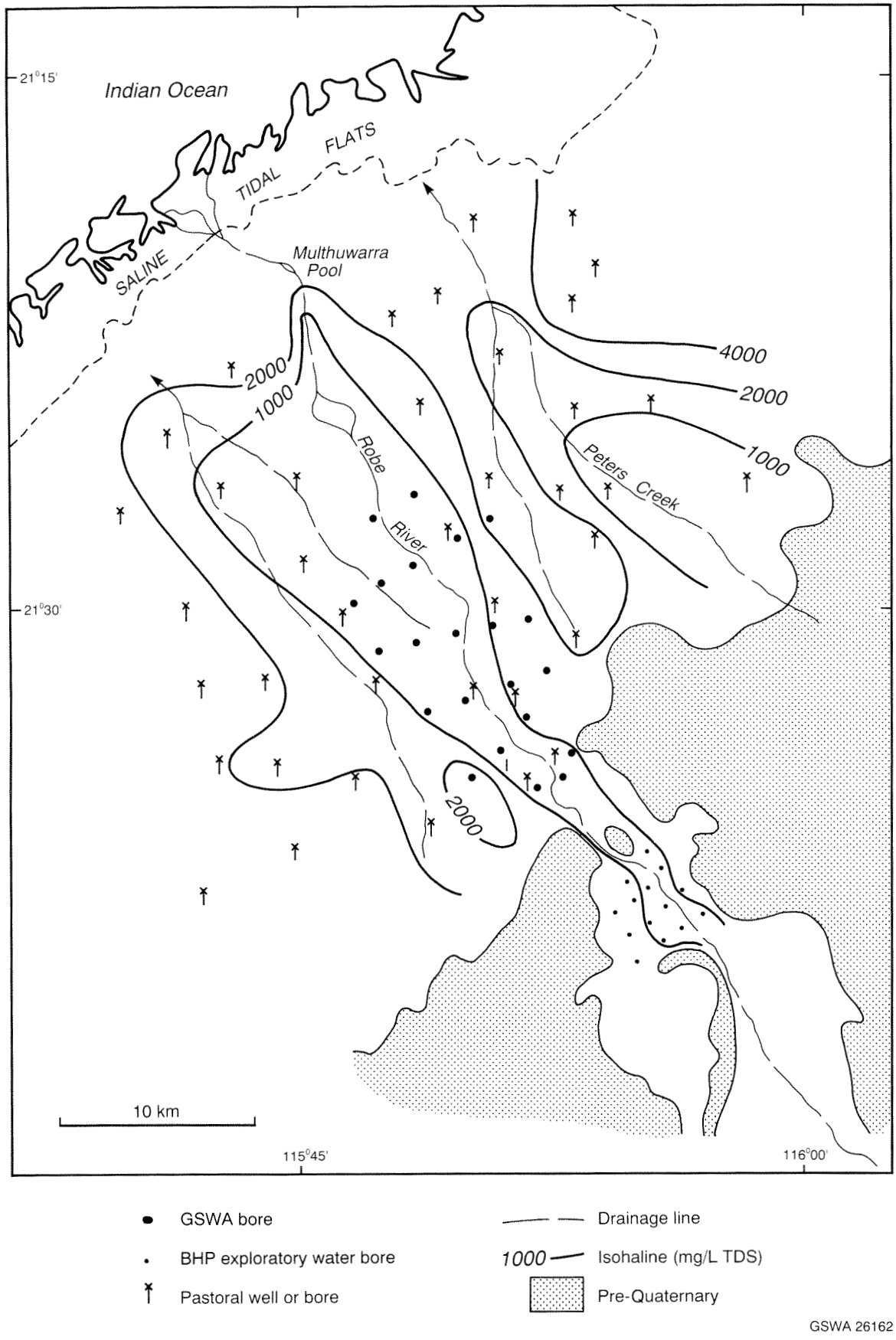

Figure 13. Regional groundwater salinity in the coastal plain alluvium

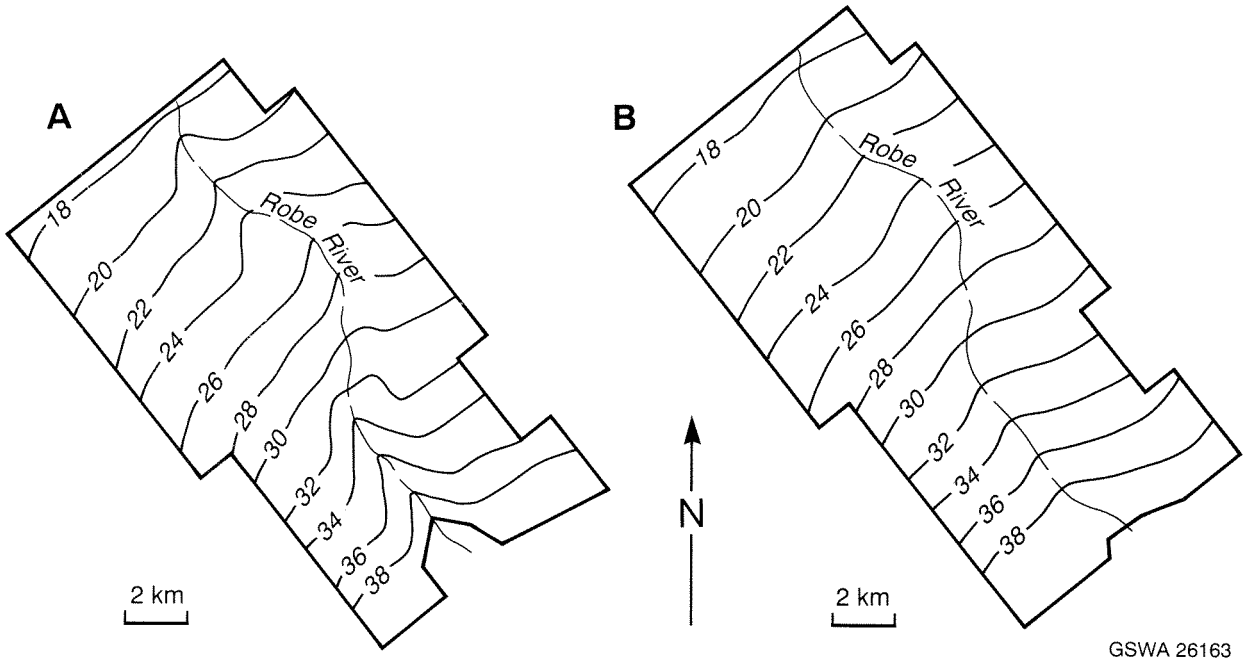

Figure 14. Simulated watertable elevation (A) 1 month and (B) 11 months after recharge

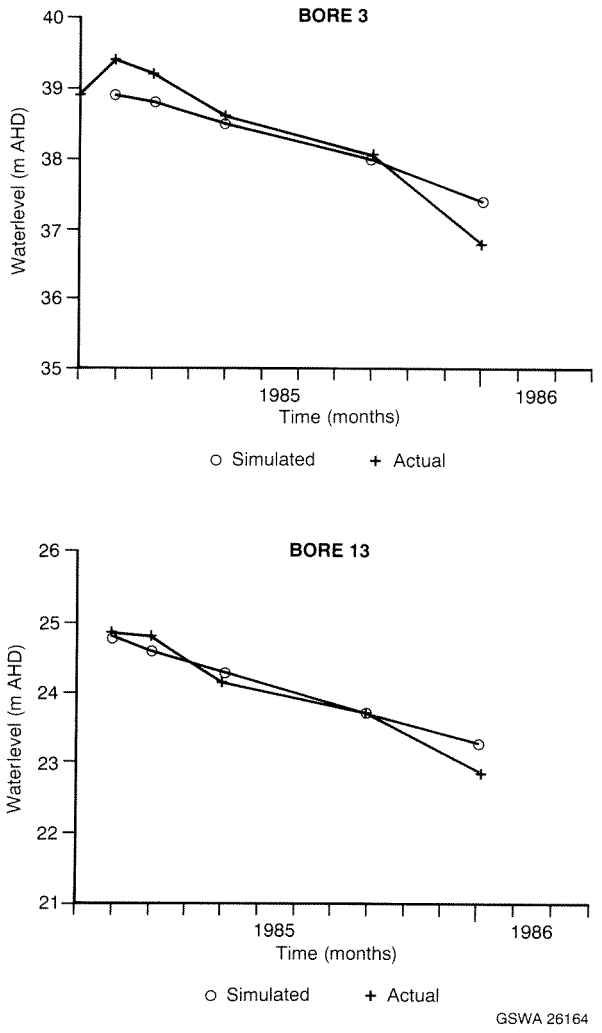

Figure 15. Comparison of simulated and actual watertable levels

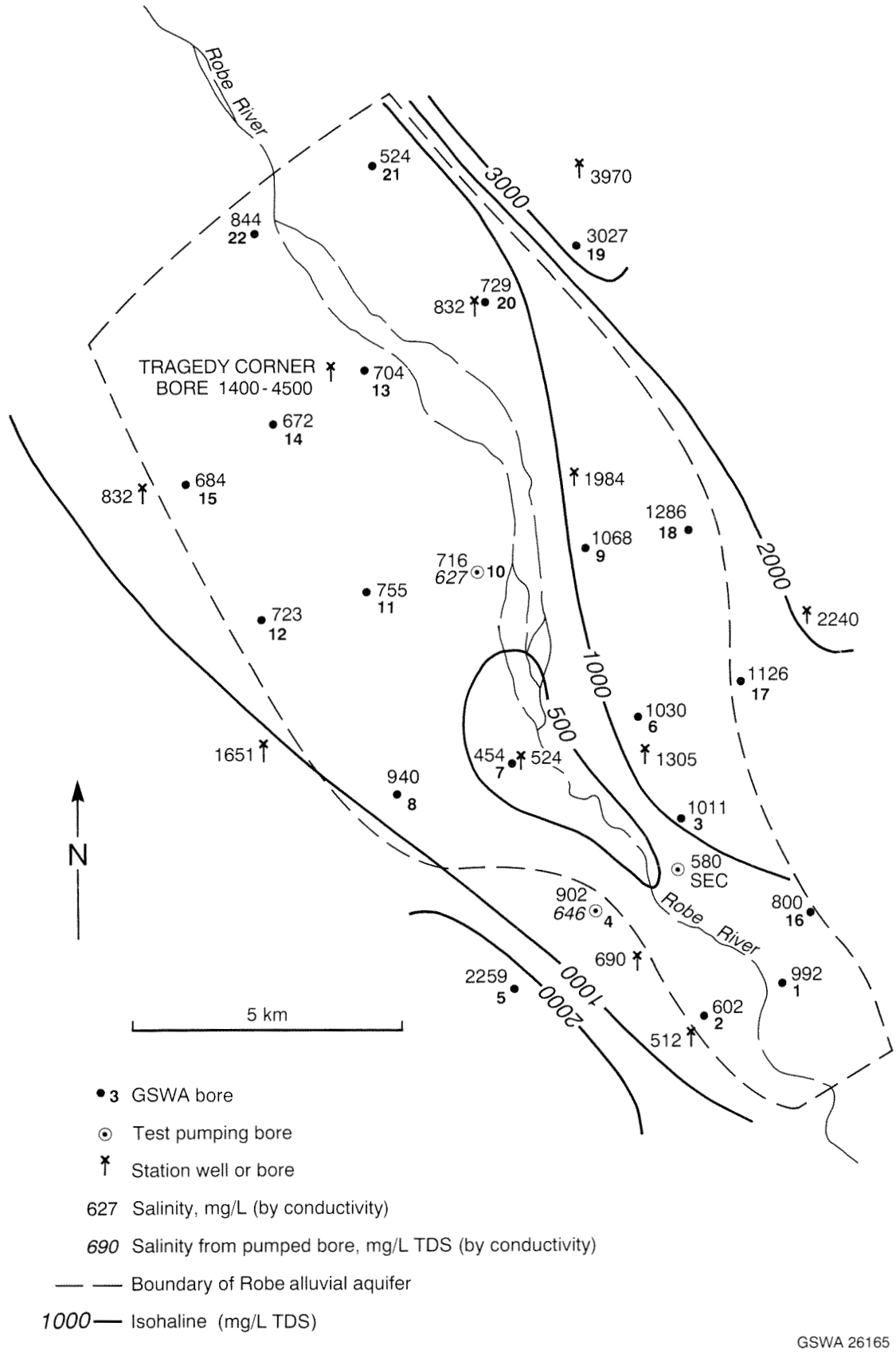

Figure 16. Groundwater salinity in the Robe River alluvium and Trealla Limestone

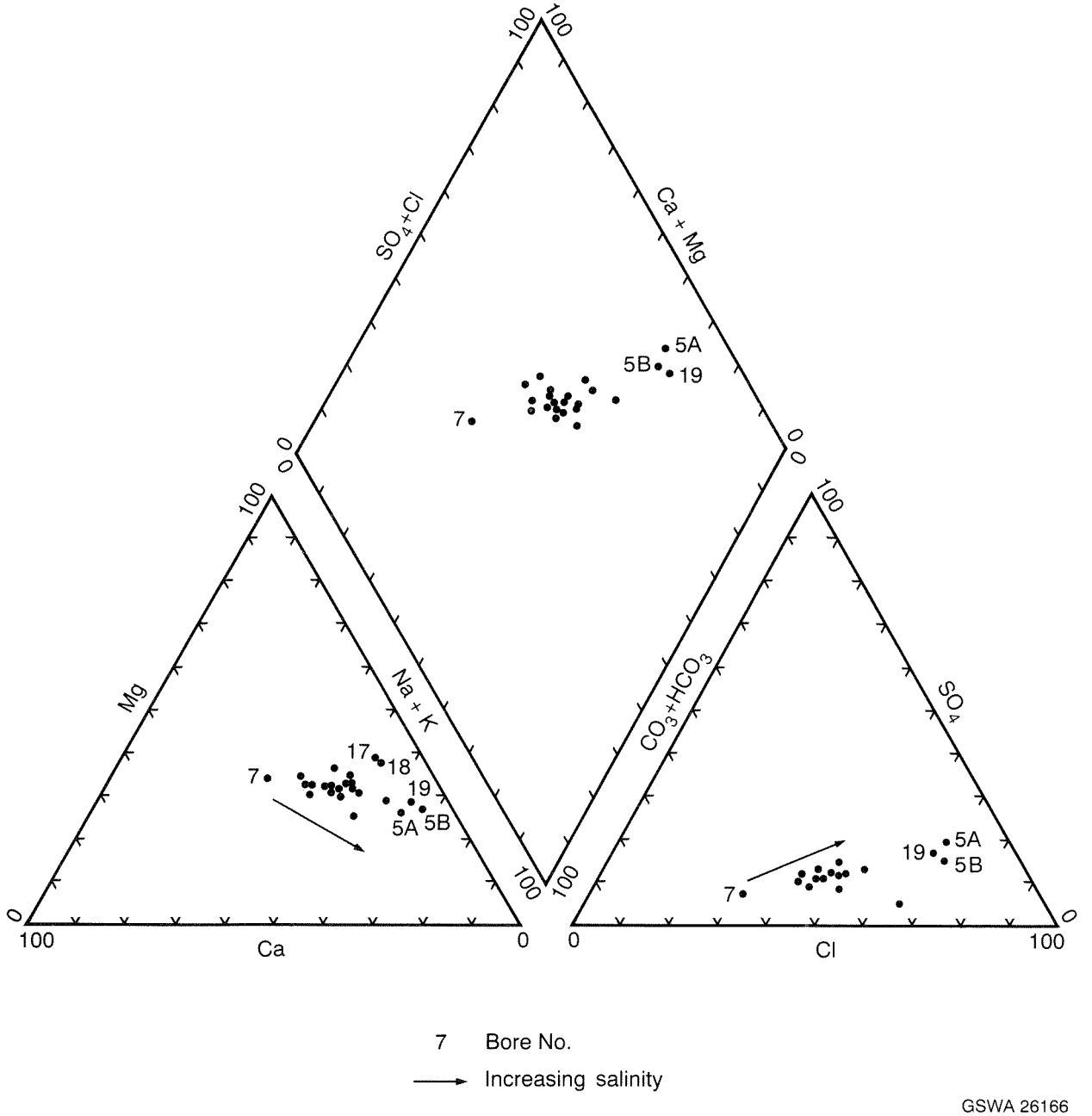

Figure 17. Piper trilinear diagram of chemical analyses

Table 11. Chemical analyses of groundwaters

Bore name	*Sample no.*	*Lab. no.*	*Sample date*	*pH*	*Conductivity*	*Total dissolved solids*	*Total hardness*	*Total alkalinity*	*Mineral matter (mg/L)*											
					(mS/m 25°C)		*($CaCo_3$)*	*($CaCO_3$)*	*Ca*	*Mg*	*Na*	*K*	*CO_3*	*HCO_3*	*Cl*	*SO_4*	*NO_3*	*SiO_2*	*B*	*F*	*Fe*
RCP1A	65662	83W 9820	07.10.83	8.0	155	855	390	285	57	60	163	12	<2	348	262	83	<1	44	0.49	0.5	
RCP2A	65663	83W 9821	12.10.83	8.3	94	526	290	210	51	39	79	7	<2	256	146	41	<1	35	0.23	0.4	
RCP3A	65664	83W 9822	08.10.83	8.2	158	892	400	316	57	62	172	12	<2	385	254	85	5	52	0.49	0.8	
RCP4A	65665	83W 9823	12.10.83	8.3	141	781	340	218	50	52	153	10	<2	266	253	83	4	43	0.38	0.6	
RCP4P	85934	86X 252	01.11.85	8.1	101	590	262	217	39	40	108	8	<2	265	159	56	4	46	0.42	0.5	<0.05
RCP5A	65666	83W 9824	30.09.83	7.8	326	1 830	580	205	71	98	440	24	<2	250	753	295	1	27	-	1.1	
RCP5B	65667	83W 9825	30.09.83	8.2	353	2 040	630	285	54	120	494	22	<2	348	805	277	12	83	-	1.1	
RCP6A	65668	83W 9826	08.10.83	8.4	161	920	420	320	56	68	174	12	6	378	263	91	6	55	0.56	0.8	
RCP7A	65669	83W 9827	15.10.83	8.3	71	420	250	222	50	30	51	5	3	265	80	26	2	40	0.23	0.4	
RCP8A	65670	83W 9828	18.10.83	8.1	147	839	340	264	50	53	165	10	<2	322	143	98	5	54	0.48	0.7	
RCP9A	65671	83W 9829	10.10.83	8.5	167	904	330	247	41	55	207	13	15	271	352	36	2	47	0.72	1.1	
RCP10A	65672	83W 9830	25.10.83	8.3	112	651	300	250	50	43	113	8	6	293	177	58	3	46	0.39	0.6	
RCP10P	85935	86X 253	06.11.85	8.3	98	590	266	248	44	38	103	8	3	296	135	57	3	46	0.39	0.6	<0.05
RCP11A	65673	83W 9831	21.10.83	8.2	118	673	270	233	49	35	138	8	<2	284	213	47	1	40	0.49	0.4	
RCP12A	65674	83W 9832	18.10.83	8.2	113	656	300	240	51	42	114	8	<2	293	184	62	2	46	0.38	0.5	
RCP13A	65675	83W 9833	20.10.83	8.2	110	650	280	239	48	40	118	8	<2	291	179	61	3	47	0.40	0.6	
RCP14A	65676	83W 9834	19.10.83	8.3	105	602	310	220	57	41	94	7	6	256	167	53	2	47	0.31	0.4	
RCP15A	65677	83W 9835	19.10.83	8.4	107	627	310	260	57	42	100	7	15	287	151	58	3	50	0.41	0.5	
RCP16A	65687	84X 2039	30.08.84	8.2	125	740	355	267	50	56	125	10	<2	326	215	70	3	46	0.4	0.6	
RCP17A	65688	84X 2040	23.08.84	8.3	176	1 030	427	333	36	82	199	17	3	400	321	104	6	58	-	1.1	
RCP18A	65689	84X 2041	21.08.84	8.2	201	1 180	476	331	39	92	236	18	<2	404	392	125	8	64	-	1.2	
RCP19A	65690	84X 2042	20.08.84	8.2	473	2 810	807	365	63	158	721	40	<2	445	1 180	347	11	69	-	1.6	
RCP20A	65691	84X 2043	24.08.84	8.2	114	680	303	246	49	44	123	9	<2	300	185	71	<1	46	0.44	0.6	
RCP21A	65692	84X 2044	28.08.84	8.2	83	490	236	198	45	30	77	6	<2	241	123	41	1	49	0.31	0.5	
RCP22A	65693	84X 2045	15.06.84	8.1	132	780	364	286	62	51	132	9	<2	349	222	73	2	52	0.43	0.7	
SEC BF2-1			22.10.81	8.0	92	-	-	-	61	34	77	6	<1	285	136	52	2	-	-	0.3	<0.05
SEC BF2-1	85936	86X 254	11.11.85	-	-	-	-	-	-	-	-	-	-	-	-	-	-	-	-	-	0.13
SEC BF2-2			30.10.81	8.1	91	-	-	-	62	34	75	6	<1	276	136	52	2	-	-	0.3	<0.05
SEC BF2-2	85937	86X 255	14.11.85	-	-	-	-	-	-	-	-	-	-	-	-	-	-	-	-	-	0.08

Note: total dissolved solids calculated to be equivalent to evaporation to dryness at 180°C

5000 mg/L in oil exploration bores near RCP 13, and to 20 000 mg/L at the coast (Thomas, 1978).

The low permeability, very low potentiometric gradient, relatively high salinity, and small area of potential recharge indicate that recharge (and therefore leakage from the Robe River alluvium) is likely to be very small.

Development

The area of the Robe River alluvium (including a small area of Trealla Limestone) most suitable for ground-water abstraction is a 2 km-wide strip extending about 7 km along the river from RCP 4 and the SEC bores north-westwards to RCP 10. Within this area, the aggregate saturated thickness is at least 5 m, and the salinity range is 450–700 mg/L.

Bore yields of 1000–1300 m^3/day have been demonstrated by pumping tests, and the potential yield of one bore (SEC 2/2), which was not pumped to the limit of the available drawdown, is projected to be 3000 m^3/day.

The yield of the aquifer is limited ultimately by the recharge from flows in the Robe River. Recharge, in turn, depends on the duration of flow and the storage level in the aquifer. The mean annual runoff (1972–85) is 51 x 10^6 m^3; but in the driest five-year period (1975–79), the average annual streamflow was only 11 x 10^6 m^3. However, since these flows do not reach the sea, a high proportion must contribute to groundwater recharge.

The estimated recharge (based on the decline in storage in a year of no river flow) and the limitation of river flow suggest that 10 x 10^6 m^3 would be a reasonable upper limit for annual abstraction. The estimated groundwater in storage, 70 x 10^6 m^3, could be utilized in periods of below-average runoff.

The infiltration capacity of the aquifer could be increased by abstraction close to the river. This would lower the watertable, and create a larger immediately available storage capacity to be filled when the river flowed. By artificially slowing the flow of the river, and by increasing the area available for direct infiltration, the storage capacity of the normally unsaturated gravel above the watertable away from the river could also be utilized.

The salinity of the groundwater may also be modified as increased infiltration may capture a higher proportion of the low-salinity water available at flow peaks.

Conclusions

Alluvial gravels underlying and adjacent to the Robe River are a significant and presently unutilized resource of fresh groundwater in a region generally deficient in such resources. This resource is sufficiently large to supply a town or support irrigated agriculture.

The aquifer has the potential to yield about 10 x 10^6 m^3/year of groundwater, and individual bores may yield as much as 3000 m^3/day. A production borefield close to the river would lower the local watertable. This would, in turn, induce increased recharge of the aquifer, and allow the utilization of surface water that normally flows into the sea during periods of flood. A concurrent lowering of the groundwater salinity would be expected.

Acknowledgements

The assistance and cooperation during the drilling program of the Patterson family of Yarraloola Pastoral Lease is gratefully acknowledged.

References

ALLEN, A. D., 1987, Groundwater, *in* Geology of the Carnarvon Basin Western Australia *by* R. M. HOCKING, H. T. MOORS, and W. J. E. van de GRAAFF: Western Australia Geological Survey, Bulletin 133.

BARNETT, J. C., and COMMANDER, D. P., 1986, Hydrogeology of the western Fortescue Valley, Pilbara region, Western Australia: Western Australia Geological Survey, Record 1986/8.

BEARD, J. S., 1975, Pilbara, explanatory notes to sheet 5: University of Western Australia Press, Vegetation Survey of Western Australia, 1:1 000 000 series.

COMMANDER, D. P., 1988, Robe River coastal plain bore completion reports: Western Australia Geological Survey, Hydrogeology Report 1988/3 (unpublished).

CONDON, M. A., 1954, Progress report on the statigraphy and structure of the Carnarvon Basin, Western Australia: Australia Bureau of Mineral Resources, Report 15.

DAVIDSON, W. A., 1975, Hydrogeological reconnaissance of the northwest Pilbara region: Western Australia Geological Survey, Record 1975/12.

de la HUNTY, L. E., 1965, Mount Bruce, W.A.: Western Australia Geological Survey, 1:250 000 Geological Series Explanatory Notes.

GILL, M. A., 1985, Bank storage characteristics of a finite aquifer due to a sudden rise and fall of river level: Journal of Hydrology, v. 76, p. 133–142.

HOCKING, R. M., and van de GRAAFF, W. J. E., 1978, Cretaceous stratigraphy and sedimentology, northeast margin of the Carnarvon Basin, Western Australia: Western Australia Geological Survey, Annual Report 1977, p. 36–41.

HOCKING, R. M., MOORS, H. T., and van de GRAAFF, W. J. E., 1987, Geology of the Carnarvon Basin Western Australia: Western Australia Geological Survey, Bulletin 133.

JOHNSTONE, D., CONDON, M. A., and PLAYFORD, P. E., 1958, The stratigraphy of the lower Murchison River area and Yaringa North Station, Western Australia: Royal Society of Western Australia, Journal, v. 41, p. 13–16.

McDONALD, M. G., and HARBAUGH, A. W., 1984, A modular three-dimensional finite-difference ground-water flow model: United States Geological Survey, Reston, Virginia, p. 528.

McTAVISH, R. A., 1968, Yarraloola No.1 well completion report: West Australian Petroleum Pty Ltd, Petroleum Search Subsidy Act Report (unpublished).

MUGGERIDGE, G. D., 1978, Final report on exploration completed within TRs 6649H, 6650H, 6694H, West Pilbara, W.A.: CRA Exploration Ltd (unpublished).

NOWAK, I. R., 1979, Fortescue and Robe Rivers coastal plain geophysical survey 1979: Western Australia Geological Survey, Geophysical Report 7/79 (unpublished).

PUBLIC WORKS DEPARTMENT, 1984, Streamflow records of Western Australia to 1982: Western Australia Public Works Department.

ROCKWATER, 1982, State Energy Commission of W.A. Dampier to Perth natural gas pipeline hydrostatic-testing water supplies, completion report for borefields BF 1–BF 12: (unpublished).

SHEAHAN, N. T., 1971, Type curve solution of step drawdown test: Groundwater, v. 9, no.1, p. 25–29.

THOMAS, B.M., 1978, Robe River — An onshore shallow oil accumulation: APEA Journal, v. 18, pt. 1, p. 3–12.

TYRWHITT, D. S., and SARGEANT, D. W., 1978, Final reports on exploration completed within TRs 6566, 6567, West Pilbara, W.A.: Newmont Pty Ltd (unpublished).

WILLIAMS, I. R., 1968, Yarraloola, W.A.: Western Australia Geological Survey, 1:250 000 Geological Series Explanatory Notes.

Hydrogeology of the Fortescue River alluvium, Ashburton Plain, Carnarvon Basin

by

D.P. Commander

Abstract

Thirty-four exploratory bores were drilled to define a Quaternary alluvial aquifer along the Fortescue River on the Ashburton Plain in the Carnarvon Basin 100 km southwest of Karratha. This aquifer extends over a former delta up to 15 km northwest of the river and has a saturated thickness of as much as 15 m. It consists of pebbles up to 100 mm diameter, similar to the present river bed gravels, and passes laterally into flood plain clay and silt. The unit rests unconformably on Precambrian banded iron-formation and basalt, Cretaceous conglomerate and siltstone, and on Tertiary pisolite and limestone.

The aquifer is recharged by periodic streamflow directly from the Fortescue River, which has a median annual flow of 121 x 10^6 m^3. The average annual recharge to the aquifer is estimated to be 11 x 10^6 m^3, and the storage in the aquifer is estimated to be about 130 x 10^6 m^3 based on a specific yield of 0.1. The groundwater salinity in the aquifer rises from 345 mg/L (TDS) close to the river to more than 1000 mg/L near the tidal flats where there is a saltwater interface. Test-pumping bores at four sites demonstrated that bores screened in the gravel aquifer are capable of yields ranging up to 800 m^3/day. There is an appreciable thickness of unsaturated gravel above the watertable, which could be used for artificial recharge, and pumping close to the river would allow a greater infiltration rate.

KEYWORDS: Hydrogeology, ground water, alluvium, drilling, salinity, streamflow, pumping tests

Introduction

Location

The Fortescue River crosses the Ashburton Plain near Mardie Homestead in the Pilbara Region of Western Australia (Fig. 1). The nearest towns are Karratha, 110 km to the northeast, and Pannawonica 100 km by road to the southeast. The North West Coastal Highway crosses the Fortescue River south of the investigation area, and access to the area is provided by station tracks.

Purpose and scope

The Geological Survey of Western Australia (GSWA) has carried out a number of exploratory drilling projects to locate groundwater supplies for towns along the Pilbara coast. Alluvium along the Fortescue River was recognized as having potential for large supplies of potable groundwater and this report describes the results of the exploratory drilling and test pumping of the alluvium carried out between 1983 and 1985. The investigation was jointly funded by the State and Commonwealth Governments under the National Water Resources Assessment Program.

Previous investigations

A census of station wells was carried out in 1963–64 during the course of regional geological mapping (Williams, 1968), and the mound spring at Mount Salt recognized (Williams, 1965).

In 1965, exploratory bores were drilled along the Fortescue River to locate a water supply for Cliffs Western Australian Mining's proposed iron-ore pelletizing plant at Cape Preston, 20 km north of the river mouth (Bradberry Associates, 1965). The investigation consisted of fifteen exploratory bores, of which six were test pumped, and proved the existence of an extensive shallow gravel aquifer. It was concluded that the aquifer could supply 3 x 10^6 m^3/year, however the plant was relocated and the groundwater resources were not developed.

The distribution of low-salinity groundwater associated with the Fortescue River was mapped, based on the salinity of pastoral bores (Davidson, 1975), and a seismic survey (Lines FA, FB) was later carried out to determine the thickness of water-bearing strata (Nowak, 1979).

In a survey of options for the West Pilbara water supply, serving Karratha, Dampier, Roebourne and Wickham, Dames and Moore (1979) described the

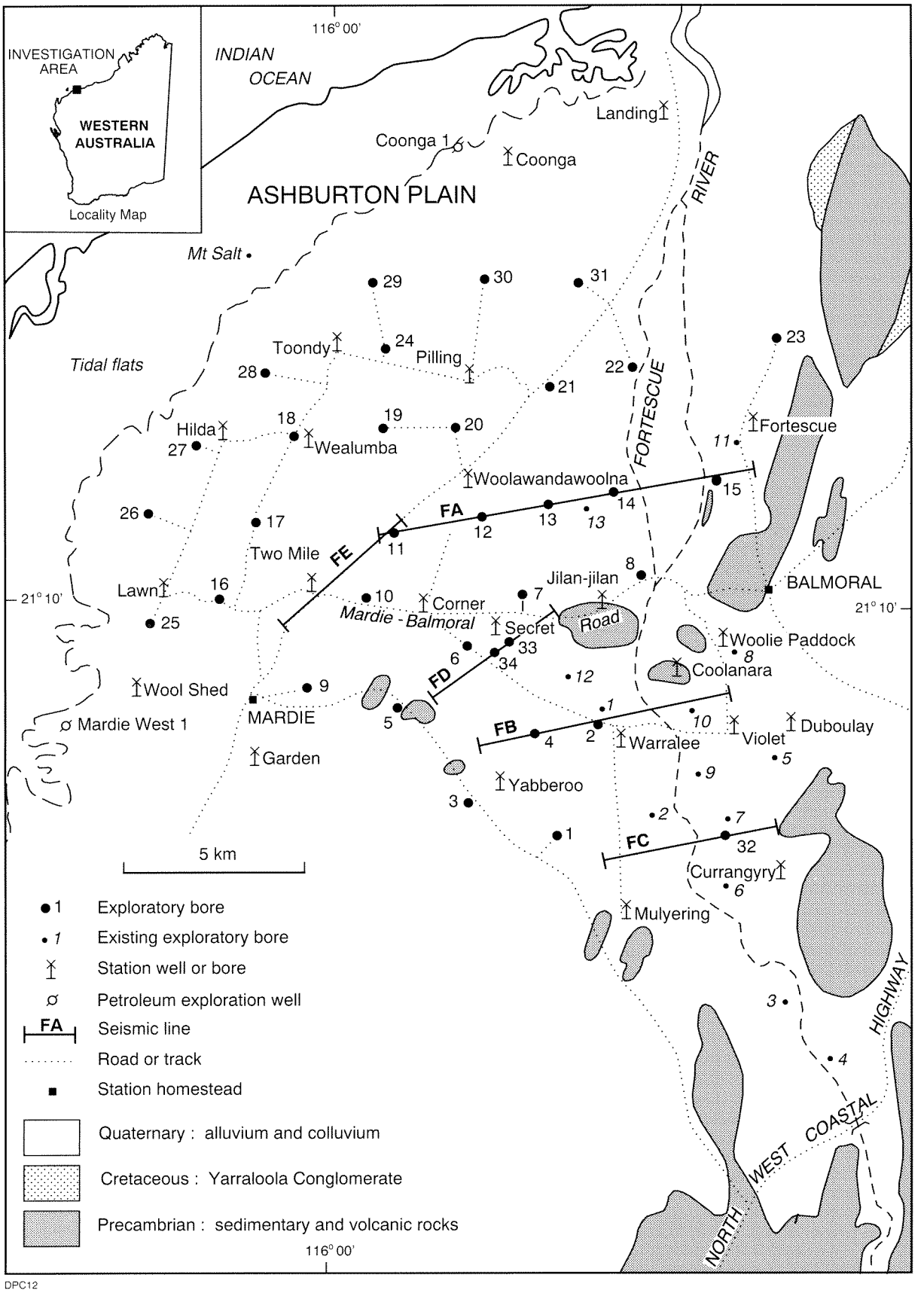

Figure 1. Location and geology

potential of a lower Fortescue borefield, based on the report by Bradberry Associates (1965). Allen (1987), in a review of the groundwater in the Carnarvon Basin, has also briefly described the groundwater resources of the area.

Two petroleum exploration wells, Mardie West (135 m) and Coonga (176 m), were drilled in 1972 (Hematite Petroleum Pty Ltd, 1973), and there has also been drilling for uranium in the area (Tyrwhitt, 1978).

Investigation program

The Fortescue Coastal Plain exploratory bores (prefix FCP) were drilled by the Mines Department Drilling Branch over a three-year period, using the mud-rotary drilling method. In 1983, twenty-six exploratory bores were drilled at 24 sites, including two drilled to bedrock to test low-velocity material shown by the seismic survey. In 1984 the bore network was extended to the northwest with seven bores, and additional seismic lines (FC, FD and FE) were run in an attempt to define the bedrock surface (Kevi, 1984). In 1985, three further exploratory bores were drilled on seismic targets. One of these (FCP 34A) was converted to a shallow test-pumping bore, and two other test-pumping bores, each with an observation bore, were also drilled and pump tested.

The bores ranged in depth from 14.5 to 75.5 m but were generally 20 to 30 m deep (Table 1) and the aggregate depth drilled was 1128 m. The shallow exploratory bores ranged in diameter from 125 to 171 mm and were completed with 80 mm PVC casing (100 mm in FCP 31A) slotted over the water-bearing interval. A protective 100 mm steel casing or in-line steel casing was used at the surface. The deep exploratory bores (FCP 2A, 14A, 32A) and the test-pumping bores FCP 4P, 11P and 34A were 200 to 311 mm diameter and were completed with 155 mm diameter steel casing (200 mm in FCP 32A) and in-line 155 mm stainless steel screens. At the three test-pumping sites, an additional observation bore was drilled 20 m away from each pumping bore and constructed with 80 mm PVC casing slotted at the same depth as the screens in the pumping bore.

The strata were lithologically logged during drilling to permit differentiation of thin gravel beds, and samples retained at 3 m intervals. Gamma-ray logs were run in the cased bores in August 1984. On completion, the bores were developed by airlifting to obtain a clear water sample for chemical analysis by the Chemistry Centre (W.A.).

Pumping tests, consisting of a six-stage step-drawdown test followed by an eight-hour constant-rate test at rates of up to 1063 m^3/day, were carried out in the three test-pumping bores and the two deep exploratory bores during October/November 1985. FCP 14A could not be developed properly, as the water contained a large amount of sediment, and the maximum pumping rate was 120 m^3/day.

During 1983–85 the waterlevels in the bores were monitored at intervals of between two weeks and three months, depending on river stage and access (closer spaced measurements were made immediately following river flow). Since 1986, the waterlevels have been recorded in November each year by the Water Authority of Western Australia (WAWA). The bores have been levelled to the Australian Height Datum (AHD).

Salinity–depth profiles in FCP 25–29, where there is a saltwater interface, were measured in September 1984 and repeated in August 1985 to confirm that the profiles had stabilized.

A summary of the bore data is given in Table 1 and more detailed bore completion reports are available in Commander (1989).

Environment

Physiography and vegetation

The investigation area lies on the Ashburton Plain (Hocking et al., 1987). This is a coastal plain which rises gently inland from the tidal flats of the Cane and Robe Rivers, and is broken by isolated hills of Precambrian and Cretaceous bedrock. The investigation area comprises the flood plain of the Fortescue River (Fig. 1). The Fortescue River crosses the plain in a narrow channel, which is incised as much as 5 m below the general level of the plain. In the lower reaches there are several anastomosing branches.

Mount Salt (Fig. 1), a prominent bare, rounded hill formed by a mound spring, rises to about 8 m above the tidal flats (Williams, 1965).

The surface of the coastal plain is flat and composed of cracking clay soils (gilgai), on which grow mixed grasses, and open shrubland or open woodland (Beard, 1975). The river banks are lined with river gums and a tree- or shrub-savannah of mixed grasses and scattered eucalypts occurs along the river. The vegetation along the river banks becomes progressively thicker downstream from the investigation area. Areas around outcrops of bedrock are covered by a veneer of gravel and are vegetated with spinifex.

North of the Mardie–Balmoral Road (the former alignment of the North West Coastal Highway) the native vegetation is overrun with mesquite. This was introduced in the early part of the century as a browse shrub after severe degradation of the natural vegetation by stock. The mesquite grew into dense impenetrable thickets after the 1945 flood, reaching its maximum extent in 1953 (Sharpe, R., 1986, pers. comm.), since when it has been periodically controlled by poisoning.

Climate

The region is arid with hot summers and warm winters. Rainfall is infrequent and intense; it usually results from tropical cyclones and thunderstorms between December and March, and from cold fronts between May and July. The average annual rainfall is 264 mm at Mardie and 263 mm at Balmoral, but annual totals since 1885 range

Table 1. Summary of bore data

Bore	*Date drilled*	*Elevation casing top (m AHD)*	*Total depth (m)*	*Slotted interval (m)*	*Static water level(a) (m)*	*Salinity(b) (mg/L TDS)*	*Airlift yield (m^3/day)*
FCP1A	06.07.83	28.473	18	7–11	7.60	998	–
FCP2A	13–26.07.83	27.199	75.5	43.8–70.8	7.96	454	120
FCP2B	21–22.07.83	27.760	21	6–21	8.46	480	40
FCP3A	07.07.83	25.217	20	6–16	7.37	1 337	15
FCP4A	11–12.07.83	24.342	25.5	6–21	6.97	537	20
FCP4P	19–20.06.85	–	20	(d)13.9–20	–	473	288
FCP5A	11.07.83	19.410	25.5	6–18	8.46	1 715	(f)
FCP6A	01–05.07.83	21.240	25	0–16.4	9.13	403	–
FCP7A	15–18.08.83	21.757	32	3.2–9.2	–	–	(f)
FCP7B	30.08.83	21.583	14.5	5–11	8.57	–	(f)
FCP8A	16–17.08.83	24.887	26	4.7–21.7	9.67	505	70
FCP9A	25–26.07.83	15.855	33	6–13	9.51	819	–
FCP10A	03.08.83	15.115	26	10–23	7.18	480	–
FCP11A	04.08.83	14.558	32	6–23	6.91	691	–
FCP11P	23.05–05.06.85	–	22	(d) 13–22	–	678	178
FCP12A	17–18.08.83	17.748	35	6–27	8.46	409	100
FCP13A	18–19.08.83	19.334	20.3	7–18	8.23	486	80
FCP14A	06–12.09.83	19.605	74	50.5–73.5	8.06	480	120
FCP14B	22.08.83	20.221	30	5–19	7.03	390	120
FCP15A	27.07–02.08.83	19.971	20	5.5–13.5	9.13	460	–
FCP16A	23–29.08.83	–	19.5	(e)	–	–	–
FCP16B	23–29.08.83	11.894	14.5	2.4–10.4	8.75	710	15
FCP17A	24.08.83	9.985	26	5–13 18–21	7.15	793	100
FCP18A	25.08.83	8.997	25.5	4–17 21–23	6.15	742	85
FCP19A	05.08.83	12.488	29.5	4.5–22	7.58	633	85
FCP20A	08.08.83	14.737	29	4.7–22.7	8.52	640	125
FCP21A	11.08.83	14.301	28	5–17	8.05	806	100
FCP22A	09–10.08.83	16.288	29.5	5–13	9.22	601	40
FCP23A	26–27.07.83	14.826	17.5	6–12	7.07	2 278	(f)
FCP24A	26.08.83	9.423	21.3	4–14 18–20	6.49	832	30
FCP25A	03.08.84	6.437	20.5	5–20	4.77	7 040	108
FCP26A	02.08.84	7.205	20.5	2.5–20	6.37	47 040	69
FCP27A	31.07.84	6.429	20.5	5–13	5.75	16 064	–
FCP28A	30.07.84	6.853	23.5	4–17	5.58	10 560	14
FCP29A	24–26.07.84	7.514	30	5–10 14–20	6.06	17 024	15
FCP30A	18–20.07.84	9.723	29.5	5–21	6.83	1 158	216
FCP31A	16.07.84	11.978	29.5	6–19	8.07	774	28
FCP32A	27–28.06.85	(c) 32.864	53	41.5–51.5	8.25	492	9
FCP32B	04.07.85	(c) 32.864	18.5	3.4–12.4	8.38	345	17
FCP33A	06.06.85	22.429	44.5	11–21	8.97	550	86
FCP34A	12.06.85	21.627	44.7	(d)13.8–20	7.97	441	103

Notes: (a) 12.11.85; (b) electrical conductivity (mS/m @ 25°C) x 6.4; (c) casing cut to same height; (d) screen; (e) not cased; (f) very low

from 9 mm (1936) to 758 mm (1973). Potential annual evaporation is about 2500 mm. Monthly rainfalls for the investigation period at Mardie and Balmoral Homesteads are shown in Table 2.

Streamflow

Streamflow in the Fortescue River has been measured since 1968 at the Jimbegnyinoo Pool gauging station, 4.5 km upstream of the North West Coastal Highway bridge (Public Works Department, 1984). Annual flow has ranged from 4 x 10^6 m^3 (1977) to 1186 x 10^6 m^3 (1975), with a median flow of 121 x 10^6 m^3 (Fig. 2). Large floods, comparable with the Cyclone 'Joan' flood in 1975, were also recorded in 1898 (which demolished the old Balmoral Homestead near Violet Well) and in 1945.

During the investigation period there were three major flows caused by the following rainfall events: Cyclone 'Chloë' in February/March 1984, frontal rain in May 1984, and Cyclone 'Gertie' in February 1985. Flow persisted for several months following the flood peaks (Fig. 3).

The salinity of large flows for which multiple samples have been taken (Public Works Department, 1984) was

Table 2. Monthly rainfall 1983–86 (mm)

Year	*Jan*	*Feb*	*Mar*	*Apr*	*May*	*Jun*	*Jul*	*Aug*	*Sep*	*Oct*	*Nov*	*Dec*	***Total***
Mardie (station no. 5008)													
1983	8	9	17	11	0	16	12	0	19	0	0	1	**93**
1984	16	80	60	14	149	0	36	6	0	0	0	25	**386**
1985	8	63	0	77	7	12	24	0	0	0	3	0	**194**
1986	22	194	19	1	0	73	6	0	9	0	0	0	**324**
Balmoral (station no. 5040)													
1983	10	26	7	22	0	3	9	0	8	0	3	0	**88**
1984	28	89	86	2	176	0	17	7	0	0	0	11	**416**
1985	17	36	7	67	8	9	16	0	0	0	0	0	**160**
1986	1	134	24	0	4	52	3	0	11	0	0	0	**229**

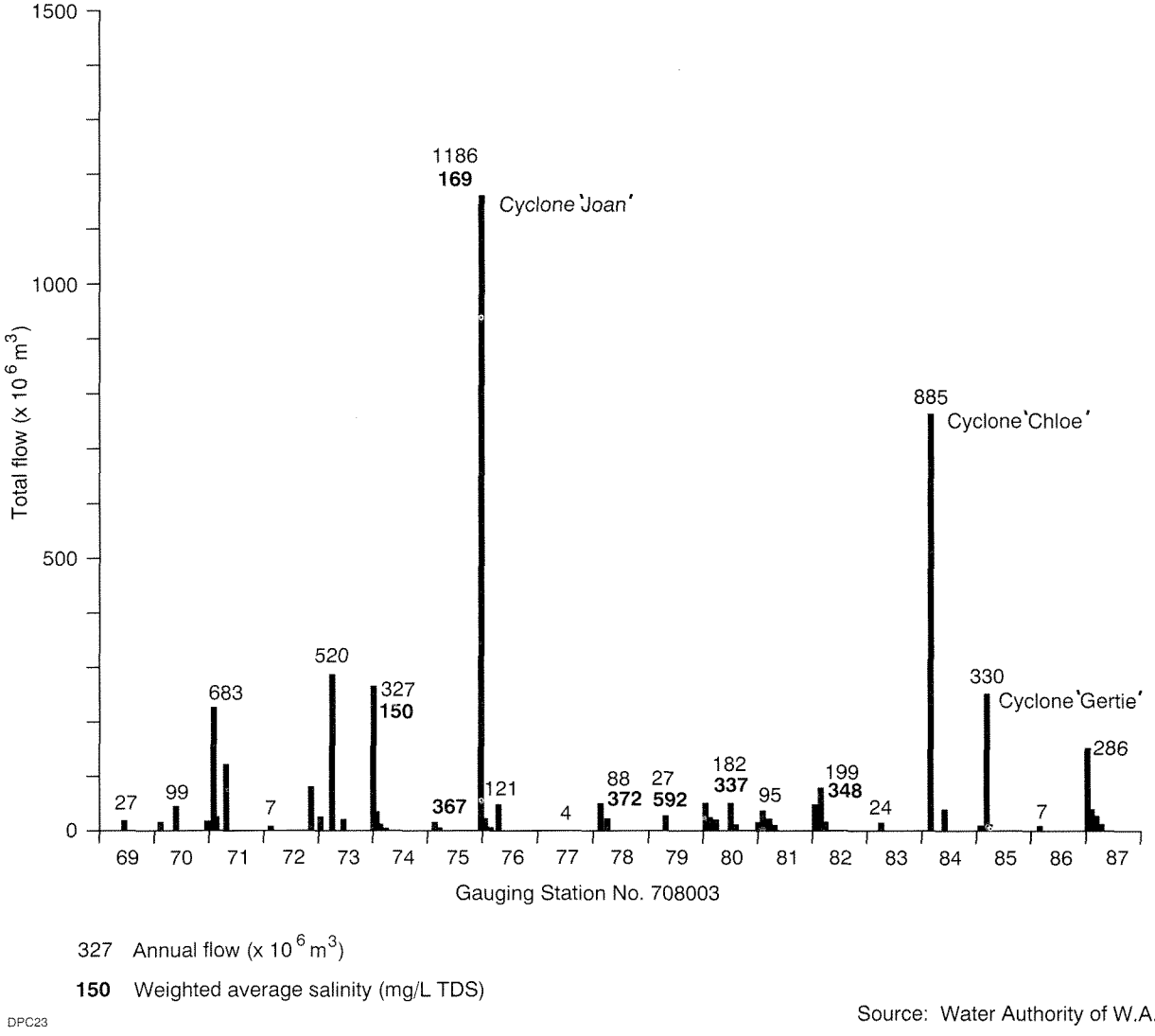

Figure 2. Fortescue River streamflow 1969–1987 and weighted average salinity

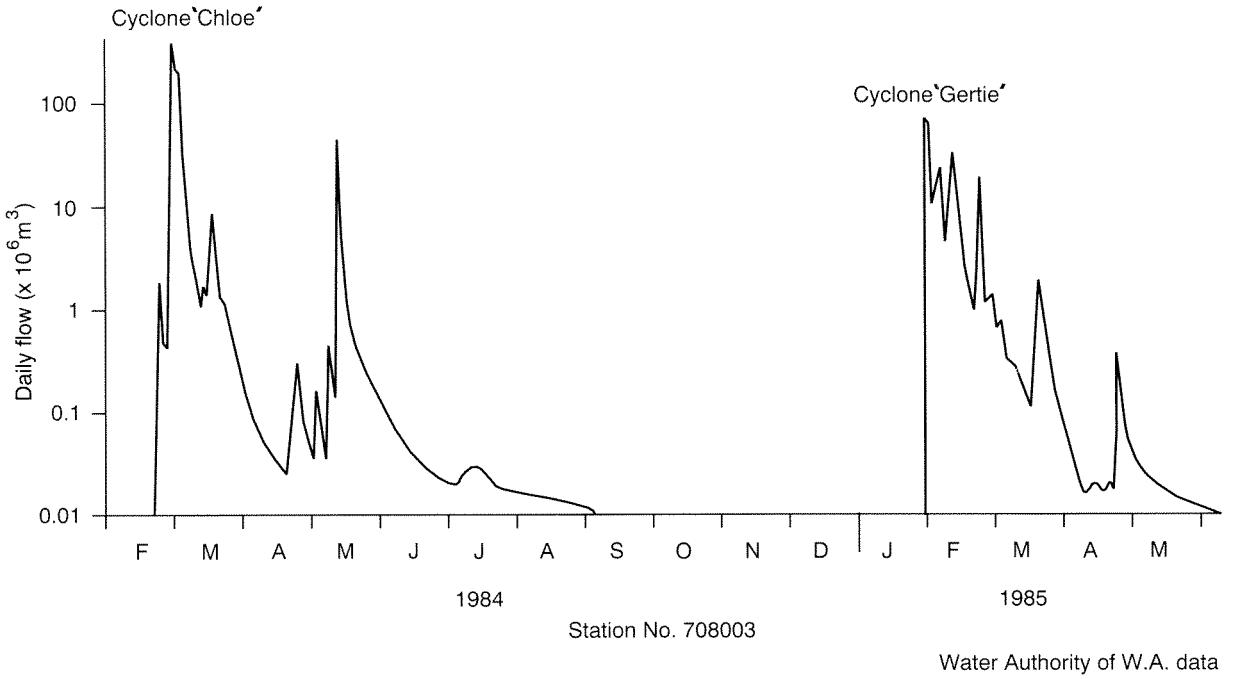

Figure 3. Fortescue River — daily flow February–July, 1984–1985

150 mg/L total dissolved solids (TDS) in 1973/4 and 169 mg/L in 1975/6 (Cyclone 'Joan' flood). In 1984, the field salinity of the flow at the North West Coastal Highway bridge was 100 mg/L on 9 March (about 4 days after the peak resulting from Cyclone Chloë), and had stabilized at 250 mg/L from 29 March to 1 May. In 1985, following the Cyclone 'Gertie' flood, the field salinity at the North West Coastal Highway bridge remained at about 250 mg/L from 22 February to 7 May 1985.

Geology

The investigation area lies in the northern part of the Carnarvon Basin on the Peedamullah Shelf (Hocking et al., 1987). It is underlain by up to 90 m of gently northwest-dipping Cretaceous sedimentary rocks, which are overlain by as much as 50 m of Tertiary and Quaternary sediments. The Carnarvon Basin sequence overlies a basement of Precambrian sedimentary and volcanic rocks of the Hamersley Basin.

The stratigraphic succession in the area is shown in Table 3.

Stratigraphy

Mt Bruce Supergroup

Rocks of the Mount Bruce Supergroup outcrop in the hills on each side of the upper reaches of the Fortescue River, and in small inliers on the coastal plain (Fig. 1). They were intersected in the deeper bores FCP 2, 14, 32, 33, and 34 (Fig. 4).

The rock types intersected are basalt (correlated with the Maddina Basalt) and chert (correlated with the Brockman Iron Formation). Ferruginized shale is common in outcrops within the investigation area.

The Mount Bruce Supergroup is of Precambrian age (latest Archaean to earliest Proterozoic) and is unconformably overlain by Cretaceous, Tertiary and Quaternary sedimentary rocks.

Yarraloola Conglomerate

The Yarraloola Conglomerate (Williams, 1968) outcrops in places adjacent to the inliers of Precambrian bedrock (Fig. 1). It was intersected in the subsurface in FCP 2A, 14A and 32A (Fig. 4), but is absent in Coonga 1 and Mardie West 1 (Hematite Petroleum Pty Ltd, 1973). The formation unconformably overlies the Precambrian bedrock.

The Yarraloola Conglomerate in FCP 2A, 14A and 32A consists of granule to pebble gravel of rounded red-brown siliceous ironstone, red jaspilite, grey chert, yellowish ironstained and clear quartz, dolomite, and basalt, with minor beds of sand and red-brown to green clay.

The formation in the subsurface appears to infill a valley incised in the Precambrian rocks by an antecedent of the Fortescue River. It is Early Cretaceous in age and was deposited in a fluvial environment. Elsewhere on the Peedamulla Shelf the formation grades laterally into the Nanutarra Formation and Birdrong Sandstone (Hocking and van de Graaff, 1978).

Table 3. Stratigraphic sequence

Age		*Formation*	*Thickness (a) (m)*	*Lithology*
QUATERNARY		Alluvium	30	Clay, gravel, calcrete close to watertable
		~~ *unconformity* ~~~~~~~~~~		
TERTIARY	Miocene	Trealla Limestone	17	Limestone, clay, marl
		~~ *unconformity* ~~~~~~~~~~		
CRETACEOUS		Muderong Shale	0	Shale
		Mardie Greensand Mbr		
		Yarraloola Conglomerate	23	Conglomerate, sand, clay
		~~ *unconformity* ~~~~~~~~~~		
PRECAMBRIAN		Mt Bruce Supergroup		
		Brockman Iron Fm		Jaspilite, shale
		Maddina Basalt		Basalt, tuff

Note: (a) maximum thickness intersected during drilling

Muderong Shale

The Muderong Shale has been identified only in Coonga 1 and Mardie West 1 petroleum exploration wells (Hematite Petroleum Pty Ltd, 1973) where it is 93 m and 74 m thick respectively. The Fortescue Coastal Plain bores were generally stopped in the overlying Trealla Limestone.

The formation, which is Early Cretaceous in age, unconformably overlies Precambrian rocks and consists of grey to green siltstone with a basal greensand (Mardie Greensand Member).

Trealla Limestone

Sedimentary rocks correlated with the Trealla Limestone occur throughout the northern part of the investigation area. They unconformably overlie the Yarraloola Conglomerate or the Muderong Shale.

The formation consists of interbedded yellow to cream clay, soft marl, and fine-grained to finely crystalline limestone.

The Trealla Limestone is a marine or lagoonal deposit of Middle Miocene age (Hocking et al., 1987).

Fortescue River alluvium

Alluvial deposits of the Fortescue River are up to 30 m thick and form an alluvial fan extending from the base of the scarp bordering the coastal plain to the coast. At the surface the sediments are mainly overbank deposits of clay and silt. Gravel bed-load deposits occur in the present river bed and in the subsurface. The Fortescue River alluvium unconformably overlies an irregular topography on Precambrian, Cretaceous, and Tertiary rocks.

The overbank deposits consist of dense red or yellow clay, and pink to white silty clay with granules and pebbles. The yellow clay is difficult to distinguish from the clay facies of the Trealla Limestone. The clay on the edge of the alluvial fan in FCP 3 and 5, and below the alluvial gravels in FCP 13 and 32, has been ferruginized and silicified. The ferruginous deposits in FCP 5 and 32 are also pisolitic.

The gravel consists of rounded pebbles of basalt, tuff, chert, jaspilite, and minor quartz, up to 100 mm in diameter, which have been derived from nearby outcrops of the Mount Bruce Supergroup. The gravel is partially cemented in outcrops near semi-permanent river pools. The basalt pebbles in the deeper gravel layers commonly have weathered surfaces, and in FCP 29A the basalt has been almost completely weathered to blue clay. Limonite-coated quartz also occurs in the deeper gravel layers in 24A.

Calcrete has been formed by hydrochemical action, close to the zone of watertable fluctuation, at depths of 4–12 m below the surface. The deposits vary from carbonate-cemented fine-grained sandstone to earthy limestone with rare calcite veins.

The alluvium forms an alluvial fan that has been deposited by the Fortescue River where it discharges onto the Ashburton Plain. It is considered to be of Quaternary age and is being periodically reworked by river floods.

Hydrogeology

Fortescue River alluvium

Gravel in the Fortescue River alluvium forms a major aquifer which extends over the alluvial fan west of the river (Fig.5). The gravel contains fresh groundwater in an area of about 200 km^2 (Fig.6). The aquifer grades laterally into the overbank silt and clay which have a very much lower transmissivity.

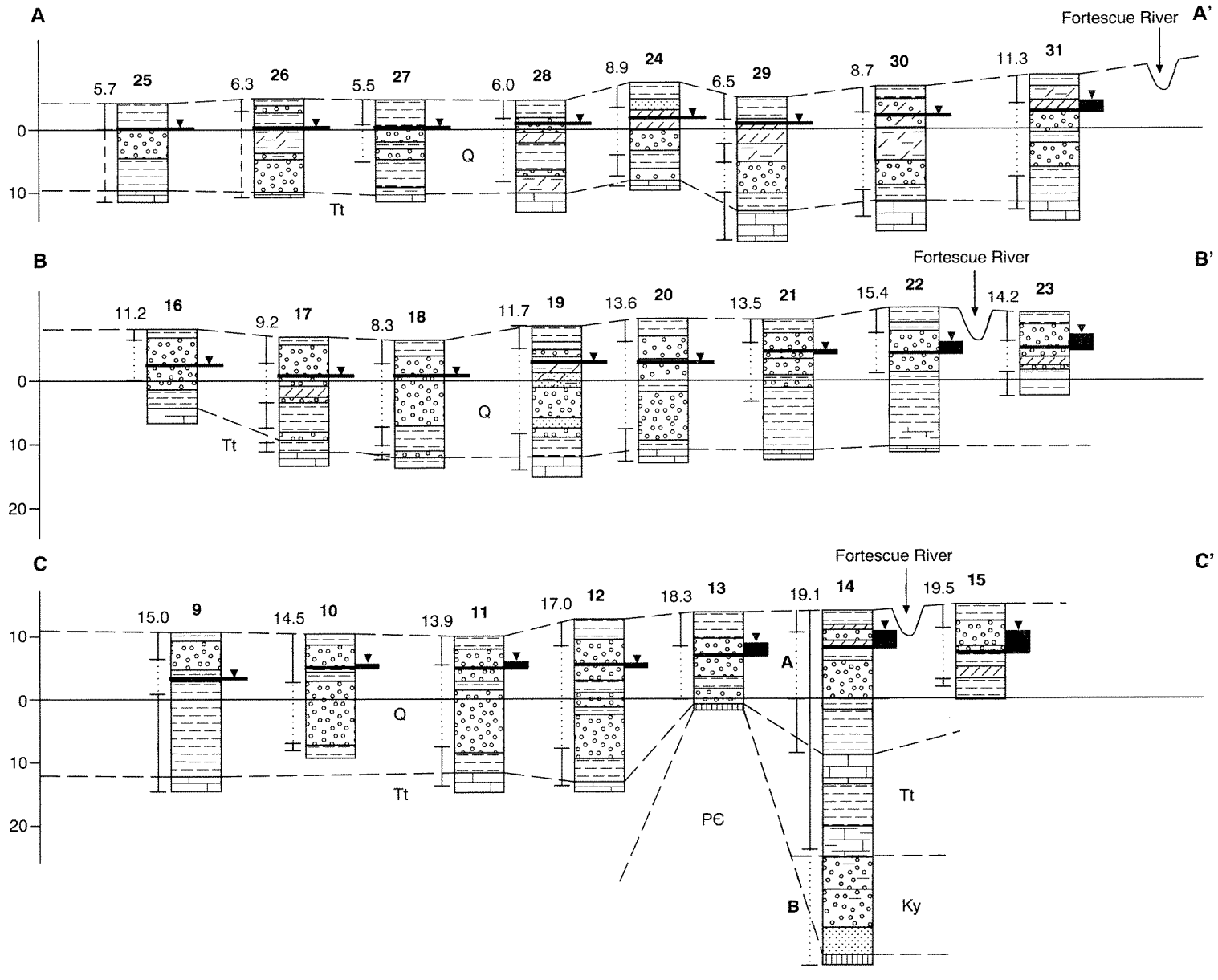
A
A'
Fortescue River
5.7 25
6.3 26
5.5 27
6.0 28
8.9 24
6.5 29
8.7 30
11.3 31
0
10
Q
Tt
B
B'
Fortescue River
11.2 16
9.2 17
8.3 18
11.7 19
13.6 20
13.5 21
15.4 22
14.2 23
0
10
20
Q
Tt
C
C'
Fortescue River
15.0 9
14.5 10
13.9 11
17.0 12
18.3 13
19.1 14
19.5 15
10
0
10
20
Q
Tt
A
PЄ
B
Tt
Ky

DPC25

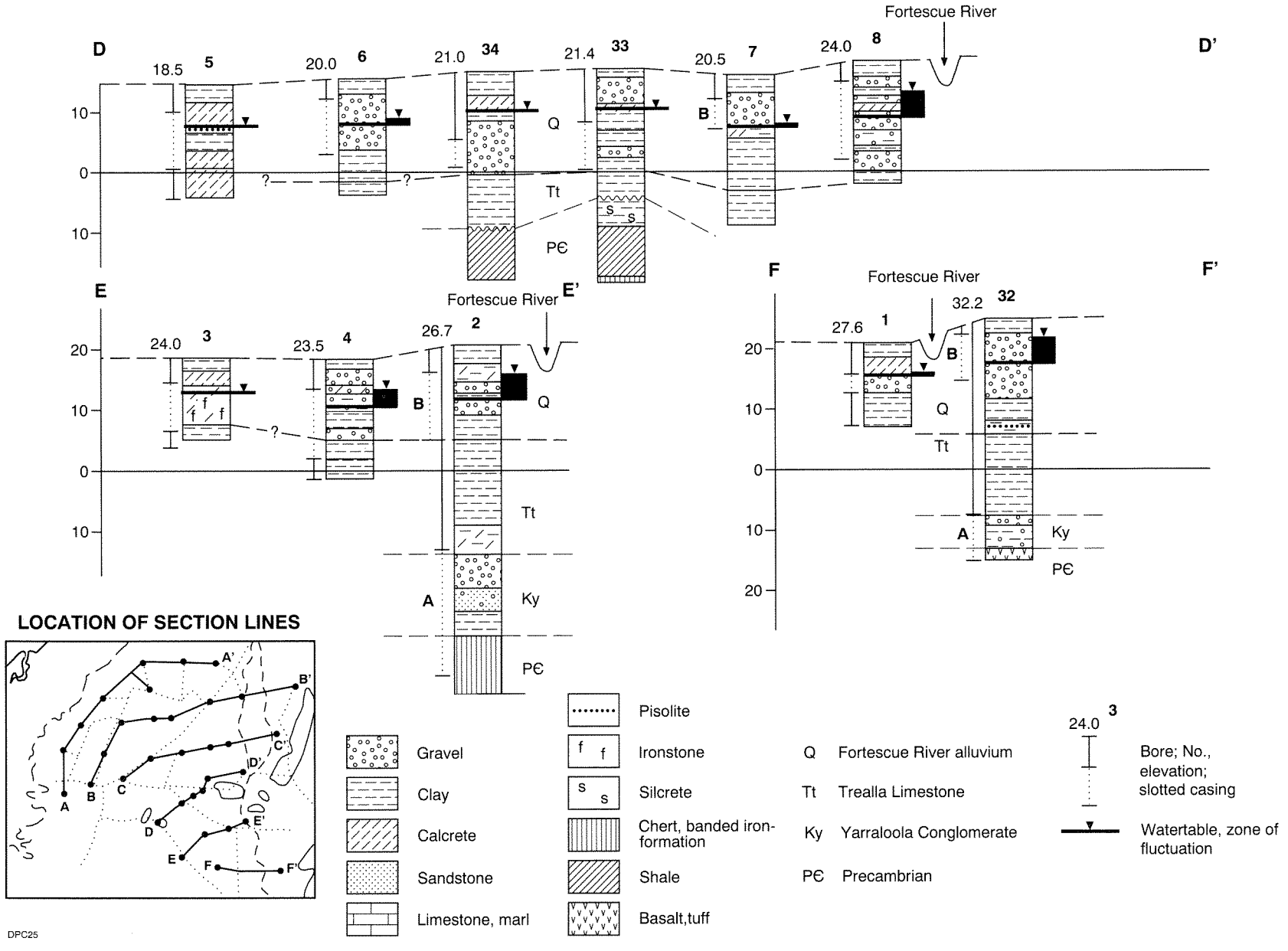

Figure 4. Geological sections

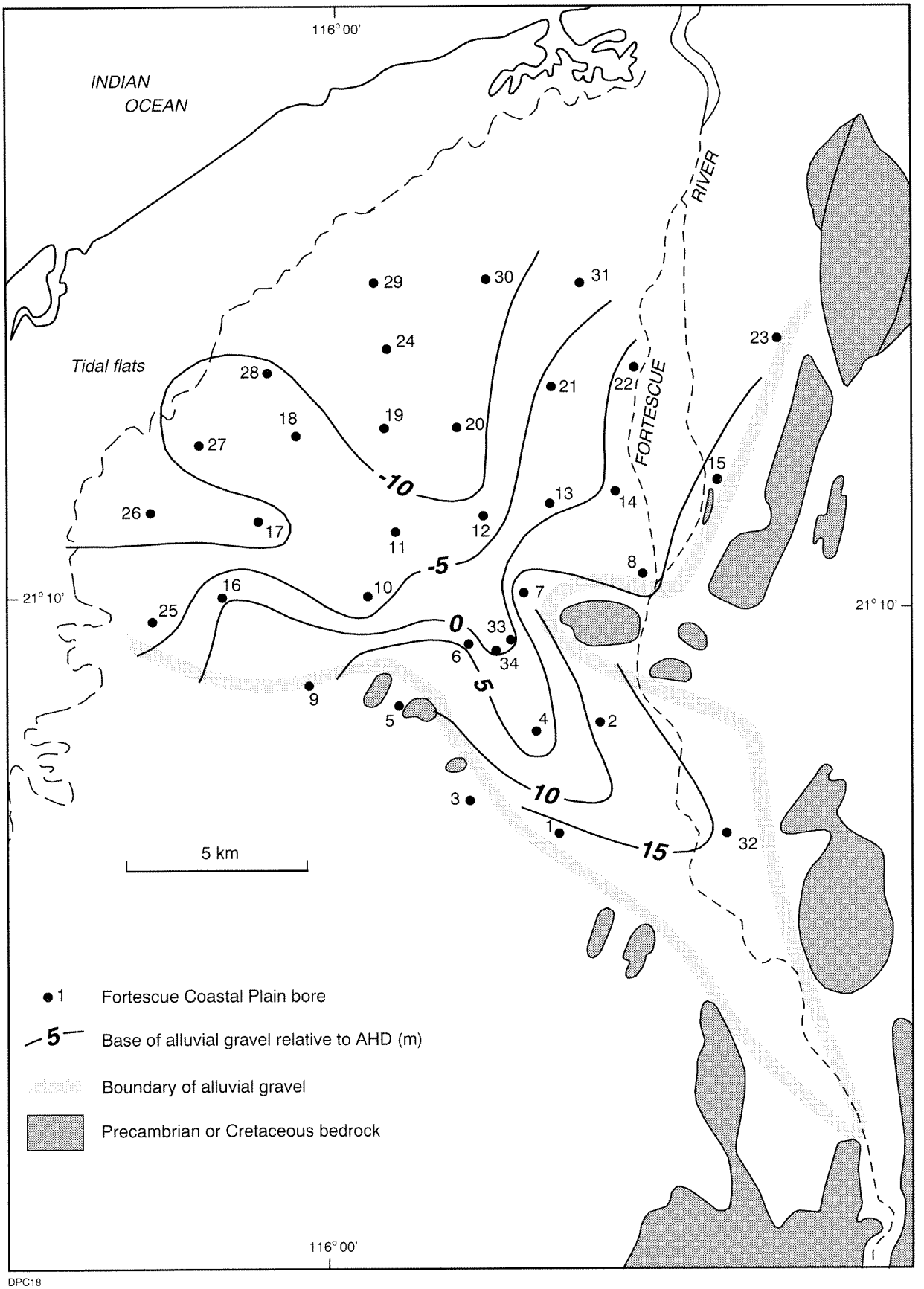

Figure 5. Structure contours on base of alluvial gravel

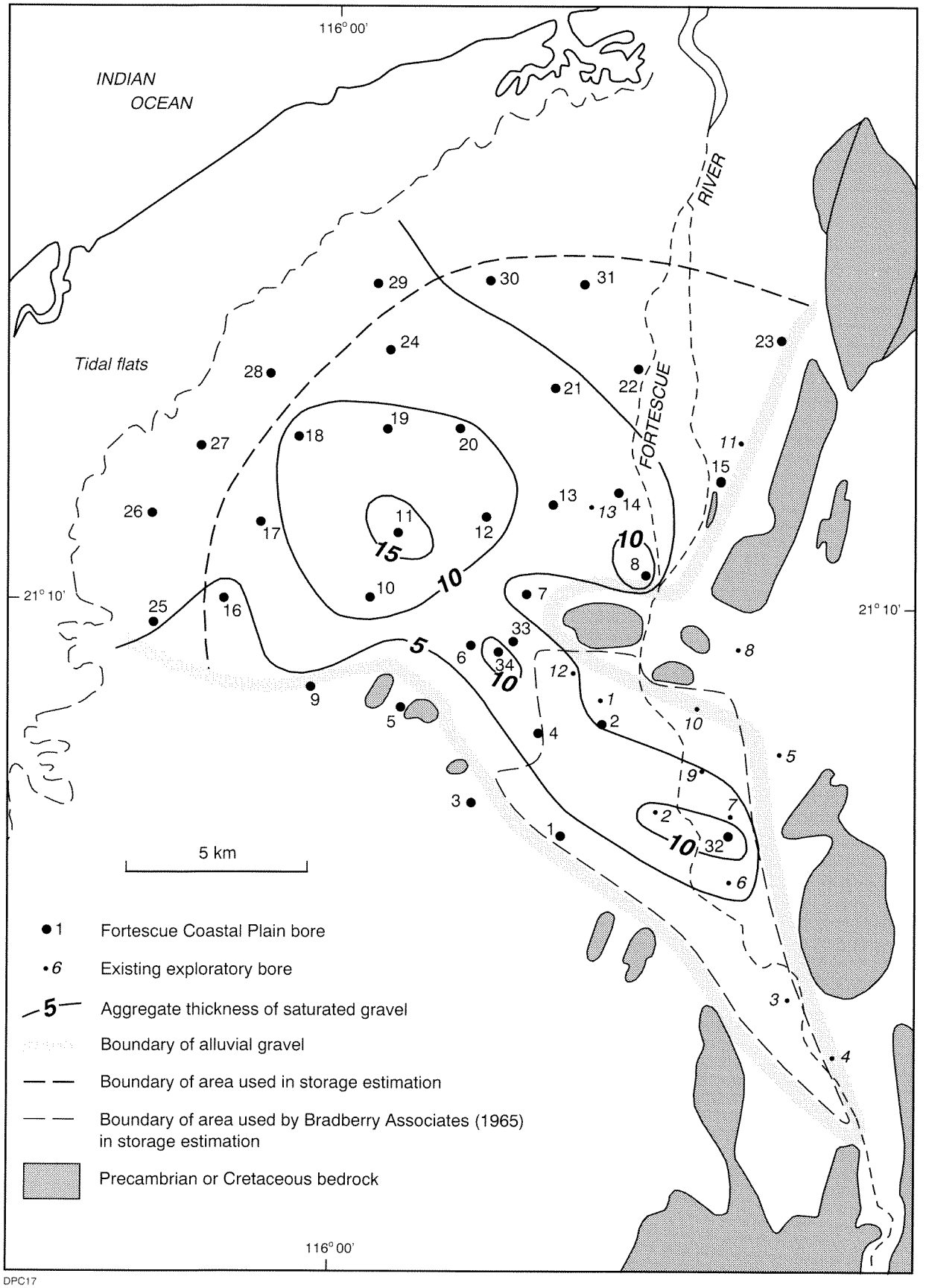

Figure 6. Extent and thickness of saturated alluvial aquifer

The gravel generally occurs in one or two layers, interbedded with the overbank clay deposits (Fig.4), and has an aggregate saturated thickness of up to 15 m (Fig. 6). It overlies relatively impermeable Tertiary and Precambrian rocks.

Watertable configuration

The watertable is generally between 5 and 12 m below ground (Fig. 4), but it is subject to seasonal and annual fluctuations of as much as 6 m in bores close to the river (Fig. 7).

The watertable slopes towards the northwest, away from the river, from about 25 m AHD in the south of the investigation area to less than 1 m AHD within 2 km of the tidal flats (Fig. 8).

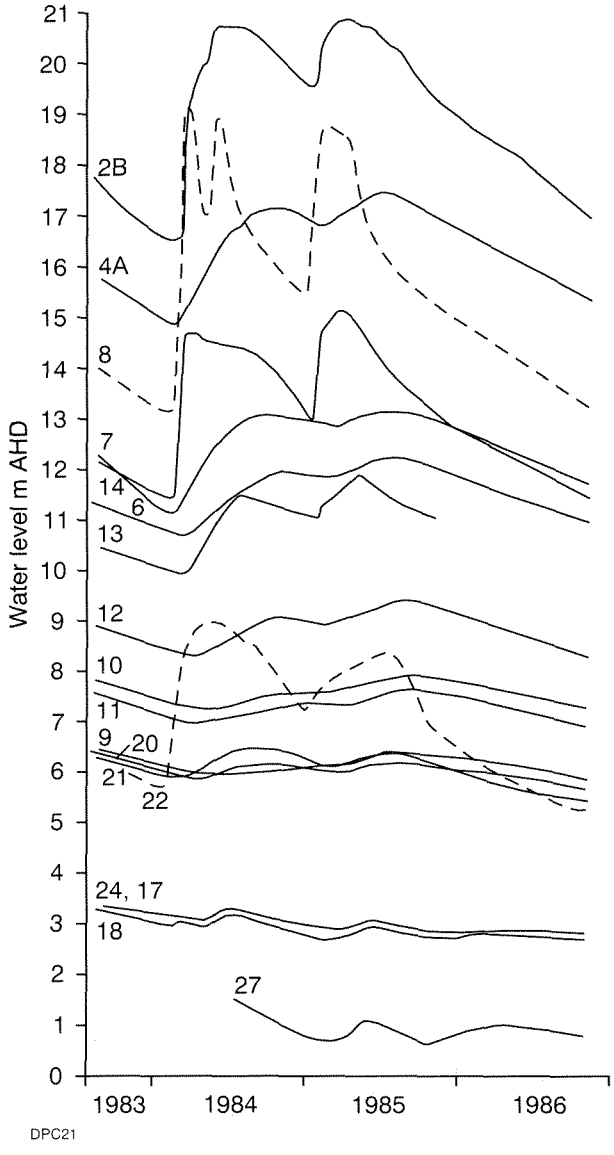

Figure 7. Hydrographs of Fortescue Coastal Plain bores

Recharge

Recharge to the alluvium takes place by direct infiltration through the river bed during periods of streamflow. The amount of recharge is controlled by the duration of flow, and by the available storage capacity in the aquifer near the river. Direct recharge may also occur on the floodplain since, during the Cyclone 'Chloë' flood, the area extending north west from Warralee Well to Corner Well (Fig. 1) was inundated.

Direct recharge apparently occurs in the northwest of the area, as the watertable in FCP 18 and 27 (Fig. 7) rose following local rain in February 1986 that did not give rise to significant streamflow.

Waterlevels in bores close to the river rise rapidly when the river flows, and decline soon after the river ceases to flow (Fig. 7). With increasing distance from the river, there is a progressively greater time lag for waterlevels to rise, and for maximum groundwater levels to occur. Maximum waterlevels occur in FCP 10 and 11 (7 km from the river) eight months after the waterlevel peak in FCP 8 (adjacent to the river). The time lag demonstrates that the waterlevel rise, hence recharge, due to river flow is very much greater than that due to direct recharge from the surface.

The amount of groundwater recharge resulting from the 1984 flow (Fig. 3) was estimated by calculating the volumetric change in the saturated aquifer between March and July 1984. The increase in saturated thickness between the March and July waterlevels was estimated from the hydrographs. These were contoured and the increase in volume of saturated aquifer calculated from areal measurement (Fig. 9), using an assumed specific yield of 0.1. The specific yield of disturbed samples of river bed gravel was measured to be 0.3, but a value of 0.1 is appropriate in this calculation because the gravel normally has a proportion of clay in the matrix. Based on this volume, the recharge in the area shown in Figure 9 west of the river was calculated to be 22.7 x 10^6 m^3. Additional recharge, not taken into account, also occurs east of the river and upstream of this area.

Storage

The total groundwater storage in the alluvial gravel can be calculated by multiplying the volume of saturated aquifer by the assumed specific yield. The volume of groundwater in storage on 12 November 1985 within the area shown on Figure 6, and based on the calculations shown in Table 4, is 126 x 10^6 m^3.

Between May 1985 and the end of 1986 there was only a small river flow (Fig. 2), and waterlevels in the aquifer declined. The resultant decrease in aquifer storage between 12 November 1985 and 26 November 1986 west of the river, in the area shown in Figure 10, was calculated to be 11 x 10^6 m^3, assuming a specific yield of 0.1.

Historical waterlevel changes

Waterlevels have been measured in station wells at intervals since 1964, and the data from wells in the area

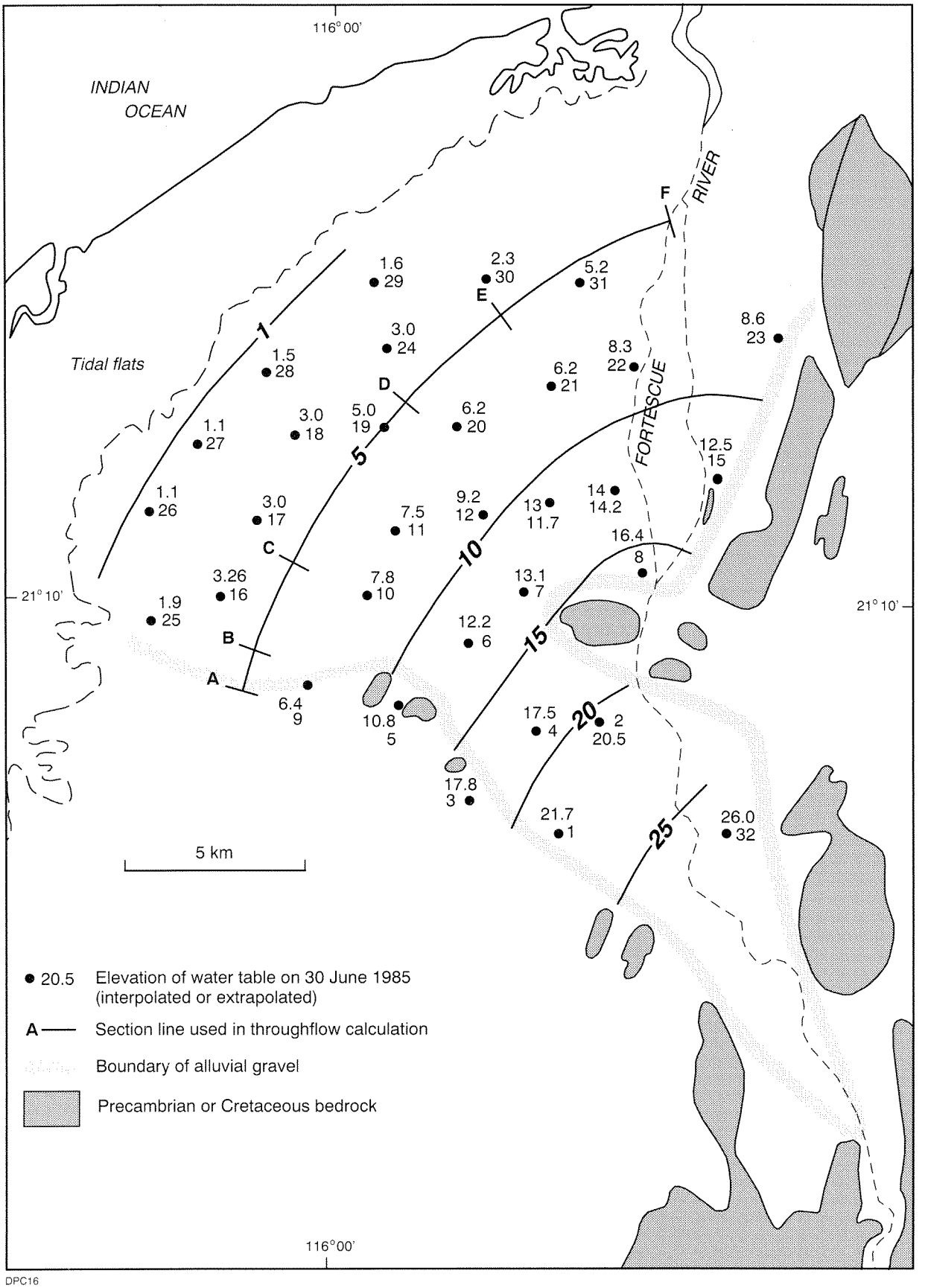

Figure 8. Watertable elevation

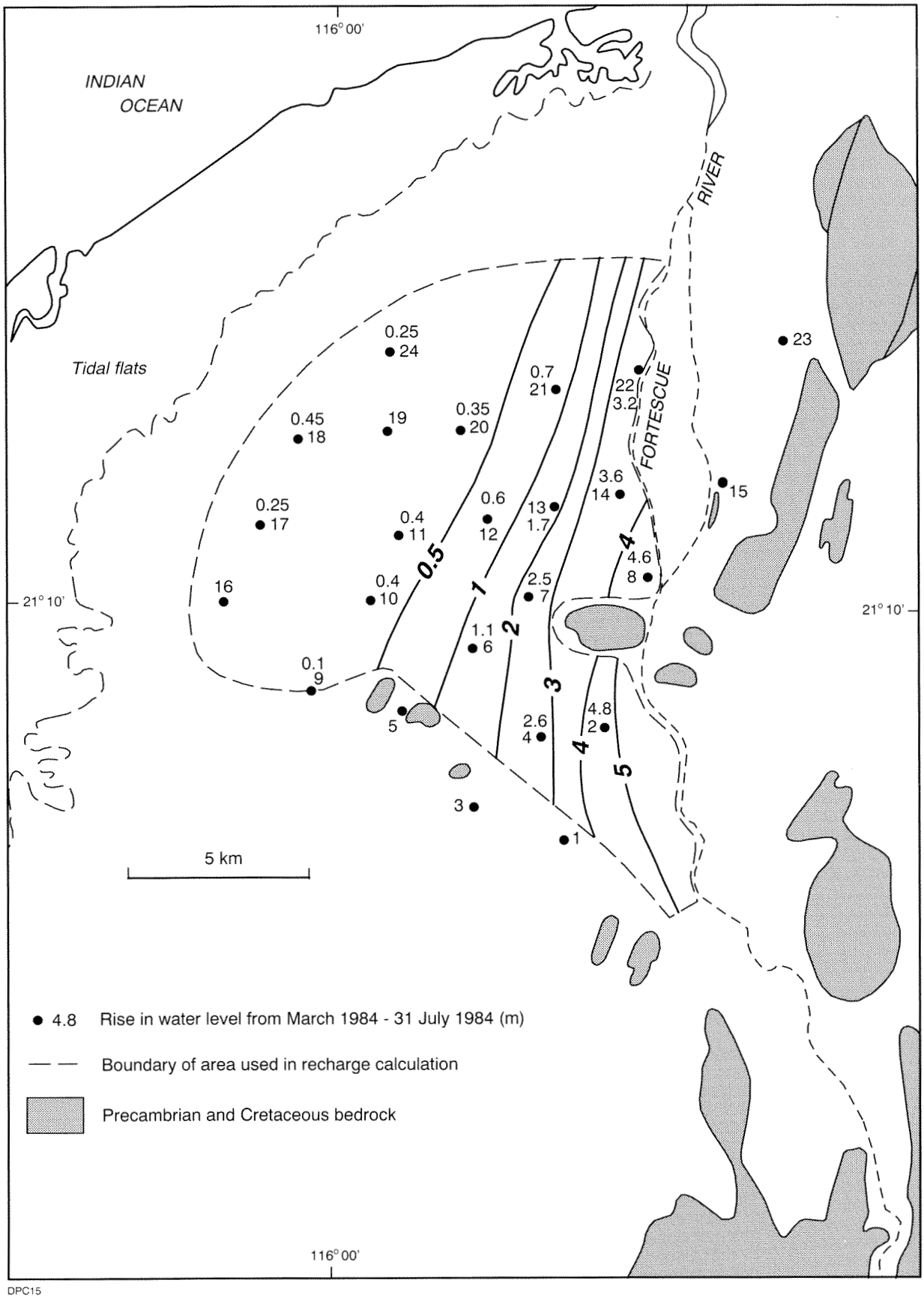

Figure 9. Rise in waterlevels from March 1984 to 31 July 1984

Table 4. Groundwater storage (based on Fig. 6)

Isopach interval (m)	*Average thickness (m)*	*Area (km^2)*	*Volume[a] ($10^6 m^3$)*
>15	15	2.6	4
10–15	12.5	32	40
5–10	7.5	83	62
0–5	2.5	82	20
		Total	**126**

Note: (a) specific yield of 0.1

are given in Table 5. Most of the lowest waterlevels that have been measured occurred in 1983–84 following a comparatively small river flow in 1983. At this time some of the wells were dry, and similar waterlevels can be inferred to have occurred after other years of low flows.

The rapid growth of mesquite north of the Mardie–Balmoral Road between 1945 and 1953 is reported to have lowered waterlevels in local station wells by about 2m. Waterlevels subsequently recovered as the mesquite was removed (Sharpe, R., 1986, pers. comm.).

Hydraulic conductivity

Eight-hour constant-rate pumping tests were under-taken on FCP 4P, 11P and 34A (Table 6). Transmissivities, derived from matching time–drawdown data from observation bores to non-equilibrium delayed-yield type curves, ranged from 380 to 1760 m^2/day (Commander, 1989). Estimates of hydraulic conductivity in the Fortescue River alluvium, derived from the pumping tests, ranged from 63 m/day at FCP 4P to 190 m/day at FCP 11P.

A pumping rate of 1690 m^3/day with a drawdown of 0.5 m was achieved by Bradberry Associates (1965) in Cliffs No.2B.

Throughflow

Groundwater in the alluvium generally flows away from the river in a northwesterly direction (Fig. 8). For a short period during streamflow, a groundwater mound builds up beneath the river bed, and there is easterly groundwater flow, which reverses when the river ceases to flow.

The throughflow, Q, across the 5 m watertable contour (A–F on Fig. 8), can be estimated from the Darcy equation:

$$Q = kbil$$

where:

k = hydraulic conductivity (m/day)
b = aquifer thickness (m)
i = hydraulic radient (dimensionless)
l = cross-section width (m)

The aggregate thickness of saturated gravel is estimated from Figure 6, and the hydraulic gradient is based on the watertable configuration in June 1985. Both can be assumed to be steady-state conditions as waterlevel fluctuations are small along the 5 m watertable contour. The range of hydraulic conductivities assumed are based on the results of the pumping tests. The estimated average annual groundwater throughflow in the gravel across section A–F on Figure 8 is in the order of 2.3–9.2 x 10^6 m^3, depending on the adopted hydraulic conductivity (Table 7).

Discharge

The decline in storage in a year with no recharge can be equated to the average annual discharge. Between December 1985 and November 1986 there was no streamflow, and the storage depletion (Fig. 10) was estimated to be 11 x 10^6 m^3 (assuming a specific yield of 0.1). The conservative value used for the specific yield gives a minimum estimate of the annual storage depletion, but this estimate is still much greater than the minimum groundwater throughflow based on the low hydraulic conductivity of 50 m/day (Table 7). This suggests that the higher hydraulic conductivity (200 m/day) derived

Table 5. Waterlevels in Mardie Station wells 1964–85

Well	*9/64*	*4/65*	*5/65*	*8/65*	*6/74*	*11/79*	*8/83*	*4/84*	*9/84*	*5/85*
				(metres below natural surface)						
Corner	7.0	7.41	7.36	7.19	7.10	6.51	8.66	9.18	8.60	–
Currangyry	8.5	6.33	7.01	8.07	6.90	10.1	10.19	6.20	–	6.76
Hilda	2.7	–	–	–	3.35	4.3	5.30	–	5.26	–
Lawn	3.6	–	–	–	4.25	5.03	6.31	–	6.28	–
Mulyering	9.1	9.90	9.63	8.90	7.85	10.70	10.92	10.83	–	9.05
Pilling	4.5	–	–	–	4.95	6.95	7.44	7.83	7.60	–
Secret	7.3	7.55	7.31	7.16	6.35	7.56	9.79	8.37	7.20	–
Toondy	3.3	–	–	–	3.40	5.0	5.61	5.52	5.43	–
Two Mile	5.5	–	–	–	5.75	6.51	7.25	7.49	–	–
Violet	8.5	6.94	6.70	6.92	5.80	9.08	9.67	7.12	–	–
Warralee	7.6	6.49	6.58	6.58	5.80	8.74	9.53	6.73	–	–
Wealumba	3.3	–	–	–	3.90	4.8	5.56	5.90	5.80	–
Woolawanda	6.7	–	–	–	6.8	8.32	9.08	9.59	9.31	–
Woolie Pdk.	5.2	4.39	4.29	–	3.6	6.20	–	4.86	–	–
Yabberoo	9.1	7.74	7.46	7.10	6.35	7.73	8.65	8.82	7.63	–

Table 6. Test-pumping data

Bore	Pump bore				20 m Observation bore		
	Pump rate	Drawdown (8 hrs)	Specific capacity (8 hrs)	Specific capacity(a) (30 min)	Drawdown (8 hrs)	T	k
	(m^3/d)	(m)	(m^2/d)	(m^2/d)	(m)	(m^2/d)	(m/d)
FCP4P	591	6.7	88	263	0.23	380	63
FCP11P	(b) 424	1.6	265	666	0.12	1 760	190
FCP34A	230	2.8	82	181	0.068	1 020	170

Notes: T = transmissivity; k = hydraulic conductivity
(a) calculated according to the method of Sheahan (1971); both specific capcities are affected by delayed yield or vertical leakage;
(b) limited by pump, potential yield about 900 m^3/day

Table 7. Throughflow calculations

Section	Aquifer thickness (m)	Hydraulic gradient ($x10^{-3}$)	Length (km)	Annual throughflow ($x10^6 m^3$) k = 50 m/d	k = 100 m/d	k = 200 m/d
AB	2	1.05	1.0	0.04	0.08	0.16
BC	7	1.05	2.5	0.33	0.67	1.32
CD	12	1.05	5.5	1.26	2.52	5.04
EF	2	1.05	5.0	0.19	0.38	0.76
			Total	**2.29**	**4.58**	**9.16**

Note: (a) average aggregate saturated thickness of gravel

Table 8. Salinity variation in Mardie Station wells 1964–84 (mg/L TDS, EC x 6.4)

Well	1964 GSWA	1965 BA(a)	1974 GSWA	1979 GSWA(b)	1983 GSWA(a)	1984 GSWA(a)
Corner	535	560	440	(c) 440	–	380
Coolanarra	552	–	690	–	–	–
Coonga	1 909	–	3 570	2 380	1 750	–
Currangyry	948	832	910	760	770	–
Garden	7 678	–	9 050	9 800	–	–
Hilda	1 875	–	1 820	1 150	1 040	980
Homestead	800	–	760	810	–	–
Jilanjilan	1 120	1 344	980	1 600	–	–
Lawn	1 379	–	1 600	1 970	2 100	2 070
Mulyering	1 121	1 344	1 290	1 190	1 152	–
Pilling	877	–	870	(c) 860	750	890
Secret	581	704	550	550	470	505
Toondy	2 368	–	3 310	1 600	1 250	1 320
Two Mile	646	–	560	550	563	–
Violet	693	672	420	460	480	–
Warralee	509	576	720	460	440	–
Wealumba	1 140	–	1 600	910	860	860
Woolawandawoolna	877	–	880	480	450	470
Woolie Paddock	732	896	820	720	–	–
Wool Shed	2 857	–	2 700	(c)1 790	–	–
Yabberoo	796	832	760	760	710	720

Notes: (a) Bradberry Associates (1965): quoted electrical conductivity (mS/m at 25°C) x 6.4;
(b) field conductivity converted to Chemistry Centre conductivity; (c) standard analysis

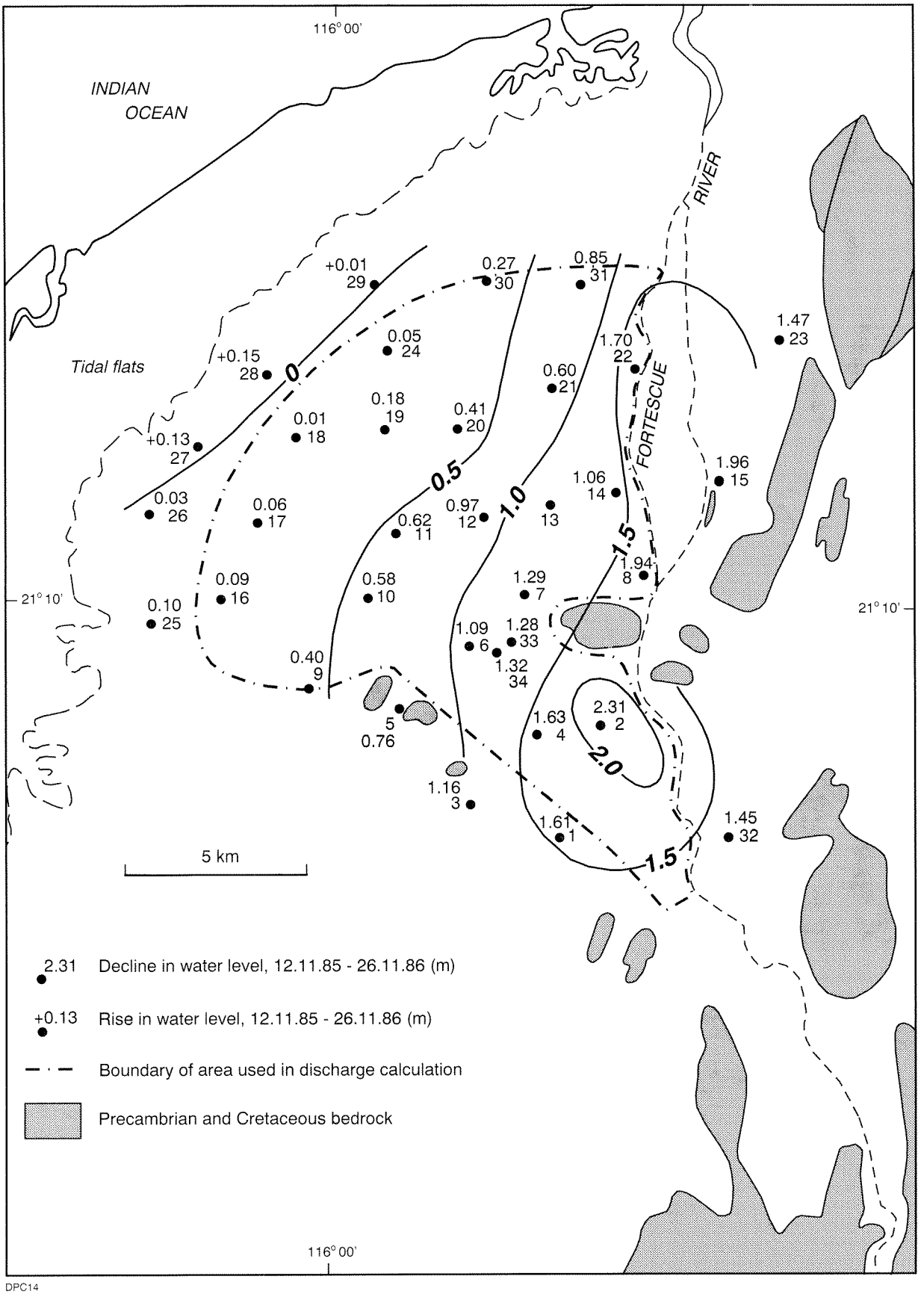

Figure 10. Decline in waterlevels from 12 November 1985 to 26 November 1986

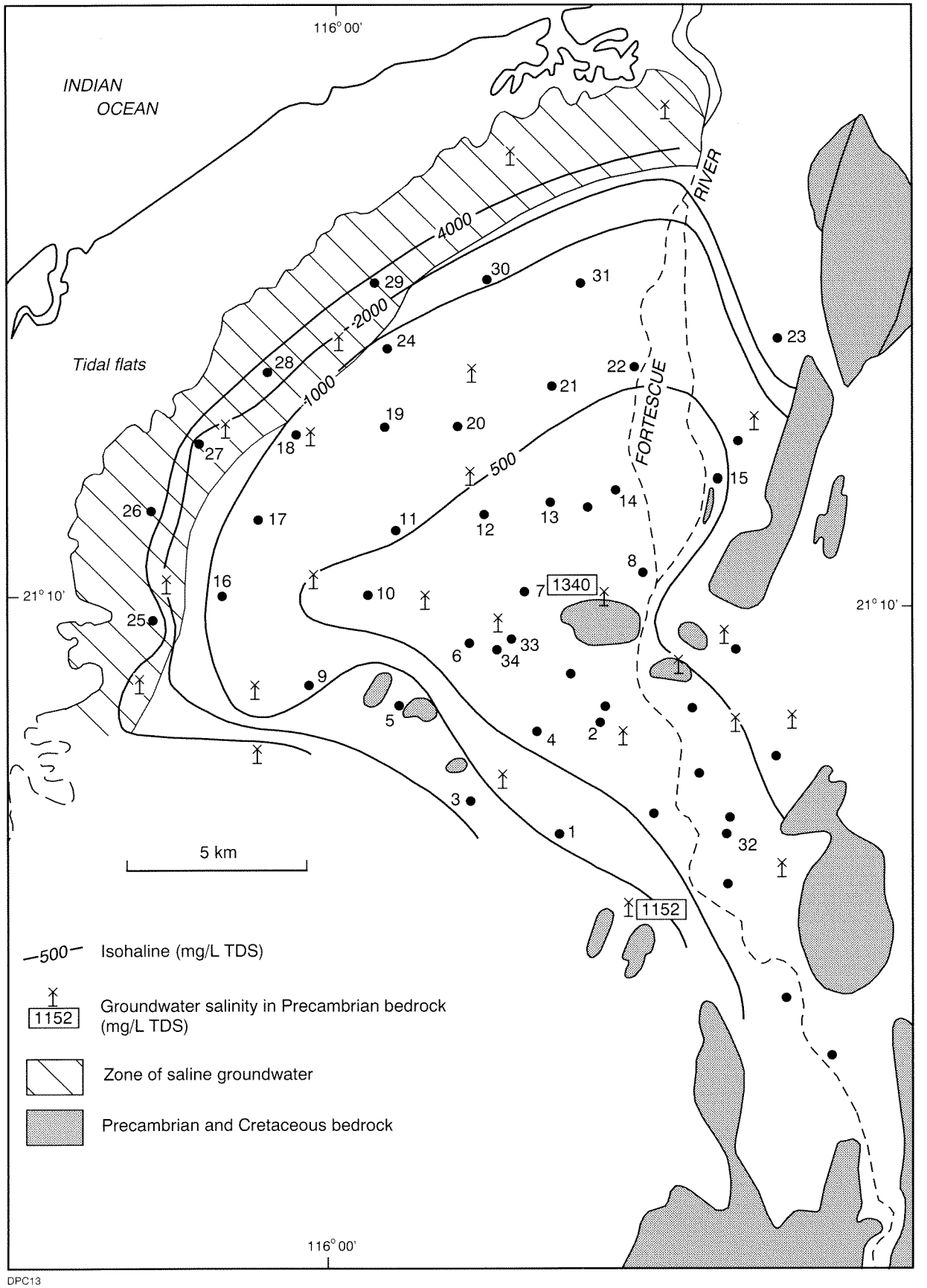

Figure 11. Groundwater salinity in the Fortescue River alluvium

from the pumping tests and used in the throughflow calculations is more likely to be of the correct order of magnitude.

Discharge from the alluvial gravel is by evapotranspiration from phreatophytic vegetation in the northwest of the area, and by evaporation from the bare tidal flats. Evapotranspiration by mesquite is considerable and the effect on the watertable has been discussed (see ***'Historical waterlevel changes'***). A study of mesquite in an area of Arizona where the watertable is 5 m deep (similar to the northwest of the study area) found evapotranspiration rates approach the summer pan-evaporation rate (Tromble, 1977). At an evapotranspiration rate of 80% pan evaporation, an area of only 5.5 km^2 is required to account for the estimated annual discharge of 11 x 10^6 m^3.

Before the advent of mesquite, it is likely that most of the groundwater discharge was to the bare tidal flats, with groundwater flow taking place over a saltwater interface.

Salinity

A lobe of low-salinity groundwater, coinciding with the distribution of the gravel, extends from the Fortescue River to the tidal flats in the northwest (Fig. 11). The groundwater salinity ranges from 345 mg/L TDS in FCP 32B to 1158 mg/L in FCP 30A in the central part of the lobe, and up to 2278 mg/L in FCP 23A on the margin of the gravel. The groundwater salinity is controlled by the low-salinity recharge water from the river, which itself varies according to the characteristics of different streamflow events.

Close to the tidal flats in the northwest of the area is a saline interface at depths of between 4 and 8 m below the watertable (Fig. 12). The salinity at the watertable in the exploratory bores in this area ranged from about 1850 mg/L in FCP 27 to 18 500 mg/L in FCP 26, and the salinity of the saline groundwater below the interface ranged from 18 000 mg/L in FCP 28 to an unusually high salinity of 75 000 mg/L in FCP 26.

The groundwater salinity in most of the shallow station wells in the alluvial gravel appears to have remained relatively constant since 1964 (Table 8). However, wells abstracting groundwater from above the saltwater interface, such as Coonga, Hilda, Lawn and Toondy Wells, show relatively large fluctuations in salinity.

Hydrochemistry

As total salinity increases, the groundwater in the Fortescue Coastal Plain bores shows a progressive enrichment of sodium chloride at the expense of calcium and bicarbonate (Fig. 13). Evidence of calcrete formation close to the watertable suggests that the calcium and bicarbonate is removed by precipitation. There is also a slight decrease in the proportion of magnesium and an increase in the proportion of sulfate with increasing salinity.

The groundwater is slightly hard to very hard (Table 9). Nitrate is present at concentrations ranging up to 5 mg/L,

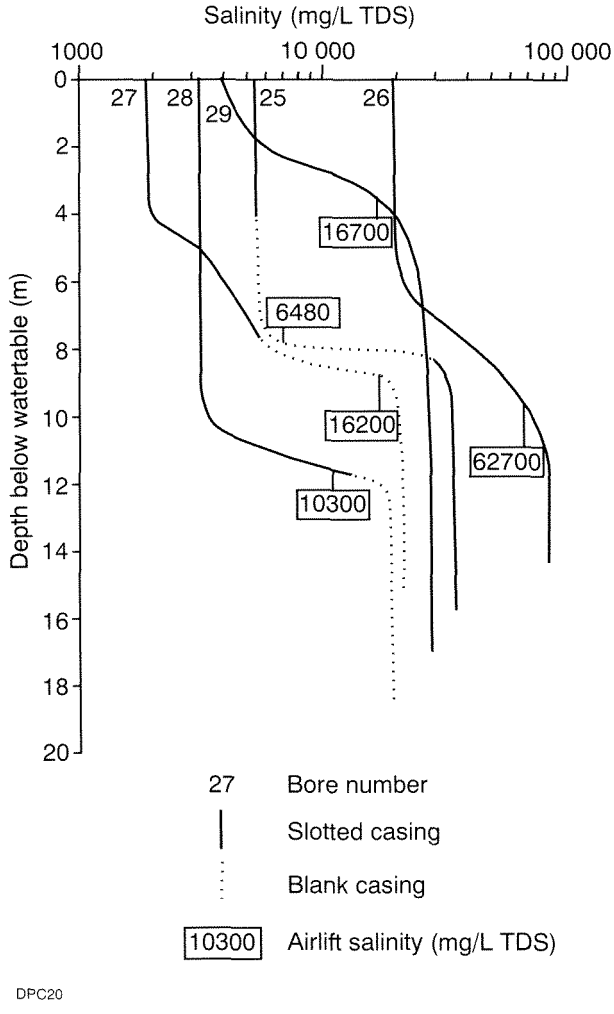

Figure 12. Salinity–depth profiles in FCP25–29 showing saltwater interface

and fluoride concentrations range from 0.3 to 0.6 mg/L. Boron ranges in concentration from 0.2 to 0.8 mg/L and silica concentrations range from 13 to 38 mg/L. Iron was analysed only in the non-aerated samples from pumped bores where it ranged from 0.05 to 0.59 mg/L.

Temperature

The temperature of groundwater measured during the pumping tests was 31.5°C.

Yarraloola Conglomerate

The Yarraloola Conglomerate was intersected below the Trealla Limestone in FCP 2, FCP 14 and FCP 32, and appears to be present only in a narrow channel which coincides approximately with the present position of the Fortescue River (Fig. 14). It is a confined aquifer, and is confined by up to 30 m of Trealla Limestone in the exploratory bores.

The potentiometric head in the Yarraloola Conglomerate decreases northwards from 26 m in FCP 32 to

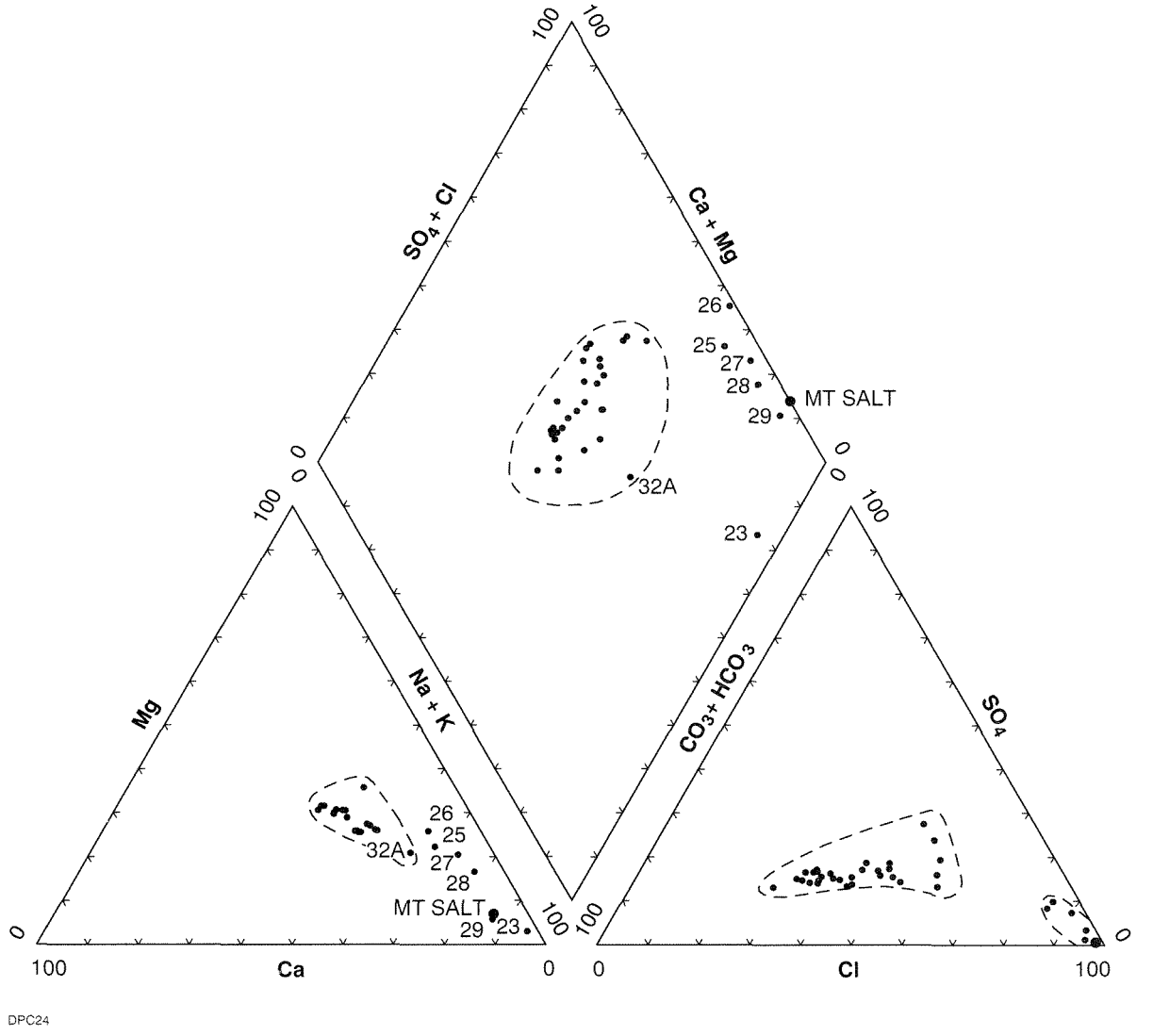

Figure 13. Piper trilinear diagram of chemical analyses

12 m in FCP 14 (August 1985). Recharge is presumed to be by downward leakage from the alluvium as the watertable in FCP 2A and 14A is higher than the potentiometric head, and the waterlevel changes are similar in both aquifers. At FCP 32 there is usually a slight upward head between the Yarraloola Conglomerate and the alluvium of 10–15 cm, which suggests that recharge takes place upstream of FCP 32 as well as downstream.

FCP 2A was test pumped at 1063 m^3/day for 26 m drawdown after 8 hours, and a match of the time–drawdown data to a late-stage non-equilibrium type curve gives a transmissivity of 65 m^2/day (Commander, 1989). In FCP 14A, a maximum yield of only 120 m^3/day could be obtained, giving a calculated transmissivity of 3 m^2/day.

The groundwater salinity in the Yarraloola Conglomerate ranges from 454 to 492 mg/L TDS. The ionic composition is similar to that of groundwater of similar salinity in the alluvium (Table 9).

A seepage of saline water (27 800 mg/L) occurs from below the summit of the mound of calcareous tufa at Mount Salt (Williams, 1965). This seepage is probably derived from the Mardie Greensand, as the Yarraloola Conglomerate is not present in Coonga 1 and Mardie West 1 petroleum exploration wells. The high salinity of the Mount Salt spring is consistent with the groundwater salinity which is found elsewhere in the basal Cretaceous sands (Thomas, 1978), and contrasts with the fresh groundwater in the Yarraloola Conglomerate in the investigation area.

The groundwater temperature in FCP 2A during the pumping test was 32°C.

Development

The area of the Fortescue River alluvium (including a small area of Yarraloola Conglomerate) which is most suitable for groundwater development is close to the present river bed, where rapid recharge can occur during streamflow. Bore yields of up to 900 m^3/day in the alluvium have been demonstrated by pumping tests.

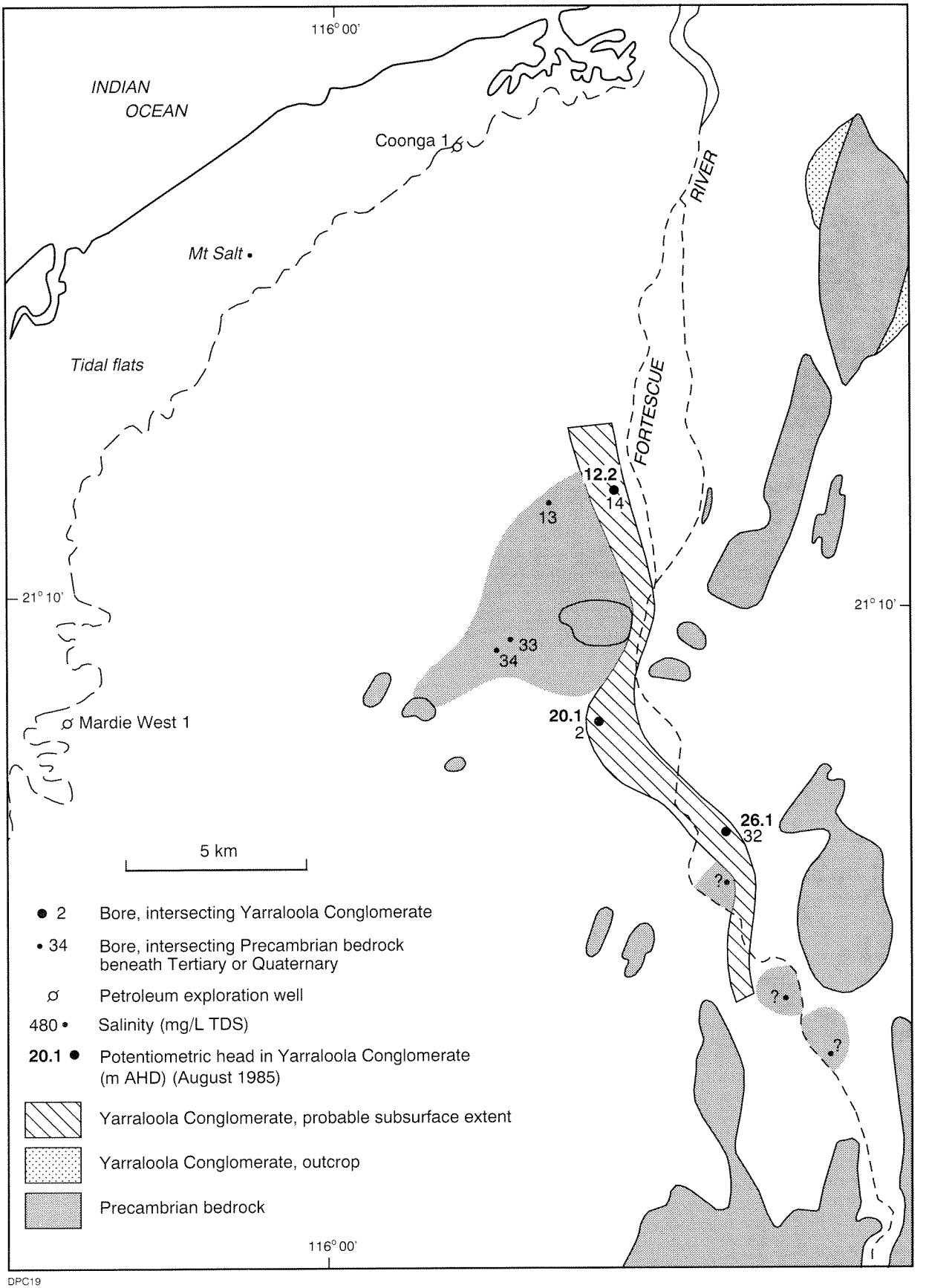

Figure 14. Yarraloola Conglomerate; distribution and hydrogeology

Table 9. Chemical analyses of groundwater

Bore	*Sample no.*	*Lab. no.*	*Sample date*	*pH*	*E.C.(b) mS/m*	*TDS(c) @ 180°C*	*T.H.(d) $CaCO_3$*	*T.A.(e) $CaCO_3$*	*Ca*	*Mg*	*Na*	*K*	*CO_3*	*HCO_3*	*Cl*	*SO_4*	*NO_3*	*SiO_2*	*B*	*F*	*Fe*	*Mn*
						mineral matter (mg/L)																
FCP1A	65638	6965	11.07.83	8.0	156	889	430	325	79	56	163	11	<2	397	243	100	1	37	0.4	0.5	-	
FCP2A (a)	65639	6966	25.07.83	8.2	71	417	160	141	28	21	82	7	<2	172	107	51	2	33	0.2	0.5	-	
FCP2A (a)	85905	2284	17.07.85	8.4	71	410	154	140	27	21	82	7	4	163	102	51	2	34	0.2	0.5	0.05	<0.02
FCP2B	65640	6967	25.07.83	8.2	76	444	210	179	42	26	76	7	<2	218	100	56	2	26	0.5	0.4	-	
FCP3A	65641	6968	12.07.83	8.2	209	1 190	540	252	72	87	213	14	<2	308	439	125	5	76	0.4	1	-	
FCP4A	65642	6969	15.07.83	7.9	84	496	230	206	43	30	88	7	<2	251	112	61	1	28	0.3	0.5	-	
FCP4P	85906	2285	23.07.85	8.5	74	420	186	175	35	24	75	6	7	199	89	57	3	28	0.2	0.4	0.17	<0.02
FCP5A	65643	6970	21.07.83	7.3	268	1 600	660	279	131	81	315	13	<2	340	496	348	2	46	1.3	1.0	-	
FCP6A	65644	6971	05.07.83	7.8	63	365	170	161	30	22	64	6	<2	196	74	45	<1	26	0.2	0.5	-	
FCP8A	65645	6972	18.08.83	7.7	79	458	220	192	44	28	79	7	<2	234	104	53	<1	26	0.8	0.3	-	
FCP9A	65646	6973	11.08.83	8.1	128	759	350	290	64	46	138	8	<2	354	196	93	1	36	0.4	0.5	-	
FCP10A	65647	6974	12.08.83	7.9	75	436	200	167	37	27	74	6	<2	204	103	57	2	28	0.2	0.3	-	
FCP11A	65648	6975	12.08.83	8.4	108	618	320	184	61	40	95	7	6	212	186	82	3	32	0.2	0.4	-	
FCP11P	85907	2286	06.08.85	8.4	106	590	296	184	56	38	92	7	5	214	168	80	3	32	0.2	0.4	0.59	<0.02
FCP12A	65649	6976	22.08.83	7.9	64	377	180	158	35	23	60	6	<2	193	80	50	<1	26	0.2	0.3	-	
FCP13A	65650	6977	22.08.83	7.9	76	461	220	232	44	27	78	6	<2	283	84	50	<1	30	0.8	0.3	-	
FCP14B	65651	6978	23.08.83	7.8	61	360	170	155	33	22	56	6	<2	189	75	48	<1	25	0.2	0.3	-	
FCP15A	65652	6979	09.08.83	7.8	72	427	180	189	36	22	82	5	<2	230	85	52	1	29	0.2	0.4	-	
FCP16B	65653	6980	29.08.83	8.5	111	643	290	203	53	39	114	8	6	235	188	82	2	33	0.4	0.4	-	
FCP17A	65654	6981	25.08.83	8.2	124	720	340	200	61	45	126	8	<2	244	224	94	5	35	0.3	0.4	-	
FCP18A	65655	6982	26.08.83	8.5	116	673	310	194	56	41	123	9	6	224	205	81	4	36	0.3	0.5	-	
FCP19A	65656	6983	15.08.83	8.2	99	567	270	180	53	34	96	7	<2	219	155	79	2	31	0.2	0.4	-	
FCP20A	65657	6984	16.08.83	8.2	100	580	300	227	59	36	90	7	<2	277	144	71	1	33	0.2	0.4	-	
FCP21A	65658	6985	17.08.83	7.9	126	724	370	200	72	46	114	7	<2	244	219	109	3	32	0.3	0.4	-	
FCP22A	65659	6986	16.08.83	7.9	95	555	270	242	52	33	94	7	<2	295	122	66	<1	33	0.2	0.5	-	
FCP23A	65660	6987	08.08.83	9.9	356	2 150	77	591	11	12	678	167	175	365	573	325	4	25	0.8	0.9	-	
FCP24A	65661	6988	29.08.83	8.2	130	725	350	196	66	45	125	8	<2	239	237	82	4	38	0.3	0.5	-	
FCP25A	65680	2032	06.08.84	7.7	1 100	6 480	1 840	326	249	297	1 770	36	<2	398	3 420	461	5	43	-	0.5	-	
FCP26A	65681	2033	02.08.84	7.4	7 350	62 700	20 300	225	2 320	3 540	16 700	136	<2	275	37 600	2 200	1	34	-	<0.1	-	
FCP27A	65682	2034	01.08.84	7.6	2 510	16 200	36 900	335	378	669	4 680	89	<2	409	9 220	937	3	42	-	0.7	-	
FCP28A	65683	2035	31.07.84	7.7	1 650	10 300	1 920	395	208	340	3 170	93	<2	482	5 360	815	1	52	-	0.7	-	
FCP29A	65684	2036	27.08.84	7.7	2 660	16 700	1 870	402	399	213	5 560	163	<2	491	10 000	33	<1	39	-	0.3	-	
FCP30A	65685	2037	08.07.84	8.1	181	1 020	455	212	82	61	183	9	<2	259	376	134	3	38	-	0.6	-	
FCP31A	65686	2038	18.07.84	8.2	121	720	297	230	58	37	138	7	<2	281	197	110	1	35	0.3	0.5	-	
FCP32A (a)	85901	2280	04.07.85	8.1	77	430	134	145	24	18	106	6	<2	177	118	59	<1	13	0.6	0.5	-	
FCP32B	85902	2281	06.07.85	8.3	54	300	148	128	28	19	49	7	2	152	61	38	1	22	0.5	0.3	-	
FCP33A	85903	2282	10.06.85	8.3	87	490	227	169	40	31	85	7	3	200	127	66	2	32	0.2	0.4	-	
FCP34A	85904	2283	10.08.85	8.4	69	400	163	157	29	22	77	7	4	183	83	54	3	29	0.2	0.4	0.18	<0.02

Table 9. (*continued*)

Bore	*Sample no.*	*Lab. no.*	*Sample date*	*pH*	*E.C.(b) mS/m*	*TDS(c) @ 180°C*	*T.H.(d) $CaCO_3$*	*T.A.(e) $CaCO_3$*	*Ca*	*Mg*	*Na*	*K*	*CO_3*	*HCO_3*	*Cl*	*SO_4*	*NO_3*	*SiO_2*	*B*	*F*	*Fe*	*Mn*
						mineral matter (mg/L)																
Mt Salt (a)	65694	2046	03.08.83	7.6	4 170	27 800	3 300	135	680	389	9 310	268	<2	165	17 000	<2	31	17	-	0.2	0.18	<0.02
Corner	12427	0025	11.11.79	6.9	68	390	188	151	34	25	63	5	0	184	93	48	3	22	0.2	0.3	-	
Woolshed	12428	0026	12.11.79	7.2	279	1 510	531	265	74	84	356	14	0	323	604	167	6	40	0.9	-	-	
Pilling	12429	0027	13.11.79	6.9	134	770	405	200	85	47	112	8	0	244	243	111	9	33	0.2	0.4	-	

Notes: (a) samples from Yarraloola Conglomerate (all others are from alluvium); (b) electrical conductivity (mS/m at 25°C); (c) total dissolved solids by evaporation to dryness at 180°C; (d) total hardness; (e) total alkalinity

The yield of the aquifer is limited ultimately by the amount and frequency of recharge from the Fortescue River. Based on the estimated recharge and throughflow, about 10 x 10^6 m^3 could be abstracted from the Fortescue River alluvium. The estimated groundwater in storage of 126 x 10^6 m^3 provides additional capacity in years of low streamflow.

The infiltration capacity of the aquifer could be increased by lowering the watertable close to the river and creating a larger immediately available storage capacity to be filled when the river flowed. By artificially slowing river flow (or controlling release from a dam upstream), and by increasing the area available for direct infiltration, the storage capacity of the normally unsaturated gravel above the watertable away from the river could also be utilized.

Conclusions

Alluvial gravel extending over an area of 200 km^2, underlying and adjacent to the Fortescue River, contains a fresh unutilized groundwater resource in a region that is generally deficient in fresh water. The resources are sufficiently large to maintain a town water supply or irrigated agriculture.

Based on natural recharge rates the aquifer has the potential to yield about 10 x 10^6 m^3/year of groundwater with a salinity ranging between 400 and 800 mg/L. The yield could be increased by conjunctive use with a dam on the Fortescue River.

References

ALLEN, A. D., 1987, Groundwater, *in* Geology of the Carnarvon Basin: Western Australia Geological Survey, Bulletin 133, p. 237–244.

BEARD, J. S., 1975, The vegetation of the Pilbara area: University of Western Australia, 1:100 000 Vegetation Series Explanatory Notes.

BRADBERRY ASSOCIATES, 1965, Water resources of the lower Fortescue River area: Report for Raymond International (unpublished).

COMMANDER, D. P., 1989, Fortescue River Coastal Plain bore completion reports: Western Australia Geological Survey, Hydrogeology Report 1989/13 (unpublished).

DAMES AND MOORE, 1979, Preliminary environmental review, alternative water sources, West Pilbara Region, Western Australia, v. I and II (unpublished).

DAVIDSON, W. A., 1975, Hydrogeological reconnaissance of the Northwest Pilbara Region: Western Australia Geological Survey, Record 1975/12.

HEMATITE PETROLEUM PTY LTD, 1973, Final well report for Woorawa 1, Windoo 1, Surprise 1, Mardie West 1, Coonga 1, phase II drilling operations, Robe River Block EP/40, Western Australia (unpublished).

HOCKING, R. M., and van de GRAAFF, W. J. E., 1978, Cretaceous stratigraphy and sedimentology, northeast margin of the Carnarvon Basin, Western Australia: Western Australia Geological Survey, Annual Report 1977, p. 36–41.

HOCKING, R. M., MOORS, H. T., and van de GRAAFF, W. J. E., 1987, Geology of the Carnarvon Basin: Western Australia Geological Survey, Bulletin 133.

KEVI, L., 1984, Fortescue seismic refraction survey: Western Australia Geological Survey, Geophysical Report 4/84 (unpublished).

NOWAK, I. R., 1979, Fortescue and Robe Rivers Coastal Plain geophysical survey 1979: Western Australia Geological Survey, Geophysical Report 7/79 (unpublished).

PUBLIC WORKS DEPARTMENT, 1984, Streamflow records of Western Australia to 1982: Perth, Public Works Department, Volumes 1–3.

SHEAHAN, N. T., 1971, Type curve solution of step drawdown test: Groundwater, v. 9, no. 1, p. 25–29.

THOMAS, B. M., 1978, Robe River — an onshore shallow oil accumulation: APEA Journal 1978, p. 3–12.

TROMBLE, J. M., 1977, Water requirements for mesquite (*Prosopis juliflora*): Journal of Hydrology, v. 34, p. 171–179.

TYRWHITT, D. S., 1978, Final report on exploration completed within Temporary Reserve 6566, Fortescue River, West Pilbara, W.A.: Newmont Pty Ltd, Report (unpublished).

WILLIAMS, I. R., 1965, Notes on a mound spring on Mardie Station, near Cape Preston: Western Australia Geological Survey, Annual Report 1964, p. 36.

WILLIAMS, I. R., 1968, Yarraloola, W.A.: Western Australia Geological Survey, 1:250 000 Geological Series Explanatory Notes.

14732/1/94—500—L/6284